universität wien

DISSERTATION

Von Biomolekülen zu organometallischen Verbindungen mit tumorhemmenden Eigenschaften

angestrebter akademischer Grad

Doktor der Naturwissenschaften (Dr. rer. nat.)

Verfasserin / Verfasser:	Muhammad Hanif
Matrikel-Nummer:	0748758
Dissertationsgebiet (lt. Studienblatt):	Chemie (A091 419)
Betreuerin / Betreuer:	O. Univ.-Prof. DDr. Bernhard K. Keppler

Wien, am 02. November 2010

universität wien

Ph.D. Thesis

From Biomolecules to Organometallic Compounds with Tumor-Inhibiting Properties

Submitted in part fulfillment of the requirements for the degree

Doctor of Sciences (Dr. rer. nat.)

Author:	Muhammad Hanif
Matriculation number:	0748758
Doctoral subject:	Chemistry (A091 419)
Supervisor:	O. Univ.-Prof. DDr. Bernhard K. Keppler

Vienna, November 2, 2010

This Ph.D thesis is based on the following publications and manuscripts to be submitted for publication:

Osmium(II)- *versus* Ruthenium(II)-Arene Carbohydrate-based Anticancer Compounds: Similarities and Differences

Muhammad Hanif, Alexey A. Nazarov, Christian G. Hartinger, Wolfgang Kandioller, Michael A. Jakupec, Vladimir B. Arion, Paul J. Dyson, Bernhard K. Keppler

Dalton Transactions, **2010,** 39, 7345–7352.

From Hydrolytically Labile to Hydrolytically Stable Ru(II)-Arene Anticancer Complexes with Carbohydrate-Derived Co-ligands

Muhammad Hanif, Samuel M. Meier, Wolfgang Kandioller, Anna Bytzek, Michaela Hejl, Christian G. Hartinger, Alexey A. Nazarov, Vladimir B. Arion, Michael A. Jakupec, Paul J. Dyson, Bernhard K. Keppler

Journal of Inorganic Biochemistry, **2010,** in Press

The Arene Moiety as Anticancer Activity Determining Parameter in Organometallic Ru(II) Complexes with Carbohydrate Derived Ligands

Muhammad Hanif, Samuel M. Meier, Alexey A. Nazarov, Michael A. Jakupec, Paul J. Dyson, Bernhard K. Keppler, Christian G. Hartinger

Unpublished results

Is the Reactivity of M(II)–Arene Complexes of 3-Hydroxy-2(1H)-pyridones to Biomolecules the Anticancer Activity Determining Parameter?

Muhammad Hanif, Helena Henke, Samuel M. Meier, Sanela Martic, Mahmoud Labib, Wolfgang Kandioller, Michael A. Jakupec, Vladimir B. Arion, Heinz-Bernhard Kraatz, Bernhard K. Keppler, Christian G. Hartinger

Inorganic Chemistry, **2010,** 49 (17), 7953–7963.

Tuning the Anticancer Activity of Ruthenium(II)–Arene Complexes of 3-hydroxy-2-pyridinone derived Ligands

Muhammad Hanif, Helena Henke, Samuel M. Meier, Wolfgang Kandioller, Michaela Hejl, Vladimir B. Arion, Michael A. Jakupec, Bernhard K. Keppler, Christian G. Hartinger

Unpublished results

Dedication

To the memory of my beloved mother who had always cheered me up.

May her soul rest in eternal peace!

Acknowledgements

I would like to thank Prof. DDr. Bernhard Keppler for providing me the opportunity to work in his research group for my PhD thesis.

With deep sense of gratitude and appreciation, I would like to express my sincere thanks to my supervisor Dr. Christian Hartinger for his inspiring guidance, advice, support and encouragement throughout the project, for proofreading and correcting of all my manuscripts, abstracts, posters, presentations and the PhD thesis. He has been not only a caring mentor, but also a great friend and I am privileged to have worked for him.

I am also extremely grateful to Dr. Alexey Nazarov for his support and advice particularly in the synthesis of sugar-derived ligands and their metal-arene complexes.

I am highly indebted to many people for their cooperation in the completion of my dissertation: Alexander Roller and Prof. Arion for X-ray data collection and structure refinement; Mag. Anatoli Dobrov and Samuel M. Meier for ESI-MS measurements; Michaela Hejl and Dr. Michael Jakupec for the MTT assays; Prof. Dr. Markus Galanski for 2D NMR measurement and NMR service measurement team (past & present). I am also thankful to Dr. Jessica Gätjens, Dr. Iryna Stepanenko and Dr. Wolfgang Kandioller for their support in synthesis; Mag. Sergey Abramkin and Dr. Wolfgang Kandioller for NMR measurement training and Samuel M. Meier for training me on gel electophoresis and ESI-MS experiments.

I am highly grateful to all colleagues and members of the working group, especially Alex Roller, Elfi, Mihai Odoleanu, Werner, Helena, and Andrea for their help and nice cooperation.

I am also extremely thankful to Prof. Dr. Saeed Ahmad (my supervisor of M. Phil thesis), for his guidance, motivation and all fruitful discussions. He has been really a great supervisor and friend who inspired me to study so-called "Bioinorganic Chemistry".

For financial support, I am thankful to Higher Education commission of Pakistan and University of Vienna.

No acknowledgement would ever adequately express my gratitude to my whole family for their years of love, care and emotional support.

Finally, I would like to say a big thank you to all my friends (both in Austria and Pakistan) for their much appreciated support and encouragement throughout the last three years.

Muhammad Hanif

Table of contents

Abbreviations

1D	one-dimensional (NMR)	***J***	coupling constant (NMR)
2D	two-dimensional (NMR)	**L-Cys**	L-cysteine
AMP	adenosine 5'-mono-phosphate	**L-His**	L-histidine
brs	broad singlet (NMR)	**L-Met**	L-methionine
°C	degree Celsius	**m**	multiplet (NMR)
Cyt	cytochrome c	**mg**	milligram
$CDCl_3$	deuterated chloroform	**min**	minute
d	doublet (NMR)	**µM**	micromolar
δ	chemical shift	**mL**	milliliter
d_6 - DMSO	deuterated dimethyl sulfoxide	**mM**	millimolar
DNA	2'-deoxyribonucleic acid	**mmol**	millimol
D_2O	deuterated water	**m.p.**	melting point
e.g.	*exempli gratia* (for example)	**MS**	mass spectrometry
et al.	*et alii* (and others)	**NMR**	nuclear magnetic resonance (spectroscopy)
etc.	*et cetera* (and other things)	**pH**	**p**ondus **H**ydrogenii (power of hydrogen)
ESI	electrospray ionization	**pK_a**	log K_a (acid dissociation constant)
g	gram	**ppm**	parts per million
h	hour	**RNA**	ribonucleic acid
Gly	glycine	**s**	singlet (NMR)
GMP	guanosine 5'-monophosphate	**t**	triplet (NMR)
Hz	hertz	**Tf**	transferrin
IR	infrared (spectroscopy)	**Ub**	ubiquitin

Abstract

Cisplatin is one of the most widely used anticancer drugs, however, its clinical efficacy is hampered by severe side effects and acquired or intrinsic resistance. These limitations have prompted a search for metal-based antitumor drugs with improved effectiveness. Consequently, a large number of metal complexes were synthesized and biologically tested. Switching from platinum to other metal ions may result in altered cytotoxicity profiles due to different targets, or chemical and biological properties in general. Complexes of gallium (KP46) and ruthenium (KP1019 and NAMI-A) have already entered clinical trials. Very recently, half-sandwich ruthenium(II)- and osmium(II)-arene complexes have shown great potential for the development of anticancer drugs. Different approaches have been explored in this regard which resulted in compounds with cytotoxicity comparable or even superior to cisplatin.

In this thesis, different strategies were employed, including coordination of biomolecules to the metal-arene scaffold, with the aim to improve pharmacological properties such as bioavailability, lipophilicity and solubility as well as anticancer activity. The first part of this thesis comprises the synthesis and biological evaluation of ruthenium(II)- and osmium(II)-arene compounds bearing sugar-derived bicyclophosphite ligands. The complexes were characterized with regard to their stability in aqueous solution, and reaction with proteins and the DNA models 5'-GMP and 9-ethylguanine. In order to establish structure-activity relationships, structural modifications such as change of arene, metal center and leaving group were made.

The second part of this thesis deals with the synthesis as well as chemical and biological characterization of ruthenium(II)- and osmium(II)-arenes complexes of 3-hydroxy-2-pyridones. Hydrolysis, reactivity to biomolecules and CDK2/Cyclin A protein kinase inhibition were investigated, which is discussed with regard to anticancer activity and reactivity to biomolecules.

The chemical and biological data presented in this thesis provide the basis and rationale to follow in future drug design strategies with carbohydrate- and pyridone-derived metal complexes.

Zusammenfassung

Cisplatin ist eines der meistverwendeten Chemotherapeutika in der Krebstherapie, jedoch wird die klinische Anwendung und Wirksamkeit von Cisplatin durch starke Nebenwirkungen und erworbene oder intrinsische Resistenz eingeschränkt. Diese Einschränkungen waren der Anlass metallbasierte Antitumormedikamente mit anderen Zentralatomen als Platin zu untersuchen. Die Metallionen wurden mit dem Ziel ausgewählt geänderte Zytotoxizitätsprofile und Aktivität an einem weiteren Tumorspektrum zu erhalten. Der Galliumkomplex KP46 und die beiden Ru(III) Verbindungen KP1019 und NAMI A werden zurzeit in klinischen Studien untersucht. Ruthenium(II)- und Osmium(II)-Aren Komplexe zeigen großes Potential zur Entwicklung tumorhemmender Medikamente und verschiedene Ansätze wurden in dieser Hinsicht erforscht. Einige dieser Verbindungen besitzen vergleichbare oder sogar bessere Zytotoxizität in Zellkulturen als Cisplatin.

Im Rahmen dieser Dissertation wurden unterschiedliche Strategien angewandt, inklusive Koordination von Biomolekülen an das Metall-Aren Gerüst, um pharmakologische Eigenschaften, wie Bioverfügbarkeit, Lipophilie, Löslichkeit und tumorhemmende Aktivität zu verbessern. Im ersten Teil der Doktorarbeit werden die Synthese und biologische Evaluierung von Ruthenium(II)- und Osmium(II)-Arenverbindungen mit von Zuckern abgeleiteten Bicyclophosphit-Liganden beschrieben. Die Komplexe wurden in Bezug auf ihre chemische Stabilität in wässriger Lösung und die Reaktivität mit Proteinen und den DNA-Modellverbindungen 5'-GMP und 9-Ethylguanin charakterisiert. Verschiedene strukturelle Modifikationen wie zum Beispiel Austausch der Arengruppe, des Metallzentrums oder der Abgangsgruppe wurden durchgeführt, um Struktur-Aktivitätsbeziehungen abzuleiten.

Der zweite Teil dieser Doktorarbeit behandelt die Synthese und Charakterisierung von Ruthenium(II)- und Osmium(II)-Arenkomplexen mit 3-Hydroxy-2-pyridonen als Liganden. Das Verhalten in wässrigen Systemen, die Reaktion mit diversen Aminosäuren und die CDK2/Cyclin A Proteinkinase-Inhibition werden in Bezug auf ihre Zytotoxizität diskutiert.

1. Introduction

1.1 Platinum-based anticancer drugs

The serendipitious discovery of the anticancer activity of cisplatin in the 1960ies has opened new horizons for the development of metal-based drugs and the last four decades have seen immense interest in metallopharmaceuticals. The increasing knowledge of molecular structural biology, in particular information of genomic, proteomic and other cellular functions has not only helped in understanding mechanism of action of existing metal-based drugs but also set the basis for the rational design of new metal-therapeutics.

Cisplatin [cis-diamminedichloridoplatinum(II)] (Fig. 1) was first synthesized by Michele Peyrone in 1844[1] and about hundred years later, its tumor-inhibiting properties were discovered accidentally[2] by Barnett Rosenberg who was investigating the influence of an electric field on the growth of *Escherichia coli* bacteria.

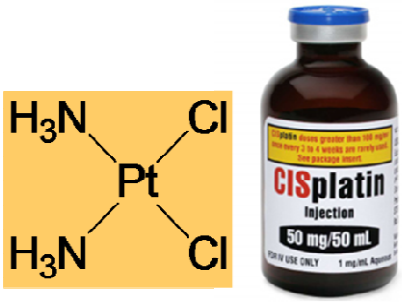

Figure 1. Cisplatin, the first metal-based anticancer drug approved by the FDA

Today cisplatin is one of the most widely used anticancer drugs with a very impressive cure-rate, particularly in testicular and ovarian cancer, and is also used in combination therapy of many other solid tumors, such as bladder, head and neck and

[1] Peyrone M. Ann Chemie Pharm. (1844) 51 (1): 1–29

[2] Rosenberg, Barnett; Van Camp, Loretta; Krigas, Thomas, Nature (1965), 205, 698-699.

small cell lung cancers.[3] The success of cisplatin in cancer therapy stimulated scientists to search for novel metal-based antitumor drugs, with improved effectiveness, broader spectrum of activity and fewer side effects. Thus thousands of other platinum complexes have been synthesized and biologically evaluated for their antitumor properties, from which about fourty entered clinical phase I trials but only two carboplatin[4] and oxaliplatin[5] (Fig. 2) have received worldwide approval so far. Carboplatin exhibits a tumor inhibiting profile identical to that of cisplatin, however with fewer side effects, whereas oxaliplatin is used in a combination therapy against metastatic colorectal cancer.[6] In addition three platinum-based drugs have gained regional approval. These include nedaplatin (Japan), lobaplatin (China) and heptaplatin (South Korea).

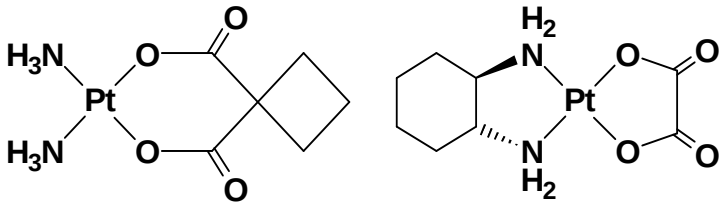

Figure 2. Structures of carboplatin (left) and oxaliplatin (right)

1.2 Mode of action of cisplatin and analogous drugs

In the last 30 years, much research has been focused on the understanding of the mechanism by which cisplatin and its analogues induce apoptosis; however, the exact mode of action is still elusive. Cisplatin is administered by intravenous injection or infusion into the bloodstream,[7,8,9] where it remains intact due to the presence of

[3] Galanski, Markus; Jakupec, Michael A.; Keppler, Bernhard K. Current Medicinal Chemistry (2005), 12(18), 2075-2094.

[4] O'Dwyer, Peter J.; Stevenson, James P.; Johnson, Steven W., Drugs (2000), 59(Suppl. 4), 19-27.

[5] Cvitkovic, Esteban; Bekradda, Mohamed, Seminars in Oncology (1999), 26(6), 647-662.

[6] Graham, Joanne; Muhsin, Mohamed; Kirkpatrick, Peter., Nature Reviews Drug Discovery (2004), 3(1), 11-12.

[7] Kelland, Lloyd. Nature Reviews Cancer (2007), 7(8), 573-584.

relatively high chloride concentration (100 mM), resulting in the suppression of hydrolysis of the drug. It enters the cell by passive diffusion or by active transport mechanisms[10] such as the copper transporter Ctr1.[11,12] Inside the cell, the hydrolysis is promoted due to low chloride concentration (4 mM). Cisplatin undergoes aquation to form mainly monoaqa species *cis*-$[Pt(NH_3)_2Cl(OH_2)]^+$ by exchange of one chlorido ligand with a water molecule.[13] This reactive species then binds preferably to nitrogen atoms of the DNA bases, particularly to the N7 of guanine, forming initially monofunctional DNA adducts and later on bifunctional intrastrand cross-links of the type 1,2-d(GpG) and 1,2-d(ApG).[14] These adducts induce a kink (conformational changes) in the DNA, resulting in the inhibition of DNA replication and transcription which leads towards the programmed cell death in cancerous tissue.

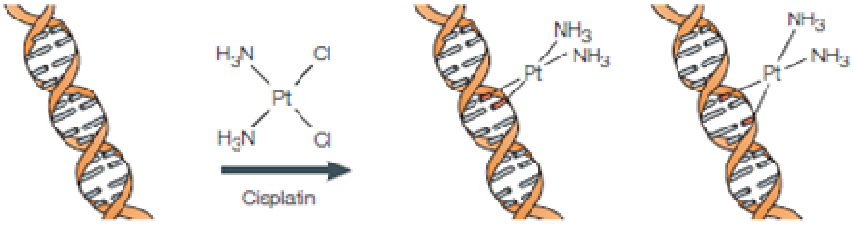

Figure 3. DNA adduct formation with cisplatin.[8]

---

[8] Wang, Dong; Lippard, Stephen J. Nature Reviews Drug Discovery (2005), 4(4), 307-320.

[9] Jakupec, M. A.; Galanski, M.; Keppler, B. K., Reviews of Physiology, Biochemistry and Pharmacology (2003), 146 1-53.

[10] Gately, D. P.; Howell, S. B., British Journal of Cancer (1993), 67(6), 1171-6.

[11] shida, Seiko; Lee, Jaekwon; Thiele, Dennis J.; Herskowitz, Ira, Proceedings of the National Academy of Sciences of the United States of America (2002), 99(22), 14298-14302.

[12] Lin, Xinjian; Okuda, Tsuyoshi; Holzer, Alison; Howell, Stephen B., Molecular Pharmacology (2002), 62(5), 1154-1159.

[13] Appleton, Trevor G.; Hall, John R.; Ralph, Stephen F.; Thompson, Craig S. M., Inorganic Chemistry (1989), 28(10), 1989-93.

[14] Fichtinger-Schepman, Anne Marie J.; Van der Veer, Johannis L.; Den Hartog, Jeroen H. J.; Lohman, Paul H. M.; Reedijk, Jan., Biochemistry (1985), 24(3), 707-13.

1.3 Non-platinum metal complexes as anticancer agents

Platinum compounds are widely used in cancer therapy but they are not devoid of problems like toxic side effects, limited spectrum of activity and intrinsic or acquired resistance. There is an increasing demand for novel anti-cancer drugs which show reduced side effects, higher selectivity towards tumor cells, and a broader spectrum of activity. This stimulated investigations in the design of drugs based on metals other than platinum, such as gold, galliun, titanium, rhodium, iron, ruthenium and osmium. Non-platinum metals may have different chemical behavior (oxidation state, redox potential, coordination geometry, additional coordination sites, binding preferences to biomolecules according to the HSAB principle etc.), rate of hydrolysis or kinetics of ligand exchange reactions and the ability to replace essential metals.[15] Therefore, it is likely that non-platinum metal-based compounds may have different mechanisms of action, biodistribution and biological activity. The antitumor properties of a number of different metal ions and their complexes have been evaluated, but only a few non-platinum metal-based drugs are currently in clinical studies, the most promising ones contain ruthenium and gallium ions.[16]

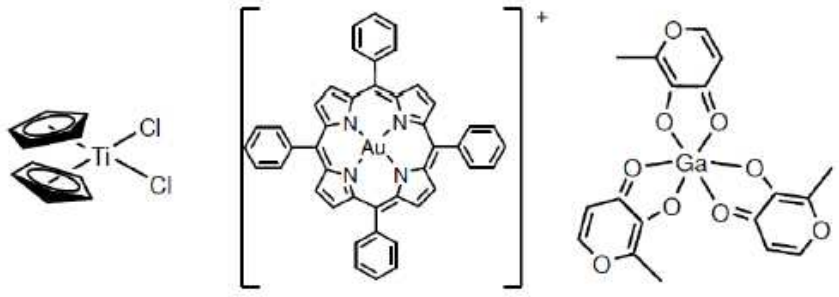

Figure 4. The chemical structures of titanocene dichloride, gold tetraphenylporphyrin and gallium maltolate.

[15] Clarke, Michael J.; Zhu, Fuchun; Frasca, Dominic R., Chemical Reviews, (1999), 99, 2511-2533.

[16] Jakupec, Michael A.; Galanski, Markus; Arion, Vladimir B.; Hartinger, Christian G.; Keppler, Bernhard K., Dalton Transactions (2008), (2), 183-194.

1.4. Ruthenium and Osmium Anticancer Complexes

1.4.1 General features

Both ruthenium and osmium, along with iron, are members of group 8 and are placed in the second and third row of the periodic table, respectively. They are classified as the 'Platinum group' along with rhodium, palladium, iridium and platinum. All these metals often occur together in the same mineral deposits and have closely related physical and chemical properties. Although osmium was discovered before ruthenium, however its chemistry and also its anticancer activity are much less explored than that of its homologue in the second row, most likely due to the higher cost of the metal and the greater difficulty with compound synthesis.[17]

The application of group 8 metal complexes in anticancer drug design has long tradition with iron in the ferrocenyl derivative of tamoxifen (ferrocifen) as the leading example[18], and ruthenium in two drug candidates NAMI-A and KP1019 in clinical trials.

1.4.2 Ruthenium(III) and Osmium(III) complexes

Among the non-platinum complexes tested so far, ruthenium-based compounds have shown great promise for the development of anticancer agents. The ruthenium(III) drug candidates NAMI-A and KP1019 are already in clinical trials.[19,20,21,22] In addi-

---

[17] Lay, Peter A.; Harman, W. Dean, Advances in Inorganic Chemistry (1991), 37 219-379.

[18] Jaouen, Gerard; Top, Siden; Vessieres, Anne, Bioorganometallics (2006), 65-95.

[19] Rademaker-Lakhai, Jeany M.; Van Den Bongard, Desiree; Pluim, Dick; Beijnen, Jos H.; Schellens, Jan H. M, Clinical Cancer Research (2004), 10(11), 3717-3727.

[20] Hartinger, Christian G.; Zorbas-Seifried, Stefanie; Jakupec, Michael A.; Kynast, Bernd; Zorbas, Haralabos; Keppler, Bernhard K., Journal of Inorganic Biochemistry (2006), 100(5-6), 891-904.

[21] Hartinger, Christian G.; Dyson, Paul J., Chemical Society Reviews (2009), 38(2), 391-401.

[22] Lentz, Frederike; Drescher, Anne; Lindauer, Andreas; Henke, Magdalena; Hilger, Ralf A.; Hartinger, Christian G.; Scheulen, Max E.; Dittrich, Christian; Keppler, Bernhard K.; Jaehde, Ulrich, Anti-Cancer Drugs (2009), 20(2), 97-103.

tion to the well developed synthetic coordination chemistry and predictable geometries, ruthenium compounds have a number of unique properties which make them ideal candidates for the design of therapeutics. The drugable features associated with ruthenium are low ligand exchange rates (similar to platinum complexes), low systemic toxicity, a range of oxidation states accessible under physiological conditions, some physicochemical properties similar to iron and more importantly its affinity to serum transport proteins such as albumin and transferrin.[15,16,23] For example, transferrin receptors are overexpressed in tumor cells due to their high demand for iron, therefore ruthenium species can be better delivered owing to their high affinity to bind with serum transferin and transferin-bound metal ions can be easily released in the relatively low pH of tumor cells. Moreover, ruthenium(III) complexes are usually considered as prodrugs that can be activated by reduction to ruthenium(II) species in vivo. The reduced form of ruthenium can bind more rapidly to biomolecules.[15,24] As the tumor cells have relatively low electrochemical potential due to the low oxygen content and low pH, the reduction of Ru(III) to Ru(II) is favored in tumor tissue relative to healthy ones. Biomolecules such as glutathione, ascorbate and redox proteins in the cell also play a part in reduction of Ru(III).

In recent years, the anticancer activity of Ru drug candidates has often been compared to that of their Os analogues; however, no clear-cut structure-activity relationship could be derived. The growing family of ruthenium compounds with antitumor activity has sparked interest in the investigation of the heavier homologue osmium. Sadler et al. have shown that the design of osmium compounds with tumor inhibiting properties can be realized by effectively tuning the reactivity, particularly the hydrolysis and nucleobase binding, by systematic variation of ancillary ligands. Nevertheless, there are only few studies on the antitumor activity of osmium complexes.[25,26,27,28] Osmium offers several features distinct from ruthenium including

---

[23] Allardyce, Claire S.; Dyson, Paul J., Platinum Metals Review (2001), 45(2), 62-69.

[24] Clarke, Michael J., Coordination Chemistry Reviews (2003), 236(1-2), 209-233.

[25] Peacock, Anna F. A.; Habtemariam, Abraha; Fernandez, Rafael; Walland, Victoria; Fabbiani, Francesca P. A.; Parsons, Simon; Aird, Rhona E.; Jodrell, Duncan I.; Sadler, Peter J., Journal of the American Chemical Society (2006), 128(5), 1739-1748.

synthetic approaches to coordination and organometallic compounds, the preference for higher oxidation states, slow ligand exchange kinetics, the stronger π back-donation from lower oxidation states and the much stronger spin-orbit coupling. These properties can be exploited to design osmium compounds with sufficient stability and inertness under physiological conditions.[29,30]

1.4.2.1 NAMI-A

The first ruthenium complex entered clinical trials in 1999 is NAMI-A, HIm[*trans*-$RuCl_4$(DMSO)(Im)] (Im = imidazole). This complex has demonstrated potent activity against tumor metastasizing processes, but its activity against the primary tumor is low. Reduction of NAMI-A to the corresponding dianionic ruthenium(II) species can be rapidly accomplished by biological reductants such as ascorbic acid, glutathione or cysteine. Reduction is then followed by stepwise hydrolysis of chlorido ligands without dissociation of the dimethylsulfoxide and imidazole ligands. Chloride hydrolysis under physiological conditions is tremendously accelerated upon prior reduction but since NAMI-A is unstable under physiological conditions and hydrolysis products have higher redox potentials than the parent compound, hydrolysis prior to reduction is also possible. Anyhow, reduction seems to be slightly advantageous for inhibition of metastasis growth in vivo. Eventually, hydrolysis

---

[26] Peacock, Anna F. A.; Parsons, Simon; Sadler, Peter J., Journal of the American Chemical Society (2007), 129(11), 3348-3357.

[27] Dorcier, Antoine; Ang, Wee Han; Bolano, Sandra; Gonsalvi, Luca; Juillerat-Jeannerat, Lucienne; Laurenczy, Gabor; Peruzzini, Maurizio; Phillips, Andrew D.; Zanobini, Fabrizio; Dyson, Paul J., Organometallics (2006), 25(17), 4090-4096.

[28] Dorcier, Antoine; Dyson, Paul J.; Gossens, Christian; Rothlisberger, Ursula; Scopelliti, Rosario; Tavernelli, Ivano, Organometallics (2005), 24(9), 2114-2123.

[29] Stepanenko, Iryna N.; Cebrian-Losantos, Berta; Arion, Vladimir B.; Krokhin, Artem A.; Nazarov, Alexey A.; Keppler, Bernhard K., European Journal of Inorganic Chemistry (2007), (3), 400-411.

[30] Peacock, Anna F. A.; Parsons, Simon; Sadler, Peter J., Journal of the American Chemical Society (2007), 129(11), 3348-3357.

results in formation of uncharacterized oxo-bridged polymeric species.[31] The finding that partially hydrolyzed species and in particular poly-oxo products are taken up to a higher extent than freshly dissolved NAMI-A by metastatic tumor cells *in vitro* with maintained effects on the cell cycle have prompted investigators to attribute the activity of NAMI-A to hydrolysis products.

In serum, NAMI-A binds to proteins such as albumin and transferrin to a high extent. Reactivity with albumin is increased upon reduction of the complex. However, *in vitro* and *in vivo* experiments employing both albumin- and transferrin-bound NAMI-A in comparison for pure NAMI-A argue against a tumor-targeting effect of binding to these proteins rather than for deactivation.[32,33]

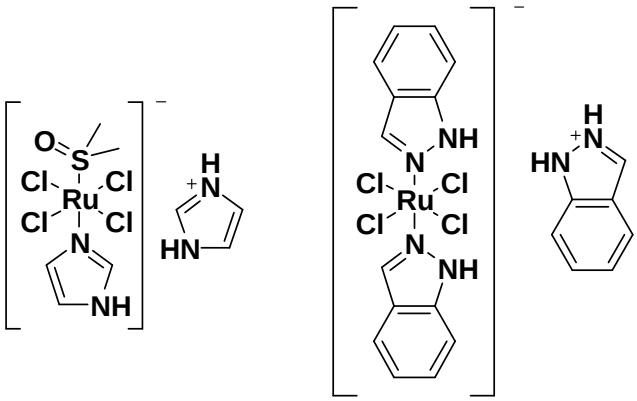

Figure 5. Ruthenium antitumor complexes: NAMI-A (left), KP1019 (right).

1.4.2.2 KP1019

Another ruthenium(III) drug candidate currently in clinical trials is KP1019, HInd[*trans*-$RuCl_4(Ind)_2$] (Ind = indazole). In order to increase the solubility of KP1019, its corresponding sodium salt Na [*trans*-$[RuCl_4(Ind)_2]$ has also been prepared and biologically evaluated for its anticancer activity. Both *in vitro* and *in vivo*

[31] Alessio, Enzo; Mestroni, Giovanni; Bergamo, Alberta; Sava, Gianni, Current Topics in Medicinal Chemistry, 2004, 4, 1525-1535.

[32] Bergamo, A.; Sava, G., Dalton Transactions (2007), (13), 1267-1272.

[33] Dyson, Paul J.; Sava, Gianni, Dalton Transactions (2006), (16), 1929-1933.

*e*xperiments with KP1019 have shown high anti-proliferative activity in human colon carcinoma cell lines and tumor models. Protein-binding studies have been performed and it was shown that KP1019 interacts with serum proteins especially with albumin and transferrin. For the latter binding preference toward the histidine residues in the iron-binding site was determined with lactoferrin as model protein.[34] A comparison of DNA binding studies of KP1019 and cisplatin showed that KP1019 is capable of binding to DNA irreversibly by affecting its conformation in a different mode than that of cisplatin.[35]

1.4.3 Metal-Arene Compounds as Anticancer Agents

In recent years, Ru(arene) compounds have become a focus of interest due to their applications in medicine. Different approaches have been explored in this regard including Ru(arene) complexes with *P*- or *N*- donor ligands or *N*,*N*-, *N*,*O*- or *O*,*O*-chelating ligands, dinuclear complexes, oxo caped trinuclear clusters, photoactive tetranuclear porphyrin derivatives, hexanuclear cages or attaching bioactive molecules such as paullone derivatives to the arene ruthenium unit.[36,37] The first organometallic ruthenium compound tested for anticancer activity was [Ru(η^6-C_6H_6)Cl_2(metronidazole)] (metronidazole = 1-β-hydroxyethyl-2-methyl-5-nitroimidazole). The metronidazole ligand itself is used for the treatment of infections and marketed under the tradename Flagyl®. When bound to ruthenium, it exhibited more selective cytotoxicity than metronidazole itself under hypoxic reducing conditions.[38] The two best investigated examples of this class are RAPTA

[34] Kratz, F.; Keppler, B. K.; Messori, L.; Smith, C.; Baker, E. N, Metal-Based Drugs (1994), 1(2-3), 169-73.

[35] Malina, Jaroslav; Novakova, Olga; Keppler, Bernhard K.; Alessio, Enzo; Brabec, Viktor. Journal of Biological Inorganic Chemistry (2001), 6(4), 435-445.

[36] Peacock, Anna F. A.; Sadler, Peter J., Chemistry--An Asian Journal (2008), 3(11), 1890-1899.

[37] Suess-Fink, Georg, Dalton Transactions (2010), 39(7), 1673-1688.

[38] Dale, L. D.; Tocher, J. H.; Dyson, T. M.; Edwards, D. I.; Tocher, D. A., Anti-Cancer Drug Design (1992), 7(1), 3-14.

$[Ru^{II}(arene)(pta)Cl_2]$ (pta = 1,3,5-triaza-7-phoshatricyclo-[3.3.1.1]decane) and $[Ru^{II}(arene)(en)Cl]^+$ (en=1,2-diaminoethane) compounds.

1.4.3.1 Monofunctional M(II)-arene complexes

Sadler and coworkers found that Ru(II)-arene complexes of general formula [(η^6-arene)Ru(X)(Y)(Z)] where X is a leaving group such as Cl^-, and YZ is a chelating diamine such as ethylenediamine (en), are cytotoxic to cancer cells, including cis-platin-resistant cell lines.[39,40,41] It has been shown that cytotoxicity increases with the size of the arene ligand. The complexes with more hydrophobic arenes like tetrahydroanthracene are much more cytotoxic than those having the less hydrophobic benzene ligand. The cytotoxicity increases in the following order benzene < cymene < biphenyl < dihydroanthracene < tetrahydroanthracene. It has been found that the presence of a hydrophobic arene, a single ligand exchange site and the other two coordination sites being occupied by a stable bidentate chelating ligand are associated with high cytotoxicity for Ru(arene) compounds.[42] These complexes are activated by the formation of reactive aqua complexes $[(\eta^6\text{-arene})Ru(en)(H_2O)]^{2+}$ by exchange of the chlorido ligand with water. This active species has shown reactivity with DNA models. Under physiologically-relevant conditions in the bloodstream ($[Cl^-]$ *ca*. 100 mM), Ru(arene) complexes should remain largely in the form of the less-reactive chlorido complexes, whereas in the cell nucleus at chloride concentrations of *ca*. 4 mM significant amounts of the more reactive aqua species are formed. Deprotonation of the coordinated aqua ligand of $[(\eta^6\text{-arene})Ru(en)(H_2O)]^{2+}$ gives hydroxido complexes $[(\eta^6\text{-arene})Ru(en)(OH)]^+$.[43] A number of neutral Ru(arene)

---

[39] Morris, Robert E.; Aird, Rhona E.; Murdoch, Piedad del Socorro; Chen, Haimei; Cummings, Jeff; Hughes, Nathan D.; Parsons, Simon; Parkin, Andrew; Boyd, Gary; Jodrell, Duncan I.; Sadler, Peter J.. Journal of Medicinal Chemistry (2001), 44(22), 3616-3621.

[40] Aird, R. E.; Cummings, J.; Ritchie, A. A.; Muir, M.; Morris, R. E.; Chen, H.; Sadler, P. J.; Jodrell, D. I. British Journal of Cancer (2002), 86(10), 1652-1657.

[41] Bruijnincx, Pieter C. A.; Sadler, Peter J., Advances in Inorganic Chemistry (2009), 61, 1-62.

[42] Ronconi, Luca; Sadler, Peter J., Coordination Chemistry Reviews (2007), 251, 1633-1648.

[43] Chen, Haimei; Parkinson, John A.; Morris, Robert E.; Sadler, Peter J., Journal of the American Chemical Society (2003), 125(1), 173-186.

complexes bearing *N,O*- or *O,O*-chelating ligands has also been investigated. These compounds show low activity as compared to complexes with *N,N*-chelating ligands and were also less stable and form hydroxido-bridged dimers in aqueous solution.[44,45,46]

Recently, Os(arene) complexes have demonstrated potential for the design of anticancer drugs. Influence on the ligand systems such *N,N*-, *N,O*- and *O,O*-chelating moieties have been investigated for their tumor inhibiting properties. Interestingly, $[(\eta^6\text{-biphenyl})Os(en)Cl]^+$ exhibits promising anticancer activity against the human ovarian cancer A2780 cell line (IC_{50} 9 μM),[47] although it hydrolyzes about 40 times slower than the Ru^{II} analogue. A switch from a neutral *N,N*-chelating (ethylenediamine, en) to an anionic *O,O*-chelating ligand (acetylacetonate, acac) has a remarkable effect on both the extent and rate of hydrolysis. The hydrolysis rate of $[(\eta^6\text{-arene})Os(acac)Cl]$ is too fast to be monitored by NMR spectroscopy at 298 K and aqua species are immediately converted into the hydroxido-bridged dimer, $[(\eta^6\text{-arene})Os(\mu_2\text{-}OH)_3Os(\eta^6\text{-arene})]^+$, with the release of the acac ligand. This hydroxido-bridged dimeric species is present predominantly at micromolar concentrations in solutions used in biological cell culture tests.[48]

Os(arene) complexes with anionic *O,O*-chelating ligands such as maltolato also hydrolyze and bind to purine nucleobases rapidly. The hydrolytic stability of these

---

[44] Habtemariam, Abraha; Melchart, Michael; Fernandez, Rafael; Parsons, Simon; Oswald, Iain D. H.; Parkin, Andrew; Fabbiani, Francesca P. A.; Davidson, James E.; Dawson, Alice; Aird, Rhona E.; Jodrell, Duncan I.; Sadler, Peter J., Journal of Medicinal Chemistry (2006), 49(23), 6858-6868.

[45] Fernandez, Rafael; Melchart, Michael; Habtemariam, Abraha; Parsons, Simon; Sadler, Peter J., Chemistry--A European Journal (2004), 10(20), 5173-5179.

[46] Melchart, Michael; Habtemariam, Abraha; Parsons, Simon; Moggach, Stephen A.; Sadler, Peter J., Inorganica Chimica Acta (2006), 359(9), 3020-3028.

[47] Kostrhunova, Hana; Florian, Jakub; Novakova, Olga; Peacock, Anna F. A.; Sadler, Peter J.; Brabec, Viktor., Journal of Medicinal Chemistry (2008), 51(12), 3635-3643.

[48] Peacock, Anna F. A.; Habtemariam, Abraha; Fernandez, Rafael; Walland, Victoria; Fabbiani, Francesca P. A.; Parsons, Simon; Aird, Rhona E.; Jodrell, Duncan I.; Sadler, Peter J., Journal of the American Chemical Society (2006), 128(5), 1739-1748.

Os(arene) complexes is increased by the presence of a five-membered maltolato chelate ring, compared to the acac analogues.

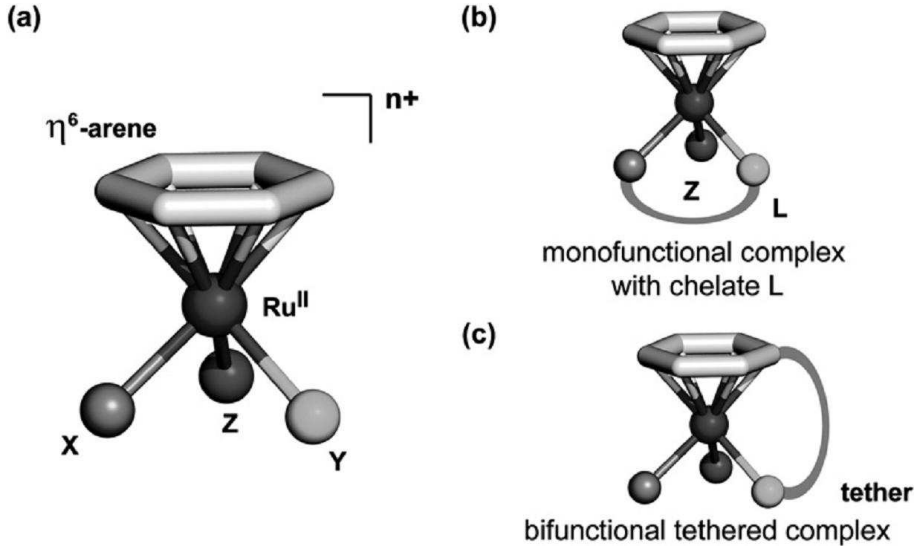

Figure 6. General structures of half-sandwich, piano-stool configurated Ru(arene) complexes.[41]

However, they are still deactivated to a significant extent due to the formation of hydroxido-bridged dimers at biologically relevant (micromolar) concentrations. Owing to the unstability of the aqua complex which leads to the formation of hydroxido-bridged adducts, compounds containing *O,O*-chelators such as maltolato or acetylacetonato are biologically inactive toward human ovarian (A2780) and human lung (A549) cancer cell lines.[49]

However, Os(arene) complexes containing anionic *N,O*-chelators such as picolinate (pico) exhibit rates of hydrolysis intermediate between those of the neutral *N,N*- and anionic *O,O*-chelated compounds. These are stable in aqueous solution at micromolar concentrations and some of them display promising activity toward a human ovarian cancer cell line with IC_{50} values (4.5 μM) similar to that of carboplatin.[50,51] It

[49] Peacock, Anna F. A.; Melchart, Michael; Deeth, Robert J.; Habtemariam, Abraha; Parsons, Simon; Sadler, Peter J., Chemistry--A European Journal (2007), 13(9), 2601-2613.

[50] Van Rijt, Sabine H.; Hebden, Andrew J.; Amaresekera, Thakshila; Deeth, Robert J.; Clarkson, Guy J.; Parsons, Simon; McGowan, Patrick C.; Sadler, Peter J., Journal of Medicinal Chemistry (2009), 52(23), 7753-7764.

is obvious from these studies that both the kinetics and thermodynamics have significant impact on the biological activity of these complexes. These factors can be controlled by choice and design of ligands for the optimization of anticancer activity of Os(arene) compounds.[52,]

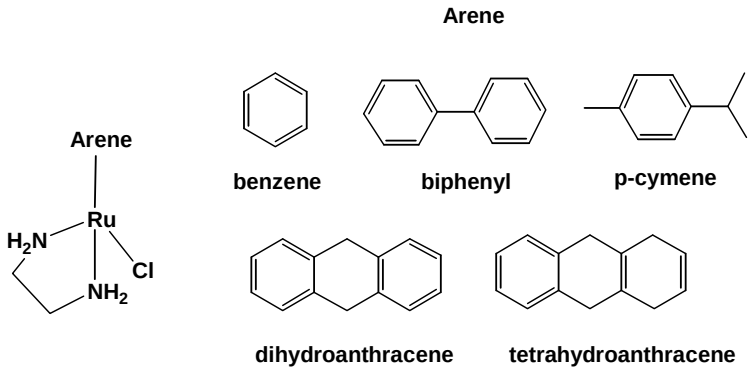

Figure 7. Ru(II) arene complexes with various arene ligands

1.4.3.2 Bifunctional M(II)-arene complexes

RAPTA is a class of anticancer active organometallic M(arene) complexes with one (or two) monodentate 1,3,5-triaza-7-phosphatricyclo[3.3.1.1]decane (pta) ligand, chlorido ligand(s) and a η^6-arene moiety (Fig. 8).[53,54,55,56] RAPTA complexes undergo hydrolysis of the chloride ligands in aqueous solution. The extent of the hydrolysis depends on the concentration of the complex in solution, the amount of

---

[51] Peacock, Anna F. A.; Parsons, Simon; Sadler, Peter J., Journal of the American Chemical Society (2007), 129(11), 3348-3357.

[52] Van Rijt, Sabine H.; Peacock, Anna F. A.; Johnstone, Russell D. L.; Parsons, Simon; Sadler, Peter J., Inorganic Chemistry (2009), 48(4), 1753-1762.

[53] Allardyce, Claire S.; Dyson, Paul J.; Ellis, David J.; Heath, Sarah L., Chemical Communications (2001), (15), 1396-1397.

[54] Allardyce, Claire S.; Dyson, Paul J.; Ellis, David J.; Salter, Paul A.; Scopelliti, Rosario, Journal of Organometallic Chemistry (2003), 668(1-2), 35-42.

[55] Ang, Wee Han; Dyson, Paul J., European Journal of Inorganic Chemistry (2006), (20), 4003-4018.

[56] Scolaro, Claudine; Bergamo, Alberta; Brescacin, Laura; Delfino, Riccarda; Cocchietto, Moreno; Laurenczy, Gabor; Geldbach, Tilmann J.; Sava, Gianni; Dyson, Paul J., Journal of Medicinal Chemistry (2005), 48(12), 4161-4171.

chloride present and the pH. Hydrolysis was found to be suppressed in the blood plasma with its high chloride concentration (*ca*. 100 mM), but occurs once the compound penetrates into the cell cytoplasm. This represents a possible activation pathway for the compound.[57]

The reaction with DNA under *in vitro* conditions is pH dependent: at pH < 7, which is characteristic of poorly oxygen-supplied cancer cells, DNA is damaged, whereas normal cells with pH > 7 are not affected. Such behavior was attributed to the basicity of the pta ligand and the protonation of pta-*N*.[58] The reaction of RAPTA-C with model oligonucleotides and proteins results in adducts under loss of chlorides and in some cases of the arene ring.[58] The arene ligand appears to be more labile than the pta ligand, an observation supported by calculations. However, *in vitro* studies have shown that proteins and RNAs are more probable targets than DNA.[57] Similar to NAMI-A, RAPTA-C exhibited very low *in vitro* activity on primary tumors, however, excellent inhibition of lung metastases in CBA mice bearing MCa mammary carcinoma. RAPTA-C was shown to reduce the weight and number of the metastases,[58] at low general toxicity combined with excellent clearance rates. In fact, RAPTA-C resulted in 40% of the animals being completely free of metastasis after treatment and in general only drug combination therapies showed better cure rates.[59]

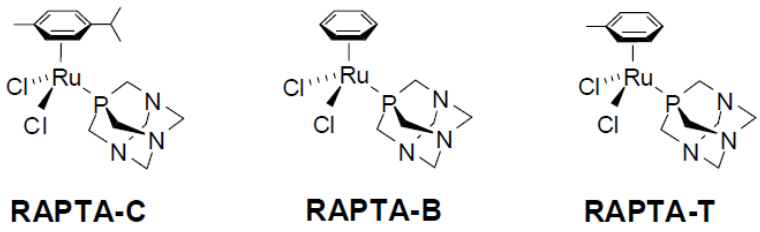

Figure 8. RAPTA complexes with various arene ligands

[57] Gossens, Christian; Dorcier, Antoine; Dyson, Paul J., Rothlisberger, Ursula., Organometallics (2007), 26(16), 3969-3975.

[58] Dorcier, Antoine; Dyson, Paul J.; Gossens, Christian; Rothlisberger, Ursula; Scopelliti, Rosario; Tavernelli, Ivano., Organometallics (2005), 24(9), 2114-2123.

[59] Khalaila, Isam; Bergamo, Alberta; Bussy, Francois; Sava, Gianni; Dyson, Paul J., International Journal of Oncology (2006), 29(1), 261-268.

In order to improve their efficacy, a number of structural modifications have been made to the basic RAPTA framework such as introduction of H-bonding functionalities,[60] change of the arene ligand[61] or the leaving group[62] and tethering to bioactive segments such as ethacrynic acid[63] or human serum albumin,[64] the latter resulted in a twenty-fold increase in cytotoxicity with respect to prototype RAPTA-C.

1.5 Linking biological molecules to an organometallic motif

To achieve tumor specificity is an important goal in drug design. Specificity means that drugs should ideally target the tissue or organ for which it is designed. One very promising approach is to conjugate drugs with biomolecules or antibodies. These biomolecules, often called vectors can be essential nutrients for cells (sugars and amino acid) or cofactors (e.g., vitamin B12).[65] This strategy has already been successfully used to incorporate an organometallic motif into biologically active molecules such as tamoxifen,[66,67,68] or staurosporine.[69,70,71] The resulting conjugates have

---

[60] Scolaro, Claudine; Geldbach, Tilmann J.; Rochat, Sebastien; Dorcier, Antoine; Gossens, Christian; Bergamo, Alberta; Cocchietto, Moreno; Tavernelli, Ivano; Sava, Gianni; Rothlisberger, Ursula; Dyson, Paul J., Organometallics (2006), 25(3), 756-765.

[61] Serli, Barbara; Zangrando, Ennio; Gianferrara, Teresa; Scolaro, Claudine; Dyson, Paul J.; Bergamo, Alberta; Alessio, Enzo., European Journal of Inorganic Chemistry (2005), (17), 3423-3434.

[62] Ang, Wee Han; Daldini, Elisa; Scolaro, Claudine; Scopelliti, Rosario; Juillerat-Jeannerat, Lucienne; Dyson, Paul J., Inorganic Chemistry (2006), 45(22), 9006-9013.

[63] Ang, Wee Han; Parker, Lorien J.; De Luca, Anastasia; Juillerat-Jeanneret, Lucienne; Morton, Craig J.; Lo Bello, Mario; Parker, Michael W.; Dyson, Paul J., Angewandte Chemie, International Edition (2009), 48(21), 3854-3857.

[64] Ang, Wee Han; Daldini, Elisa; Juillerat-Jeanneret, Lucienne; Dyson, Paul J., Inorganic Chemistry (2007), 46(22), 9048-9050.

[65] Metzler-Nolte, Nils., Chimia (2007), 61(11), 736-741.

[66] Hillard, Elizabeth; Vessieres, Anne; Thouin, Laurent; Jaouen, Gerard; Amatore, Christian., Angewandte Chemie, International Edition (2006), 45(2), 285-290.

[67] Plazuk Damian; Vessieres Anne; Hillard Elizabeth A; Buriez Olivier; Labbe Eric; Pigeon Pascal; Plamont Marie-Aude; Amatore Christian; Zakrzewski Janusz; Jaouen Gerard, Journal of medicinal chemistry (2009), 52(15), 4964-7.

enhanced activity than parent compounds. The metal ion in these bioorganometallic compounds has either a structural or a functional role, important for biological activity (Fig. 9).

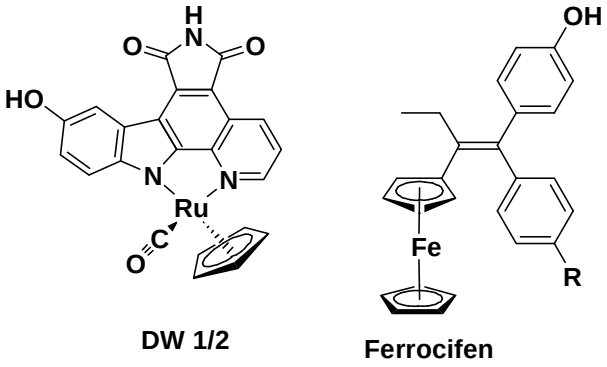

Figure 9. Biocojugates of staurosporine (DW1/2) and tamoxifen (ferrocifen) with organometallic moiety.

---

[68] Hamels Didier; Dansette Patrick M; Hillard Elizabeth A; Top Siden; Vessieres Anne; Herson Patrick; Jaouen Gerard; Mansuy Daniel, Angewandte Chemie, 2009, 48(48), 9124-9126.

[69] Meggers, Eric., Chemical Communications (2009), (9), 1001-1010.

[70] Meggers, Eric., Current Opinion in Chemical Biology (2007), 11(3), 287-292.

[71] Meggers, Eric; Atilla-Gokcumen, G. Ekin; Bregman, Howard; Maksimoska, Jasna; Mulcahy, Seann P.; Pagano, Nicholas; Williams, Douglas S., Synlett (2007), (8), 1177-1189.

2. Results

2.1. Designing carbohydrate-based anticancer drugs

Carbohydrates are fundamental biomolecules and are the constitutional parts of many lipids (glycolipids), proteins (glycoprotein), nucleic acids and ADP/ATP (energy storage system). Sugars perform a range of (bio)chemical and cellular functions in living organisms such as modification of many proteins and fats on cell surfaces, participation in immunity and cell to cell communication, etc.[72] Moreover, carbohydrates play critical roles in diseases from viral infections to cancer and, therefore, they have been increasingly targeted for design and development of new medicines. In recent years, modified carbohydrates and their specific glycoconjugates have not only been targeted for effective vaccines for viral, bacterial and parasitic infections as well as cancer but have also been developed as adjuvants and drug delivery systems. Furthermore, modified carbohydrate structures can interfere with carbohydrate-protein interactions, and subsequently inhibit cell-cell recognition and adhesion processes, both of which play a critical role in tumor growth and progression.[73]

2.1.1 Tumor-induced alterations in carbohydrate metabolism

Tumor cells exhibit a number of distinct biophysical properties which distinguish them from normal cells. Alterations of carbohydrate metabolism, structures and their organization are a hallmark of the tumor cells. These features can be potentially exploited to design drugs which can selectively target the tumor cell.

[72] Steinborn, Dirk; Junicke, Henrik., Chemical Reviews (2000), 100(12), 4283-4317.

[73] Nangia-Makker, Pratima; Conklin, Jeffrey; Hogan, Victor; Raz, Avraham, Trends in Molecular Medicine (2002), 8(4), 187-192.

2.1.2. Switch in energy supply and increased glucose uptake

Healthy cells generate their energy in the form of ATP by glycolysis in the cytoplasm and oxidative phosphorylation in mitochondria. In glycolysis, one molecule of glucose is converted into two molecules of pyruvate with the production of two ATP in a sequence of reactions. Pyruvate then is converted into acetyl co-enzyme A that enters into citric acid cycle to produce NADH and $FADH_2$ which upon oxidation in the respiratory chain results in 36 ATP per 1 molecule glucose (oxidative phosphorylation, Fig. 10). Therefore a single glucose molecule is converted into a total of about 38 mol of ATP (2 during glycolysis and 36 from oxidative phosphorylation). As tumor tissues are often under hypoxia due to rapid tumor growth and insufficient vascularization, oxidative phosphorylation does not remain functional to the same extent and cancer cells have to rely on glycolysis for their energy. Consequently, in order to meet the increasing energy demand, cancer cells must upregulate glycolytic activity.[74] This results in upregulation of certain metabolic enzymes and glucose transporters and eventually, to increased glucose uptake.[75] This physiological difference has been exploited in the development of an oncological imaging tool, namely ^{18}fluorodeoxyglucose positron emission tomography (FdG PET). FdG is injected intravenously and is ingested by the cells but cannot be metabolized (Fig. 11). This leads to an increased intracellular accumulation of the radio labeled glucose analogue in cancer cells and hence, a higher local radioactivity.[76,77]

---

[74] Kim, Jung-whan; Gardner, Lawrence B.; Dang, Chi V., Drug Discovery Today: Disease Mechanisms (2005), 2(2), 233-238.

[75] Gatenby, Robert A.; Gillies, Robert J., Nature Reviews Cancer (2004), 4(11), 891-899.

[76] Talbot, J. N.; Petegnief, Y.; Kerrou, K.; Montravers, F.; Grahek, D.; Younsi, N Nuclear Instruments & Methods in Physics Research, Section A: Accelerators, Spectrometers, Detectors, and Associated Equipment (2003), 504(1-3), 129-138.

[77] Bourguet P; Blanc-Vincent M P; Boneu A; Bosquet L; Chauffert B; Corone C; Courbon F; Devillers A; Foehrenbach H; Lumbroso J D; Mazselin P; Montravers F; Moretti J L; Talbot J N British journal of cancer (2003), 89 Suppl 1 S84-91.

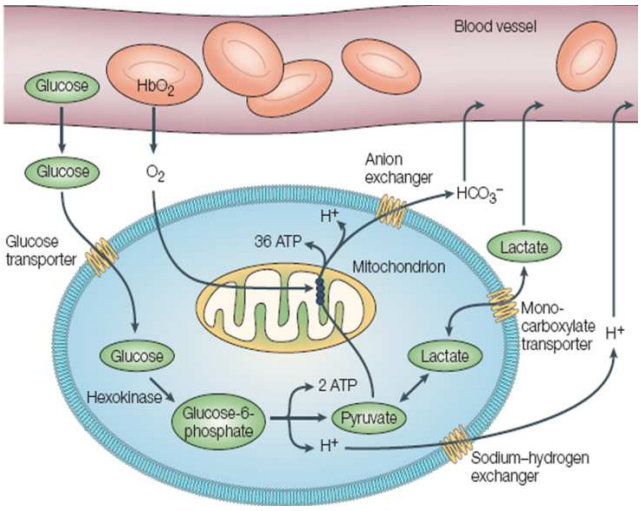

Figure . 10 Glucose metabolism in healthy cell and generation of ATP.[75]

2.1.3 Manipulation of tumor cell metabolism for therapeutic purposes

Alterations in tumor micro-environments, offers many possibilities to design drugs that can selectively target tumor tissue. Many approaches such as designing glycolysis inhibitors, linking drugs to carbohyderates and glycosylation have been investigated to exploit these alterations in tumor micro-environments. The following two strategies are described briefly.

2.1.3.1 Designing glycolysis inhibitors

Due to increased energy demand, cancer cells are much more sensitive to lack of glucose than normal cells. Therefore, the absence of glucose in cancer cells results in cellular stress subsequently followed by cell death.[78] The tumor growth can be suppressed by modified glucose derivatives that can inhibit glycolysis by interfering

[78] Kitzman, Harvey H., Jr.; McMahon, Robert J.; Williams, Martin G.; Frost, Susan C., Journal of Biological Chemistry (1993), 268(2), 1320-5.

with involved enzymes, depriving the cancer cells from its energy supply.[79] One example of a glycolysis inhibitor is 2-deoxyglucose, being in phase I clinical trials (Fig. 12). [80,81] Preliminary *in vivo* and *in vitro* studies showed that 2-deoxyglucose can induce apoptosis in cancer cells.[82]

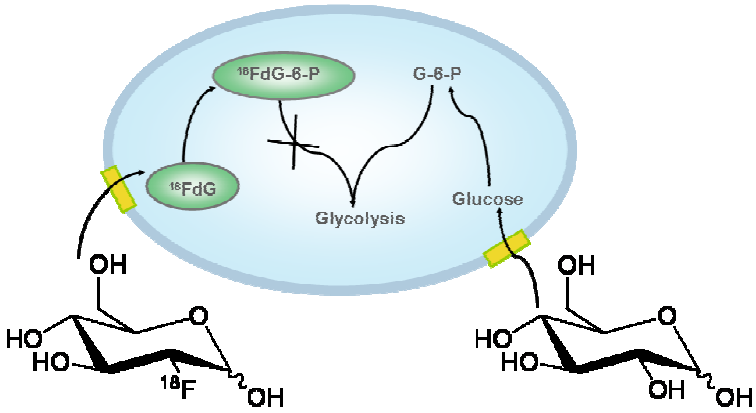

Figure 11. Comparison of metabolism of ^{18}FdG and glucose, ^{18}FdG is ingested by the cell but cannot be metabolized because ^{18}FdG-6-P (= ^{18}fluorodeoxyglucose-6-phosphate) is not a substrate for glycolysis.

2.1.3.2 Linking carbohydrates to drugs

Another approach is to link carbohydrates with drugs in order to enhance the cellular uptake. Since a tumor cell has high desire for glucose, the drug may be preferentially transported into cancer cells as compared to normal cells. Inside cells, the active drug component is released by cleavage of the linker between glucose and the drug. This strategy had already been used for ifosfamide-mustard, a known cytotoxic alky-

---

[79] Spitz, Douglas R.; Sim, Julia E.; Ridnour, Lisa A.; Galoforo, Sandra S.; Lee, Yong J. Annals of the New York Academy of Sciences (2000), 899, 349-362.

[80] http://www.thresholdpharm.com/sec/pipe_2deoxyglucose

[81] G. Tidmarsh, PCT Int. Appl., WO 2006124573 A2 20061123

[82] Zhu, Zongjian; Jiang, Weiqin; McGinley, John N.; Thompson, Henry J., Cancer Research (2005), 65(15), 7023-7030.

lating compound. The glucose conjugate of ifosfamide is called glufosfamide (Fig. 12) that entered clinical trials phase III as drug candidate for second line treatment of pancreatic cancer but failed in February 2007 due to insignificant increase of the overall survival time. The same drug is currently undergoing phase I and II clinical trials as a first-line treatment of pancreatic cancer.[80,81]

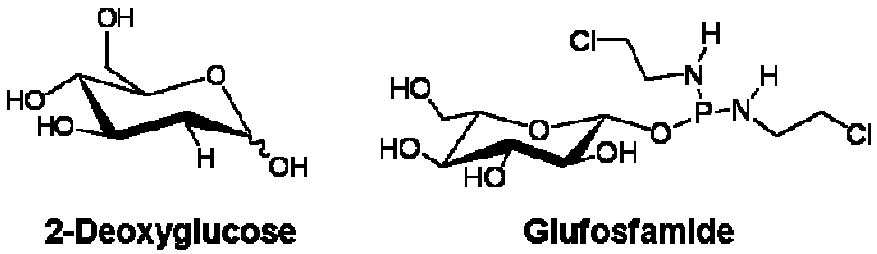

Figure 12. Structures of 2-deoxyglucose and glufosfamide.

2.2 Osmium(II)- *versus* Ruthenium(II)-Arene Carbohydrate-based Anticancer Compounds: Similarities and Differences

Muhammad Hanif, Alexey A. Nazarov, Christian G. Hartinger, Wolfgang Kandioller, Michael A. Jakupec, Vladimir B. Arion, Paul J. Dyson, Bernhard K. Keppler

Dalton Transactions, **2010,** 39, 7345–7352.

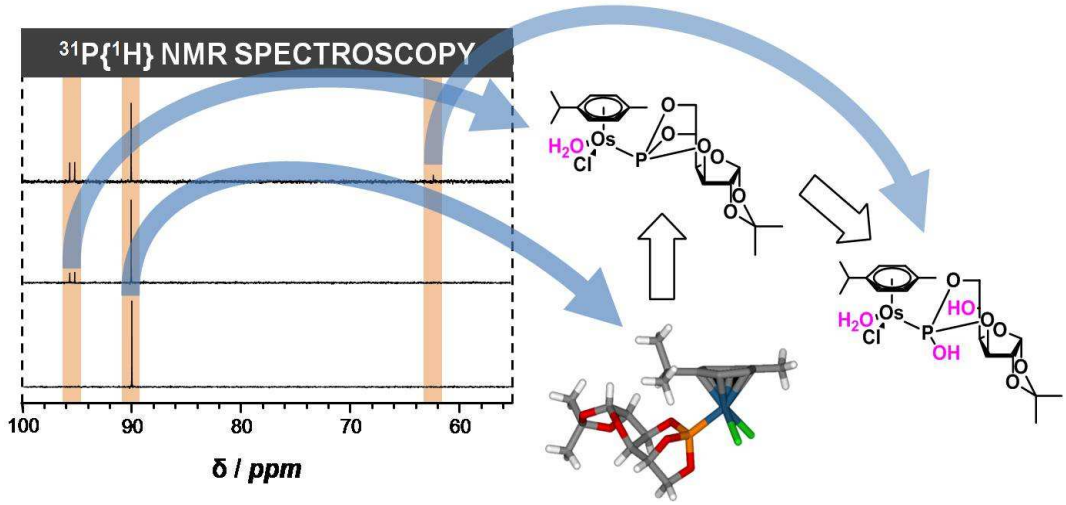

Osmium(II)–*versus* ruthenium(II)–arene carbohydrate-based anticancer compounds: similarities and differences†‡

Muhammad Hanif,[a] Alexey A. Nazarov,*[a,b] Christian G. Hartinger,*[a,c] Wolfgang Kandioller,[a] Michael A. Jakupec,[a,c] Vladimir B. Arion,[a] Paul J. Dyson[b] and Bernhard K. Keppler[a,c]

Received 15th February 2010, Accepted 19th May 2010
First published as an Advance Article on the web 2nd July 2010
DOI: 10.1039/c003085f

The synthesis and *in vitro* anticancer activity of Os^{II}–arene complexes with carbohydrate-derived phosphite co-ligands are reported. The compounds were characterized by standard methods and the molecular structure of dichlorido(η⁶-*p*-cymene)(3,5,6-bicyclophosphite-1,2-*O*-isopropylidene-α-D-glucofuranoside)osmium(II) was determined by X-ray diffraction analysis. Complexes with chlorido leaving groups undergo hydrolysis by consecutive formation of aqua compounds, followed by cleavage of a P–O bond of sugar phosphite ligands, as demonstrated by NMR studies. These observations are similar to those of analogous Ru^{II}–arene complexes; however the rate of hydrolysis is very slow for osmium compounds. The complexes with oxalato leaving groups resist hydrolysis; no hydrolytic species were detected by $^{31}P\{^1H\}$ NMR spectroscopy over several days. Within this series of Os compounds, *in vitro* anticancer activity is highest for the most lipophilic chlorido complex dichlorido(η⁶-*p*-cymene)(3,5,6-bicyclophosphite-1,2-*O*-cyclohexylidene-α-D-glucofuranoside)osmium(II).

Introduction

The limitations of current metal-based chemotherapeutics have prompted a search for novel antitumor drugs with improved effectiveness and fewer side effects.[1–3] Thousands of novel platinum and non-platinum compounds have been synthesized and evaluated for their antitumor properties.[4] Among the tested transition metal compounds, ruthenium compounds have shown considerable potential as anticancer drugs.[5-7] Ruthenium compounds are usually less toxic than cisplatin and are therefore better tolerated *in vivo*. In animal models, ruthenium compounds are effective in the treatment of cancer types which cannot be treated by platinum-based compounds, most probably due to a different mode of action. Two ruthenium(III)-based drugs, KP1019 and NAMI-A (Fig. 1), have successfully completed phase I clinical trials.[6,8] Both ruthenium(III) compounds differ considerably from cisplatin in their *in vivo* behaviour; NAMI-A strongly inhibits metastasis without effects on the primary tumour, whereas KP1019 effectively reduces colorectal tumours in which cisplatin is inactive.

Recently, half-sandwich organometallic Ru(II)–arene complexes of the general formula [(η⁶-arene)Ru(X)(Y)(Z)] have attracted great attention as putative anticancer drugs, where X is a monodentately bound moiety, often a leaving group (*e.g.* chloride), and Y and Z are bidentate chelating or two monodentate ligands, resulting in neutral or positively charged complexes (the latter often with Cl^-, BF_4^-, PF_6^-, *etc.* as counter ions). Various approaches have been investigated in this regard including coordination of ethylenediamine (en),[9,10] paullone derivatives,[11] 1,3,5-triaza-7-phosphatricyclo[3.3.1.1]decane (pta),[12] pyr(id)ones[13–15] or *per se* bioactive groups, such as staurosporine derivatives,[16] to the metal centre. These water-soluble ruthenium–arene complexes offer a

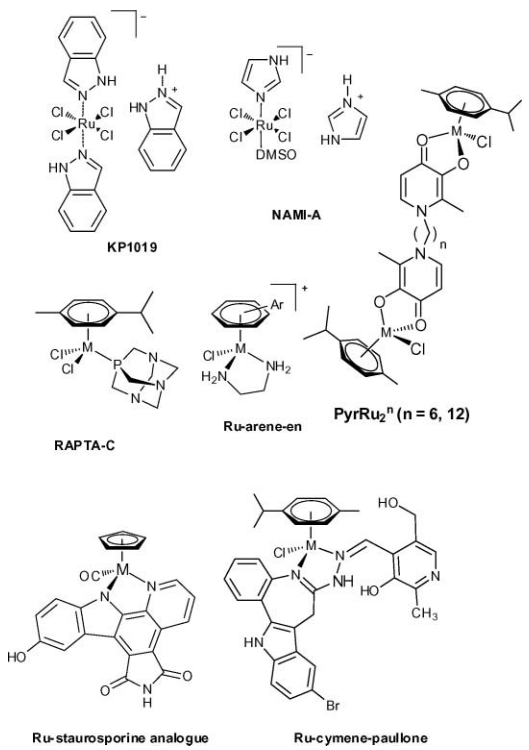

Fig. 1 Ruthenium compounds evaluated in clinical trials (KP1019, NAMI-A), and Ru–arene complexes and their Os analogues with biological activity (M = Ru, Os).

[a]*University of Vienna, Institute of Inorganic Chemistry, Waehringer Str. 42, A-1090, Vienna, Austria. E-mail: christian.hartinger@univie.ac.at, alex.nazarov@univie.ac.at; Fax: +43-1-4277-52680; Tel: +43-1-4277-52609*
[b]*Institut des Sciences et Ingénierie Chimiques, Ecole Polytechnique Fédérale de Lausanne (EPFL), CH-1015, Lausanne, Switzerland*
[c]*University of Vienna, Research Platform "Translational Cancer Therapy Research", Waehringer Str. 42, A-1090, Vienna, Austria*

† CCDC reference number 766305. For crystallographic data in CIF or other electronic format see DOI: 10.1039/c003085f

‡ Dedicated to Prof. Tamás Kiss on the occasion of his 60th birthday.

potential to fine-tune the lipophilicity of the molecule, which is an important parameter for drug development. For example, Ru(II) complexes of the type [(η⁶-arene)Ru(en)X]⁺ (X = halide) exhibit high cytotoxicity *in vitro* comparable or, in some cases, superior to that of cisplatin.[17,18] On the other hand, RAPTA complexes of the type [(η⁶-arene)Ru(pta)Cl] exhibit selective cytotoxicity towards the TS/A tumourigenic cell line as opposed to the HBL-100 non-tumourigenic cell line, and notably *in vivo* some of the compounds reduce significantly the growth of lung metastases in CBA mice bearing MCa mammary carcinoma.[12] Other Ru–arene complexes target kinases or other proteins, some of them being very inert.[11,16,19] Osmium analogues of many of these half-sandwich organometallic complexes have been synthesized and shown to inhibit cancer cell growth *in vitro*, in some cases with potencies comparable to the clinical drugs carboplatin and cisplatin.[11,13,16,20–23] There are no clear-cut structure–activity relationships allowing to predict the effect of exchanging ruthenium for osmium in anticancer compounds: as observed by Sadler *et al.* the Os compounds can be more active than their Ru analogues,[21] whereas in other cases no difference was observed,[11,16] probably due to an exclusively structural function of the metal centre.[16]

In this paper we describe the influence of the metal centre (Ru *vs.* Os) on hydrolysis and cytotoxicity of a series of carbohydrate–metal complexes. With the intention to target Ru–arene compounds selectively to the tumour micro-environment,[24] we have linked such metal moieties to glucose-derived ligands *via* a phosphorus atom, resulting in RAPTA-C analogues with increased *in vitro* activity.[25] Glucose uptake is increased in cancer cells due to upregulation of glycolysis and glucose transporters.[26] This property is being exploited for the visualization of tumours by using the glucose analogue tracer ^{18}fluorodeoxyglucose in positron emission tomography (FdG-PET).[26] As far as we are aware, these are the first examples of osmium compounds with carbohydrate-based ligands, and in addition to their synthesis, their solid state structures, behaviour in aqueous solution and cytotoxicity in cancer cells are discussed.

Experimental

Materials

All reactions were carried out in dry solvents under an inert atmosphere. All chemicals were obtained from commercial suppliers and used as received and were of analytical grade. OsO_4 (99.8%) and $N_2H_4{\cdot}2HCl$ were purchased from Johnson Matthey and Fluka, respectively. Methanol and CH_2Cl_2 were dried using standard procedures. The dimer bis[dichlorido(η⁶-*p*-cymene)osmium(II)] [(η⁶-*p*-cymene)OsCl(μ-Cl)]$_2$ **a**,[27] 3,5,6-bicyclophosphite-1,2-*O*-isopropylidene-α-D-glucofuranoside **1** and 3,5,6-bicyclophosphite-1,2-*O*-cyclohexylidene-α-D-glucofuranoside **2**[28] and disilver oxalate[29] were synthesized using literature procedures. ^{1}H, ^{13}C{^{1}H} and ^{31}P{^{1}H} NMR spectra were recorded at 25 °C on a Bruker FT NMR spectrometer Avance III 500 MHz at 500.10 (^{1}H), 125.75 (^{13}C{^{1}H}) and 202.44 MHz (^{31}P{^{1}H}). 2D NMR spectra were collected in a gradient-enhanced mode. Specific optical rotations were determined on a Perkin-Elmer 341 polarimeter in a 10 cm cell at 20 °C. Melting points were measured on a Büchi B-540 apparatus and are uncorrected. Elemental analysis was determined by the Laboratory for Elemental Analysis, Faculty of Chemistry, University of Vienna, on a Perkin-Elmer 2400 CHN Elemental Analyzer. Electrospray ionization mass spectra were recorded on a Bruker esquire$_{3000}$.

Table 1 Crystal data and details of data collection for **3**†

Compound	**3**
Chemical formula	$C_{19}H_{23.70}Cl_2O_{6.35}Os\,P$
M/g mol^{-1}	645.75
T/K	100(2)
Crystal size/mm	0.30 × 0.30 × 0.20
Crystal colour, habit	Orange, block
Crystal system	Orthorhombic
Space group	$P2_12_12_1$
a/Å	8.7180(4)
b/Å	14.8768(7)
c/Å	17.0012(8)
V/Å^3	2204.99(18)
Z	4
D_c/g cm^{-3}	1.945
μ/cm^{-1}	6.133
$F(000)$	1254
Θ range for data collection/°	2.71 to 30.09
h range	−12/12
k range	−20/20
l range	−23/23
No. refls. used in refinement	6470
No. parameters	269
R_{int}	0.075
R_1 (obs.)	0.0240
wR_2 (all data)	0.0505
Flack parameter	−0.010(4)
S	1.011

Refinement was by full-matrix least-squares (F_o^2) for all reflections, $R_1 = \sum\|F_o| - |F_c\|/\sum w|F_o|$, $wR_2 = [\sum(F_o^2 - F_c^2)^2/\sum wF_o^4]^{1/2}$, $w = 1/[(\sigma^2(F_o^2) + (0.0173P)^2 + 5.64P$, with $P = \{[F_o^2 + 2F_c^2)/3\}$. Goodness of fit, $S = \sum[(F_o^2 - F_c^2)^2]/(n-p)^{1/2}$.

X-Ray diffraction measurements of **3** were performed on a Bruker X8 APEXII CCD diffractometer at 100 K. The crystal was positioned at 35 mm from the detector and 1522 frames for 5 s over 1° were measured. The data were processed using the SAINT software package.[30] Crystal data, data collection parameters, and structure refinement details are given in Table 1.

The structure was solved by direct methods and refined by full-matrix least-squares techniques. Non-hydrogen atoms were refined with anisotropic displacement parameters. H atoms were inserted at calculated positions and refined with a riding model. The following computer programs were used: structure solution, SHELXS-97;[31] refinement, SHELXL-97;[32] molecular diagrams, ORTEP-3;[33] computer, Pentium IV; scattering factors.[34]

Dichlorido(η⁶-*p*-cymene)(3,5,6-bicyclophosphite-1,2-*O*-isopropylidene-α-D-glucofuranoside)osmium(II) (3). A solution of bis[dichlorido(η⁶-*p*-cymene)osmium(II)] **a** (79 mg, 0.1 mmol) in dry CH_2Cl_2 (5 mL) was added to a solution of 3,5,6-bicyclophosphite-1,2-*O*-isopropylidene-α-D-glucofuranoside (50 mg, 0.2 mmol) in dry CH_2Cl_2 (15 mL). The reaction mixture was stirred at 40 °C for 2 h. The solvent was reduced to *ca.* 5 mL and the product was precipitated by the addition of pentane (*ca.* 20 mL). The solid was filtered, washed with pentane (3 × 2 mL) and dried under vacuum. Crystals suitable for X-ray diffraction studies were grown from D_2O in the NMR tube.

Yield: 126 mg (98%), m.p. 186–187 °C (decomp.), Elemental analysis, found% C, 35.02; H, 4.14; calcd. for $C_{19}H_{27}Cl_2O_6POs\cdot 0.15CH_2Cl_2$, C, 35.05; H, 4.19. MS (ESI$^+$): *m/z*: 667.0 $[M + Na]^+$, 1309.7 $[2M + Na]^+$; $[\alpha]_D^{20} = 6$ (c 0.25, CH_2Cl_2).

^{1}H NMR (500.10 MHz, $CDCl_3$, 25 °C): $\delta = 6.13$ (d, $J = 3.5$ Hz, 1 H, H-1), 5.75 (d, $J = 6.0$ Hz, 1 H, H-Ar), 5.60 (d, $J = 8.2$ Hz, 2 H, H-Ar), 5.59 (d, $J = 8.2$ Hz, 2 H, H-Ar), 5.04 (m, 1 H, H-5), 4.78 (d, $J = 2.0$ Hz, 1 H, H-3), 4.67 (d, $J = 3.5$ Hz, 1 H, H-2), 4.45 (dd, $J = 9.4$, 11.8 Hz, 1 H, H-6), 4.32 (m, 2 H, H-6′, H-4), 2.86 (m, 1 H, C*H*$(CH_3)_2$), 2.33 (s, 3 H, CH_3), 1.51 (s, 3 H, C$(CH_3)_2$), 1.36 (s, 3 H, C$(CH_3)_2$), 1.28 (d, $J = 6.9$ Hz, 6H, CH(C*H*$_3)_2$). ^{13}C{^{1}H} NMR (125.75 MHz, $CDCl_3$, 25 °C): $\delta = 112.6$ (*C*$(CH_3)_2$), 105.7 (C-1), 102.5 (C-Ar), 100.6 (C-Ar), 83.6 ($J = 7.3$ Hz, C-2), 82.0 (C-Ar), 81.8 (C-Ar), 81.4 (C-Ar), 78.6 ($J = 8.2$ Hz, C-3), 76.7 ($J = 5.5$ Hz, C-4), 74.5 ($J = 4.5$ Hz, C-5), 69.6 ($J = 8.2$ Hz, C-6), 30.8 (*C*H$(CH_3)_2$), 26.9 (C$(CH_3)_2$), 26.2 (C$(CH_3)_2$), 22.4 (CH$(CH_3)_2$), 22.4 (CH$(CH_3)_2$), 18.4 (CH_3) ppm. ^{31}P{^{1}H} NMR (202.44 MHz, $CDCl_3$, 25 °C): $\delta = 87.3$ ppm.

Dichlorido(η^6-*p*-cymene)(3,5,6-bicyclophosphite-1,2-*O*-cyclohexylidene-α-D-glucofuranoside)osmium(II) (4). A solution of bis[dichlorido(η^6-*p*-cymene)osmium(II)] **a** (79 mg, 0.1 mmol) in dry CH_2Cl_2 (5 mL) was added to a solution of 3,5,6-bicyclophosphite-1,2-*O*-cyclohexylidene-α-D-glucofuranoside (58 mg, 0.2 mmol) in dry CH_2Cl_2 (15 mL). The mixture was stirred at 40 °C for 2 h. The solvent was then reduced to *ca.* 5 mL and the compound was precipitated as yellow powder by the addition of pentane (*ca.* 20 mL). The solid was filtered, washed with pentane (3 × 2 mL) and dried under vacuum.

Yield: 135 mg (98%), m.p. 159–161 °C (decomp.), Elemental analysis, found% C, 37.48; H, 4.42; calcd. for $C_{22}H_{31}Cl_2O_6POs\cdot 0.15CH_2Cl_2$, C, 37.22; H, 4.44. MS (ESI$^+$): *m/z*: 649.0 $[M - 2 H_2O + H]^+$, 705.0 $[M + Na]^+$; $[\alpha]_D^{20} = 12$ (c 0.25, CH_2Cl_2).

^{1}H NMR (500.10 MHz, $CDCl_3$, 25 °C): $\delta = 6.13$ (d, $J = 3.8$ Hz, 1 H, H-1), 5.75 (d, $J = 6.0$ Hz, 1 H, H-Ar), 5.60 (d, $J = 8.2$ Hz, 1 H, H-Ar), 5.58 (d, $J = 8.2$ Hz, 2 H, H-Ar), 5.03 (m, 1 H, H-5), 4.79 (d, $J = 2.5$ Hz, 1 H, H-3), 4.67 (d, $J = 3.5$ Hz, 1 H, H-2), 4.45 (dd, $J = 7.0$, 11.8 Hz, 1 H, H-6), 4.32 (m, 2 H, H-6′, H-4), 2.86 (m, 1 H, C*H*$(CH_3)_2$), 2.33 (s, 3 H,CH_3), 1.68 (m, 4 H, C_6H_{10}), 1.56 (m, 6 H, C_6H_{10}), 1.28 (d, $J = 6.9$ Hz, 6H, CH(C*H*$_3)_2$). ^{13}C{^{1}H} NMR (125.75 MHz, $CDCl_3$, 25 °C): $\delta = 113.3$ (*C*$(CH_3)_2$), 105.3 (C-1), 102.5 (C-Ar), 100.7 (C-Ar), 83.2 ($J = 6.4$ Hz, C-2), 82.0 (C-Ar), 81.6 (C-Ar), 81.4 (C-Ar), 78.8 ($J = 8.2$ Hz, C-3), 76.6 ($J = 5.5$ Hz, C-4), 74.5 ($J = 4.5$ Hz, C-5), 69.4 ($J = 9.1$ Hz, C-6), 36.5 (C_6H_{10}), 35.7 (C_6H_{10}), 30.8 (*C*H$(CH_3)_2$), 24.8 (C_6H_{10}), 23.8 (C_6H_{10}), 23.5 (C_6H_{10}), 22.4 (CH$(CH_3)_2$), 22.4 (CH$(CH_3)_2$), 18.4 (CH_3) ppm. ^{31}P{^{1}H} NMR (202.44 MHz, $CDCl_3$, 25 °C): $\delta =$ 87.3 ppm.

Oxalato(η^6-*p*-cymene)(3,5,6-bicyclophosphite-1,2-*O*-isopropylidene-α-D-glucofuranoside)osmium(II) (5). [(η^6-Cymene)OsCl(μ-Cl)]$_2$ (158 mg, 0.2 mmol) and silver oxalate (133 mg, 0.44 mmol) were stirred in distilled water (25 mL) for 12 h. The mixture was filtered through a bed of Celite to remove the AgCl precipitate. The solvent was removed under vacuum, and the residue was redissolved in methanol (25 mL) and 3,5,6-bicyclophosphite-1,2-*O*-isopropylidene-α-D-glucofuranose (100 mg, 0.4 mmol) was added. The reaction mixture was stirred for 2 h, the volume of the solvent was reduced to *ca.* 5 mL and diethyl ether (25 mL) was added. The slurry was cooled to 4 °C for 12 h to complete the precipitation. The yellow crystalline product was filtered, washed with diethyl ether (2 × 5 mL) and dried under vacuum.

Yield: 195 mg (74%), m.p. 190–192 °C (decomp.), Elemental analysis, found% C, 37.14; H, 3.98; calcd. for $C_{21}H_{27}O_{10}POs\cdot 0.75H_2O$, C, 37.41; H, 4.26., MS (ESI$^+$): *m/z*: 683 $[M + Na]^+$; $[\alpha]_D^{20} = -2$ (c 0.25, CH_2Cl_2).

^{1}H NMR (500.10 MHz, $CDCl_3$, 25 °C): $\delta = 6.06$ (d, $J = 3.5$ Hz, 1H; H-1), 5.97 (d, $J = 4.7$ Hz, 1H; H-Ar), 5.94 (d, $J = 5.0$ Hz, 1H; H-Ar), 5.80 (d, $J = 4.7$ Hz, 2H; H-Ar), 5.10 (m, 1H; H-5), 4.71 (brs, 1H; H-3), 4.63 (d, $J = 3.2$ Hz, 1H; H-2), 4.52 (m, 1H; H-6), 4.40 (s, 1H; H-4), 4.35 (m, 1H; H-6′), 2.76 (m, 1H; C*H*$(CH_3)_2$), 2.29 (s, 3H; CH_3), 1.48 (s, 3H; C$(CH_3)_2$), 1.31 (s, 3H; C$(CH_3)_2$), 1.29 (d, $J = 6.6$ Hz, 3H; CH(C*H*$_3)_2$), 1.28 (d, $J = 6.7$ Hz, 3H; CH(C*H*$_3)_2$) ppm; ^{13}C{^{1}H} NMR (125.75 MHz, $CDCl_3$, 25 °C): $\delta = 165.1$ ($J = 6.0$ Hz; C=O), 112.7 (*C*$(CH_3)_2$), 105.7 (C-1), 102.7 (C-Ar), 99.1 (C-Ar), 83.6 ($J = 6.1$ Hz; C-2), 81.5 (C-Ar), 80.9 (C-Ar), 80.1 (C-Ar), 78.5 ($J = 7.8$ Hz; C-3), 76.7 ($J = 10.1$ Hz; C-4), 74.6 ($J = 3.8$ Hz; C-5), 69.5 ($J = 7.1$ Hz; C-6), 31.2 (*C*H$(CH_3)_2$), 26.9 (C(*C*H$_3)_2$), 26.2 (C(*C*H$_3)_2$), 22.7 (CH(*C*H$_3)_2$), 22.6 (CH(*C*H$_3)_2$), 18.2 (CH_3) ppm; ^{31}P{^{1}H} NMR (202.44 MHz, $CDCl_3$, 25 °C): $\delta = 94.7$ ppm.

Oxalato(η^6-*p*-cymene)(3,5,6-bicyclophosphite-1,2-*O*-cyclohexylidene-α-D-glucofuranoside)osmium(II) (6). [(η^6-Cymene)OsCl(μ-Cl)]$_2$ (158 mg, 0.2 mmol) and silver oxalate (133 mg, 0.44 mmol) were stirred in distilled water (25 mL) for 12 h. The mixture was filtered through a bed of Celite to remove the AgCl precipitate. The solvent was removed under vacuum, the residue was redissolved in methanol (25 mL) and 3,5,6-bicyclophosphite-1,2-*O*-cyclohexylidene-α-D-glucofuranose (115 mg, 0.4 mmol) was added. The reaction mixture was stirred for 2 h, the volume of the solvent was reduced to *ca.* 5 mL and diethyl ether (25 mL) was added. The slurry was cooled to 4 °C for 12 h to complete the precipitation. The yellow crystalline product was filtered off, washed with diethyl ether (2 × 5 mL) and dried under vacuum.

Yield: 213 mg, (76%), m.p. 183–184 °C (decomp.), Elemental analysis, found% C, 40.12; H, 4.27; calcd. for $C_{24}H_{31}O_{10}POs\cdot 0.75H_2O$, C, 40.36; H, 4.59; MS (ESI$^+$): *m/z*: 725 $[M + Na]^+$; $[\alpha]_D^{20} = 4$ (c 0.25, CH_2Cl_2). ^{1}H NMR (500.10 MHz, $CDCl_3$, 25 °C): $\delta = 6.07$ (d, $J = 3.2$ Hz, 1 H, H-1), 5.94 (brs, 1 H, H-Ar), 5.78 (brs, 1 H, H-Ar), 5.58 (brs, 2 H, H-Ar), 5.08 (m, 1 H, H-5), 4.71 (brs, 1 H, H-3), 4.62 (d, $J = 3.2$ Hz, 1 H, H-2), 4.49 (m, 1 H, H-6), 4.38 (m, 1 H, H-4), 4.32 (m, 1 H, H-6′), 2.76 (m, 1 H, C*H*$(CH_3)_2$), 2.29 (s, 3 H,CH_3), 1.65 (m, 4 H, C_6H_{10}), 1.53 (m, 6 H, C_6H_{10}), 1.29 (d, $J = 6.4$ Hz, 3 H, CH(C*H*$_3)_2$), 1.28 (d, $J = 6.5$ Hz, 3H, CH(C*H*$_3)_2$) ppm; ^{13}C{^{1}H} NMR (125.75 MHz, $CDCl_3$, 25 °C): $\delta = 165.0$ ($J = 6.0$ Hz; C=O), 113.4 (C$(CH_3)_2$), 105.3 (C-1), 102.7 (C-Ar), 99.1 (C-Ar), 83.1 ($J = 6.1$ Hz; C-2), 81.5 (C-Ar), 80.9 (C-Ar), 80.1 (C-Ar), 78.7 ($J = 7.8$ Hz; C-3), 76.7 ($J = 10.1$ Hz; C-4), 74.7 ($J = 3.8$ Hz; C-5), 69.6 ($J = 7.1$ Hz; C-6), 36.5 (C_6H_{10}), 35.6 (C_6H_{10}), 31.2 (*C*H$(CH_3)_2$), 24.7 (C_6H_{10}), 23.8 (C_6H_{10}), 23.5 (C_6H_{10}), 22.7 (CH(*C*H$_3)_2$-Ar), 22.6 (CH(*C*H$_3)_2$-Ar), 18.2 (CH_3-Ar) ppm; ^{31}P{^{1}H} NMR (202.44 MHz, $CDCl_3$, 25 °C): $\delta = 94.6$ ppm.

Hydrolysis and reactivity with 5′-GMP

For hydrolysis studies, the compounds were dissolved in D_2O and the samples were analyzed by ^{31}P{^{1}H} NMR spectroscopy once a day for 5 days. The ^{31}P{^{1}H} NMR spectra for the kinetic

experiments were recorded on a Bruker Avance 400 instrument at 161.98 MHz. For GMP binding experiments, the complexes were mixed at molar ratios of 1 : 2 (complex : GMP) in D_2O and kept at room temperature for 2 days.

Cytotoxicity in cancer cell lines

Cell lines and culture conditions. CH1 cells originate from an ascites sample of a patient with a papillary cystadenocarcinoma of the ovary and were a generous gift from Lloyd R. Kelland, CRC Centre for Cancer Therapeutics, Institute of Cancer Research, Sutton, UK. SW480 (adenocarcinoma of the colon, human), and A549 (non-small cell lung cancer, human) cells were kindly provided by Brigitte Marian (Institute of Cancer Research, Department of Medicine I, Medical University of Vienna, Austria). All cell culture reagents were obtained from Sigma-Aldrich Austria. Cells were grown in 75 cm^2 culture flasks (Iwaki) as adherent monolayer cultures in Eagle's Minimal Essential Medium (MEM) supplemented with 10% heat-inactivated foetal calf serum, 1 mM sodium pyruvate and 2 mM L-glutamine. Cultures were maintained at 37 °C in a humidified atmosphere containing 95% air and 5% CO_2.

MTT assay conditions. Cytotoxicity was determined by the colorimetric MTT (3-(4,5-dimethyl-2-thiazolyl)-2,5-diphenyl-2*H*-tetrazolium bromide, purchased from Fluka) microculture assay. For this purpose, cells were harvested from culture flasks by trypsinization and seeded in 100 μL aliquots MEM supplemented with 10% heat-inactivated foetal calf serum, 1 mM sodium pyruvate, 4 mM L-glutamine and 1% non-essential amino acids (100×) into 96-well microculture plates (Iwaki). Cell densities of 1.5×10^3 cells/well (CH1), 2.5×10^3 cells/well (SW480) and 4×10^3 cells/well (A549) were chosen in order to ensure exponential growth of untreated controls throughout the experiment. Cells were allowed to settle and resume exponential growth for 24 h. The test compounds were dissolved and serially diluted in the same medium and added in 100 μL aliquots to the microcultures (if necessary due to limited solubility, the maximum concentration tested was added in 200 μL aliquots after removal of the medium), and cells were exposed to the test compounds for 96 h. At the end of the exposure period, all media were replaced by 100 μL/well RPMI1640 culture medium (supplemented with 10% heat-inactivated foetal calf serum) plus 20 μL/well MTT solution in phosphate-buffered saline (5 mg ml^{-1}). After incubation for 4 h, the supernatants were removed, and the formazan crystals formed by vital cells were dissolved in 150 μL DMSO per well. Optical densities at 550 nm were measured with a microplate reader (Tecan Spectra Classic), using a reference wavelength of 690 nm to correct for unspecific absorption. The quantity of vital cells was expressed in terms of T/C values by comparison to untreated control microcultures, and 50% inhibitory concentrations (IC_{50}) were calculated from concentration-effect curves by interpolation. Evaluation is based on means from at least three independent experiments, each comprising at least three replicates per concentration level.

Results and discussion

In recent years, the tumour microenvironment has become one of the focuses of targeted cancer chemotherapy. Carbohydrate compounds have been extensively studied as they could potentially exploit the altered metabolism associated with cancer cells, such as increased glucose uptake as compared to healthy tissues. In previous work, we linked carbohydrate-derived ligands to organometallic Ru^{II}–arene moieties to afford RAPTA-C analogues such as dichlorido(η^6-*p*-cymene)(3,5,6-bicyclophosphite-1,2-*O*-cyclohexylidene-α-D-glucofuranoside)ruthenium(II) **4**^{Ru}, which is more cytotoxic than RAPTA-C, probably due to its higher lipophilicity and, hence, increased uptake. The complexes were shown to undergo aquation of a halido ligand in aqueous solution, followed by hydrolysis of a P–O bond of the phosphite ligand, and finally formation of dinuclear species.[25] In order to investigate the influence of the metal centre on hydrolysis and cytotoxicity, we prepared similar compounds based on osmium, the heavier homologue of ruthenium.

The organometallic Os^{II}-chlorido complexes **3** and **4** were synthesized in very good yield by reacting the dimer bis[dichlorido(η^6-*p*-cymene)osmium(II)] **a** in CH_2Cl_2 at 40 °C with 3,5,6-bicyclophosphite-1,2-*O*-isopropylidene-α-D-glucofuranoside **1** and 3,5,6-bicyclophosphite-1,2-*O*-cyclohexylidene-α-D-glucofuranoside **2**, respectively (Scheme 1). In contrast, the oxalato analogues **5** and **6** were prepared *via* a two step synthesis, following a literature procedure.[29] In the first step, [oxalato(η^6-*p*-cymene)(H_2O)osmium(II)] was formed by reacting bis[dichlorido(η^6-*p*-cymene)osmium(II)] with disilver oxalate ($Ag_2C_2O_4$). In the second step the active aqua species was stirred for 2 h in CH_3OH with the respective carbohydrate-based phosphorus ligand and the compounds ultimately precipitated from the reaction mixture. The reason for choosing this reaction sequence was to avoid side reactions involving the silver ions and the phosphorus ligand.

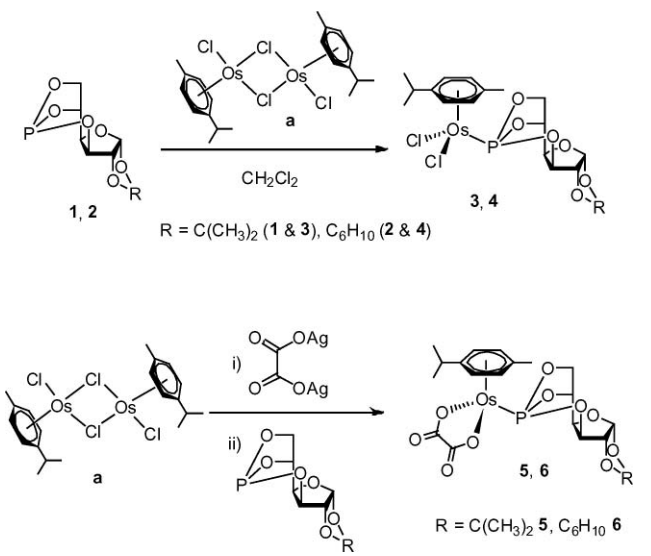

Scheme 1 Synthesis of the dichlorido– (**3**, **4**) and oxalato–Os^{II} (**5**, **6**) compounds of P-derived sugar ligands (**1**, **2**).

All the complexes were fully characterized by 1D and 2D NMR spectroscopy, ESI-MS, elemental analysis, and the solid state structure of complex **3** was determined by single crystal X-ray diffraction analysis. Upon coordination of the P-containing ligands to the Os centre, a change in chemical shift of the $^{31}P\{^1H\}$ NMR signals was observed from approximately 117 ppm to about 87 ppm in the case of the chlorido complexes and to 94 ppm

in the case of the oxalato complexes. For the analogous Ru compounds low-field shifts to about 130 ppm were observed.[25] In the $^{13}C\{^1H\}$ NMR spectra of **5** and **6**, the most indicative signal for complex formation is found at 165.0 ppm, which corresponds to the carboxylate moieties of the coordinated oxalato ligand. ^1H NMR spectra of oxalato complexes in $CDCl_3$ gave two sets of signals (two doublets) for the Ar-CH$(CH_3)_2$ protons, which is in contrast to NMR in D_2O where the methyl groups are observed as a single doublet, since the inversion of the metal centre only occurs in protic solvents.[35] A similar observation was previously reported for related complexes.[36]

X-Ray diffraction analysis of **3** demonstrated the presence of piano-stool geometry (Fig. 2), as usually observed for such metal–arene organometallics.[11,14,36] Complex **3** crystallizes in the orthorhombic space group $P2_12_12_1$. The osmium–centroid$_{arene}$ distance is 1.713 Å in **3** and the Os–Cl1, Os–Cl2, and Os–P bond lengths are 2.4203(8), 2.4106(9) and 2.2411(9), respectively. The Os–Cl bonds are slightly longer than the Ru–Cl bonds observed in $\mathbf{3}^{Ru}$, whereas the Os–P bond length is similar.[25] As compared

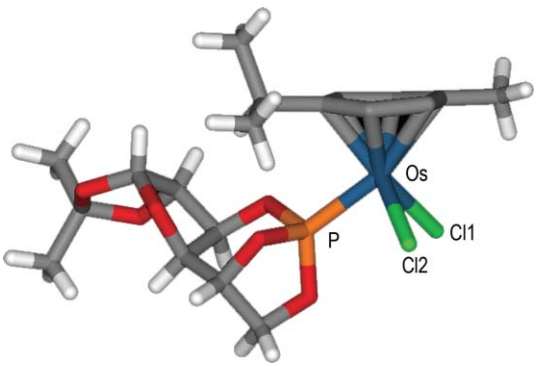

Fig. 2 Molecular structure of **3**. Selected bond lengths (Å) and angles (°) are: Os–Cl1 2.4203(8), Os–Cl2 2.4106(9), Os–P 2.2411(9); P–Os–Cl2 88.51(3), P–Os–Cl1 88.74(3), Cl2–Os–Cl1 86.29(3).

to the RAPTA-C analogous Os compound, the Os–centroid$_{arene}$ distance is slightly longer (1.698 Å), whereas the Os–Cl and Os–P bonds are shorter [2.4344(15), 2.4194(15); 2.3324(16) Å].[37]

The hydrolysis of **3** was studied by $^{31}P\{^1H\}$ NMR spectroscopy. Initially only a single peak is observed at 90.0 ppm which was assigned to unmodified **3** (Fig. 3). After 24 h, two additional peaks of equal relative intensity at 95.8 and 95.3 ppm appear due to formation of diastereomers by exchange of a single chlorido ligand with an aqua molecule (Scheme 2). These observations are similar to those made for related ruthenium(II) compounds,[12,25,38] as is the next step in the hydrolysis mechanism which involves cleavage of a P–O bond (after approximately 4 d; peak at $\delta(^{31}P) = 62.1$ ppm, Fig. 3). In contrast to the Ru compounds, the rate of hydrolysis is very slow for the Os compounds, as also observed in other cases.[39] Within 24 h only 5% of the complex undergo hydrolysis in the case of Os complex, whereas for the Ru analogue more than 50% of the initial complex was degraded. For the ruthenium(II) compounds the formation of mono-aqua species and the hydrolysis of the P–O bond of the phosphite was observed already after 12 h and a dimeric species had formed within 24 h. The diaqua complex was not observed in the NMR spectrum, probably because it is converted immediately into the dimeric species. In contrast to the Ru complexes, no dimeric species were detected for the Os compound after 72 h. Since the dimer is believed to be not cytotoxic,[14,36] avoiding the formation of a dimeric species could prove advantageous (see below). Forced hydrolysis of **3** by addition of two equivalents of $AgNO_3$ resulted in a release of both chlorido ligands and formation of aqua species with hydrolyzed P–O bonds ($\delta(^{31}P) = 99.1$ and 97.9 for $\mathbf{3}^{Ru}$ and 62.2 ppm for **3**).

Introduction of bidentate ligands has been demonstrated to be an option to overcome the instability problem of titanocene anticancer compounds and has also proven useful for platinum drugs by leading to higher stability, reduced side-effects and extending the range of treatable tumors.[7,40] In order to study the influence of chelating oxalato ligands on the hydrolysis behaviour, **5** and **6** were prepared (Scheme 1) and similar hydrolysis studies

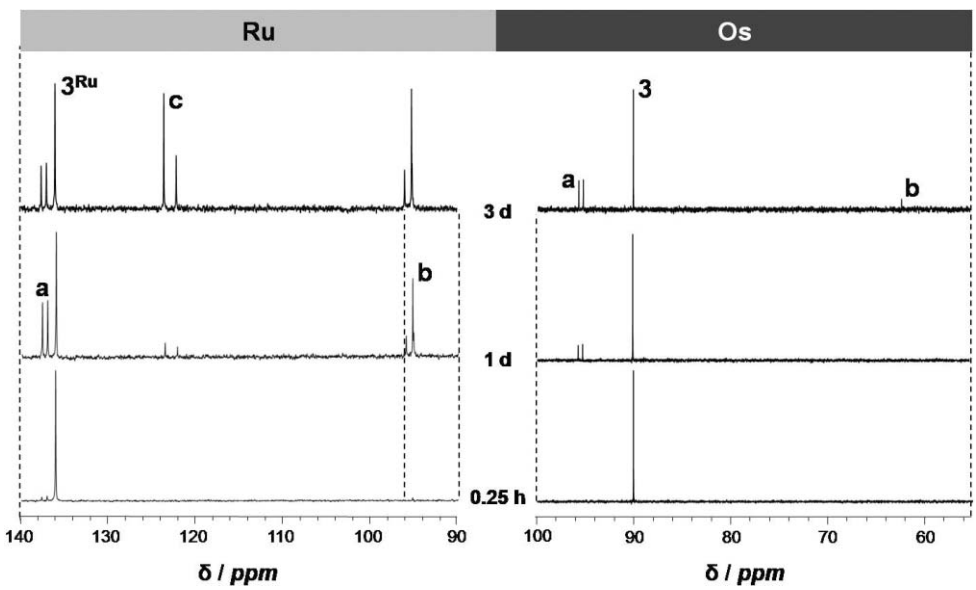

Fig. 3 $^{31}P\{^1H\}$ NMR spectra for the hydrolysis of $\mathbf{3}^{Ru}$ and **3** in D_2O up to 72 h. Peak assignment: **a**, monoaqua complex; **b**, products obtained by cleavage of the P–O bond; **c**, dimeric species.

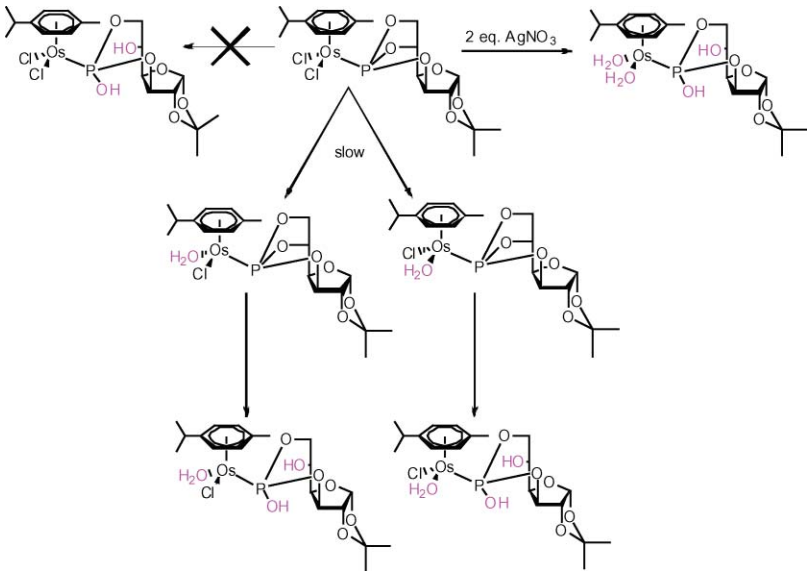

Scheme 2 Reaction scheme for the hydrolysis of **3** (charges/counter ions were omitted for clarity).

Table 2 *In vitro* anticancer activity in human ovarian cancer (CH1), colon cancer (SW480) and non-small cell lung cancer (A549) cells (exposure time 96 h unless stated otherwise). Values are means ± standard deviations, obtained from at least three independent experiments

	IC_{50} values/μM		
Compound	CH1	SW480	A549
3	113 ± 24	n.d.[a]	n.d.[a]
4	50 ± 6	215 ± 7	> 640
5	436 ± 72	> 640	> 640
6	764 ± 215	> 640	> 640
$\mathbf{3}^{Ru}$	60 ± 14[b]	361 ± 122[b]	498 ± 17[bc]
$\mathbf{4}^{Ru}$	29 ± 4[b]	150 ± 19[b]	223 ± 14[ac]

[a] Not determined. [b] From ref. 25. [c] Exposure time 72 h.

as for **3** were conducted. The exchange of the chlorido ligands by oxalato stabilized the compounds and there were no hydrolysis products identified during a week of incubation (after two weeks a very small peak at 59.1 ppm was assigned to a P–O bond hydrolysis product). A similar approach was followed for RAPTA-C and most notably such modification did not alter the anticancer activity of the compounds.[29] In contrast, **5** and **6** are much less active in *in vitro* anticancer assays than their Ru counterparts (see below; Table 2).

In an attempt to study the reactivity of the compounds to 5′-GMP, $^{31}P\{^1H\}$ NMR studies were conducted on mixtures with 5′-GMP in 1 : 2 ratio in D_2O. However, none of the complexes reacted with 5′-GMP within 48 h, whereas the Ru organometallics are relatively reactive and form adducts *via* the *N*7 atoms of guanine. Hydrolysis prior to reaction with biomolecular targets can be considered an essential step for Ru and Pt compounds in their modes of action.[1,5] However, for the studied derivatives, although hydrolysis is observed, no binding of Os(II) to *N*-donor ligands occurs. This property has been noted for similar Os(II) complexes,[18,21] but might also be related to the insufficient detection limit of NMR spectroscopy, since only a minor fraction of the Os compound was found to hydrolyze within the experimental time.

Evaluation of the *in vitro* anticancer activity

The antiproliferative potential of **3–6** was determined in human SW480 colon adenocarcinoma, CH1 ovarian cancer and A549 non-small cell lung cancer cells by means of the MTT assay, and the obtained results are compared to those of the analogous Ru(II) compounds (Table 2). Structure–activity relationships can best be assessed in CH1 cells, the most sensitive of these cell lines, and concentration–effect curves of **3**, **4**, $\mathbf{3}^{Ru}$ and $\mathbf{4}^{Ru}$ are depicted in Fig. 4.

Among the series of Os derivatives, **4** is the most cytotoxic in CH1 cells, followed by the chlorido species **3** and the oxalate complexes **5** and **6**. As in the case of the Ru compounds with chlorido ligands, the Os analogue bearing the lipophilic cyclohexylidene protection group, *i.e.*, **4**, is more cytotoxic than the isopropylidene derivative. The Ru–chlorido compounds are approximately twice as potent as their Os counterparts **3** and **4**. The Ru complexes exhibited activity in cisplatin-resistant A2780 cells, which suggests a mode of action different from that of DNA-targeted agents, and furthermore selectivity for non-tumourigenic cells was observed.[25] A non-DNA-related mode of action is also supported by the fact that the Ru analogues form inactive dimers which are not detectable for the Os compounds. However, the Os complexes still lack reactivity to 5′-GMP and the cytotoxicity is low. In general, the cytotoxicities of the tested Os and Ru organometallics cover a broad range of IC_{50} values of 30–760 μM in the most sensitive cell line CH1.

Such a low anticancer potency *in vitro* has often been observed for osmium and ruthenium drug candidates, including the clinically tested NAMI-A and certain organometallic RAPTA compounds, especially when compared to platinum-based drugs. Nevertheless, the Ru compounds exhibit excellent *in vivo* activities, in particular against tumour metastases.[12,41–43] Ru and Pt complexes bearing carbohydrate ligands were shown to be generally less cytotoxic than structural analogues,[24] but they often exhibit considerable activity *in vivo*, which makes them promising compounds for further development.[12,44]

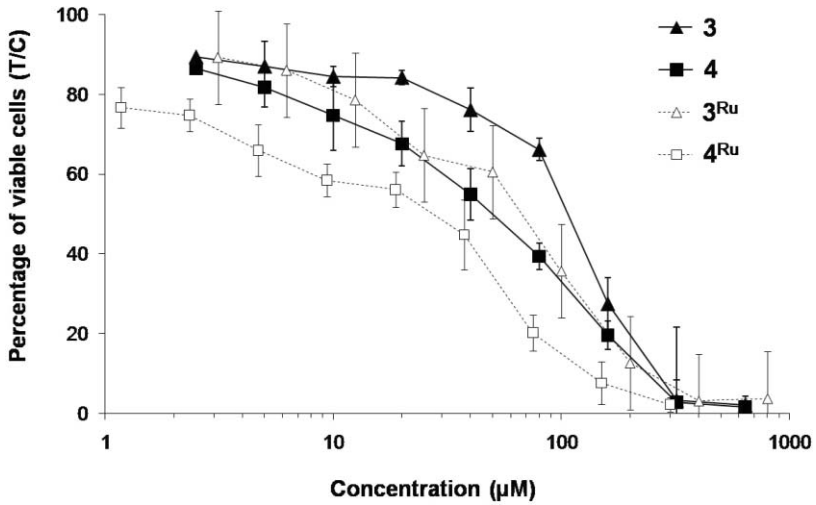

Fig. 4 Concentration–effect curves of Os and Ru carbohydrate complexes in CH1 cells.

Conclusions

RAPTA-type complexes are among the best studied and most promising Ru–arene anticancer agents. In an attempt to confer to the basic scaffold tumour-targeting properties, sugar moieties had been linked to Ru complexes of this kind, which yielded compounds with selectivity for tumourigenic cell lines. In this paper, we report on the synthesis of Os analogues with carbohydrate-derived phosphorus-containing ligands. These compounds exhibit slightly higher IC_{50} values than their Ru counterparts. In contrast to the Ru compounds, studies on the reactivity to 5′-GMP showed that the Os complexes do not react with this DNA model within 48 h, which may account for their lower cytotoxicity.

In addition, the chlorido ligands were replaced by oxalate groups, in order to increase the stability of the compounds. In aquation studies, both the Os–chlorido and –oxalato complexes were significantly more stable than the Ru counterparts, as demonstrated by $^{31}P\{^{1}H\}$ NMR spectroscopy, though structurally similar species are formed, including a species in which an intramolecular P–O bond break occurs upon replacement of a chlorido ligand by an aqua moiety. These oxalato compounds inhibit cancer cell growth with a much lower potency *in vitro* than the chlorido analogues.

Acknowledgements

We thank the Higher Education Commission of Pakistan, the Austrian Exchange Service (ÖAD), the Hochschuljubiläumsstiftung Vienna, the Theodor-Körner-Fonds, the FFG – Austrian Research Promotion Agency (811591), the Austrian Council for Research and Technology Development (IS526001), COST D39 and CM0902 and the Austrian Science Fund for financial support. This research was supported by a Marie Curie Intra European Fellowship within the 7th European Community Framework Programme project 220890-SuRuCo (A.A.N.). We gratefully acknowledge Alexander Roller for collecting the X-ray diffraction data, Michaela Hejl for performing the *in vitro* anticancer assays and Prof. Markus Galanski for recording the 2D NMR spectra.

References

1 M. Galanski, M. A. Jakupec and B. K. Keppler, *Curr. Med. Chem.*, 2005, **12**, 2075–2094.
2 P. Heffeter, U. Jungwirth, M. Jakupec, C. Hartinger, M. Galanski, L. Elbling, M. Micksche, B. Keppler and W. Berger, *Drug Resist. Updates*, 2008, **11**, 1–16.
3 P. J. Sadler, *Dalton Transactions* themed issue on Metal Anticancer Compounds, *Dalton Trans.*, 2009, 10629–10936.
4 Z. Guo and P. J. Sadler, *Angew. Chem., Int. Ed.*, 1999, **38**, 1512–1531.
5 C. G. Hartinger, S. Zorbas-Seifried, M. A. Jakupec, B. Kynast, H. Zorbas and B. K. Keppler, *J. Inorg. Biochem.*, 2006, **100**, 891–904.
6 C. G. Hartinger, M. A. Jakupec, S. Zorbas-Seifried, M. Groessl, A. Egger, W. Berger, H. Zorbas, P. J. Dyson and B. K. Keppler, *Chem. Biodiversity*, 2008, **5**, 2140–2155.
7 C. G. Hartinger and P. J. Dyson, *Chem. Soc. Rev.*, 2009, **38**, 391–401.
8 J. M. Rademaker-Lakhai, D. Van Den Bongard, D. Pluim, J. H. Beijnen and J. H. M. Schellens, *Clin. Cancer Res.*, 2004, **10**, 3717–3727.
9 R. E. Morris, R. E. Aird, P. d. S. Murdoch, H. Chen, J. Cummings, N. D. Hughes, S. Parsons, A. Parkin, G. Boyd, D. I. Jodrell and P. J. Sadler, *J. Med. Chem.*, 2001, **44**, 3616–3621.
10 R. E. Aird, J. Cummings, A. A. Ritchie, M. Muir, R. E. Morris, H. Chen, P. J. Sadler and D. I. Jodrell, *Br. J. Cancer*, 2002, **86**, 1652–1657.
11 W. F. Schmid, R. O. John, V. B. Arion, M. A. Jakupec and B. K. Keppler, *Organometallics*, 2007, **26**, 6643–6652.
12 C. Scolaro, A. Bergamo, L. Brescacin, R. Delfino, M. Cocchietto, G. Laurenczy, T. J. Geldbach, G. Sava and P. J. Dyson, *J. Med. Chem.*, 2005, **48**, 4161–4171.
13 M. G. Mendoza-Ferri, C. G. Hartinger, A. A. Nazarov, R. E. Eichinger, M. A. Jakupec, K. Severin and B. K. Keppler, *Organometallics*, 2009, **28**, 6260–6265.
14 W. Kandioller, C. G. Hartinger, A. A. Nazarov, C. Bartel, M. Skocic, M. A. Jakupec, V. B. Arion and B. K. Keppler, *Chem.–Eur. J.*, 2009, **15**, 12283–12291.
15 M. G. Mendoza-Ferri, C. G. Hartinger, M. A. Mendoza, M. Groessl, A. E. Egger, R. E. Eichinger, J. B. Mangrum, N. P. Farrell, M. Maruszak, P. J. Bednarski, F. Klein, M. A. Jakupec, A. A. Nazarov, K. Severin and B. K. Keppler, *J. Med. Chem.*, 2009, **52**, 916–925.
16 J. Maksomiska, D. S. Williams, G. E. Atilla-Gokcumen, K. S. M. Smalley, P. J. Carroll, R. D. Webster, P. Filippakopoulos, S. Knapp, M. Herlyn and E. Meggers, *Chem.–Eur. J.*, 2008, **14**, 4816–4822.
17 Y. K. Yan, M. Melchart, A. Habtemariam and P. J. Sadler, *Chem. Commun.*, 2005, 4764–4776.
18 A. F. A. Peacock, A. Habtemariam, R. Fernandez, V. Walland, F. P. A. Fabbiani, S. Parsons, R. E. Aird, D. I. Jodrell and P. J. Sadler, *J. Am. Chem. Soc.*, 2006, **128**, 1739–1748.
19 C. A. Vock, W. H. Ang, C. Scolaro, A. D. Phillips, L. Lagopoulos, L. Juillerat-Jeanneret, G. Sava, R. Scopelliti and P. J. Dyson, *J. Med. Chem.*, 2007, **50**, 2166–2175.

20 A. Dorcier, W. H. Ang, S. Bolano, L. Gonsalvi, L. Juillerat-Jeannerat, G. Laurenczy, M. Peruzzini, A. D. Phillips, F. Zanobini and P. J. Dyson, *Organometallics*, 2006, **25**, 4090–4096.
21 A. F. A. Peacock, S. Parsons and P. J. Sadler, *J. Am. Chem. Soc.*, 2007, **129**, 3348–3357.
22 S. H. van Rijt, A. J. Hebden, T. Amaresekera, R. J. Deeth, G. J. Clarkson, S. Parsons, P. C. McGowan and P. J. Sadler, *J. Med. Chem.*, 2009, **52**, 7753–7764.
23 S. H. van Rijt, A. F. A. Peacock, R. D. L. Johnstone, S. Parsons and P. J. Sadler, *Inorg. Chem.*, 2009, **48**, 1753–1762.
24 C. G. Hartinger, A. A. Nazarov, S. M. Ashraf, P. J. Dyson and B. K. Keppler, *Curr. Med. Chem.*, 2008, **15**, 2574–2591.
25 I. Berger, M. Hanif, A. A. Nazarov, C. G. Hartinger, R. O. John, M. L. Kuznetsov, M. Groessl, F. Schmitt, O. Zava, F. Biba, V. B. Arion, M. Galanski, M. A. Jakupec, L. Juillerat-Jeanneret, P. J. Dyson and B. K. Keppler, *Chem.–Eur. J.*, 2008, **14**, 9046–9057.
26 R. A. Gatenby and R. J. Gillies, *Nat. Rev. Cancer*, 2004, **4**, 891–899.
27 S. Stahl and H. Werner, *Organometallics*, 1990, **9**, 1876–1881.
28 N. K. Kochetkov, E. E. Nifant'ev, M. P. Koroteev, Z. K. Zhane and A. A. Borisenko, *Carbohydr. Res.*, 1976, **47**, 221–231.
29 W. H. Ang, E. Daldini, C. Scolaro, R. Scopelliti, L. Juillerat-Jeannerat and P. J. Dyson, *Inorg. Chem.*, 2006, **45**, 9006–9013.
30 M. R. Pressprich and J. Chambers, Bruker Analytical X-ray systems, Madison, Editon edn, 2004.
31 G. M. Sheldrick, University Göttingen (Germany), Editon edn, 1997.
32 G. M. Sheldrick, University Göttingen (Germany), Editon edn, 1997.
33 L. J. Farrugia, *J. Appl. Crystallogr.*, 1997, **30**, 565.
34 *International Tables for X-ray Crystallography*, Kluwer Academic Press, Dordrecht, The Netherlands, 1992.
35 R. Lang, K. Polborn, T. Severin and K. Severin, *Inorg. Chim. Acta*, 1999, **294**, 62–67.
36 A. F. A. Peacock, M. Melchart, R. J. Deeth, A. Habtemariam, S. Parsons and P. J. Sadler, *Chem.–Eur. J.*, 2007, **13**, 2601–2613.
37 A. Dorcier, P. J. Dyson, C. Gossens, U. Rothlisberger, R. Scopelliti and I. Tavernelli, *Organometallics*, 2005, **24**, 2114–2123.
38 C. Scolaro, C. G. Hartinger, C. S. Allardyce, B. K. Keppler and P. J. Dyson, *J. Inorg. Biochem.*, 2008, **102**, 1743–1748.
39 J. Reedijk, *Platinum Met. Rev.*, 2008, **52**, 2–11.
40 M. A. Jakupec, M. Galanski and B. K. Keppler, *Rev. Physiol., Biochem., Pharmacol.*, 2003, **146**, 1–53.
41 E. Alessio, G. Mestroni, A. Bergamo and G. Sava, *Curr. Top. Med. Chem.*, 2004, **4**, 1525–1535.
42 A. Bergamo, A. Masi, P. J. Dyson and G. Sava, *Int. J. Oncol.*, 2008, **33**, 1281–1289.
43 S. Chatterjee, S. Kundu, A. Bhattacharyya, C. G. Hartinger and P. J. Dyson, *JBIC, J. Biol. Inorg. Chem.*, 2008, **13**, 1149–1155.
44 I. Berger, A. A. Nazarov, C. G. Hartinger, M. Groessl, S.-M. Valiahdi, M. A. Jakupec and B. K. Keppler, *ChemMedChem*, 2007, **2**, 505–514.

2.3. From Hydrolytically Labile to Hydrolytically Stable Ru(II)-Arene Anticancer Complexes with Carbohydrate-Derived Co-ligands

Muhammad Hanif, Samuel M. Meier, Wolfgang Kandioller, Anna Bytzek, Michaela Hejl, Christian G. Hartinger, Alexey A. Nazarov, Vladimir B. Arion, Michael A. Jakupec, Paul J. Dyson, Bernhard K. Keppler

Journal of Inorganic Biochemistry, **2010,** in Press

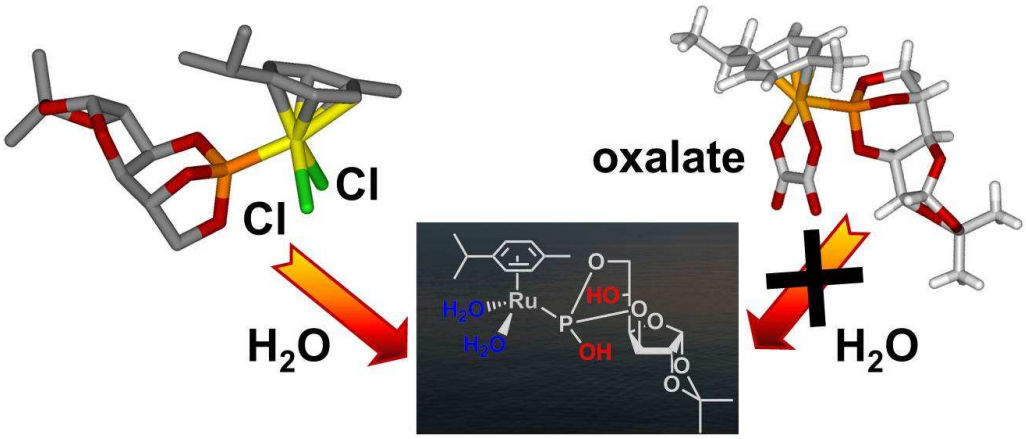

Journal of Inorganic Biochemistry xxx (2010) xxx–xxx

Contents lists available at ScienceDirect

Journal of Inorganic Biochemistry

journal homepage: www.elsevier.com/locate/jinorgbio

From hydrolytically labile to hydrolytically stable Ru(II)–arene anticancer complexes with carbohydrate-derived co-ligands

Muhammad Hanif [a], Samuel M. Meier [a,c], Wolfgang Kandioller [a], Anna Bytzek [a], Michaela Hejl [a], Christian G. Hartinger [a,c,*], Alexey A. Nazarov [a,b,*], Vladimir B. Arion [a,c], Michael A. Jakupec [a,c], Paul J. Dyson [b], Bernhard K. Keppler [a,c]

[a] University of Vienna, Institute of Inorganic Chemistry, Waehringer Str. 42, A-1090 Vienna, Austria
[b] Institut des Sciences et Ingénierie Chimiques, Ecole Polytechnique Fédérale de Lausanne (EPFL), CH-1015 Lausanne, Switzerland
[c] University of Vienna, Research Platform "Translational Cancer Therapy Research", Waehringer Str. 42, A-1090 Vienna, Austria

ARTICLE INFO

Article history:
Received 13 August 2010
Received in revised form 30 September 2010
Accepted 6 October 2010
Available online xxxx

Keywords:
Anticancer activity
Aquation
Bioorganometallic chemistry
Carbohydrate ligands
Ruthenium

ABSTRACT

The synthesis, characterization, reactivity and *in vitro* anticancer activity of a series of Ru^{II}–arene complexes with carbohydrate-derived phosphite and biscarboxylato co-ligands are reported. The compounds were characterized by NMR spectroscopy and electrospray ionization (ESI) mass spectrometry, and the molecular structures of oxalato(η^6-*p*-cymene)(3,5,6-bicyclophosphite-1,2-*O*-isopropylidene-α-d-glucofuranoside)ruthenium(II) and oxalato(η^6-*p*-cymene)(3,5,6-bicyclophosphite-1,2-*O*-cyclohexylidene-α-d-glucofuranoside)ruthenium(II) were determined by X-ray diffraction analysis. In contrast to their dichlorido counterparts, the biscarboxylato complexes did not exhibit significant reactivity towards biomolecules, such as cysteine, methionine, ubiquitin or the DNA model 5′-GMP, and resist hydrolysis; no hydrolytic species were detected by ^{1}H and ^{31}P{^{1}H} NMR spectroscopy over several days. These structural alterations led to a decrease in the tumor-inhibiting potency of the compounds in human cancer cell lines.

1. Introduction

Organometallic medicinal chemistry is an emerging research area with considerable potential [1]. In recent years many examples of organometallic compounds appeared that exhibit potent anticancer activity [1–4], including compounds that selectively inhibit enzymes [5–9], block receptors [2], or have been used to label peptides or other biomolecules [10,11]. Indeed, titanocene dichloride, Cp_2TiCl_2, entered clinical trials as an anticancer agent [12,13], and other compounds are expected to follow.

One of the most investigated class of organometallic compounds are based on the Ru^{II}–arene unit linked to ethylenediamine (en) [14,15], 1,3,5-triaza-7-phosphatricyclo[3.3.1.1]decane (pta) [16], pyr(id)ones [17–19] or bioactive groups [5,6,8,9,20]. For example, the so-called RAPTA compounds are a large family of organometallic compounds with general formula [Ru^{II}(η^6-arene)(pta)Cl_2] (for RAPTA-C, see Fig. 1), which have been extensively investigated for their tumor-inhibiting properties. *In vivo* studies on some RAPTA compounds have shown excellent inhibition of metastases growth in CBA mice bearing the MCa mammary carcinoma while exhibiting selective, but mild cytotoxicity towards the TS/A tumorigenic cell line as opposed to the HBL-100 non-tumorigenic cell line in *in vitro* anticancer assays [16]. RAPTA complexes undergo aquation of the chloride ligand(s) in aqueous solution [21]. The extent of the aquation depends on the concentration of the complex in solution, the amount of chloride present and the pH. Hydrolysis was found to be suppressed at the high chloride concentration found in blood plasma (*ca.* 100 mM), but occurs at chloride concentrations typical of cell cytoplasm (*ca.* 4 mM), representing a possible activation pathway.

In order to improve their efficacy, a number of structural modifications have been made to the basic RAPTA framework such as introduction of H-bonding functionalities [22], change of the arene ligand [16] or the leaving group (Fig. 1) [23] and tethering to bioactive segments such as human serum albumin which resulted in a twentyfold increase in cytotoxicity with respect to prototype RAPTA-C [24].

By replacing the pta moiety with sugar-phosphite ligands with similar hydrophilicity [25,26], RAPTA-like analogues were obtained, capable of targeting cancer cells by exploiting the increased glucose uptake resulting from overexpression of glucose transporters and glycolytic enzymes [25,27]. This concept led to the development of compounds with the general formula [Ru^{II}(η^6-*p*-cymene)(3,5,6-bicyclophosphite-α-d-glucofuranoside)Cl_2]. The complexes showed moderate cytotoxicity, with certain selectivity for tumor cells over non-tumorigenic cells, and

* Corresponding authors. University of Vienna, Institute of Inorganic Chemistry, Waehringer Str. 42, A-1090 Vienna, Austria. Tel.: +43 1 4277 52609; fax: +43 1 4277 52680.
E-mail addresses: christian.hartinger@univie.ac.at (C.G. Hartinger), alex.nazarov@univie.ac.at (A.A. Nazarov).

0162-0134/$ – see front matter © 2010 Published by Elsevier Inc.
doi:10.1016/j.jinorgbio.2010.10.004

Please cite this article as: M. Hanif, et al., From hydrolytically labile to hydrolytically stable Ru(II)–arene anticancer complexes with carbohydrate-derived co-ligands, J. Inorg. Biochem. (2010), doi:10.1016/j.jinorgbio.2010.10.004

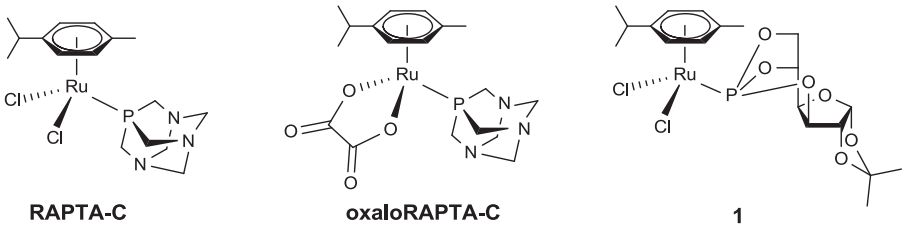

Fig. 1. Structures of anticancer RAPTA complexes and an analogues carbohydrate-derived compound.

importantly activity in cisplatin-resistant cells [26]. The cytotoxicity appears to be determined, to some extent, by lipophilicity, *i.e.*, the most lipophilic compound was the most cytotoxic. These compounds are prone to aquation/hydrolysis similar to RAPTA compounds in that they undergo aquation of the first halido ligand in aqueous solution, but additionally the hydrolysis of a P–O bond of the phosphite ligand, and ultimately the formation of inert dinuclear species takes place [26,28].

Use of anionic chelating ligands such as oxalate instead of halido ligands has already been employed to overcome the problem of solubility problems and stability in platinum compounds and with titanocenes [1,3,29], and the replacement of the two chlorido ligands in RAPTA-C by oxalate resulted in a complex which resists aquation [23]. In this paper we describe the influence of the leaving group on hydrolysis, binding to biomolecules, and cytotoxicity for a series of carbohydrate–ruthenium(II)-arene complexes, with oxalato and malonato leaving groups, and compare it to data obtained for structurally similar Os compounds [30].

2. Experimental

All reactions were carried out in dry solvents under argon atmosphere. Chemicals were obtained from commercial suppliers and used as received. Ubiquitin from bovine red blood cells was purchased from Sigma, L-cysteine from Fluka and L-methionine from Sigma-Aldrich and used as obtained. MeOH (VWR Int., 20864.320, HiPerSolv CHROMANORM), formic acid (Fluka) and milliQ H_2O were used as solvents for MS studies. For the microemulsion electrokinetic chromatography studies sodium dodecyl sulfate (SDS), dodecanophenone, 1-butanol and sodium monohydrogenphosphate were purchased from Sigma-Aldrich. Sodium hydroxide solution (0.1 M), hydrochloric acid, heptane and sodium dihydrogenphosphate were obtained from Fluka, and DMSO from Fisher Scientific. Methanol and CH_2Cl_2 used in synthesis were dried using standard procedures. Dichlorido(η^6-*p*-cymene)(3,5,6-bicyclophosphite-1,2-*O*-isopropylidene-α-d-glucofuranoside)ruthenium(II) **1** [26], the dimer bis [dichlorido(η^6-*p*-cymene)ruthenium(II)] {[Ru^{II}(cym)Cl(μ-Cl)]$_2$ **a** [31]}, 3,5,6-bicyclophosphite-1,2-*O*-isopropylidene-α-d-glucofuranoside **I** [32], 3,5,6-bicyclophosphite-1,2-*O*-cyclohexylidene-α-d-glucofuranoside **II** [32], 1,2-*O*-(2,2,2-trichloroethylidene)-α-d-glucofuranose 3,5,6-bicyclophosphite **III** [33], disilver oxalate [23] and oxalato(η^6-*p*-cymene)(3,5,6-bicyclophosphite-1,2-*O*-isopropylidene-α-d-glucofuranoside)osmium(II) **2^{Os}** and oxalato(η^6-*p*-cymene)(3,5,6-bicyclophosphite-1,2-*O*-cyclohexylidene-α-d-glucofuranoside)osmium(II) **3^{Os}** [23] were synthesized using literature procedures. ^{1}H, ^{13}C{^{1}H} and ^{31}P{^{1} H} NMR spectra were recorded at 25 °C on a Bruker FT NMR spectrometer Avance III 500 MHz at 500.10 (^{1}H), 125.75 (^{13}C{^{1}H}) and 202.44 MHz (^{31}P{^{1}H}). The ^{31}P NMR spectra were referenced to 85% phosphoric acid. 2D NMR spectra were collected in a gradient-enhanced mode. Specific optical rotations were determined on a Perkin-Elmer 341 polarimeter in a 10 cm cell at 20 °C. Melting points were measured on a Büchi B-540 apparatus and are uncorrected. Elemental analysis was determined by the Laboratory for Elemental Analysis, Faculty of Chemistry, University of Vienna, on a Perkin-Elmer 2400 CHN Elemental Analyzer. Electrospray ionization mass spectra were recorded on a Bruker esquire$_{3000}$.

2.1. General procedure for the synthesis of 2–6

The dimer [(η^6-cymene)RuCl(μ-Cl)]$_2$ (122 mg, 0.20 mmol) and silver dicarboxylate (0.44 mmol) were stirred in water (25 mL) for 12 h. The mixture was filtered through a bed of Celite to remove the AgCl precipitate. The solvent was removed under vacuum, and the residue was redissolved in methanol (25 mL) and the carbohydrate ligand (0.40 mmol) was added. The reaction mixture was stirred for 2 h, then the volume of the solution was reduced to 5 mL and diethyl ether (25 mL) was added. The slurry was cooled to 4 °C for 12 h to afford a yellow crystalline product that was isolated by filtration, washed with diethyl ether (2×5 mL) and dried under vacuum.

Oxalato(η^6-*p*-cymene)(3,5,6-bicyclophosphite-1,2-*O*-isopropylidene-α-d-glucofuranoside)ruthenium(II) 2 was prepared following the general procedure, using silver oxalate (133 mg, 0.44 mmol) and 1,2-*O*-isopropylidene-α-d-glucofuranose 3,5,6-bicyclophosphite (100 mg, 0.40 mmol). Crystals suitable for X-ray diffraction studies were grown by slow diffusion from diethyl ether and methanol. Yield: 190 mg (83%), m.p. 175–177 °C (decomp.), Elemental analysis, found % C, 43.37; H, 4.91; calcd. for $C_{21}H_{27}O_{10}PRu\cdot0.5H_2O$, C, 43.45; H, 4.86. MS (ESI$^+$): *m/z*: 572.7 (573.0) [M + H]$^+$, 595.1 (595.0) [M + Na]$^+$; ^{1}H NMR (500.10 MHz, $CDCl_3$, 25 °C, d = doublet, m = multiplet, s = singlet, brs = broad singlet): δ = 6.08 (d, J = 4 Hz, 1H; H-1), 5.88 (d, J = 6 Hz, 1H; H–Ar), 5.86 (d, J = 6 Hz, 1H; H–Ar), 5.74 (d, J = 5 Hz, 1H; H–Ar), 5.71 (d, J = 5 Hz, 1H; H–Ar), 5.15–5.18 (m, 1H; H-5), 4.71 (brs, 1H; H-3), 4.60 (d, J = 4 Hz, 1H; H-2), 4.56 (brs, 1H; H-6), 4.34 (brs, 2H; H-4, H-6′), 2.77–2.82 (m, 1H; C*H*(CH_3)$_2$), 2.22 (s, 3H; CH_3), 1.46 (s, 3H; C(CH_3)$_2$), 1.30 (s, 3H; C(CH_3)$_2$), 1.29 (d, J = 7 Hz, 3H; CH(C*H*$_3$)$_2$), 1.28 (d, J = 7 Hz, 3H; CH(C*H*$_3$)$_2$) ppm; ^{13}C{^{1}H} NMR (125.75 MHz, $CDCl_3$, 25 °C): δ = 165.2 (J = 4 Hz; C=O), 112.6 (*C*(CH_3)$_2$), 109.3 (C–Ar), 105.7 (C-1), 105.0 (C–Ar), 89.8 (*C*H–Ar), 89.6 (*C*H–Ar), 89.0 (*C*H–Ar), 88.2 (*C*H–Ar), 83.6 (J = 5 Hz; C-2), 78.6 (J = 8 Hz; C-3), 76.9 (J = 6 Hz; C-4), 74.7 (J = 5 Hz; C-5), 69.3 (J = 8 Hz; C-6), 31.2 (*C*H(CH_3)$_2$), 26.9 (C(*C*H$_3$)$_2$), 26.2 (C(*C*H$_3$)$_2$), 22.5 (CH(*C*H$_3$)$_2$), 22.4 (CH(*C*H$_3$)$_2$), 18.3 (CH_3) ppm; ^{31}P{^{1}H} NMR (202.44 MHz, $CDCl_3$, 25 °C): δ = 134.1 ppm.

Oxalato(η^6-*p*-cymene)(3,5,6-bicyclophosphite-1,2-*O*-cyclohexylidene-α-d-glucofuranoside)ruthenium(II) 3 was prepared following the general procedure, using silver oxalate (133 mg, 0.44 mmol) and 1,2-*O*-cyclohexylidene-α-d-glucofuranose 3,5,6-bicyclophosphite (115 mg, 0.40 mmol). Crystals suitable for X-ray diffraction studies were grown by slow diffusion from diethyl ether and methanol. Yield: 191 mg, (78%), m.p. 181–183 °C (decomp.), Elemental analysis, found % C, 46.24; H, 4.87; calcd. for $C_{24}H_{31}O_{10}PRu\cdot0.5H_2O$, C, 46.45; H, 5.19. MS (ESI$^+$): *m/z*: 612.8 (613.1) [M + H]$^+$, 635.3 (635.1) [M + Na]$^+$; ^{1}H NMR (500.10 MHz, $CDCl_3$, 25 °C): δ = 6.08 (d, J = 3 Hz, 1H, H-1), 5.87 (d, J = 6 Hz, 1H; H–Ar), 5.85 (d, J = 6 Hz, 1H; H–Ar), 5.72 (d, J = 5 Hz, 1H; H–Ar), 5.70 (d, J = 5 Hz, 1H; H–Ar), 5.14–5.17 (m, 1H, H–5), 4.70 (brs 1H, H-3), 4.61 (d, J = 3 Hz, 1H, H-2), 4.51–4.53 (m, 1H, H-6), 4.32 (brs, 2H, H-4, H-6′), 2.78–2.83 (m, 1H, C*H*(CH_3)$_2$), 2.22 (s, 3H,CH_3), 1.59–1.65 (m, 4H, C_6H_{10}), 1.51–1.55 (m, 6H, C_6H_{10}), 1.29 (d, J = 7 Hz, 3H; CH(C*H*$_3$)$_2$), 1.28 (d, J = 7 Hz, 3H; CH(C*H*$_3$)$_2$) ppm; ^{13}C{^{1}H} NMR (125.75 MHz, $CDCl_3$, 25 °C): δ = 165.1 (J = 4 Hz; C=O), 113.3 (C(CH_3)$_2$), 109.3 (C–Ar), 105.3 (C-1), 105.0 (C–Ar), 89.7 (C–Ar), 89.5 (C–Ar), 88.9 (C–Ar), 88.2 (C–Ar), 83.1 (J = 6 Hz; C-2), 78.7 (J = 8 Hz; C-3), 76.8 (J = 8 Hz; C-4), 74.7 (J = 6 Hz; C-5), 69.2 (J = 6 Hz; C-6), 36.5(C_6H_{10}), 35.6 (C_6H_{10}), 31.1

Please cite this article as: M. Hanif, et al., From hydrolytically labile to hydrolytically stable Ru(II)–arene anticancer complexes with carbohydrate-derived co-ligands, J. Inorg. Biochem. (2010), doi:10.1016/j.jinorgbio.2010.10.004

(CH(CH$_3$)$_2$), 24.7 (C$_6$H$_{10}$), 23.8 (C$_6$H$_{10}$), 23.5 (C$_6$H$_{10}$), 22.5 (CH(CH$_3$)$_2$–Ar), 22.4 (CH(CH$_3$)$_2$–Ar), 18.3 (CH$_3$–Ar) ppm; ^{31}P{^{1}H} NMR (202.44 MHz, CDCl$_3$, 25 °C): δ = 134.1 ppm.

Oxalato(η^6-*p*-cymene)(3,5,6-bicyclophosphite-1,2-*O*-(2,2,2-trichloroethylidene-α-d-glucofuranoside)ruthenium(II) 4 was prepared following the general procedure, using silver oxalate (133 mg, 0.44 mmol) and 1,2-*O*-(2,2,2-trichloroethylidene)-α-d-glucofuranose 3,5,6-bicyclophosphite (135 mg, 0.40 mmol). Yield: 177 mg (67%), m.p. 251–252 °C (decomp.), Elemental analysis, found% C, 35.34; H, 3.26; calcd. for C$_{20}$H$_{22}$O$_{10}$Cl$_3$PRu·0.75H$_2$O, C, 35.62; H, 3.51. MS (ESI$^+$): *m/z*: 662.6 (662.9) [M + H]$^+$; ^{1}H NMR (500.10 MHz, CDCl$_3$, 25 °C): δ = 6.29 (d, J = 4 Hz, 1H; H-1), 6.14 (d, J = 5 Hz, 1H; H–Ar), 6.12 (d, J = 5 Hz, 1H; H–Ar), 5.92 (d, J = 6 Hz, 1H; H–Ar), 5.90 (d, J = 6 Hz, 1H; H–Ar), 5.57 (s, 1H, *CH*CCl$_3$), 5.20–5.24 (m , 1H; H-5), 5.04 (d, J = 3 Hz, 1H; H-3), 4.84 (d, J = 3 Hz, 1H; H-2), 4.77–4.81 (m, 1H; H-6), 4.71 (brs, 1H; H-4), 4.06–4.10 (m, 1H; H-6′), 2.63–2.68 (m, 1H; C*H*(CH$_3$)$_2$), 2.07 (s, 3H; Ar–CH$_3$), 1.20 (d, J = 7 Hz, 6H; CH(C*H*$_3$)$_2$) ppm; ^{13}C{^{1}H} NMR (125.75 MHz, CDCl$_3$, 25 °C): δ = 164.6 (J = 6 Hz; C=O), 108.6 (C–Ar), 106.9 (C-1), 106.5 (*C*H–Ar), 104.8 (C–Ar), 97.4 (CCl$_3$), 90.8 (*C*H–Ar), 89.0 (*C*H–Ar), 88.6 (*C*H–Ar), 86.0 (J = 6 Hz; C-2), 78.6 (J = 5 Hz; C-3), 77.9 (J = 8 Hz; C-4), 74.4 (J = 5 Hz; C-5), 69.1 (J = 9 Hz; C-6), 31.1 (*C*H(CH$_3$)$_2$), 24.5 (*C*HCCl$_3$), 22.5 (CH(*C*H$_3$)$_2$), 22.4 (CH(*C*H$_3$)$_2$), 18.1 (CH$_3$) ppm; ^{31}P{^{1}H} NMR (202.44 MHz, CDCl$_3$, 25 °C): δ = 135.0 ppm.

Malonato(η^6-*p*-cymene)(3,5,6-bicyclophosphite-1,2-*O*-isopropylidene-α-d-glucofuranoside)ruthenium(II) 5 was prepared following the general procedure, using silver malonate (140 mg, 0.44 mmol) and 1,2-*O*-isopropylidene-α-d-glucofuranose 3,5,6-bicyclophosphite (100 mg, 0.40 mmol). Yield: 168 mg (72%), m.p.>200 °C (decomp.), Elemental analysis, found% C, 43.62; H, 5.05; calcd. for C$_{22}$H$_{29}$O$_{10}$PRu·H$_2$O, C, 43.78; H, 5.18. MS (ESI$^+$): *m/z*: 608.9 (609.0) [M + Na]$^+$; ^{1}H NMR (500.10 MHz, CDCl$_3$, 25 °C): δ = 6.09 (d, J = 4 Hz, 1H; H-1), 5.81 (d, J = 7 Hz, 1H; H–Ar), 5.80 (d, J = 7 Hz, 1H; H–Ar), 5.68 (d, J = 6 Hz, 2H; H–Ar), 5.64 (d, J = 6 Hz, 2H; H–Ar), 5.17–5.20 (m, 1H; H-5), 4.73 (brs, 1H; H-3), 4.66 (d, J = 3.5 Hz, 1H; H-2), 4.52–4.56 (m, 1H; H-6), 4.33–4.34 (m, 2H; H-4 and H-6′), 3.41 (d, J = 17 Hz, 1H, CH$_2$COO), 3.20 (d, J = 17 Hz, 1H, CH$_2$COO), 2.80–2.86 (m, 1H; C*H*(CH$_3$)$_2$), 2.19 (s, 3H; CH$_3$), 1.49 (s, 3H; C(CH$_3$)$_2$), 1.32 (s, 3H; C(CH$_3$)$_2$), 1.26 (d, J = 7 Hz, 3H; CH(C*H*$_3$)$_2$) ppm; ^{13}C{^{1}H} NMR (125.75 MHz, CDCl$_3$, 25 °C): δ = 175.4 (J = 10 Hz; C=O), 112.7 (C(CH$_3$)$_2$), 109.6 (C–Ar), 106.7 (C–Ar), 105.7 (C-1), 90.0 (C–Ar), 89.7 (C–Ar), 89.4 (C–Ar), 88.9 (C–Ar), 83.4 (J = 5 Hz; C-2), 78.7 (J = 8 Hz; C-3), 76.7 (J = 10 Hz; C-4), 74.7 (J = 5 Hz; C-5), 69.0 (J = 9 Hz; C-6), 46.8 (*C*H$_2$COO), 30.7 (*C*H(CH$_3$)$_2$), 26.8 (C(*C*H$_3$)$_2$), 26.1 (C(*C*H$_3$)$_2$), 22.2 (CH(*C*H$_3$)$_2$), 18.1 (CH$_3$) ppm; ^{31}P{^{1}H} NMR (202.44 MHz, CDCl$_3$, 25 °C): δ = 137.4 ppm.

Malonato(η^6-*p*-cymene)(3,5,6-bicyclophosphite-1,2-*O*-cyclohexylidene-α-d-glucofuranoside)ruthenium(II) 6 was prepared following the general procedure, using silver malonate (140 mg, 0.44 mmol) and 1,2-*O*-cyclohexylidene-α-d-glucofuranose 3,5,6-bicyclophosphite (115 mg, 0.40 mmol). Yield: 185 mg (74%), m.p.> 200 °C (decomp.), Elemental analysis, found% C, 46.39; H, 5.75; calcd. for C$_{25}$H$_{33}$O$_{10}$PRu·H$_2$O, C, 46.65; H, 5.48. MS (ESI$^+$): *m/z*: 648.8 (649.1) [M + Na]$^+$; ^{1}H NMR (500.10 MHz, CDCl$_3$, 25 °C): δ = 6.09 (d, J = 4 Hz, 1H; H-1), 5.80 (d, J = 7 Hz, 1H; H–Ar), 5.79 (d, J = 7 Hz, 1H; H–Ar), 5.67 (d, J = 6 Hz, 2H; H–Ar), 5.62 (d, J = 6 Hz, 2H; H–Ar), 5.16–5.19 (m, 1H; H-5), 4.74 (brs, 1H; H-3), 4.65 (d, J = 4 Hz, 1H; H-2), 4.50–4.54 (m, 1H; H-6), 4.33 (brs, 2H; H-4 and H-6′), 3.40 (d, J = 17 Hz, 1H, CH$_2$COO), 3.20 (d, J = 17 Hz, 1H, CH$_2$COO), 2.81–2.86 (m, 1H; C*H*(CH$_3$)$_2$), 2.20 (s, 3H; CH$_3$), 1.64–1.67 (m, 4H, C$_6$H$_{10}$), 1.53–1.55 (m, 6H, C$_6$H$_{10}$), 1.26 (d, J = 7 Hz, 3H; CH(C*H*$_3$)$_2$), 1.25 (d, J = 7 Hz, 3H; CH(C*H*$_3$)$_2$) ppm; ^{13}C{^{1}H} NMR (125.75 MHz, CDCl$_3$, 25 °C): δ = 175.4 (J = 9 Hz; C=O), 113.4 (C(CH$_3$)$_2$), 109.6 (C–Ar), 106.7 (C–Ar), 105.3 (C-1), 90.1 (C–Ar), 89.7 (C–Ar), 89.4 (C–Ar), 88.8 (C–Ar), 83.0 (J = 5 Hz; C-2), 78.8 (J = 8 Hz; C-3), 76.7 (J = 5 Hz; C-4), 74.7 (J = 5 Hz; C-5), 68.9 (J = 9 Hz; C-6), 46.8 (*C*H$_2$COO), 36.4 (C$_6$H$_{10}$), 35.6 (C$_6$H$_{10}$), 30.7 (*C*H(CH$_3$)$_2$), 24.7 (C$_6$H$_{10}$), 23.8 (C$_6$H$_{10}$), 23.4 (C$_6$H$_{10}$), 22.2 (CH(*C*H$_3$)$_2$–Ar), 22.4 (CH(*C*H$_3$)$_2$–Ar), 18.1 (CH$_3$–Ar) ppm; ^{31}P{^{1}H} NMR (202.44 MHz, CDCl$_3$, 25 °C): δ = 137.5 ppm.

2.2. X-ray diffraction analysis

X-ray diffraction measurements of **2** and **3** were performed on a Bruker X8 APEXII CCD diffractometer at 100 K. The crystals were positioned at 40 and 35 mm from the detector and 1386 and 1345 frames, each for 10 and 80 s over 1°, were measured. The data were processed using the SAINT software package [34]. Crystal data, data collection parameters, and structure refinement details are given in Table 1. The structures were solved by direct methods and refined by full-matrix least-squares techniques. Non-hydrogen atoms were refined with anisotropic displacement parameters. H atoms were inserted at calculated positions and refined with a riding model. One of the four co-crystallized methanol molecules was refined with 75% occupancy. The following computer programs were used: structure solution SHELXS-97, refinement SHELXL-97 [35], molecular diagrams ORTEP-3 [36]. Crystallographic data for the structural analysis of **2** and **3** has been deposited with the Cambridge Crystallographic Data Centre, CCDC 785120 and 785121, respectively. These data can be obtained free of charge from The Cambridge Crystallographic Data Centre via www.ccdc.cam.ac.uk/data_request/cif.

2.3. Reactions with biomolecules

2.3.1. NMR spectroscopy

Solutions of **1** or **2** containing either Cys, Met (both 1:1) or GMP (1:2) were prepared in D$_2$O (pH 4–5) and kept at room temperature for 5 days. The reaction progress was monitored by ^{1}H and ^{31}P NMR spectroscopy at 0.5, 48 and 120 h. *ESI-MS.* The complexes were incubated at 37 °C with Cys and Met at a molar ratio of 1:1 and with ubiquitin at 2:1 molar ratio in milliQ water (18.2 MΩ; Millipore Synergy 185 UV Ultrapure Water system; Molsheim, France). The

Table 1
Crystal data and details of data collection for **2** and **3**.

Compound	**2**	**3**
Chemical formula	C$_{22}$H$_{31}$O$_{11}$PRu	C$_{25.88}$H$_{38.50}$O$_{11.88}$PRu
M (g mol^{-1})	603.51	671.61
Temperature (K)	100(2)	100(2)
Crystal size (mm)	0.20 × 0.10 × 0.03	0.25 × 0.08 × 0.04
Crystal color, habit	yellow, plate	orange, stick
Crystal system	orthorhombic	monoclinic
Space group	$P2_12_12_1$	$P2_1$
a (Å)	8.2719(7)	15.1978(9)
b (Å)	12.9548(14)	13.0153(7)
c (Å)	22.785(2)	15.7673(9)
V (Å^3)	2441.7(4)	2964.0(3)
Z	4	4
D_c (g cm^{-3})	1.642	1.505
μ (cm^{-1})	7.67	6.42
F(000)	1240	1391
Θ range for data collection (°)	2.92 to 26.00	2.72 to 26.00
h range	−10/10	−18/18
k range	−15/15	−16/16
l range	−28/28	−19/19
No. refls. used in refinement	4781	11628
No. parameters	319	731
R_{int}	0.1242	0.0775
R_1 (obs.)[a]	0.0503	0.0374
wR_2 (all data)[b]	0.1266	0.0837
Flack parameter	0.01(5)	−0.05(2)
S[c]	1.053	1.006

[a] Refinement was by full-matrix least-squares (Fo2) for all reflections, R1 = Σ||Fo|−|Fc||/Σ|Fo|.
[b] wR2 = {Σ[w(Fo2−Fc2)2]/Σ[w(Fo2)2]}1/2.
[c] Goodness of fit, S = {Σ[w(Fo2−Fc2)2]/(n−p)}1/2.

Please cite this article as: M. Hanif, et al., From hydrolytically labile to hydrolytically stable Ru(II)–arene anticancer complexes with carbohydrate-derived co-ligands, J. Inorg. Biochem. (2010), doi:10.1016/j.jinorgbio.2010.10.004

samples containing amino acids were diluted with MeOH, and the protein incubation mixtures were diluted with H_2O/MeOH/formic acid (50:50:0.1). Mass spectra were recorded after 3, 6, 24, 72 h and 7 days at concentrations of 1–10 μM, using a Bruker esquire3000 ion trap mass spectrometer with direct infusion at a flow rate of 5 μl/min. The experimental conditions were as follows: capillary 4.5 kV, end plate offset 0.5 kV, skim1 45.5 V, skim2 6 V, cap exit offset 78.4 V and dry temperature 200 °C. The spectra were recorded using ESI Compass 1.3 (Bruker) and DataAnalysis 4.0 software. Deconvolution was obtained by the maximum entropy algorithm with a 0.1 *m/z*-mass step and an instrument peak width of 1.

2.4. Aquation studies

For hydrolysis studies, the compounds were dissolved in D_2O and the samples were analyzed by $^{31}P\{^1H\}$ NMR spectroscopy once a day over 15 days. The $^{31}P\{^1H\}$ NMR spectra were recorded on a Bruker Avance 400 instrument at 161.98 MHz.

2.5. Cytotoxicity studies

2.5.1. Cell lines and culture conditions

CH1 (ovarian carcinoma, human) cells were a gift from Lloyd R. Kelland, CRC Centre for Cancer Therapeutics, Institute of Cancer Research, Sutton, UK. SW480 (adenocarcinoma of the colon, human) and A549 (non-small cell lung cancer, human) cells were provided by Brigitte Marian (Institute of Cancer Research, Department of Medicine I, Medical University of Vienna, Austria). All cell culture reagents were purchased from Sigma-Aldrich. Cells were grown in 75 cm² culture flasks (Iwaki) as adherent monolayer cultures in Eagle's Minimal Essential Medium (MEM) supplemented with 10% heat-inactivated fetal calf serum, 1 mM sodium pyruvate and 2 mM l-glutamine at 37 °C under a humidified atmosphere containing 95% air and 5% CO_2.

2.5.2. MTT assay conditions

Cytotoxicity was determined by the colorimetric MTT (3-(4,5-dimethyl-2-thiazolyl)-2,5-diphenyl-2*H*-tetrazolium bromide, Fluka) microculture assay. For this purpose, cells were harvested from culture flasks by trypsinization and seeded in 100 μL aliquots of MEM supplemented with 10% heat-inactivated fetal calf serum, 1 mM sodium pyruvate, 4 mM l-glutamine and 1% non-essential amino acids (100×) into 96-well microculture plates (Iwaki). The following cell densities were chosen to ensure exponential growth of untreated controls throughout the experiment: 1.5×10^3 cells/well (CH1), 2.5×10^3 cells/well (SW480) and 4×10^3 cells/well (A549). Cells were allowed to settle and resume exponential growth for 24 h. The test compounds were dissolved and serially diluted in the same medium and added in aliquots of 100 μL/well. After exposure for 96 h, all media were replaced by 100 μL/well RPMI1640 medium (supplemented with 10% heat-inactivated fetal calf serum) plus 20 μL/well MTT in phosphate-buffered saline (5 mg/mL). After incubation for 4 h, the supernatants were removed, and the formazan crystals formed by viable cells were dissolved in 150 μL DMSO per well. Optical densities at 550 nm were measured with a microplate reader (Tecan Spectra Classic), using a reference wavelength of 690 nm to correct for unspecific absorption. The quantity of viable cells was expressed as percentages of untreated controls, and 50% inhibitory concentrations (IC_{50}) were calculated from concentration–effect curves by interpolation. The results given are mean values from at least three or two independent experiments in case of activity or inactivity, respectively, each comprising three replicates per concentration level.

2.6. Microemulsion electrokinetic chromatography (MEEKC) studies

CE separations were carried out on an HP^{3D} CE system (Agilent, Waldbronn, Germany) equipped with an on-column diode-array detector and the analytes were detected by UV absorption at 200 nm. For all measurements, capillaries of 48.5 cm total length (40 cm effective length; 50 μm ID) were used (Polymicro Technologies, Phoenix, AZ, USA). Capillary and sample tray were thermostatted at 25 °C. The sample injection was carried out by hydrodynamic injection at 10 mbar for 15 s with a separation voltage of 25 kV. New capillaries were conditioned with 0.1 M HCl, water, 0.1 M NaOH, and again with water (10 min each). The capillary was flushed with 0.1 M NaOH, water, and BGE for 5 min each before the first run each run. Before each injection the capillary was purged with 0.1 M NaOH, water and the BGE for 2 min each.

The following component ratios (wt.%) were used to establish a stable microemulsion: 91.22% sodium phosphate buffer (20 mM, pH 7.4), 0.84% heptane, 1.47% SDS, and 6.48% 1-butanol. For the preparation of the MEEKC solutions, surfactant, alcohol, oil, and a small portion of buffer were mixed by sonication for 5 min. The residual buffer was then slowly added to the mixture. Afterwards, the solution was kept for 30 min at room temperature before use. The analytes were dissolved in the microemulsion to give concentrations between 0.45 and 0.6 mg/ml. DMSO and dodecanophenone were used as markers for the electroosmotic flow (EOF) and the microemulsion droplets, respectively: to 1 ml of the sample solution 1 μl DMSO and 20 μl dodecanophenone (18 mg/ml in methanol) were added.

The capacity factor, k, is defined as the ratio n_{me}/n_{aq} (n_{me} = total number of moles of solute in the microemulsion phase, n_{aq} = total number of moles of solute in the aqueous phase) and this mass distribution coefficient can be calculated according to Eq. (1) [t_o = migration time of an unretained substance (EOF marker), t_{me} = migration time of the microemulsion, t_R = solute migration time] [37,38].

$$k = \frac{t_R - t_0}{t_0\left(1 - {}^{t_R}/_{t_{me}}\right)} \quad (1)$$

3. Results and discussion

In previous work, we prepared RAPTA-C analogues by linking various carbohydrate-derived ligands to Ru^{II}–arene scaffold, and some examples such as dichlorido(η^6-*p*-cymene)(3,5,6-bicyclophosphite-1,2-*O*-isopropylidene-α-d-glucofuranoside)ruthenium(II) **1** were more anticancer active than RAPTA-C in *in vitro* assays. The complexes were found to exhibit aquation of the first halido ligand in aqueous solution, followed by hydrolysis of a P–O bond of the phosphite ligand, and finally formation of dinuclear species [26]. In order to study the influence of chelating ligands on the hydrolysis, reactivity towards biomolecules and cytotoxicity of the complexes, we synthesized carbohydrate containing Ru^{II}–arene dicarboxylato compounds. This concept proved successful in case of RAPTA complexes [23], which undergo rapid hydrolysis in aqueous media, although they can be stabilized by high concentrations of NaCl [21]. These dicarboxylate species were found to be highly soluble and kinetically more stable than their RAPTA precursors with the two chlorido ligands and notably, the anticancer activity was maintained, as was their reactivity with biomolecules [23].

3.1. Synthesis and characterization

The preparation of the Ru^{II}–arene biscarboxylato complexes, **2**–**6**, is summarized in Scheme 1, and follows a literature procedure [23]. In the first step, [biscarboxylato(η^6-*p*-cymene)(H_2O)ruthenium(II)] was formed by reacting bis[dichlorido(η^6-*p*-cymene)ruthenium(II)] with disilver oxalate or malonate (obtained by reacting 2.2 eq. of $AgNO_3$ with disodium oxalate and malonate) in water. In the second step the aqua species was stirred for 2 h in CH_3OH with the respective

Please cite this article as: M. Hanif, et al., From hydrolytically labile to hydrolytically stable Ru(II)–arene anticancer complexes with carbohydrate-derived co-ligands, J. Inorg. Biochem. (2010), doi:10.1016/j.jinorgbio.2010.10.004

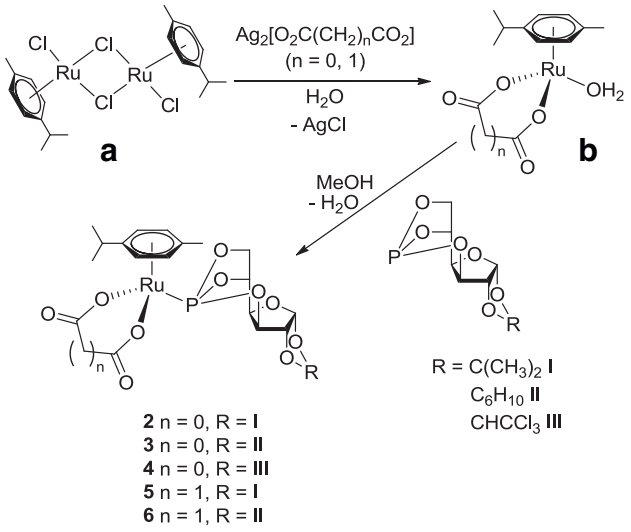

Scheme 1. Synthetic route to biscarboxylato Ru^{II}–arene compounds with sugar-derived co-ligands.

carbohydrate-based phosphorus ligand. This reaction sequence avoids side reactions involving the silver ions and the phosphorus ligand.

The complexes were characterized by 1D and 2D NMR spectroscopy, ESI-MS, and elemental analysis (see Experimental for full details). ^{31}P NMR spectroscopy is very informative as coordination of the P-containing sugar ligands to the metal center results in a significant change in frequency from 117 ppm to 134–137 ppm. These values are in the same range as those observed for the analogous Ru compounds with chlorido ligands [26]. In the ^{1}H NMR spectra of malonato Ru–arene complexes, the methylene protons of the malonic acid become diastereotopic upon complexation and give two doublets centered at about $\delta = 3.4$ and 3.2 ppm with a geminal coupling constant $^{2}J_{(H,H)} = 17$ Hz, as expected for an AB system. The $^{13}C\{^{1}H\}$ NMR spectra of **2**–**6** contain prominent signals at *ca.* 165 and 175 ppm that correspond to coordinated carboxylates of oxalato and malonato ligands, respectively.

Single crystals of **2** and **3** suitable for X-ray diffraction studies were grown by slow diffusion of diethyl ether into a solution of the complex in methanol. Their molecular structures are shown in Fig. 2, and as expected, confirm the piano-stool geometry typical of such systems [5,18,23,39]. The ruthenium–centroid$_{arene}$ distances are 1.703 and 1.704 Å in **2** and **3**, which are similar to that observed in the dichlorido analogue (1.711 Å) [26]. Both **2** and **3** are solvated by methanol which forms H-bonds with a carbonyl oxygen of the oxalato ligand. The key binding parameters, such as Ru–P and Ru–O bond lengths, are similar to those of oxalo-RAPTA-C (see Table 2) [23].

3.2. Aquatic stability

In order to study the influence of chelating biscarboxylate ligands on the behaviour of carbohydrate-based Ru^{II}–arene complexes in aqueous solution, **2** and **5** were dissolved in D_2O and the reaction was monitored by ^{1}H and $^{31}P\{^{1}H\}$ NMR spectroscopy over 15 days. As expected, the exchange of the chlorido ligands by biscarboxylato resulted in enhanced stability of the compounds. Both the oxalato and malonato derivatives are stable towards aquation over one week and no aquation products were identified. In the case of the dichlorido Ru^{II}–arene analogues mono aqua species are formed within a few hours followed by cleavage of the P–O(C5) bond of the sugar-derived phosphorous ligand, terminating in the formation of dinuclear species [26]. The same trends were basically confirmed by ESI-MS, but in addition, a peak at *m/z* 564.88 ± 0.02 that may be assigned to $[(cym)_2Ru_2(\mu\text{-}MeO)_3]^+$ (19%, exact mass 565.08) was observed. This species presumably results from the exchange of the hydroxido ligands in $[(cym)_2Ru_2(\mu\text{-}OH)_3]^+$ with the methanol added to assist the spraying/ionization process.

3.3. Reactivity with biomolecules

As shown above, in water the complexes are inert, but it has previously been shown that in the presence of other ligands (such as in biological media) reactions may occur more rapidly [23,26]. Consequently, the reactivity of **1** and **2** with the sulfur-containing amino acids Cys and Met, with the small protein ubiquitin as well as 5′-GMP as a DNA model were carried out in aqueous solution. In particular, the binding to proteinaceous targets appears to be of relevance to the mode of action of organometallic Ru(arene) complexes [9,40–44], although they are also known to have high affinity to DNA [44,45].

Analysis of samples containing **1** and Met by ESI-MS revealed adduct formation during the first hours of incubation, with the formation of a signal at *m/z* 649.84 ± 0.02 (relative intensity 76%, exact mass 650.11) assignable to the ion $[\mathbf{1}\text{–}2Cl + Met + OH]^+$ (Table 3). With time the main peak observed in the spectrum is

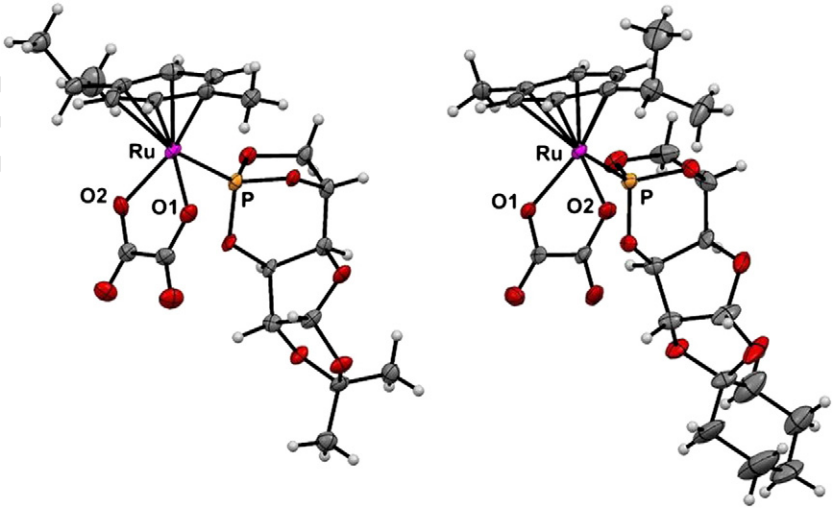

Fig. 2. Molecular structures of **2** and one of the two crystallographically independent molecules of **3** (**3A**); thermal ellipsoids are drawn at 50% probability level and solvent molecules were omitted for clarity.

Please cite this article as: M. Hanif, et al., From hydrolytically labile to hydrolytically stable Ru(II)–arene anticancer complexes with carbohydrate-derived co-ligands, J. Inorg. Biochem. (2010), doi:10.1016/j.jinorgbio.2010.10.004

Table 2
Selected bond lengths (Å) and bond angles (°) of **1**–**3** and the structurally related compound OxaloRAPTA for comparison purposes.

	1[a]	**2**	**3**[c]		OxaloRAPTA-C[b]
			A	B	
Ru–O1	–	2.073 (4)	2.071 (3)	2.071 (3)	2.093 (2)
Ru–O2	–	2.109 (4)	2.087 (3)	2.088 (3)	2.095−(1)
Ru–P	2.2406 (11)	2.2491 (16)	2.2500 (11)	2.2492 (12)	2.310 (1)
Ru-centroid	1.711	1.703 (3)	1.701 (2)	1.704 (2)	1.690
O–Ru–O	–	79.11 (17)	78.89 (11)	78.62 (12)	78.43 (7)
O1–Ru–P	–	85.95 (12)	86.25 (8)	85.40 (8)	82.83 (5)
O2–Ru–P	–	89.37 (14)	89.05 (9)	89.21 (9)	88.79 (5)

[a,b] Taken from Refs. [26] and [23], respectively.
[c] There are two crystallographically independent molecules of **3** in the asymmetric unit.

Table 3
Relative abundance of selected adducts between **1** and **2** and Met, Cys and Ub referenced to the most abundant species in the ESI mass spectra recorded after 24, 72 and 168 h of incubation.

Bioligand	Compound	Adduct	Relative abundance / %		
			24 h	72 h	168 h
Met	**1**	$[(cym)Ru(Met)-H]^+$	37	100	100
		$[\mathbf{1}-2Cl+OH]^+$	100	26	0
	2	$[(cym)Ru(Met)-H]^+$	3	24	100
		$[\mathbf{2}+H]^+$	100	100	9
Cys	**1**	$[(cym)Ru(Cys)-H]^+$	10	0	–[a]
		$[\mathbf{1}-2Cl+OH]^+$	100	100	–[a]
	2	$[(cym)Ru(Cys)-H]^+$	0	4	0
		$[\mathbf{2}+H]^+$	100	100	100
Ub	**1**	$[Ub+\{Ru(cym)\}]^+$	66	100	100
		$[Ub]^+$	100	51	31
		$[y_{58}]^+$	38	17	59
	2	$[Ub+\mathbf{2}]^+$	0	0	0
		$[Ub]^+$	100	100	100
		$[y_{58}]^+$	13	16	34

[a] Cysteine appears to decompose the complexes completely within 168 h.

found at *m/z* 383.83 ± 0.02 (100% after 72 h, exact mass 384.06), which corresponds to $[(cym)Ru(Met)-H]^+$.

Incubation of **1** with Cys leads to defined products only within the first 24 h where the most abundant signal at *m/z* 500.83 ± 0.02 corresponds to $[\mathbf{1}-2Cl+OH]^+$, followed by *m/z* 355.90 (14%, exact mass 356.04; $[(cym)Ru(Cys)-H]^+$) and *m/z* 855.95 (37%, exact mass 856.06; $[(cym)_2Ru_2(Cys)_3-2H+Na]^+$ and the hydrolysis products discussed before. Over time the intensities of those peaks decrease dramatically and after 72 h they are not assignable to defined reaction products, probably due to Cys decomposing the Ru^{II}–arene complexes present in solution.

In the spectrum of a solution containing **2** and Met recorded after 24 h of reaction, there were only traces of Ru–Met adducts visible in the mass spectrum (Table 3), indicating a much lower reaction rate for the dicarboxylato species. After 72 h, a signal assignable to $[(cym)Ru(Met)-H]^+$ (24%) was observed, which increases in relative intensity over 7 days of incubation to become the most abundant species, similar to the reaction of **1** with Met. In contrast to the reaction with Met, there is no significant interaction of **2** with Cys indicated by mass spectrometric methods over 7 days of incubation. These observations were also confirmed by NMR spectroscopy.

The reaction of **1** and **2** with the model protein Ub (8564.2 ± 0.2 Da) was monitored over 7 days, and in the case of the dichlorido complex **1**, a steady increase in relative intensity of the mono-adduct $[(cym)Ru+Ub]$ at *m/z* 8797.4 ± 0.6 Da was observed in the deconvoluted mass spectrum (Fig. 3). The phospite ligand is lost during the binding process, as also observed for other Ru^{II}–arene complexes [28]. Although **1** was present in a 2-fold excess no peaks corresponding to bis-adducts were observed. Furthermore, the protein appears to undergo degradation over time, as indicated by the appearance of, *e.g.*, the $[y_{59}+H]^+$ fragment (51% after 72 h). When incubating **2** with Ub, no evidence for adduct formation was found during 7 days of incubation.

The reactivity of **2** with 5′-GMP was evaluated by means of ^1H and $^{31}P\{^1H\}$ NMR spectroscopy and compared to **1**. Samples containing

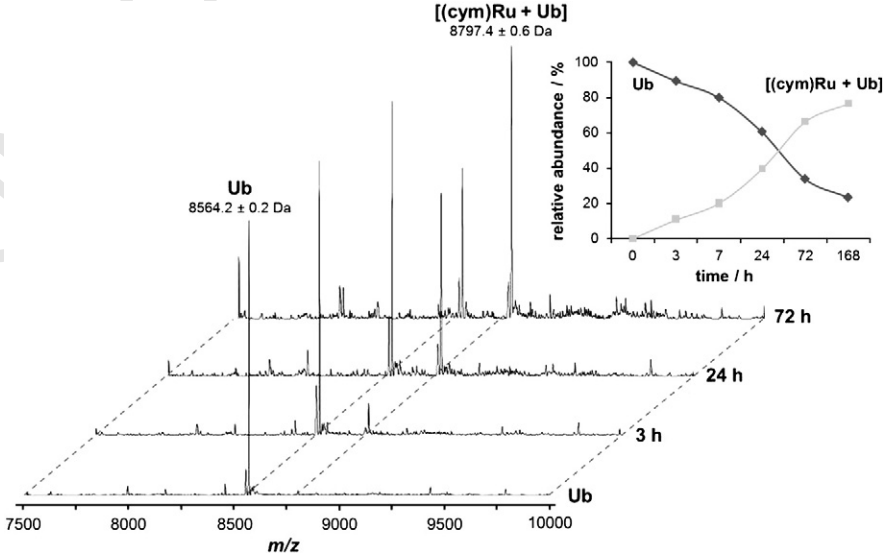

Fig. 3. The reaction of **1** with Ub studied by ESI-MS over a period of 3 days. Upon adduct formation, the carbohydrate ligand of **1** is cleaved.

Please cite this article as: M. Hanif, et al., From hydrolytically labile to hydrolytically stable Ru(II)–arene anticancer complexes with carbohydrate-derived co-ligands, J. Inorg. Biochem. (2010), doi:10.1016/j.jinorgbio.2010.10.004

molar ratios of 1:2 (metal complexes : 5′-GMP) were prepared in D_2O and analyzed after 0.5, 48 and 120 h. These studies reveal low reactivity for **2** with 5′-GMP, whereas **1** and other dichlorido Ru compounds are relatively reactive and form adducts *via* the *N*7 atoms of guanine [26,46].

3.4. Evaluation of the in vitro anticancer activity

The antiproliferative potential of **2**, **3**, **5** and **6** (**4** is not sufficiently soluble in water to be included in the biological assay) was determined in human SW480 colon adenocarcinoma, CH1 ovarian cancer and A549 non-small cell lung cancer cells using the MTT assay, and the obtained results are compared to those of the analogous dichlorido compound **1** and the Os analogues of **2** and **3**, *i.e.*, $\mathbf{2}^{Os}$ and $\mathbf{3}^{Os}$ (Table 4) [30]. In general, only modest antiproliferative activity was observed for this series of sugar compounds, which is not unexpected considering recent literature reports on the tumor-inhibiting properties of different carbohydrate–metal conjugates [25]. Low *in vitro* cytotoxicity is common for many ruthenium drug candidates, including NAMI-A and some Ru^{II}–arene compounds, which nevertheless are often potent *in vivo*, *e.g.*, certain RAPTA complexes against tumor metastases [16,47,48].

In the series of compounds reported here, the replacement of the labile chlorido ligands by chelating biscarboxylates significantly alters the biological activity of the compounds. The IC_{50} values in the CH1 and SW480 cells are approximately 5–7 times lower for the biscarboxylato complexes compared to their dichlorido counterparts [26], with the malonato complexes **5** and **6** being somewhat more active than their oxalato analogues **2** and **3**, suggesting an influence of ligand stability on cytotoxic potency (Fig. 4). In contrast, similar modifications in the RAPTA-type complexes had only a minor effect on their tumor-inhibiting potencies [23]. The variation of the phosphite ligand has a minor influence on anticancer activity, although potential binding to the glucose receptor might by influenced by the substituents at the carbohydrate-derived moiety.

In order to estimate the relative lipophilicity of the compounds, being of relevance for the cellular uptake and therefore for the intracellular concentration, microemulsion electrokinetic chromatography (MEEKC) experiments were conducted and the capacity factors log k were determined for **2**, **3**, **4**, **6** and the Os analogues of **2** and **3**, *i.e.*, $\mathbf{2}^{Os}$ and $\mathbf{3}^{Os}$ (Table 4), using a literature method [25,49]. The separation in MEEKC is not only based on the analytes electrophoretic mobility but on their hydrophobic interaction with the microemulsion droplets. The most active compound **6** was found to have the highest lipophilicity whereas the log k values of the other compounds are in a rather similar range, as are their IC_{50} values.

Table 4
In vitro anticancer activity (mean IC_{50} values ± standard deviations) of **2**, **3**, **5** and **6** in human ovarian cancer (CH1), colon cancer (SW480) and non-small cell lung cancer (A549) cells (exposure time 96 h), compared to **1**, $\mathbf{2}^{Os}$ and $\mathbf{3}^{Os}$, and the correlation to the capacity factor log k.

Compound	IC_{50} values / μM			log k
	CH1	SW480	A549	
1[a]	60 ± 14	361 ± 122	–	–
2	425 ± 43	>640	>640	−0.212
3	354 ± 31	>640	>640	−0.178
$\mathbf{2}^{Os}$[b]	436 ± 72	>640	>640	−0.386
$\mathbf{3}^{Os}$[b]	764 ± 215	>640	>640	0.296
5	301 ± 16	613 ± 11	>640	–
6	198 ± 7	204 ± 19	>640	2.124

[a] IC_{50} values taken from Ref. [26].
[b] IC_{50} values taken from Ref. [23].

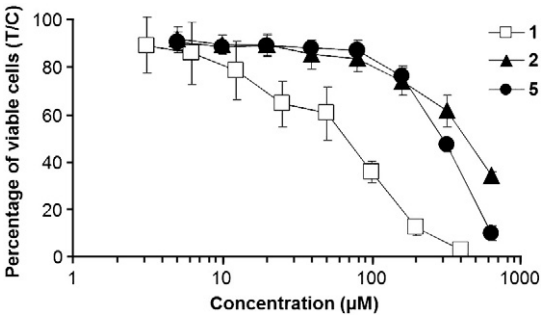

Fig. 4. Concentration–effect curves of 3,5,6-bicyclophosphite-1,2-*O*-isopropylidene-α-d-glucofuranoside complexes **1** (dichlorido), **2** (oxalato) and **5** (malonato) in CH1 cells (exposure time 96 h).

4. Conclusions

RAPTA-type complexes with their P-based pta ligand are among the best studied and most promising Ru^{II}–arene anticancer agents that appear to interfere with enzymatic targets and in vivo show selective antitumor activity. By maintaining the structural features around the Ru center, but modifying the carrier ligand, we have prepared closely related sugar-derived Ru^{II}–arene complexes. In order to study the role of the leaving group, the dichlorido ligands were replaced by the chelating biscarboxylates, *i.e.*, oxalate and malonate. These structural modifications have a dramatic influence on the chemical and biological properties of the compounds. As expected, and in analogy to the RAPTA counterparts, hydrolysis is markedly inhibited. The reactivity of the organometallic species to the biological nucleophiles Met, Cys, Ub and 5′-GMP is significantly reduced, and compared to the respective dichlorido complexes, essentially the same adducts are formed, but at a significantly lowered rate. Since the introduction of the biscarboxylate ligands resulted in significantly reduced *in vitro* anticancer activity in all tested cell lines, it appears that covalent binding to biological targets is a prerequisite for the compound type to exhibit their desired biological properties. Q1

Acknowledgements

We thank the Higher Education Commission of Pakistan, the Austrian Exchange Service (ÖAD), the Hochschuljubiläumsstiftung Vienna, the Theodor-Körner-Fonds, the FFG—Austrian Research Promotion Agency (811591), the Austrian Council for Research and Technology Development (IS526001), COST D39 and CM0902 and the Austrian Science Fund for the financial support. This research was supported by a Marie Curie Intra European Fellowship within the 7th European Community Framework Programme project 220890-SuRuCo (A.A.N.). We gratefully acknowledge Alexander Roller for collecting the X-ray diffraction data and Prof. Markus Galanski for recording the 2D NMR spectra.

Appendix A. Supplementary data

Supplementary data to this article can be found online at doi:10.1016/j.jinorgbio.2010.10.004.

References

[1] C.G. Hartinger, P.J. Dyson, Chem. Soc. Rev. 38 (2009) 391–401.
[2] A. Nguyen, A. Vessieres, E.A. Hillard, S. Top, P. Pigeon, G. Jaouen, Chimia 61 (2007) 716–724.
[3] K. Strohfeldt, M. Tacke, Chem. Soc. Rev. 37 (2008) 1174–1187.
[4] Dalton transactions themed issue on metal anticancer compounds, Dalton Trans. (2009) 10629–10936.
[5] W.F. Schmid, R.O. John, V.B. Arion, M.A. Jakupec, B.K. Keppler, Organometallics 26 (2007) 6643–6652.

Please cite this article as: M. Hanif, et al., From hydrolytically labile to hydrolytically stable Ru(II)–arene anticancer complexes with carbohydrate-derived co-ligands, J. Inorg. Biochem. (2010), doi:10.1016/j.jinorgbio.2010.10.004

[6] W.H. Ang, A. De Luca, C. Chapuis-Bernasconi, L. Juillerat-Jeanneret, M. Lo Bello, P.J. Dyson, ChemMedChem 2 (2007) 1799–1806.
[7] C.A. Vock, W.H. Ang, C. Scolaro, A.D. Phillips, L. Lagopoulos, L. Juillerat-Jeanneret, G. Sava, R. Scopelliti, P.J. Dyson, J. Med. Chem. 50 (2007) 2166–2175.
[8] J. Maksomiska, D.S. Williams, G.E. Atilla-Gokcumen, K.S.M. Smalley, P.J. Carroll, R.D. Webster, P. Filippakopoulos, S. Knapp, M. Herlyn, E. Meggers, Chem. Eur. J. 14 (2008) 4816–4822.
[9] W.H. Ang, L.J. Parker, A. De Luca, L. Juillerat-Jeanneret, C.J. Morton, M. Lo Bello, M.W. Parker, P.J. Dyson, Angew. Chem. Int. Ed. 48 (2009) 3854–3857.
[10] N. Metzler-Nolte, Angew. Chem. Int. Ed. 40 (2001) 1040–1043.
[11] N. Metzler-Nolte, Chimia 61 (2007) 736–741.
[12] C.V. Christodoulou, D.R. Ferry, D.W. Fyfe, A. Young, J. Doran, T.M.T. Sheehan, A. Eliopoulos, K. Hale, J. Baumgart, G. Sass, D.J. Kerr, J. Clin. Oncol. 16 (1998) 2761–2769.
[13] P. Köpf-Maier, Anticancer Res. 19 (1999) 493–504.
[14] R.E. Morris, R.E. Aird, P.d.S. Murdoch, H. Chen, J. Cummings, N.D. Hughes, S. Parsons, A. Parkin, G. Boyd, D.I. Jodrell, P.J. Sadler, J. Med. Chem. 44 (2001) 3616–3621.
[15] R.E. Aird, J. Cummings, A.A. Ritchie, M. Muir, R.E. Morris, H. Chen, P.J. Sadler, D.I. Jodrell, Br. J. Cancer 86 (2002) 1652–1657.
[16] C. Scolaro, A. Bergamo, L. Brescacin, R. Delfino, M. Cocchietto, G. Laurenczy, T.J. Geldbach, G. Sava, P.J. Dyson, J. Med. Chem. 48 (2005) 4161–4171.
[17] M.G. Mendoza-Ferri, C.G. Hartinger, A.A. Nazarov, R.E. Eichinger, M.A. Jakupec, K. Severin, B.K. Keppler, Organometallics 28 (2009) 6260–6265.
[18] W. Kandioller, C.G. Hartinger, A.A. Nazarov, C. Bartel, M. Skocic, M.A. Jakupec, V.B. Arion, B.K. Keppler, Chem. Eur. J. 15 (2009) 12283–12291.
[19] M.G. Mendoza-Ferri, C.G. Hartinger, M.A. Mendoza, M. Groessl, A.E. Egger, R.E. Eichinger, J.B. Mangrum, N.P. Farrell, M. Maruszak, P.J. Bednarski, F. Klein, M.A. Jakupec, A.A. Nazarov, K. Severin, B.K. Keppler, J. Med. Chem. 52 (2009) 916–925.
[20] W.F. Schmid, R.O. John, G. Mühlgassner, P. Heffeter, M.A. Jakupec, M. Galanski, W. Berger, V.B. Arion, B.K. Keppler, J. Med. Chem. 50 (2007) 6343–6355.
[21] C. Scolaro, C.G. Hartinger, C.S. Allardyce, B.K. Keppler, P.J. Dyson, J. Inorg. Biochem. 102 (2008) 1743–1748.
[22] C. Scolaro, T.J. Geldbach, S. Rochat, A. Dorcier, C. Gossens, A. Bergamo, M. Cocchietto, I. Tavernelli, G. Sava, U. Rothlisberger, P.J. Dyson, Organometallics 25 (2006) 756–765.
[23] W.H. Ang, E. Daldini, C. Scolaro, R. Scopelliti, L. Juillerat-Jeannerat, P.J. Dyson, Inorg. Chem. 45 (2006) 9006–9013.
[24] W.H. Ang, E. Daldini, L. Juillerat-Jeanneret, P.J. Dyson, Inorg. Chem. 46 (2007) 9048–9050.
[25] C.G. Hartinger, A.A. Nazarov, S.M. Ashraf, P.J. Dyson, B.K. Keppler, Curr. Med. Chem. 15 (2008) 2574–2591.
[26] I. Berger, M. Hanif, A.A. Nazarov, C.G. Hartinger, R.O. John, M.L. Kuznetsov, M. Groessl, F. Schmitt, O. Zava, F. Biba, V.B. Arion, M. Galanski, M.A. Jakupec, L. Juillerat-Jeanneret, P.J. Dyson, B.K. Keppler, Chem. Eur. J. 14 (2008) 9046–9057.
[27] R.A. Gatenby, R.J. Gillies, Nat. Rev. Cancer 4 (2004) 891–899.
[28] M. Hanif, H. Henke, S.M. Meier, S. Martic, M. Labib, W. Kandioller, M.A. Jakupec, V.B. Arion, H.-B. Kraatz, B.K. Keppler, C.G. Hartinger, Inorg. Chem. 49 (2010) 7953–7963.
[29] R.W. Hay, S. Miller, Polyhedron 17 (1998) 2337–2343.
[30] M. Hanif, A.A. Nazarov, C.G. Hartinger, W. Kandioller, M.A. Jakupec, V.B. Arion, P.J. Dyson, B.K. Keppler, Dalton Trans. 39 (2010) 7345–7352.
[31] S. Stahl, H. Werner, Organometallics 9 (1990) 1876–1881.
[32] N.K. Kochetkov, E.E. Nifant'ev, M.P. Koroteev, Z.K. Zhane, A.A. Borisenko, Carbohydr. Res. 47 (1976) 221–231.
[33] M.P. Koroteev, S.B. Khrebtova, A.R. Bekker, N.M. Pugashova, V.K. Bel'skii, A.Y. Zotov, E.E. Nifant'ev, Zh. Obshch. Khim. 66 (1996) 1615–1628.
[34] M.R. Pressprich, J. Chambers, SAINT + Integration Engine, Program for Crystal Structure Integration, Madison, 2004.
[35] G.M. Sheldrick, Acta Crystallogr., Sect. A: Found. Crystallogr. 64 (2008) 112–122.
[36] L.J. Farrugia, J. Appl. Crystallogr. 30 (1997) 565.
[37] P.-E. Mahuzier, M.S. Aurora Prado, B.J. Clark, E.R.M. Kedor-Hackmann, K.D. Altria, LC GC Eur. 16 (2003) 22–29.
[38] A.K. Bytzek, M.R. Reithofer, M. Galanski, M. Groessl, B.K. Keppler, C.G. Hartinger, Electrophoresis 31 (2010) 1144–1150.
[39] A.F.A. Peacock, M. Melchart, R.J. Deeth, A. Habtemariam, S. Parsons, P.J. Sadler, Chem. Eur. J. 13 (2007) 2601–2613.
[40] A. Casini, C. Gabbiani, F. Sorrentino, M.P. Rigobello, A. Bindoli, T.J. Geldbach, A. Marrone, N. Re, C.G. Hartinger, P.J. Dyson, L. Messori, J. Med. Chem. 51 (2008) 6773–6781.
[41] A. Casini, C. Gabbiani, E. Michelucci, G. Pieraccini, G. Moneti, P.J. Dyson, L. Messori, J. Biol. Inorg. Chem. 14 (2009) 761–770.
[42] A. Casini, A. Karotki, C. Gabbiani, F. Rugi, M. Vasak, L. Messori, P.J. Dyson, Metallomics 1 (2009) 434–441.
[43] M. Groessl, M. Terenghi, A. Casini, L. Elviri, R. Lobinski, P.J. Dyson, J. Anal. At. Spectrom. 25 (2010) 305–313.
[44] A.E. Egger, C.G. Hartinger, A.K. Renfrew, P.J. Dyson, J. Biol. Inorg. Chem. 15 (2010) 919–927.
[45] M. Groessl, Y.O. Tsybin, C.G. Hartinger, B.K. Keppler, P.J. Dyson, J. Biol. Inorg. Chem. 15 (2010) 677–688.
[46] A. Dorcier, C.G. Hartinger, R. Scopelliti, R.H. Fish, B.K. Keppler, P.J. Dyson, J. Inorg. Biochem. 102 (2008) 1066–1076.
[47] M. Galanski, M.A. Jakupec, B.K. Keppler, Curr. Med. Chem. 12 (2005) 2075–2094.
[48] P. Heffeter, U. Jungwirth, M. Jakupec, C. Hartinger, M. Galanski, L. Elbling, M. Micksche, B. Keppler, W. Berger, Drug Res. Upd. 11 (2008) 1–16.
[49] C. Rappel, M. Galanski, A. Yasemi, L. Habala, B.K. Keppler, Electrophoresis 26 (2005) 878–884.

Q2

Please cite this article as: M. Hanif, et al., From hydrolytically labile to hydrolytically stable Ru(II)–arene anticancer complexes with carbohydrate-derived co-ligands, J. Inorg. Biochem. (2010), doi:10.1016/j.jinorgbio.2010.10.004

2.4. The Arene Moiety as Anticancer Activity Determining Parameter in Organometallic Ru(II) Complexes with Carbohydrate Derived Ligands

Results and Discussion

RAPTA complexes are among the most extensively studied Ru–arene anticancer agents. In order to further improve the specificity and efficacy, RAPTA-C analogues were prepared by using carbohydrate derived moieties instead of pta. The resulting organometallic compounds exhibited selectivity for tumorigenic cell lines, and dichlorido(η^6-*p*-cymene)(3,5,6-bicyclophosphite-1,2-*O*-cyclohexylidene-α-D-glucofuranoside)ruthenium(II) **1**, was found to be more cytotoxic than RAPTA-C in *in vitro* assays.[83,84] In order to investigate the influence of the nature of the arene ligand on the cytotoxicity, analogous compounds with benzene, toluene and biphenyl arene ligand were prepared.

The organometallic Ru^{II}-chlorido complexes **2-6** were synthesized in high yields by reacting 3,5,6-bicyclophosphite-1,2-*O*-isopropylidene-α-D-glucofuranoside **I** or 3,5,6-bicyclophosphite-1,2-*O*-cyclohexylidene-α-D-glucofuranoside **II** with the respective dimer bis[dichlorido(η^6-arene)ruthenium(II)] in CH_2Cl_2 (Fig. 13). All the complexes were characterized by 1D and 2D NMR spectroscopy, ESI-MS, and elemental analysis. On coordination of the P-containing ligands to the metal center, the most significant change observed was a low field chemical shift of the $^{31}P\{^1H\}$

[83] Berger, Isabella; Hanif, Muhammad; Nazarov, Alexey A.; Hartinger, Christian G.; John, Roland O.; Kuznetsov, Maxim L.; Groessl, Michael; Schmitt, Frederic; Zava, Olivier; Biba, Florian; Arion, Vladimir B.; Galanski, Markus; Jakupec, Michael A.; Juillerat-Jeanneret, Lucienne; Dyson, Paul J.; Keppler, Bernhard K., Chemistry--A European Journal (2008), 14(29), 9046-9057.

[84] Hanif, Muhammad; Nazarov, Alexey A.; Hartinger, Christian G.; Kandioller, Wolfgang; Jakupec, Michael A.; Arion, Vladimir B.; Dyson, Paul J.; Keppler, Bernhard K., Dalton Transactions (2010), 39(31), 7345-7352.

NMR signals from *ca.* 117 to approximately 135 ppm, similar to reported analogous compounds.[83]

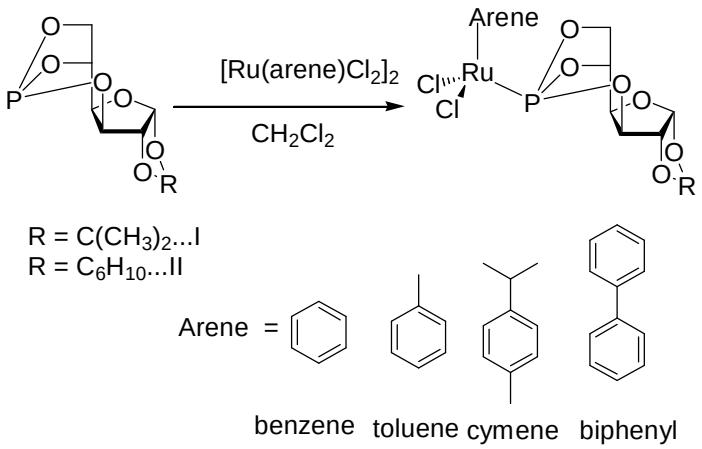

Figure 13. Synthesis of the dichlorido–Ru^{II} compounds **1-6** of P-derived sugar ligands (**I**, **II**).

Stability in aqueous solution

The hydrolysis of **2** and **3** was studied by $^{31}P\{^{1}H\}$ NMR spectroscopy. For the toluene compound only a single peak is observed at 136.1 ppm after 1 h of dissolution, which was assigned to unhydrolyzed compound, indicating stability for this time period in aqueous solution. After 24 h, two additional peaks of equal relative intensity at 137.4 and 136.8 ppm appear due to the formation of diastereomers by exchange of a single chlorido ligand with an aqua molecule. This was accompanied by the cleavage of a P–O bond as indicated by signals of equal relative intensity at 95.7 and 94.5 ppm, while an additional signal at 94.7 ppm indicates P–O bond cleavage of unhydrolyzed complex. After 48 h, two additional signals appeared at 123.8 and 122.4 ppm, potentially due to formation of dimeric species. The sequence of formation of hydrolytic species is similar to that observed for related ruthenium(II) compounds.[83] No further hydrolysis was observed for another 48 h, as the number and extent of hydrolysis products remained unchanged and account together for 30-40 %.

Reaction with 9-EtG

Complex **3** demonstrated rapid adduct formation with the DNA model 9-EtG *via* N7 of the guanine moiety, as shown by ^{1}H NMR spectroscopy. A low field shift from 7.85 to 8.29 ppm was observed for H8 of guanine, indicating N7 binding. Immediately after mixing complex **3** with 9-EtG, a single peak was obtained at 135.9 ppm in the ^{31}P{^{1}H}- NMR for the unreacted compound. Within one hour, two additional signals at 136.6 and 137.2 ppm appeared due to the formation of diastereomers by exchange of one of the chlorido ligand with 9-EtG. However, after 24 h several species were formed, including signals at 93.3 and 95.1 ppm indicative for cleavage of P-O bond.

Evaluation of the *in vitro* cytotoxicity

The tumor-inhibiting potential of **2**–**6** was determined in human SW480 colon adenocarcinoma, CH1 ovarian cancer and A549 non-small cell lung cancer cells by means of the MTT assays (Table 1). Variation in the arene ligand of metal arene complexes has demonstrated a stronge influence on the antiproliferative activity. It appears that cytotoxicity is increased with both the size of the arene ligand and the lipophilicity of carbohydrate moiety in this series of Ru(II) complexes. The most lipophilic compound **6** with biphenyl arene was the most active with IC_{50} values in low micromolar range. The following order of cytotoxicity is observed with regard to variation of arene ligand with same sugar moiety: biphenyl > cymene > toluene > benzene. This is also observed when keeping the arene ligand same while changing the carbohydrates derived moiety, the compound having the most lipophilic ligand was the most cytotoxic. As we know, for a drug to exert its desired pharmacological effects, it must reach the target sites in sufficient concentration. Therefore, more lipophilic molecules penetrate through cell membranes more easily than those with less lipophilicity. This result in greater drug uptake and subsequently enhanced activity.

Table 1. *In vitro* anticancer activity (mean IC_{50} values ± standard deviations) of **1**-**6** in human ovarian cancer (CH1), colon cancer (SW480) and non-small cell lung cancer (A549) cells (exposure time 96 h).

Compound	**IC_{50} values / µM**		
	CH1	SW480	A549
1	29 ± 4 [a]	150 ± 19 [a]	223 ± 14 [a]
2	118 ± 36	129 ± 13	417 ± 68
3	164 ± 47	276 ± 6	427 ± 163
4	92 ± 22	99 ± 13	486 ± 55
5	29 ± 3	26 ± 5	>160
6	3.9 ± 0.3	5.3 ± 0.9	56 ± 9

[a)] taken from ref.[83]

Conclusions

Organometallic compounds have gained an increasing importance in metallo-drug design. In particular, the M(η^6-arene) moiety is versatile scaffold that can be modulated to attribute desired properties to the molecule. A series of Ru^{II}(η^6-arene) complexes with carbohydrate-derived phosphorus-containing ligands was synthesized. These compounds exhibit IC_{50} values upto low micromolar range, depending on the lipophilicity of arene ligand with biphenyl containing compound the most active. In hydrolysis studies, the compounds form monoaqua species by exchange of chloride with water molecule, followed by cleavage of intramolecular P–O bond and formation of dinuclear species as demonstrated by ^{1}H and $^{31}P\{^{1}H\}$ NMR spectroscopy. Adduct formation with DNA model 9-EtG was observed.

Experimental Section

Materials: All reactions were carried out in dry solvents under an inert atmosphere. All chemicals were obtained from commercial suppliers, and were of analytical grade and used as received. $RuCl_3.xH_2O$ was purchased from Johnson Matthey, 1-methyl-1,4-cyclohexadiene from Aldrich, 1-isopropyl-4-methyl-1,3-cyclohexadiene (α-terpinene), and 3-cyclohexadiene from Acros Organics. Methanol and CH_2Cl_2 were dried using standard procedures. The dimer bis[dichlorido(η^6-biphenyl)ruthenium(II)],[85] bis[dichlorido(η^6-*p*-cymene)ruthenium(II)],[86,87] bis[dichlorido(η^6-benzene)ruthenium(II)], bis[dichlorido(η^6-toluene)ruthenium(II)], 3,5,6-bicyclophosphite-1,2-*O*-isopropylidene-α-D-glucofuranoside **I**, 3,5,6-bicyclophosphite-1,2-*O*-cyclohexylidene-α-D-glucofuranoside[88,89] **II** and dichlorido(η^6-p-cymene)(3,5,6-bicyclophosphite-1,2-*O*-cyclohexylidene-α-D-glucofuranose)ruthenium(II)[83] **1** were synthesized using literature procedures. Na_2EDTA (p.a., Fisher Scientific), NaOH (Fluka), tris(hydroxymethyl)aminoethane (TAE) and glacial acetic acid (p.a., Acros) and MilliQ H_2O (18.2 MΩ, Synergy 185 UV Ultrapure, Millipore, France) were used for the preparation of TAE buffer for gel electrophoresis studies. Loading buffer (6x), pBR322 DNA (0.5 µg/µL) and GeneRuler™ 1kb DNA Ladder (0.5 µg/µL) were obtained from Fermentas. ^1H, $^{13}C\{^1H\}$ and $^{31}P\{^1H\}$ NMR spectra were recorded at 25 °C on a Bruker FT NMR spectrometer Avance III 500 MHz at 500.10 (^1H), 125.75 ($^{13}C\{^1H\}$) and 202.44 MHz ($^{31}P\{^1H\}$). 2D NMR spectra were collected in a gradient-enhanced mode. Melting points were measured on a Büchi B-540 apparatus and are uncorrected. Elemental analysis was determined by the Laboratory for Elemental Analysis, Fac-

---

[85] Morris, R. E.; Sadler, P. J.; Chen, H.; Jodrell, D. Half-sandwich ruthenium(II) compounds comprising nitrogen containing ligands for treatment of cancer. 2000-GB4144, 2001.

[86] M. A. Bennett, T. N. Huang, T. W. Matheson, A. K. Smith, *Inorg. Synth.* **1982**, *21*, 74.

[87] M. A. Bennett, A. K. Smith, *J. Chem. Soc., Dalton Trans.* **1974**, 233.

[88] N.K. Kochetkov, E.E. Nifant'ev, M.P. Koroteev, Z.K. Zhane, A.A. Borisenko, Carbohydr. Res. 47 (1976) 221-231.

[89] M.P. Koroteev, S.B. Khrebtova, A.R. Bekker, N.M. Pugashova, V.K. Bel'skii, A.Y. Zotov, E.E. Nifant'ev, Zh. Obshch. Khim. 66 (1996) 1615-1628

ulty of Chemistry, University of Vienna, on a Perkin–Elmer 2400 CHN Elemental Analyzer. Electrospray ionization mass spectra were recorded on a Bruker esquire$_{3000}$.

General Procedure

A mixture of bis[(η^6-arene)dichloridoruthenium] (1 eq.) and phosphite ligand (2 eq.) in dry CH_2Cl_2 (25 mL) was stirred at 40 °C for 3 h. The solvent was reduced to about 3 mL under vacuum and diethyl ether (20 mL) was added resulting in orange or brown precipitate which were filtered, washed with diethyl ether (2×5 mL), and dried under vacuum.

Dichlorido(η^6-benzene)(3,5,6-bicyclophosphite-1,2-*O*-cyclohexylidene-α-D-glucofuranose)ruthenium(II) 2

The title compound was synthesized from 3,5,6-bicyclophosphite-1,2-*O*-cyclohexylidene-α-D-glucofuranose (58 mg, 0.2 mmol) and [(η^6-benzene)RuCl(μ-Cl)]$_2$ (50 mg, 0.1 mmol) following the general procedure.
Yield: 104 mg (96%); m.p. 295-297 °C (decomp); elemental analysis calcd. for $C_{18}H_{23}Cl_2O_6PRu \cdot 0.5CH_2Cl_2$: C 38.25, H 4.16; found: C 38.21, H 4.19%; MS (ESI^+): *m/z*: 560.7 $[M + Na]^+$; ^1H NMR (500.10 MHz, $CDCl_3$, 25 °C): δ = 6.20 (brs, 1 H, H-1), 5.89 (s, 6 H, H-Ar), 5.10-5.13 (m, 1 H, H-5), 4.83 (brs, 1 H, H-3), 4.75 (brs, 1 H, H-2), 4.48-4.50 (m, 1 H, H-6), 4.32-4.33 (m, 2 H, H-6', H-4), 1.57-1.70 (m, 10 H, C_6H_{10}) ppm. $^{13}C\{^1H\}$ NMR (125.75 MHz, $CDCl_3$, 25 °C): δ = 113.3 (C_{cyc}), 105.4 (C-1), 91.2 (C-Ar), 83.4 (C-2), 79.5 (C-3), 75.7 (C-4), 75.2 (C-5), 71.5 (C-6), 36.5 (C_6H_{10}), 35.8 (C_6H_{10}), 24.8 (C_6H_{10}), 23.9 (C_6H_{10}), 23.5 (C_6H_{10}) ppm. $^{31}P\{^1H\}$ NMR (202.44 MHz, $CDCl_3$, 25 °C): δ = 132.7 ppm.

Dichlorido(η^6-toluene)(3,5,6-bicyclophosphite-1,2-*O*-isopropylidene-α-D-glucofuranose)ruthenium(II) 3

The title compound was synthesized from 3,5,6-bicyclophosphite-1,2-*O*-isopropylidene-α-D-glucofuranose (99 mg, 0.4 mmol) and [(η^6-toluene)RuCl(μ-Cl)]$_2$ (106 mg, 0.2 mmol) following the general procedure.

Yield: 201 mg (97%); m.p. 180-181 °C (decomp); elemental analysis calcd. for $C_{16}H_{21}Cl_2O_6PRu \cdot 0.25CH_2Cl_2$: C 36.58, H 4.06; found: C 36.93, H 4.22%; MS (ESI^+): *m/z*: 534.6 $[M + Na]^+$; ^1H NMR (500.10 MHz, $CDCl_3$, 25 °C): δ = 6.19 (d, J = 3 Hz, 1 H, H-1), 5.81-5.82 (m, 2 H, H-Ar), 5.58 (brs, 2 H, H-Ar), 5.52 (brs, 1 H, H-Ar) , 5.09-5.12 (m, 1 H, H-5), 4.81 (brs, 1 H, H-3), 4.74 (d, J = 2 Hz, 1 H, H-2), 4.44-4.48 (m, 1 H, H-6), 4.32 (m, 2 H, H-6', H-4), 2.34 (s, 3 H, Ar-CH_3), 1.52 (s, 3 H, C(CH_3)$_2$), 1.36 (s, 3 H, C(CH_3)$_2$) ppm. $^{13}C\{^1H\}$ NMR (125.75 MHz, $CDCl_3$, 25 °C): δ = 113.0 (*C*(CH_3)$_2$), 112.6 (C-Ar), 105.7 (C-1), 91.0 (C-Ar), 90.6 (C-Ar), 83.7 (J = 6 Hz, C-2), 82.2 (C-Ar), 81.8 (C-Ar), 79.2 (J = 8 Hz, C-3), 77.2 (C-Ar), 76.8 (J = 6 Hz, C-4), 74.8 (J = 5 Hz, C-5), 69.9 (J = 8 Hz, C-6), 26.9 (C(*C*H_3)$_2$), 26.3 (C(*C*H_3)$_2$), 19.2 (Ar-*C*H_3) ppm. $^{31}P\{^1H\}$ NMR (202.44 MHz, $CDCl_3$, 25 °C): δ = 134.5 ppm.

Dichlorido(η^6-toluene)(3,5,6-bicyclophosphite-1,2-*O*-cyclohexylidene-α-D-glucofuranose)ruthenium(II) 4

The title compound was synthesized from 3,5,6-bicyclophosphite-1,2-*O*-cyclohexylidene-α-D-glucofuranose (58 mg, 0.2 mmol) and [(η^6-toluene)RuCl(μ-Cl)]$_2$ (53 mg, 0.1 mmol) following the general procedure.

Yield: 107 mg (95%); m.p. 282-283 °C (decomp); elemental analysis calcd. for $C_{19}H_{25}Cl_2O_6PRu \cdot 0.15CH_2Cl_2$: C 39.37, H 4.40; found: C 39.06, H 4.40%; MS (ESI^+): *m/z*: 574.6 $[M + Na]^+$; ^1H NMR (500.10 MHz, $CDCl_3$, 25 °C): δ = 6.18 (d, J = 4 Hz, 1 H, H-1), 5.80-5.82 (m, 2 H, H-Ar), 5.58 (brs, 2 H, H-Ar), 5.50-5.51 (m, 1 H, H-Ar), 5.08-5.12 (m, 1 H, H-5), 4.82 (brs, 1 H, H-3), 4.73 (brs, 1 H, H-2), 4.44-4.48 (m, 1 H, H-6), 4.31 (m, 2 H, H-6', H-4), 2.34 (s, 3 H, Ar-CH_3), 1.67-1.70 (m, 4 H, C_6H_{10}), 1.56-1.58 (m, 6 H, C_6H_{10}) ppm. $^{13}C\{^1H\}$ NMR (125.75 MHz, $CDCl_3$, 25 °C): δ = 113.7 (C_{cyc}), 112.7 (C-Ar), 105.3 (C-1), 91.1 (C-Ar), 90.7 (C-Ar), 83.4 (J = 7 Hz, C-2), 82.3 (C-Ar), 81.6 (C-Ar), 79.4 (J = 8 Hz, C-3), 77.4 (C-Ar), 76.6 (J = 6 Hz, C-4), 74.9 (J = 5 Hz, C-5), 69.8 (J = 8 Hz, C-6), 36.9 (C_6H_{10}), 36.2 (C_6H_{10}), 24.8 (C_6H_{10}), 24.2 (C_6H_{10}), 23.5 (C_6H_{10}), 19.2 (*C*H_3) ppm. $^{31}P\{^1H\}$ NMR (202.44 MHz, $CDCl_3$, 25 °C): δ = 134.4 ppm.

Dichlorido(η^6-biphenyl)(3,5,6-bicyclophosphite-1,2-*O*-isopropylidene-α-D-glucofuranose)ruthenium(II) 5

The title compound was synthesized from 3,5,6-bicyclophosphite-1,2-*O*-isopropylidene-α-D-glucofuranose (99 mg, 0.4 mmol) and [(η^6-biphenyl)RuCl(μ-Cl)]$_2$ (131 mg, 0.2 mmol) following the general procedure.

Yield: 217 mg (91%); m.p. 178-179 °C (decomp); elemental analysis calcd. for $C_{21}H_{23}Cl_2O_6PRu \cdot 0.25CH_2Cl_2$: C 42.85, H 3.98; found: C 42.97, H 3.88%; MS (ESI$^+$): *m/z*:: 596.6 [M + Na]$^+$; ^{1}H NMR (500.10 MHz, $CDCl_3$, 25 °C): δ = 7.69-7.71 (m, 2 H, H-Ar), 7.49-7.50 (m, 3 H, H-Ar), 6.18-6.22 (m, 3 H, H-Ar), 5.99 (d, J = 4 Hz, 1 H, H-1), 5.88 (brs, 2 H, H-Ar), 5.03-5.07 (m, 1 H, H-5), 4.72 (brs, 1 H, H-3), 4.38-4.44 (m, 2 H, H-6', H-2), 4.26 (brs, 1 H, H-4), 4.19 (brs, 1 H, H-6), 1.50 (s, 3 H, C(CH_3)$_2$), 1.33 (s, 3 H, C(CH_3)$_2$) ppm. ^{13}C{^{1}H} NMR (125.75 MHz, $CDCl_3$, 25 °C): δ = 133.7 (C-Ar), 130.1 (C-Ar), 129.0 (C-Ar), 128.8 (C-Ar), 128.7 (C-Ar), 127.3 (C-Ar), 112.5 (*C*(CH_3)$_2$), 108.3 (C-Ar), 105.7 (C-1), 91.2 (C-Ar), 90.8 (C-Ar), 89.9 (C-Ar), 88.9 (C-Ar), 88.2 (C-Ar), 83.6 (J = 5 Hz, C-4), 79.1 (J = 8 Hz, C-3), 76.8 (C-2), 74.9 (J = 5 Hz, C-5), 69.6 (C-6), 26.9 (C(*C*H_3)$_2$), 26.3 (C(*C*H_3)$_2$) ppm. ^{31}P{^{1}H} NMR (202.44 MHz, $CDCl_3$, 25 °C): δ = 132.3 ppm.

Dichlorido(η^6-biphenyl)(3,5,6-bicyclophosphite-1,2-*O*-cyclohexylidene-α-D-glucofuranose)ruthenium(II) 6

The title compound was synthesized from 3,5,6-bicyclophosphite-1,2-*O*-cyclohexylidene-α-D-glucofuranose (58 mg, 0.2 mmol) and [(η^6-biphenyl)RuCl(μ-Cl)]$_2$ (65 mg, 0.1 mmol) following the general procedure.

Yield: 119 mg (93%); m.p. 170-172 °C (decomp); elemental analysis calcd. for $C_{24}H_{27}Cl_2O_6PRu \cdot 0.3CH_2Cl_2$: C 45.61, H 4.35; found: C 45.27, H 4.38%; MS (ESI$^+$): *m/z*: 636.7 [M + Na]$^+$; ^{1}H NMR (500.10 MHz, $CDCl_3$, 25 °C): δ = 7.62-7.69 (m, 2 H, H-Ar), 7.46-7.49 (m, 3 H, H-Ar), 6.17-6.20 (m, 2 H, H-Ar), 5.97-6.01 (m, 3 H, H-Ar, H-1), 5.87 (brs, 1 H, H-Ar), 5.03-5.05 (m, 1 H, H-5), 4.73 (brs, 1 H, H-3), 4.43-4.46 (m, 2 H, H-6', H-2), 4.26 (brs, 1 H, H-4), 4.18 (brs, 1 H, H-6), 1.65-1.67 (m, 4 H, C_6H_{10}), 1.54-1.58 (m, 6 H, C_6H_{10}) ppm. ^{13}C{^{1}H} NMR (125.75 MHz,

$CDCl_3$, 25 °C): δ = 133.6 (C-Ar), 130.1 (C-Ar), 129.0 (C-Ar), 128.8 (C-Ar), 128.6 (C-Ar), 127.2 (C-Ar), 113.2 (C_{cyc}), 108.5 (C-Ar), 105.4 (C-1), 91.3 (C-Ar), 90.6 (C-Ar), 90.0 (C-Ar), 89.0 (C-Ar), 88.3 (C-Ar), 83.2 (J = 6 Hz, C-4), 79.2 (J = 8 Hz, C-3), 76.6 (C-2), 75.0 (J = 5 Hz, C-5), 70.0 (C-6), 36.5 (C_6H_{10}), 35.8 (C_6H_{10}), 24.8 (C_6H_{10}), 23.9 (C_6H_{10}), 23.5 (C_6H_{10}) ppm. $^{31}P\{^1H\}$ NMR (202.44 MHz, $CDCl_3$, 25 °C): δ = 132.4 ppm.

Hydrolysis and reactivity with 9-ethylguanine

For hydrolysis studies, **2** and **3** were dissolved in D_2O and the samples were analyzed by ^1H and $^{31}P\{^1H\}$ NMR spectroscopy after 1, 24, 48 and 96 h. For 9-ethylguanine (9-EtG) binding experiments, the complexes were mixed at molar ratios of 1 : 1 and 1 : 2 (complex :9-EtG) in D_2O and the reaction progress was monitored by ^1H and $^{31}P\{^1H\}$ NMR spectroscopy after 1, 24, and 96 h, while samples were kept at room temperature during this time period.

Cytotoxicity in cancer cell lines

Cell lines and culture conditions. CH1 cells originate from an ascites sample of a patient with a papillary cystadenocarcinoma of the ovary and were a generous gift from Lloyd R. Kelland, CRC Centre for Cancer Therapeutics, Institute of Cancer Research, Sutton, UK. SW480 (adenocarcinoma of the colon, human), and A549 (non-small cell lung cancer, human) cells were kindly provided by Brigitte Marian (Institute of Cancer Research, Department of Medicine I, Medical University of Vienna, Austria). All cell culture reagents were obtained from Sigma-Aldrich Austria. Cells were grown in 75 cm^2 culture flasks (Iwaki) as adherent monolayer cultures in Eagle's Minimal Essential Medium (MEM) supplemented with 10% heat-inactivated foetal calf serum, 1 mM sodium pyruvate and 2 mM L-glutamine. Cultures were maintained at 37 °C in a humidified atmosphere containing 95% air and 5% CO_2.

MTT assay conditions. Cytotoxicity was determined by the colorimetric MTT (3-(4,5-dimethyl-2-thiazolyl)-2,5-diphenyl-2*H*-tetrazolium bromide, purchased from Fluka) microculture assay. For this purpose, cells were harvested from culture flasks

by trypsinization and seeded in 100 µL aliquots MEM supplemented with 10% heat-inactivated foetal calf serum, 1 mM sodium pyruvate, 4 mM L-glutamine and 1% non-essential amino acids (100×) into 96-well microculture plates (Iwaki). Cell densities of 1.5×10^3 cells/well (CH1), 2.5×10^3 cells/well (SW480) and 4×10^3 cells/well (A549) were chosen in order to ensure exponential growth of untreated controls throughout the experiment. Cells were allowed to settle and resume exponential growth for 24 h. The test compounds were dissolved and serially diluted in the same medium and added in 100 µL aliquots to the microcultures (if necessary due to limited solubility, the maximum concentration tested was added in 200 µL aliquots after removal of the medium), and cells were exposed to the test compounds for 96 hours. At the end of the exposure period, all media were replaced by 100 µL/well RPMI1640 culture medium (supplemented with 10% heat-inactivated foetal calf serum) plus 20 µL/well MTT solution in phosphate-buffered saline (5 mg/ml). After incubation for 4 h, the supernatants were removed, and the formazan crystals formed by vital cells were dissolved in 150 µL DMSO per well. Optical densities at 550 nm were measured with a microplate reader (Tecan Spectra Classic), using a reference wavelength of 690 nm to correct for unspecific absorption. The quantity of vital cells was expressed in terms of T/C values by comparison to untreated control microcultures, and 50% inhibitory concentrations (IC_{50}) were calculated from concentration-effect curves by interpolation. Evaluation is based on means from at least three independent experiments, each comprising at least three replicates per concentration level.

2.5. Hydroxypyr(id)ones and their medicinal applications

Hydroxypyrones have enjoyed growing interest in medicinal inorganic chemistry as a versatile class of chelating ligands.[90] Pyrones can be converted to their *N*-heterocyclic analogous pyridones by reaction with ammonia, primary amines, or bifunctional amines such as amino acids. In these reactions the pyrone ring –O– is replaced by –NR–, providing a great variety of potentially useful ligands and even for conjugating biologically active molecules. Some 1-aryl derivatives can be synthesized by direct heating aromatic amines with maltol in a sealed tube; however, the reaction completion takes a very long time and yields are often low. [91,92]

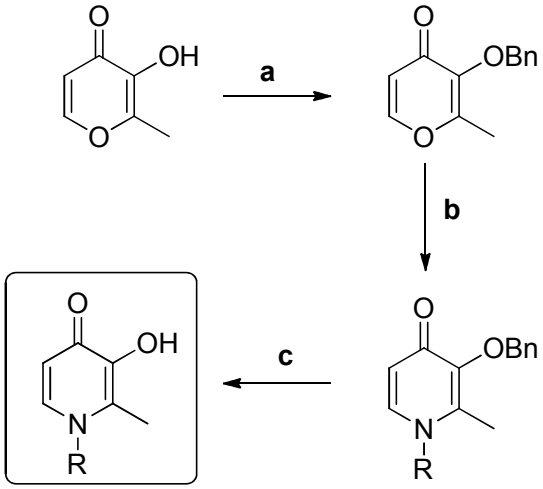

Figure 14. Synthetic strategy for conversion of pyrone to pyridone. a) BnBr, b) H_2N-R, c) H_2, Pd/C.

It is often necessary to protect the hydroxyl group via benzylation to facilitate the reaction for high yields. Cleavage of the benzyl group *via* hydrogenation affords the

[90] Santos, M. Amelia, Coordination Chemistry Reviews (2008), 252(10+11), 1213-1224.

[91] Tamhina, B.; Jakopcic, K.; Zorko, F.; Herak, M. J., Journal of Inorganic and Nuclear Chemistry (1974), 36(8), 1855-7.

[92] Tamhina, B.; Zorko, F.; Herak, M. J., Journal of Inorganic and Nuclear Chemistry (1977), 39(7), 1201-3.

desired pyridones (Fig. 14).[93,94]There are three classes of hydroxypyridones namely, 3-hydroxy-4-pyridone, 3-hydroxy-2-pyridone and 1-hydroxy-2-pyridone (Fig. 15). These are heterocyclic compounds with a hydroxyl group ortho to a ketone, and behave as *{O,O}* bidentates to form thermodynamically stable 5-membered chelate rings for metal-coordination similar to their pyrone analogues. In addition, the pyridone moiety contains a tertiary amino group which along with hydroxyl and ketone H-bonding functionalities, also contributes to enhance the solubility of the resulting complexes in comparison to pyrones.[95] Moreover, the ease of *N*-functionalization of pyridones provides the option for the development of a variety of derivatives, namely bidentate,[96,97,98] tetradentate,[99,100] hexadentate chelators[101] and tethering bioactive or biological molecules including carbohydrates and amino acids.[96]

---

[93] Dobbin, Paul S.; Hider, Robert C.; Hall, Adrian D.; Taylor, Paul D.; Sarpong, Patience; Porter, John B.; Xiao, Gaoyi; van der Helm, Dick, Journal of Medicinal Chemistry (1993), 36(17), 2448-58.

[94] Dehkordi, Lotfollah S.; Liu, Zu D.; Hider, Robert C., European Journal of Medicinal Chemistry (2008), 43(5), 1035-1047.

[95] Thompson, Katherine H.; Barta, Cheri A.; Orvig, Chris, Chemical Society Reviews (2006), 35(6), 545-556.

[96] Chaves, Silvia; Dron, Paul I.; Danalache, Florina A.; Sacoto, Diana; Gano, Lurdes; Santos, M. Amelia., Journal of Inorganic Biochemistry (2009), 103(11), 1521-1529.

[97] Kruck, Theo P. A.; Burrow, Timothy E, Journal of Inorganic Biochemistry (2002), 88(1), 19-24.

[98] Santos, M. Amelia; Gil, Marco; Gano, Lurdes; Chaves, Silvia, Journal of Biological Inorganic Chemistry (2005), 10(5), 564-580.

[99] Santos, M. Amelia; Gama, Sofia; Gano, Lurdes; Cantinho, Guilhermina; Farkas, Etelka, Dalton Transactions (2004), (21), 3772-3781.

[100] Santos, M. Amelia; Gama, Sofia; Gano, Lurdes; Farkas, Etelka, Journal of Inorganic Biochemistry , (2005), 99, 1845–1852.

[101] Grazina, Raquel; Gano, Lurdes; Sebestik, Jaroslav; Santos, M. Amélia, Journal of Inorganic Biochemistry (2009), 103(2), 262-273.

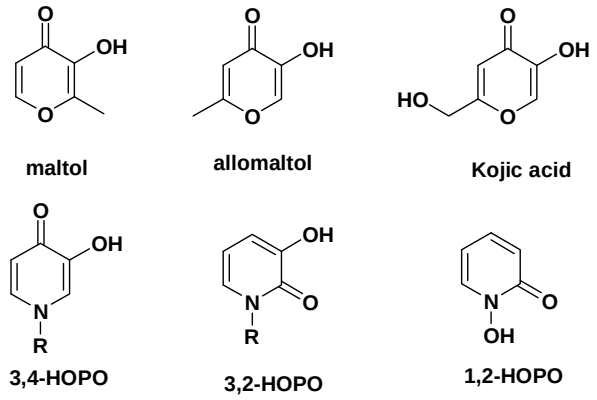

Figure 15. Examples for pyrone and pyridone ligands.

2.5.1 Medicinal applications of hydroxypyr(id)ones

Hydroxypyrones occur mostly as natural products such as maltol and kojic acid but many of them can be synthesized. Maltol is known for its biocompatibility and favorable toxicity profile and is used as food additive;[102] whereas kojic acid is extensively used as cosmetics additive and also inhibits the copper-containing enzyme tyrosinase that causes melanization in humans.[103] In the last two decades, hydroxypyr(id)ones have found many applications in medicinal inorganic chemistry and they have been extensively investigated as metal chelators,[90,101] magnetic resonance imaging (MRI) contrast agents,[104] matrix metalloprotein inhibitors,[105,106] receptors for Li^+ or Na^+,[107,108] anthrax lethal factor inhibitors,[109,110] antidiabetic,[111] antiviral,[109] and antibacterial agents.[109,112]

---

[102] Bentley, Ronald, Natural Product Reports (2006), 23(6), 1046-1062.

[103] Cabanes, Juana; Chazarra, Soledad; Garcia-Carmona, Francisco, Journal of Pharmacy and Pharmacology (1994), 46(12), 982-985.

[104] Datta, Ankona; Raymond, Kenneth N., Accounts of Chemical Research (2009), 42(7), 938-947.

[105] Jacobsen, Faith E.; Lewis, Jana A.; Cohen, Seth M., ChemMedChem (2007), 2(2), 152-171.

[106] Yan, Yi-Long; Miller, Melissa T.; Cao, Yuchen; Cohen, Seth M., Bioorganic & Medicinal Chemistry Letters (2009), 19(7), 1970-1976.

[107] Grote, Zacharias; Lehaire, Marie-Line; Scopelliti, Rosario; Severin, Kay, Journal of the American Chemical Society (2003), 125(45), 13638-13639.

[108] Grote, Zacharias; Scopelliti, Rosario; Severin, Kay, Journal of the American Chemical Society (2004), 126(51), 16959-16972.

2.5.2. Organometallic anticancer compounds of pyr(id)one ligands

Sadler and co-workers reported Ru(arene) and Os(arene) compounds of maltol. These compounds were shown to be inactive in *in vitro* assays that can be attributed to their low stability and the formation of a hydroxide-bridged dimer under physiological conditions.[113] Keppler and coworkers have synthesized Ru(arene) complexes with modified pyrone ligands (Fig. 16), and some examples have shown potent anticancer activity with IC_{50} values in the low micromolar range.[114,115,116,117] The Ru(arene)(pyronato)(halido) complexes hydrolyze to their respective aqua species under physiological conditions. The aqua ligand can be rapidly replaced by biological targets and test reactions with small biomolecules, such as the DNA model 5'-GMP, were conducted.[114-117] For the latter selective binding to the *N*7 of the guanine

---

[109] Agrawal, Arpita; de Oliveira, Cesar Augusto F.; Cheng, Yuhui; Jacobsen, Jennifer A.; McCammon, J. Andrew; Cohen, Seth M., Journal of Medicinal Chemistry (2009), 52(4), 1063-1074.

[110] Lewis, Jana A.; Mongan, John; McCammon, J. Andrew; Cohen, Seth M., ChemMedChem (2006), 1(7), 694-697.

[111] Enyedy, Eva Anna; Lakatos, Andrea; Horvath, Laszlo; Kiss, Tamas, Journal of Inorganic Biochemistry (2008), 102(7), 1473-1485.

[112] Feng, Min Hua; van der Does, Leen; Bantjes, Adriaan, Journal of Medicinal Chemistry (1993), 36(19), 2822-7.

[113] Peacock, Anna F. A.; Melchart, Michael; Deeth, Robert J.; Habtemariam, Abraha; Parsons, Simon; Sadler, Peter J., Chemistry--A European Journal (2007), 13(9), 2601-2613.

[114] Kandioller, Wolfgang; Hartinger, Christian G.; Nazarov, Alexey A.; Bartel, Caroline; Skocic, Matthias; Jakupec, Michael A.; Arion, Vladimir B.; Keppler, Bernhard K., Chemistry--A European Journal (2009), 15(45), 12283-12291.

[115] Kandioller, Wolfgang; Hartinger, Christian G.; Nazarov, Alexey A.; Kuznetsov, Maxim L.; John, Roland O.; Bartel, Caroline; Jakupec, Michael A.; Arion, Vladimir B.; Keppler, Bernhard K., Organometallics (2009), 28(15), 4249-4251.

[116] Kandioller, Wolfgang; Hartinger, Christian G.; Nazarov, Alexey A.; Kasser, Johanna; John, Roland; Jakupec, Michael A.; Arion, Vladimir B.; Dyson, Paul J.; Keppler, Bernhard K. Journal of Organometallic Chemistry (2009), 694(6), 922-929.

[117] Muhammad Hanif, Patricia Schaaf, Wolfgang Kandioller, Michaela. Hejl, Michael A. Jakupec, Alexander Roller, Bernhard K. Keppler, Christian G. Hartinger, Aust. J. Chem. (2010) in press.

moiety was shown and such adducts are stable in solution for more than 18 h, suggesting DNA as a possible target for these organometallic Ru compounds.

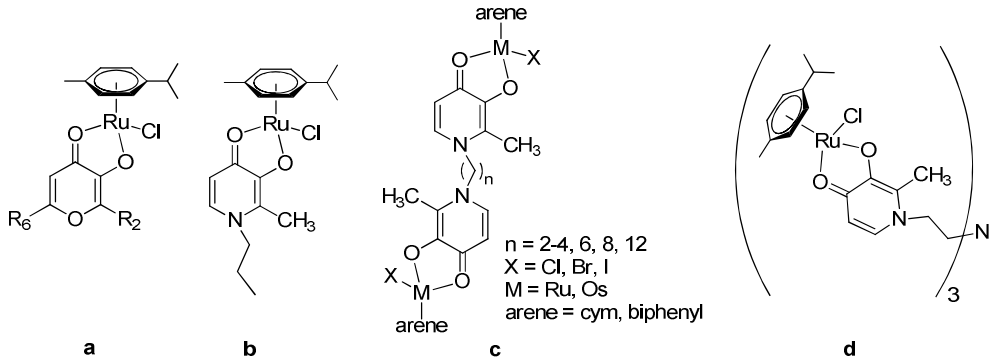

Figure 16. Structures of mono- (**a**,**b**), di- (**c**) and trinuclear (**d**) Ru/Os(arene)(pyr(id)one)X complexes with tumor-inhibiting properties.

In addition to the substitution on the pyrone scaffold, the replacement of the carbonyl oxygen by a sulfur atom resulted in improved stability of the Ru complexes.[115] In contrast to the Ru(arene) complexes of *O,O*-chelating pyrones, *in vitro* anticancer activity assays revealed potent growth inhibition for their *S,O*-chelating thiopyrone analogues with IC_{50} values in the low µM range. Thus the stronger binding of thiopyrones to the ruthenium center explains the higher stability in aqueous solution compared to their pyrone counterparts. These complexes also react rapidly with 5'-GMP to form mono-adducts, however, they show a significantly different behavior in presence of amino acids, forming stable complexes with Met and His, with the thiopyrone ligand remaining bound to the Ru center. This demonstrates again the higher stability of the thiopyrone complexes which might allow them to enter the cells to a higher degree in their unmodified form.[114, 115]

Moreover, complexes based on 4-pyridonato ligands were reported and by linking pyridones di- and trinuclear Ru and Os(arene) compounds were obtained (Fig. 16).[118,119,120,121] Out of the series of compounds, the dinuclear species proved to

[118] Mendoza-Ferri, Maria G.; Hartinger, Christian G.; Mendoza, Marco A.; Groessl, Michael; Egger, Alexander E.; Eichinger, Rene E.; Mangrum, John B.; Farrell, Nicholas P.; Maruszak, Magdalena; Bednarski, Patrick J.; Klein, Franz; Jakupec, Michael A.; Nazarov, Alexey A.; Severin, Kay; Keppler, Bernhard K, Journal of Medicinal Chemistry (2009), 52(4), 916-925.

be the most efficient in *in vitro* anticancer activity assays, in some cell lines being superior to platinum-based anticancer drugs (Fig. 16). The most potent dinuclear compound was 1,12-bis{chlorido[3-(oxo-*κO*)-2-methyl-4-pyridinonato-*κO*4]cym)ruthenium(II)}dodecane (IC_{50} = 0.29 μM) which is an order of magnitude more active than cisplatin (IC_{50} = 4.5 μM) and equally active as oxaliplatin (IC_{50} = 0.30 μM) in SW480 cells.[118] The compounds show strong affinity for transferrin, but surprisingly no interaction with the smaller cellular proteins ubiquitin and cytochrome *c* was detected. The compounds react rapidly with DNA and model nucleotides, as observed by NMR spectroscopy, DNA precipitation, mass spectrometry, and gel electrophoresis. The anticancer activity of this compound class initially appeared to be determined by their lipophilicity,[118] however, DNA and protein interaction studies revealed significant potential for DNA-protein and interduplex cross-linking.[122]

---

[119] Mendoza-Ferri, Maria-Grazia; Hartinger, Christian G.; Eichinger, Rene E.; Stolyarova, Natalya; Severin, Kay; Jakupec, Michael A.; Nazarov, Alexey A.; Keppler, Bernhard K., Organometallics (2008), 27(11), 2405-2407.

[120] Mendoza-Ferri, Maria G.; Hartinger, Christian G.; Nazarov, Alexey A.; Eichinger, Rene E.; Jakupec, Michael A.; Severin, Kay; Keppler, Bernhard K., Organometallics (2009), 28(21), 6260-6265.

[121] Mendoza-Ferri, Maria G.; Hartinger, Christian G.; Nazarov, Alexey A.; Kandioller, Wolfgang; Severin, Kay; Keppler, Bernhard K., Applied Organometallic Chemistry (2008), 22(6), 326-332.

[122] Novakova, Olga; Nazarov, Alexey A.; Hartinger, Christian G.; Keppler, Bernhard K.; Brabec, Viktor. Biochemical Pharmacology (2009), 77(3), 364-374.

2.6 Is the Reactivity of M(II)–Arene Complexes of 3-Hydroxy-2(1H)-pyridones to Biomolecules the Anticancer Activity Determining Parameter?

Muhammad Hanif, Helena Henke, Samuel M. Meier, Sanela Martic, Mahmoud Labib, Wolfgang Kandioller, Michael A. Jakupec, Vladimir B. Arion, Heinz-Bernhard Kraatz, Bernhard K. Keppler, Christian G. Hartinger

Inorganic Chemistry, **2010,** 49 (17), 7953–7963.

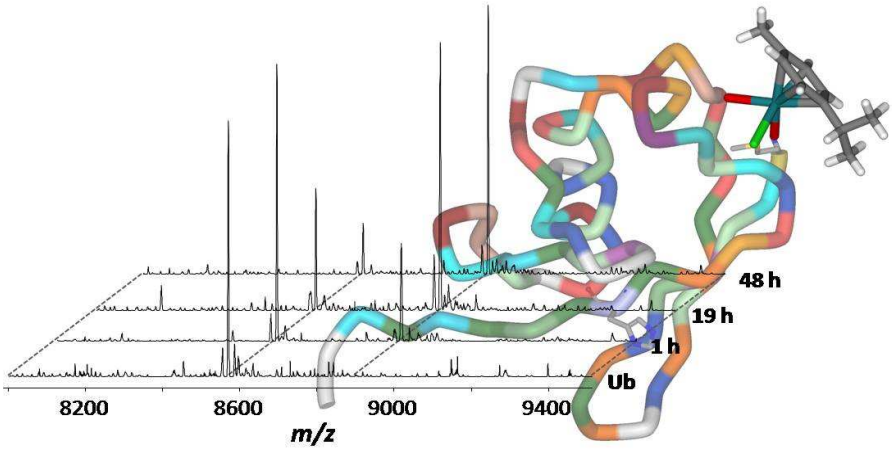

Inorganic Chemistry
Article

Inorg. Chem. **2010**, *49*, 7953–7963 **7953**
DOI: 10.1021/ic1009785

Is the Reactivity of M(II)−Arene Complexes of 3-Hydroxy-2(1*H*)-pyridones to Biomolecules the Anticancer Activity Determining Parameter?

Muhammad Hanif,[†] Helena Henke,[†,‡] Samuel M. Meier,[†,‡] Sanela Martic,[§] Mahmoud Labib,[§] Wolfgang Kandioller,[†] Michael A. Jakupec,[†,‡] Vladimir B. Arion,[†,‡] Heinz-Bernhard Kraatz,[§] Bernhard K. Keppler,[†,‡] and Christian G. Hartinger*[,†,‡]

[†] *University of Vienna, Institute of Inorganic Chemistry, Waehringer Str. 42, A-1090 Vienna, Austria,* [‡] *University of Vienna, Research Platform "Translational Cancer Therapy Research", Waehringer Str. 42, A-1090 Vienna, Austria, and* [§] *Department of Chemistry, The University of Western Ontario, London, Ontario, N6A 5B7, Canada*

Received May 17, 2010

Hydroxypyr(id)ones are versatile ligands for the synthesis of organometallic anticancer agents, equipping them with fine-tunable pharmacological properties. Herein, we report on the preparation, mode of action, and in vitro anticancer activity of Ru^{II}− and Os^{II}−arene complexes with alkoxycarbonylmethyl-3-hydroxy-2-pyridone ligands. The hydrolysis and binding to amino acids proceed quickly, as characterized by NMR spectroscopy and ESI mass spectrometry. However, the reaction with amino acids causes cleavage of the pyridone ligands from the metal center because the amino acids act as multidentate ligands. A similar behavior was also observed during the reactions with the model proteins ubiquitin and cytochrome c, yielding mainly [protein + M(η^6-*p*-cymene)] adducts (M = Ru, Os). Notably the ligand cleavage of the Os derivative was significantly slower than of its Ru analogue, which could explain its higher activity in in vitro anticancer assays. Furthermore, the reaction of the compounds to 5′-GMP was characterized and coordination to the *N7* of the guanine moiety was demonstrated by ^{1}H NMR spectroscopy and X-ray diffraction analysis. CDK2/Cyclin A protein kinase inhibition studies revealed potent activity of the Ru and Os complexes.

Introduction

Ruthenium-based coordination compounds and organometallics are promising antitumor agents, and NAMI-A and KP1019 have passed clinical phase I trials.[1−6] Ruthenium complexes benefit from low ligand exchange rates (similar to platinum complexes), low systemic toxicity, a range of oxidation states accessible under physiological conditions, some physicochemical properties similar to iron, and affinity to serum transport proteins.[7−10] In recent years, the anticancer activity of Ru drug candidates has often been compared to that of their Os analogues; however, no clear-cut structure−activity relationship could be derived. Organometallic ruthenium(II)−arene and also their analogous osmium(II)−arene compounds provide an option to fine-tune the chemical reactivity and also pharmacological properties such as water solubility, oral bioavailability, stability in plasma, pharmacokinetic behavior, etc., on the basis of the choice of ligands and coordination geometry.[5]

One of the first concepts applied in the quest for organometallic Ru anticancer drugs was to combine metal−arene moieties with bioactive ligands as in the first organometallic ruthenium species tested for anticancer activity, i.e., [Ru(η^6-C_6H_6)Cl_2(metronidazole)], containing the common antiinfective agent metronidazole.[11] This strategy was also successful with a variety of enzyme inhibitors such as paullones, ethacrynic acid, and staurosporine.[12−14] However, the combination of noncytotoxic ligands with metals also led to compounds with

*To whom correspondence should be addressed. E-mail: christian.hartinger@univie.ac.at. Phone: +43-1-4277-52609. Fax: +43-1-4277-52680.

(1) Rademaker-Lakhai, J. M.; Van Den Bongard, D.; Pluim, D.; Beijnen, J. H.; Schellens, J. H. M. *Clin. Cancer Res.* **2004**, *10*, 3717–3727.
(2) Hartinger, C. G.; Zorbas-Seifried, S.; Jakupec, M. A.; Kynast, B.; Zorbas, H.; Keppler, B. K. *J. Inorg. Biochem.* **2006**, *100*, 891–904.
(3) Hartinger, C. G.; Jakupec, M. A.; Zorbas-Seifried, S.; Groessl, M.; Egger, A.; Berger, W.; Zorbas, H.; Dyson, P. J.; Keppler, B. K. *Chem. Biodiversity* **2008**, *5*, 2140–2155.
(4) Peacock, A. F. A.; Sadler, P. J. *Chem. Asian J.* **2008**, *3*, 1890–1899.
(5) Hartinger, C. G.; Dyson, P. J. *Chem. Soc. Rev.* **2009**, *38*, 391–401.
(6) Suess-Fink, G. *Dalton Trans.* **2010**, *39*, 1673–1688.
(7) Clarke, M. J.; Zhu, F.; Frasca, D. R. *Chem. Rev.* **1999**, *99*, 2511–2533.
(8) Allardyce, C. S.; Dyson, P. J. *Platinum Met. Rev.* **2001**, *45*, 62–69.
(9) Timerbaev, A. R.; Hartinger, C. G.; Aleksenko, S. S.; Keppler, B. K. *Chem. Rev.* **2006**, *106*, 2224–2248.
(10) Jakupec, M. A.; Galanski, M.; Arion, V. B.; Hartinger, C. G.; Keppler, B. K. *Dalton Trans.* **2008**, 183–194.
(11) Dale, L. D.; Dyson, T. M.; Tocher, D. A.; Tocher, J. H.; Edwards, D. I. *Anti-Cancer Drug Des.* **1989**, *4*, 295–302.
(12) Debreczeni, J. É.; Bullock, A. N.; Atilla, G. E.; Williams, D. S.; Bregman, H.; Knapp, S.; Meggers, E. *Angew. Chem.* **2006**, *45*, 1580–1585.
(13) Schmid, W. F.; John, R. O.; Arion, V. B.; Jakupec, M. A.; Keppler, B. K. *Organometallics* **2007**, *26*, 6643–6652.

Published on Web 08/12/2010

significant anticancer activity as demonstrated for pta, ethylenediamine, and many other examples.[4−6,15]

Metal−arene complexes of the type $[M(\eta^6\text{-arene})(XY)Cl]^{n+}$ (XY = a bidentate *N*,*N*-, *N*,*O*-, *O*,*O*- or *S*,*O*-chelating ligand; $n = 0, 1$) have shown promising cytotoxicity profiles. The coordination of simple bidentate *N*,*N* ligands such as ethylenediamine to organometallic Ru(II)−arene species resulted in compounds exhibiting high cytotoxicity in cancer cells, including cisplatin-resistant cell lines.[4] Monofunctional covalent binding accompanied by a hydrogen bond to DNA nucleobases is considered essential for the mode of action,[16] with the ultimate targets of bioorganometallics still remaining unclear and controversially discussed.[4,5,17] Complexes bearing paullone-derived *N*,*N*-chelating ligands are highly active in in vitro anticancer assays, regardless of whether ruthenium or osmium is the central metal.[13] The same metal centers equipped with *N*,*O*- and *O*,*O*-chelating ligands such as those derived from the amino acids glycine, L-alanine, and L-proline, or with 8-oxyquinolinato, tropolonato, or acetylacetonato give compounds which are moderately cytotoxic,[18] whereas with picolinato and picolinamide ligands promising in vitro activities, also in cisplatin-resistant cells, were observed.[19−21]

Mononuclear ruthenium−arene complexes with *O*,*O*-bound maltol-derived ligands are not or are only marginally cytotoxic.[22,23] Switching from *O*,*O*- to *S*,*O*-donor systems increases the anticancer activity in vitro,[24] probably because of higher stability in the presence of biomolecules.[25] Exchanging pyrones by pyridones (HPs), for example in dinuclear ruthenium−arene complexes with an adjustable spacer length, results in high anticancer activity with the potential to overcome drug resistance.[26−30] Another class of *O*,*O*-donor system ligands are hydroxypyr(id)ones, and their metal complexes have demonstrated potential in different research areas, including medicinal inorganic chemistry. They have been studied extensively as metal chelators,[31,32] magnetic resonance imaging (MRI) contrast media,[33−41] matrix metalloprotein inhibitors,[42−44] receptors for Li^+ or Na^+,[45−47] anthrax lethal factor inhibitors,[48,49] antidiabetic,[50−53] antiviral,[49] and antibacterial agents.[48,49,54] We have reported a series of mono- and polynuclear metal−arene complexes of 3-hydroxy-4-pyr(id)ones and investigated their tumor inhibiting properties.[23,24,26,27,29,55] In order to extend the structure−activity relationships, a series of mononuclear metal(II)−arene complexes of ruthenium and osmium with *O*,*O*-bound alkoxycarbonylmethyl-3-hydroxy-2(1*H*)-pyridones were synthesized and characterized with regard to stability toward hydrolysis, biological activity, and interaction with DNA model nucleobases such as 5′-GMP and 9-ethylguanine and with proteins in order to correlate affinity to biomolecules with anticancer activity.

(14) Ang, W. H.; Parker, L. J.; De Luca, A.; Juillerat-Jeanneret, L.; Morton, C. J.; Lo Bello, M.; Parker, M. W.; Dyson, P. J. *Angew. Chem., Int. Ed.* **2009**, *48*, 3854–3857.
(15) Dyson, P. J. *Chimia* **2007**, *61*, 698–703.
(16) Aird, R. E.; Cummings, J.; Ritchie, A. A.; Muir, M.; Morris, R. E.; Chen, H.; Sadler, P. J.; Jodrell, D. I. *Br. J. Cancer* **2002**, *86*, 1652–1657.
(17) Scolaro, C.; Chaplin, A. B.; Hartinger, C. G.; Bergamo, A.; Cocchietto, M.; Keppler, B. K.; Sava, G.; Dyson, P. J. *Dalton Trans.* **2007**, 5065–5072.
(18) Habtemariam, A.; Melchart, M.; Fernandez, R.; Parsons, S.; Oswald, I. D. H.; Parkin, A.; Fabbiani, F. P. A.; Davidson, J. E.; Dawson, A.; Aird, R. E.; Jodrell, D. I.; Sadler, P. J. *J. Med. Chem.* **2006**, *49*, 6858–6868.
(19) Peacock, A. F. A.; Parsons, S.; Sadler, P. J. *J. Am. Chem. Soc.* **2007**, *129*, 3348–3357.
(20) van Rijt, S. H.; Hebden, A. J.; Amaresekera, T.; Deeth, R. J.; Clarkson, G. J.; Parsons, S.; McGowan, P. C.; Sadler, P. J. *J. Med. Chem.* **2009**, *52*, 7753–7764.
(21) van Rijt, S. H.; Peacock, A. F. A.; Johnstone, R. D. L.; Parsons, S.; Sadler, P. J. *Inorg. Chem.* **2009**, *48*, 1753–1762.
(22) Peacock, A. F. A.; Melchart, M.; Deeth, R. J.; Habtemariam, A.; Parsons, S.; Sadler, P. J. *Chem.—Eur. J.* **2007**, *13*, 2601–2613.
(23) Kandioller, W.; Hartinger, C. G.; Nazarov, A. A.; Kasser, J.; John, R.; Jakupec, M. A.; Arion, V. B.; Dyson, P. J.; Keppler, B. K. *J. Organomet. Chem.* **2009**, *694*, 922–929.
(24) Kandioller, W.; Hartinger, C. G.; Nazarov, A. A.; Kuznetsov, M. L.; John, R. O.; Bartel, C.; Jakupec, M. A.; Arion, V. B.; Keppler, B. K. *Organometallics* **2009**, *28*, 4249–4251.
(25) Kandioller, W.; Hartinger, C. G.; Nazarov, A. A.; Bartel, C.; Skocic, M.; Jakupec, M. A.; Arion, V. B.; Keppler, B. K., *Chem.—Eur. J.* **2009**, *15*, 12283-12291, S12283/1-S12283/32.
(26) Mendoza-Ferri, M. G.; Hartinger, C. G.; Eichinger, R. E.; Stolyarova, N.; Jakupec, M. A.; Nazarov, A. A.; Severin, K.; Keppler, B. K. *Organometallics* **2008**, *27*, 2405–2407.
(27) Mendoza-Ferri, M. G.; Hartinger, C. G.; Nazarov, A. A.; Kandioller, W.; Severin, K.; Keppler, B. K. *Appl. Organomet. Chem.* **2008**, *22*, 326–332.
(28) Mendoza-Ferri, M. G.; Hartinger, C. G.; Nazarov, A. A.; Eichinger, R. E.; Jakupec, M. A.; Severin, K.; Keppler, B. K. *Organometallics* **2009**, *28*, 6260–6265.
(29) Mendoza-Ferri, M. G.; Hartinger, C. G.; Mendoza, M. A.; Groessl, M.; Egger, A. E.; Eichinger, R. E.; Mangrum, J. B.; Farrell, N. P.; Maruszak, M.; Bednarski, P. J.; Klein, F.; Jakupec, M. A.; Nazarov, A. A.; Severin, K.; Keppler, B. K. *J. Med. Chem.* **2009**, *52*, 916–925.
(30) Nováková, O.; Nazarov, A. A.; Hartinger, C. G.; Keppler, B. K.; Brabec, V. *Biochem. Pharmacol.* **2009**, *77*, 364–374.
(31) Santos, M. A. *Coord. Chem. Rev.* **2008**, *252*, 1213–1224.
(32) Grazina, R.; Gano, L.; Sebestik, J.; Santos, M. A. *J. Inorg. Biochem.* **2009**, *103*, 262–273.
(33) Pierre, V. C.; Botta, M.; Aime, S.; Raymond, K. N. *J. Am. Chem. Soc.* **2006**, *128*, 5344–5345.
(34) Werner, E. J.; Avedano, S.; Botta, M.; Hay, B. P.; Moore, E. G.; Aime, S.; Raymond, K. N. *J. Am. Chem. Soc.* **2007**, *129*, 1870–1871.
(35) Jocher, C. J.; Botta, M.; Avedano, S.; Moore, E. G.; Xu, J.; Aime, S.; Raymond, K. N. *Inorg. Chem.* **2007**, *46*, 4796–4798.
(36) Jocher, C. J.; Moore, E. G.; Xu, J.; Avedano, S.; Botta, M.; Aime, S.; Raymond, K. N. *Inorg. Chem.* **2007**, *46*, 9182–9191.
(37) Werner, E. J.; Datta, A.; Jocher, C. J.; Raymond, K. N. *Angew. Chem., Int. Ed.* **2008**, *47*, 8568–8580.
(38) Datta, A.; Hooker, J. M.; Botta, M.; Francis, M. B.; Aime, S.; Raymond, K. N. *J. Am. Chem. Soc.* **2008**, *130*, 2546–2552.
(39) Moore, E. G.; Seitz, M.; Raymond, K. N. *Inorg. Chem.* **2008**, *47*, 8571–8573.
(40) Datta, A.; Raymond, K. N. *Acc. Chem. Res.* **2009**, *42*, 938–947.
(41) Werner, E. J.; Kozhukh, J.; Botta, M.; Moore, E. G.; Avedano, S.; Aime, S.; Raymond, K. N. *Inorg. Chem.* **2009**, *48*, 277–286.
(42) Jacobsen, F. E.; Lewis, J. A.; Cohen, S. M. *ChemMedChem* **2007**, *2*, 152–171.
(43) Zhang, Y.-M.; Fan, X.; Yang, S.-M.; Scannevin, R. H.; Burke, S. L.; Rhodes, K. J.; Jackson, P. F. *Bioorg. Med. Chem. Lett.* **2008**, *18*, 405–408.
(44) Yan, Y.-L.; Miller, M. T.; Cao, Y.; Cohen, S. M. *Bioorg. Med. Chem. Lett.* **2009**, *19*, 1970–1976.
(45) Piotrowski, H.; Polborn, K.; Hilt, G.; Severin, K. *J. Am. Chem. Soc.* **2001**, *123*, 2699–2700.
(46) Grote, Z.; Lehaire, M.-L.; Scopelliti, R.; Severin, K. *J. Am. Chem. Soc.* **2003**, *125*, 13638–13639.
(47) Grote, Z.; Scopelliti, R.; Severin, K. *J. Am. Chem. Soc.* **2004**, *126*, 16959–16972.
(48) Lewis, J. A.; Mongan, J.; McCammon, J. A.; Cohen, S. M. *ChemMedChem* **2006**, *1*, 694–697.
(49) Agrawal, A.; de Oliveira, C. A. F.; Cheng, Y.; Jacobsen, J. A.; McCammon, J. A.; Cohen, S. M. *J. Med. Chem.* **2009**, *52*, 1063–1074.
(50) Jakusch, T.; Gajda-Schrantz, K.; Adachi, Y.; Sakurai, H.; Kiss, T.; Horvath, L. *J. Inorg. Biochem.* **2006**, *100*, 1521–1526.
(51) Enyedy, E. A.; Lakatos, A.; Horvath, L.; Kiss, T. *J. Inorg. Biochem.* **2008**, *102*, 1473–1485.
(52) Jakusch, T.; Hollender, D.; Enyedy, E. A.; Gonzalez, C. S.; Montes-Bayon, M.; Sanz-Medel, A.; Pessoa, J. C.; Tomaz, I.; Kiss, T. *Dalton Trans.* **2009**, 2428–2437.
(53) Katoh, A.; Matsumura, Y.; Yoshikawa, Y.; Yasui, H.; Sakurai, H. *J. Inorg. Biochem.* **2009**, *103*, 567–574.
(54) Feng, M. H.; van der Does, L.; Bantjes, A. *J. Med. Chem.* **1993**, *36*, 2822–7.
(55) Kasser, J. H.; Kandioller, W.; Hartinger, C. G.; Nazarov, A. A.; Arion, V. B.; Dyson, P. J.; Keppler, B. K. *J. Organomet. Chem.* **2010**, *695*, 875–881.

Experimental Section

Materials and Methods. All reactions were carried out in dry solvents under an inert atmosphere. Chemicals obtained from commercial suppliers were used as received and were of analytical grade; methanol and CH_2Cl_2 were dried using standard procedures. OsO_4 (99.8%; ***Caution!*** *OsO_4 is highly toxic and volatile!*[56]) and $RuCl_3 \cdot 3H_2O$ (40.4%) were purchased from Johnson Matthey; ubiquitin from bovine red blood cells and horse heart cytochrome c from Sigma; L-alanine and α-terpinene from Acros; glycine and L-histidine from Merck; L-cysteine, 5′-dGMP, 5′-GMP, and $N_2H_4 \cdot 2HCl$ from Fluka; and L-methionine from Sigma-Aldrich. The solvents for ESI-MS studies were methanol (VWR Int., HiPerSolv CHROMANORM), formic acid (Fluka), and Milli-Q H_2O (18.2 MΩ, Synergy 185 UV Ultrapure, Millipore, France). The dimers bis[dichlorido(η^6-*p*-cymene)ruthenium(II)],[57,58] bis[dibromido(η^6-*p*-cymene)ruthenium(II)],[28] bis[diiodido(η^6-*p*-cymene)ruthenium(II)],[28] and bis[dichlorido(η^6-*p*-cymene)osmium(II)],[59] and the ligands 1-[(ethoxycarbonyl)methyl]-3-hydroxy-2-(1*H*)-pyridone **a**,[60] 1-[(methoxycarbonyl)methyl]-3-hydroxy-2-(1*H*)-pyridone **b**,[61] and 1-ethoxycarbonylmethyl-3-hydroxy-4-methyl-2-(1*H*)-pyridone **c**[62] were synthesized using literature procedures.

^{1}H, ^{31}P{^{1}H}, and ^{13}C{^{1}H} NMR spectra were recorded at 25 °C on a Bruker FT NMR spectrometer Avance III 500 MHz at 500.10 (^{1}H), 202.44 (^{31}P{^{1}H}), and 125.75 MHz (^{13}C{^{1}H}), and 2D NMR data were collected in a gradient-enhanced mode. Melting points were measured on a Büchi B-540 apparatus and are uncorrected. Elemental analysis was done on a Perkin−Elmer 2400 CHN elemental analyzer by the Laboratory for Elemental Analysis, Faculty of Chemistry, University of Vienna. Electrospray ionization mass spectra were recorded on a Bruker esquire$_{3000}$ ion trap instrument.

X-ray diffraction measurements of single crystals of **1a**, **1b**, and **5a** were performed on a Bruker X8 APEX II CCD diffractometer at 100 K. The crystals were positioned at 35 mm from the detector and 1917, 1580, and 1446 frames for 30, 50, and 60 s over 1° were measured for **1a**, **1b**, and **5a**, respectively. The data were processed using the SAINT Plus software package.[63] Crystal data, data collection parameters, and structure refinement details are given in Table 1. The structures were solved by direct methods and refined by full-matrix least-squares techniques. Non-hydrogen atoms were refined with anisotropic displacement parameters. H atoms were inserted at calculated positions and refined with a riding model. The isopropyl group of the *p*-cymene moiety in **5a** was found disordered. The disorder was resolved with constrained anisotropic displacement parameters and restrained bond distances using EADP and SADI instructions of SHELX97, respectively. The site occupation factors were refined to about 0.60:0.40. The following software programs and tables were used: structure solution, SHELXS-97;[64,65] refinement, SHELXL-97;[65,66] and molecular diagrams, ORTEP-3.[67]

Synthesis. General Procedure. A solution of 3-hydroxy-2-(1*H*)-pyridone (2.2 equiv) and NaOMe (3.5 equiv) in 20 mL MeOH was stirred for about 30 min. A solution of [(η^6-cymene)MX(μ-X)]$_2$ (1.0 equiv; M = Ru, Os; X = Cl, Br, I) in 5 mL CH_2Cl_2 was added, and the mixture was stirred for 4 h at RT. The solvent was removed under reduced pressure. The residue was redissolved in CH_2Cl_2, and filtered to remove undissolved impurities. The filtrate was evaporated under vacuum. Recrystallization from CH_2Cl_2 and diethyl ether gave the pure product.

[Chlorido(η^6-*p*-cymene){*N*-[(ethoxycarbonyl)methyl]-3-oxo-κ*O*-2-(1*H*)-pyridonato-κ*O*}ruthenium(II)] (1a). The title compound was synthesized from *N*-[(ethoxycarbonyl)methyl]-3-hydroxy-2-(1*H*)-pyridone (130 mg, 0.33 mmol), NaOMe (38 mg, 0.70 mmol), and [(η^6-*p*-cymene)RuCl(μ-Cl)]$_2$ (92 mg, 0.15 mmol), following the general procedure. Crystals suitable for X-ray diffraction analysis were grown by slow diffusion of diethyl ether into a solution of **1a** in CH_2Cl_2. Yield: 130 mg (93%), mp 221−222 °C dec. Elemental analysis: found C, 48.55; H, 4.88; N, 2.94. Calcd for $C_{19}H_{24}O_4NClRu$: C, 48.87; H, 5.18; N, 2.99; MS (ESI$^+$) *m*/*z* 432.2 [M − Cl]$^+$. ^{1}H NMR (500.10 MHz, $CDCl_3$, 25 °C): δ 6.67 (dd, $^3J_{(H5,H6)}$ = 8 Hz, $^4J_{(H4,H6)}$ = 1 Hz, 1H, H-6$_{Py}$), 6.40 (dd, $^3J_{(H4,H5)}$ = 7 Hz, $^4J_{(H4,H6)}$ = 1 Hz, 1H, H-4$_{Py}$), 6.26 (dd, $^3J_{(H5,H6)}$ = 7 Hz, $^3J_{(H4,H5)}$ = 7 Hz, 1H, H-5$_{Py}$), 5.62 (d, $^3J_{(H,H)}$ = 6 Hz; 1H, Ar-H), 5.60 (d, $^3J_{(H,H)}$ = 6 Hz, 1H, Ar-H), 5.38 (d, $^3J_{(H,H)}$ = 6 Hz, 1H, Ar-H), 5.34 (d, $^3J_{(H,H)}$ = 6 Hz, 1H, Ar-H), 5.11 (d, $^2J_{gem(H,H)}$ = 17 Hz, 1H, NCH_2CO), 4.27 (m, 3H, NCH_2CO, OCH_2CH$_3$), 2.93 (m, 1H, CH(CH$_3$)$_2$), 2.31 (s, 3H, Ar-CH$_3$), 1.33 (m, 9H, (CH_3)$_2$CH-Ar, OCH$_2$CH_3) ppm. ^{13}C{^{1}H} NMR (125.75 MHz, $CDCl_3$, 25 °C): δ 167.0 (C-2), 166.3 (C-3), 160.9 (*C*OOEt), 121.1 (C-4), 117.6 (C-6), 112.7 (C-5), 99.7 (C-Ar), 94.4 (C-Ar), 81.4 (CH-Ar), 80.5 (CH-Ar), 79.3 (CH-Ar), 77.8 (CH-Ar), 61.9 (O*C*H$_2$CH$_3$), 51.3 (N*C*H$_2$CO), 31.2 (*C*H(CH$_3$)$_2$), 22.5 (CH(*C*H$_3$)$_2$), 22.4 (CH(*C*H$_3$)$_2$), 18.5 (Ar-*C*H$_3$), 14.2 (OCH$_2$*C*H$_3$) ppm.

[Chlorido(η^6-*p*-cymene){*N*-[(methoxycarbonyl)methyl]-3-oxo-κ*O*-2-(1*H*)-pyridonato-κ*O*}ruthenium(II)] (1b). The title compound was synthesized from *N*-[(methoxycarbonyl)methyl]-3-hydroxy-2-(1*H*)-pyridone (40 mg, 0.22 mmol), NaOMe (19 mg, 0.35 mmol) and [(η^6-*p*-cymene)RuCl(μ-Cl)]$_2$ (61 mg, 0.10 mmol), following the general procedure. Crystals suitable for X-ray diffraction analysis were grown by slow diffusion of diethyl ether into a solution of **1b** in CH_2Cl_2. Yield: 81 mg (90%), mp > 200 °C dec. Elemental analysis: found C, 47.39; H, 4.63; N, 2.98. Calcd for $C_{18}H_{22}NO_4ClRu$: C, 47.74; H, 4.89; N, 3.09; MS (ESI$^+$) *m*/*z* 418.0 [M − Cl]$^+$. ^{1}H NMR (500.10 MHz, $CDCl_3$, 25 °C): δ 6.67 (dd, $^3J_{(H5,H6)}$ = 8 Hz, $^4J_{(H4,H6)}$ = 1 Hz, 1H, H-6$_{Py}$), 6.40 (d, $^3J_{(H4,H5)}$ = 7 Hz, 1H, H-4$_{Py}$), 6.26 (dd, $^3J_{(H5,H6)}$ = 7 Hz, $^3J_{(H4,H5)}$ = 8 Hz, 1H, H-5$_{Py}$), 5.51 (d, $^3J_{(H,H)}$ = 6 Hz; 1H, Ar-H), 5.50 (d, $^3J_{(H,H)}$ = 6 Hz; 1H, Ar-H), 5.31 (d, $^3J_{(H,H)}$ = 6 Hz, 1H, Ar-H), 5.31 (d, $^3J_{(H,H)}$ = 6 Hz, 1H, Ar-H), 5.11 (d, $^2J_{gem(H,H)}$ = 17 Hz, 1H, NCH_2CO), 4.27 (d, $^2J_{gem(H,H)}$ = 17 Hz, 1H, NCH_2CO), 3.81 (s, 3H, OCH_3), 2.88 (m, 1H, CH(CH$_3$)$_2$), 2.29 (s, 3H, Ar-CH_3), 1.34 (d, $^3J_{(H,H)}$ = 6.9 Hz, 3H, CH(CH_3)$_2$), 1.30 (d, $^3J_{(H,H)}$ = 6.9 Hz, 3H, CH(CH_3)$_2$) ppm. ^{13}C{^{1}H} NMR (125.75 MHz, $CDCl_3$, 25 °C): δ 167.3 (C-2), 166.2 (C-3), 160.7 (*C*OOMe), 121.1 (C-4), 117.7 (C-6), 112.8 (C-5), 99.4 (C-Ar), 94.8 (C-Ar), 81.3 (CH-Ar), 80.5 (CH-Ar), 79.2 (CH-Ar), 77.3 (CH-Ar), 52.7 (COO*C*H$_3$), 51.3 (N*C*H$_2$CO), 31.1 (*C*H(CH$_3$)$_2$), 22.4 (CH(*C*H$_3$)$_2$), 22.3 (CH(*C*H$_3$)$_2$), 18.5 (Ar-CH$_3$) ppm.

[Chlorido(η^6-*p*-cymene){*N*-[(ethoxycarbonyl)methyl]-3-oxo-κ*O*-4-methyl-2(1*H*)-pyridonato-κ*O*}ruthenium(II)] (1c). The title compound was synthesized from *N*-[(ethoxycarbonyl)methyl]-3-hydroxy-4-methyl-2(1*H*)-pyridone (85 mg, 0.40 mmol), NaOMe (25 mg, 0.44 mmol), and [(η^6-*p*-cymene)RuCl(μ-Cl)]$_2$ (122 mg,

(56) Young, J. A. *J. Chem. Educ.* **2002**, *79*, 1064.
(57) Bennett, M. A.; Smith, A. K. *J. Chem. Soc., Dalton Trans.* **1974**, 233–41.
(58) Bennett, M. A.; Huang, T. N.; Matheson, T. W.; Smith, A. K. *Inorg. Synth.* **1982**, *21*, 74–8.
(59) Kiel, W. A.; Ball, R. G.; Graham, W. A. G. *J. Organomet. Chem.* **1990**, *383*, 481–96.
(60) Streater, M.; Taylor, P. D.; Hider, R. C.; Porter, J. *J. Med. Chem.* **1990**, *33*, 1749–55.
(61) Brown, E. J.; Whitwood, A. C.; Walton, P. H.; Duhme-Klair, A.-K. *Dalton Trans.* **2004**, 2458–2462.
(62) Fox, R. C.; Taylor, P. D. *Synth. Commun.* **1998**, *28*, 1563–1574.
(63) Pressprich, M. R.; Chambers, J. *SAINT + Integration Engine, Program for Crystal Structure Integration*; Bruker Analytical X-ray Systems: Madison, WI, 2004.
(64) Sheldrick, G. M. *SHELXS-97, Program for Crystal Structure Solution*, University Göttingen: Göttingen, Germany, 1997.
(65) Sheldrick, G. M. *Acta Crystallogr., Sect. A: Found. Crystallogr.* **2008**, *A64*, 112–122.
(66) Sheldrick, G. M. *SHELXL-97, Program for Crystal Structure Refinement*; University Göttingen; Göttingen, Germany, 1997.
(67) Farrugia, L. J. *J. Appl. Crystallogr.* **1997**, *30*, 565.

Table 1. Crystal Data and Details of Data Collection for **1a**, **1b**, and **5a**[a]

compound	1a	1b	5a
chemical formula	$C_{19}H_{24}ClNO_4Ru$	$C_{18}H_{22}ClNO_4Ru$	$C_{27}H_{33}F_3N_6O_8Ru\,S$
M (g mol^{-1})	466.91	452.89	759.72
temperature (K)	100(2)	100(2)	100(2)
crystal size (mm)	0.25 × 0.20 × 0.13	0.14 × 0.10 × 0.04	0.20 × 0.13 × 0.13
crystal color, habit	orange, block	orange, block	orange, block
crystal system	triclinic	triclinic	triclinic
space group	$P\bar{1}$	$P\bar{1}$	$P\bar{1}$
a (Å)	9.5302(4)	9.4338(4)	11.6654(5)
b (Å)	10.1465(4)	10.0892(4)	12.5639(9)
c (Å)	10.5931(5)	10.2654(5)	12.6860(7)
V (Å^3)	960.63(7)	922.26(7)	1606.11(16)
Z	2	2	2
D_c (g cm^{-3})	1.614	1.631	1.571
μ (mm^{-1})	0.979	1.017	0.627
F(000)	476	460	776
Θ range (deg)	2.64 to 30.12	2.64 to 30.08	2.51 to 30.11
h range	−13/13	−13/13	−16/16
k range	−14/14	−14/14	−17/17
l range	−14/14	−14/14	−17/17
no. refls.	5610	5384	9411
no. parameters	237	227	425
R_{int}	0.0358	0.0736	0.0609
R_1 (obs.)	0.0241	0.0356	0.0366
wR_2 (all data)	0.0596	0.0802	0.0908
S	1.003	1.014	1.005

[a] Refinement was by full-matrix least-squares (F_o^2) for all reflections, $R_1 = \sum||F_o| - |F_c||/\sum|F_o|$, $wR_2 = \{\sum[w(F_o^2 - F_c^2)^2]/\sum[w(F_o^2)^2]\}^{1/2}$. Goodness of fit, $S = \{\sum[w(F_o^2 - F_c^2)^2]/(n-p)\}^{1/2}$.

0.20 mmol), following the general procedure. Yield: 110 mg (57%), mp > 200 °C dec. Elemental analysis: found C, 49.60; H, 5.23; N, 2.89. Calcd for $C_{20}H_{26}NO_4ClRu$: C, 49.95; H, 5.45; N, 2.91; MS (ESI$^+$) m/z 446.0 [M − Cl]$^+$. ^{1}H NMR (500.10 MHz, $CDCl_3$, 25 °C): δ 6.34 (d, $^3J_{(H5,H6)}$ = 7 Hz, 1H, H-6$_{Py}$), 6.18 (dd, $^3J_{(H5,H6)}$ = 7 Hz, 1H, H-5$_{Py}$), 5.52 (d, $^3J_{(H,H)}$ = 6 Hz, 1H, Ar-H), 5.49 (d, $^3J_{(H,H)}$ = 6 Hz, 1H, Ar-H), 5.25 (d, $^3J_{(H,H)}$ = 6 Hz, 1H, Ar-H), 5.24 (d, $^3J_{(H,H)}$ = 6 Hz, 1H, Ar-H), 5.13 (d, $^2J_{gem(H,H)}$ = 17 Hz, 1H, NCH_2CO), 4.28 (m, 2H, OCH_2CH$_3$), 4.19 (d, $^2J_{gem(H,H)}$ = 17 Hz, 1H, NCH_2CO), 2.89 (m, 1H, CH(CH$_3$)$_2$) 2.31 (s, 3H, Ar-CH_3), 2.19 (s, 3H, Py-CH$_3$), 1.34 (m, 9H, CH(CH_3)$_2$, OCH$_2$CH_3) ppm. ^{13}C{^{1}H} NMR (125.75 MHz, $CDCl_3$, 25 °C): δ 167.2 (C-2), 164.3 (C-3), 158.2 (*C*OOEt), 128.9 (C-4), 120.0 (C-6), 115.4 (C-5), 98.5 (C-Ar), 95.8 (C-Ar), 81.3 (CH-Ar), 80.5 (CH-Ar), 77.7 (CH-Ar), 77.1 (CH-Ar), 61.8 (O*C*H$_2$CH$_3$), 51.1 (N*C*H$_2$CO), 31.1 (*C*H(CH$_3$)$_2$), 22.4 (CH(*C*H$_3$)$_2$), 22.3 (CH(*C*H$_3$)$_2$), 18.5 (Ar-*C*H$_3$), 15.5 (Py-*C*H$_3$), 14.2 (OCH$_2$*C*H$_3$) ppm.

[Bromido(η^6-*p*-cymene){*N*-[(ethoxycarbonyl)methyl]-3-oxo-κ*O*-2-(1*H*)-pyridonato-κ*O*}ruthenium(II)] (2a). The title compound was synthesized from *N*-[(ethoxycarbonyl)methyl]-3-hydroxy-2-(1*H*)-pyridone (43 mg, 0.22 mmol), NaOMe (19 mg, 0.35 mmol), and [(η^6-*p*-cymene)RuBr(μ-Br)]$_2$ (79 mg, 0.10 mmol), following the general procedure. Yield: 90 mg (88%), mp 204−205 °C dec. Elemental analysis: found C, 44.44; H, 4.69; N, 2,78. Calcd for $C_{19}H_{24}NO_4BrRu$: C, 44.63; H, 4.73; N, 2.74; MS (ESI$^+$) m/z 432.0 [M − Br]$^+$. ^{1}H NMR (500.10 MHz, $CDCl_3$, 25 °C): δ 6.67 (dd, $^3J_{(H5,H6)}$ = 8 Hz, $^4J_{(H4,H6)}$ = 1 Hz, 1H, H-6$_{Py}$), 6.40 (dd, $^3J_{(H4,H5)}$ = 7 Hz, $^4J_{(H4,H6)}$ = 1 Hz, 1H, H-4$_{Py}$), 6.26 (dd, $^3J_{(H5,H6)}$ = 7 Hz, $^3J_{(H4,H5)}$ = 7 Hz, 1H, H-5$_{Py}$), 5.53 (d, $^3J_{(H,H)}$ = 6 Hz, 1H, Ar-H), 5.52 (d, $^3J_{(H,H)}$ = 6 Hz, 1H, Ar-H), 5.32 (d, $^3J_{(H,H)}$ = 6 Hz, 1H, Ar-H), 5.31 (d, $^3J_{(H,H)}$ = 6 Hz, 1H, Ar-H), 5.11 (d, $^2J_{gem(H,H)}$ = 17 Hz, 1H, NCH_2CO), 4.27 (m, 3H, NCH_2CO, OCH_2CH$_3$), 2.93 (m, 1H, CH(CH$_3$)$_2$) 2.31 (s, 3H, Ar-CH$_3$), 1.33 (m, 9H, CH(CH_3)$_2$, OCH$_2$CH_3) ppm. ^{13}C{^{1}H} NMR (125.75 MHz, $CDCl_3$, 25 °C): δ 167.0 (C-2), 166.3 (C-3), 160.9 (*C*OOEt), 121.1 (C-4), 117.6 (C-6), 112.7 (C-5), 99.7 (C-Ar), 94.4 (C-Ar), 81.4 (CH-Ar), 80.5 (CH-Ar), 79.3 (CH-Ar), 77.8 (CH-Ar), 61.9 (O*C*H$_2$CH$_3$), 51.3 (N*C*H$_2$CO), 31.2 (*C*H(CH$_3$)$_2$), 22.5 (CH(*C*H$_3$)$_2$), 22.4 (CH(*C*H$_3$)$_2$), 18.5 (Ar-*C*H$_3$), 14.2 (OCH$_2$*C*H$_3$) ppm.

[(η^6-*p*-Cymene){*N*-[(ethoxycarbonyl)methyl]-3-oxo-κ*O*-2-(1*H*)-pyridonato-κ*O*}iodidoruthenium(II)] (3a). The title compound was synthesized from *N*-[(ethoxycarbonyl)methyl]-3-hydroxy-2-(1*H*)-pyridone (43 mg, 0.22 mmol), NaOMe (19 mg, 0.35 mmol), and [(η^6-*p*-cymene)RuI(μ-I)]$_2$ (98 mg, 0.10 mmol), following the general procedure. Yield: 69 mg (62%), mp 214−215 °C dec. Elemental analysis: found C, 40.53; H, 4.26; N, 2.5. Calcd for $C_{19}H_{24}NO_4IRu$: C, 40.87; H, 4.33; N, 2.51; MS (ESI$^+$) m/z 432.0 [M − I]$^+$. ^{1}H NMR (500.10 MHz, $CDCl_3$, 25 °C): δ 6.66 (dd, $^3J_{(H5,H6)}$ = 1 Hz, $^4J_{(H4,H6)}$ = 7 Hz, 1H, H-6$_{Py}$), 6.41 (dd, $^3J_{(H4,H5)}$ = 7 Hz, $^4J_{(H4,H6)}$ = 1 Hz, 1H, H-4$_{Py}$), 6.26 (dd, $^3J_{(H5,H6)}$ = 7 Hz, $^3J_{(H4,H5)}$ = 8 Hz, 1H, H-5$_{Py}$), 5.58 (d, $^3J_{(H,H)}$ = 5 Hz, 1H, Ar-H), 5.54 (d, $^3J_{(H,H)}$ = 5 Hz, 1H, Ar-H), 5.38 (d, $^3J_{(H,H)}$ = 5 Hz, 1H, Ar-H), 5.31 (d, $^3J_{(H,H)}$ = 5 Hz, 1H, Ar-H), 5.02 (d, $^2J_{gem(H,H)}$ = 17 Hz, 1H, NCH_2CO), 4.28 (m, 3H, NCH_2CO, OCH_2CH$_3$), 2.95 (m, 1H, CH(CH$_3$)$_2$) 2.33 (s, 3H, Ar-CH$_3$), 1.33 (m, 9H, CH(CH_3)$_2$, OCH$_2$-CH_3) ppm. ^{13}C{^{1}H} NMR (125.75 MHz, $CDCl_3$, 25 °C): δ 167.3 (C-2), 166.7 (C-3), 161.7 (*C*OOEt), 121.0 (C-4), 117.5 (C-6), 112.8 (C-5), 100.2 (C-Ar), 94.4 (C-Ar), 80.0 (CH-Ar), 79.4 (CH-Ar), 78.9 (CH-Ar), 77.0 (CH-Ar), 61.1 (O*C*H$_2$CH$_3$), 51.4 (N*C*H$_2$CO), 31.4 (*C*H(CH$_3$)$_2$), 22.6 (CH(*C*H$_3$)$_2$), 22.5 (CH(*C*H$_3$)$_2$), 19.2 (Ar-*C*H$_3$), 14.2 (OCH$_2$*C*H$_3$) ppm.

[Chlorido(η^6-*p*-cymene){*N*-[(ethoxycarbonyl)methyl]-3-oxo-κ*O*-2-(1*H*)-pyridonato-κ*O*}osmium(II)] (4a). The title compound was synthesized from *N*-[(ethoxycarbonyl)methyl]-3-hydroxy-2-(1*H*)-pyridone (44 mg, 0.22 mmol), NaOMe (19 mg, 0.35 mmol), and [(η^6-*p*-cymene)OsCl(μ-Cl)]$_2$ (79 mg, 0.10 mmol), following the general procedure. Yield: 85 mg (76%), mp 222−223 °C dec. Elemental analysis: found C, 40.81; H, 4.14; N, 2.50. Calcd for $C_{19}H_{24}O_4NClOs$: C, 41.04; H, 4.35; N, 2.52; MS (ESI$^+$) m/z 520.2 [M − Cl]$^+$. ^{1}H NMR (500.10 MHz, $CDCl_3$, 25 °C): δ 6.68 (dd, $^3J_{(H5,H6)}$ = 8 Hz, $^4J_{(H4,H6)}$ = 1 Hz, 1H, H-6$_{Py}$), 6.41 (dd, $^3J_{(H4,H5)}$ = 7 Hz, $^4J_{(H4,H6)}$ = 1 Hz, 1H, H-4$_{Py}$), 6.26 (dd, $^3J_{(H5,H6)}$ = 7 Hz, $^3J_{(H4,H5)}$ = 7 Hz, 1H, H-5$_{Py}$), 5.51 (d, $^3J_{(H,H)}$ = 6 Hz, 1H, Ar-H), 5.50 (d, $^3J_{(H,H)}$ = 6 Hz, 1H, Ar-H), 5.31 (d, $^3J_{(H,H)}$ = 6 Hz, 1H, Ar−H), 5.30 (d, $^3J_{(H,H)}$ = 6 Hz, 1H, Ar-H), 5.11 (d, $^2J_{gem(H,H)}$ = 17 Hz, 1H, NCH_2CO), 4.27 (m, 3H, NCH_2CO, OCH_2CH$_3$), 2.93 (m, 1H, CH(CH$_3$)$_2$), 2.31 (s, 3H, Ar-CH_3), 1.33 (m, 9H, CH(CH_3)$_2$, OCH$_2$CH_3) ppm. ^{13}C{^{1}H} NMR (125.75 MHz, $CDCl_3$, 25 °C): δ 167.3 (C-2), 166.1 (C-3), 160.9 (*C*OOEt), 121.4 (C-4), 117.6 (C-6),

112.7 (C-5), 99.7 (C-Ar), 94.4 (C-Ar), 81.4 (CH-Ar), 80.5 (CH-Ar), 79.3 (CH-Ar), 77.8 (CH-Ar), 61.9 (OCH_2CH_3), 51.3 (NCH_2CO), 31.2 ($CH(CH_3)_2$), 22.5 ($CH(CH_3)_2$), 22.4 ($CH(CH_3)_2$), 18.5 ($Ar-CH_3$), 14.4 (OCH_2CH_3) ppm.

[(η^6-*p*-cymene){*N*-[(ethoxycarbonyl)methyl]-3-oxo-κO-2-(1*H*)-pyridonato-κO}(9-ethylguanine-$\kappa N7$)ruthenium(II)] trifluoromethanesulfonate (5a). A solution of $Ag(CF_3SO_3)$ (20 mg, 0.077 mmol) in H_2O (5 mL) was added to a solution of **1a** (33 mg, 0.070 mmol) in H_2O (15 mL) and stirred for 2 h at RT under light protection. The solution was filtered to remove AgCl, and 9-ethylguanine (14 mg, 0.077 mmol; 9-EtG) was added to the filtrate and stirred for 24 h at RT. The solvent was removed under reduced pressure, and the product was recrystallized from methanol and diethyl ether to give crystals suitable for X-ray diffraction analysis. Yield: 36 mg (67%), mp > 200 °C dec. Elemental analysis: found C, 42.68; H, 4.12; N, 10.94. Calcd for $C_{27}H_{33}N_6O_8F_3SRu$: C, 42.69; H, 4.38; N, 11.06; MS (ESI$^+$) m/z 432.0 $[M - 9EtG]^+$ (100%), 610.8 $[M]^+$ (9%). ^{1}H NMR (500.10 MHz, DMSO-d_4, 25 °C): δ 10.77 (s, 1H, *H*-N1 of 9-EtG), 7.70 (s, 1H, *H*-8 of 9-EtG), 7.03 (dd, $^3J_{(H5,H6)}$ = 8 Hz, $^4J_{(H4,H6)}$ = 1 Hz, 1H, H-6$_{Py}$), 6.79 (dd, $^3J_{(H4,H5)}$ = 7 Hz, $^4J_{(H4,H6)}$ = 1 Hz, 1H, H-4$_{Py}$), 6.65 (dd, $^3J_{(H5,H6)}$ = 7 Hz, $^3J_{(H4,H5)}$ = 7 Hz, 1H, H-5$_{Py}$), 6.41 (brs, 2H, H_2N of 9-EtG), 5.85 (d, $^3J_{(H,H)}$ = 6 Hz, 1H, Ar-H), 5.77 (d, $^3J_{(H,H)}$ = 6 Hz, 1H, Ar-H), 5.63 (d, $^3J_{(H,H)}$ = 6 Hz, 1H, Ar-H), 5.58 (d, $^3J_{(H,H)}$ = 6 Hz, 1H, Ar-H), 5.17 (d, $^2J_{gem(H,H)}$ = 17 Hz, 1H, NCH_2CO), 5.04 (d, $^2J_{gem(H,H)}$ = 17 Hz, 1H, NCH_2-CO), 4.20 (m, 2H, OCH_2CH_3), 3.96 (m, 2H, NCH_2CH_3), 2.84 (m, 1H, $CH(CH_3)_2$), 2.26 (s, 3H, Ar-CH_3), 1.33 (m, 3H, NCH_2-CH_3)1.24 (m, 9H, $CH(CH_3)_2$, OCH_2CH_3) ppm. $^{13}C\{^1H\}$ NMR (125.75 MHz, DMSO-d_4, 25 °C): δ 167.9 (C-2), 165.5 (C-3), 160.0 (COO), 157.3 (C6 of 9-EtG), 154.6 (C2 of 9-EtG), 151.4 (C4 of 9-EtG), 137.4 (C6 of 9-EtG), 129.3 (C-4), 123.5 (C-6), 117.8 (C-5), 117.2 (C5 of 9-EtG), 99.8 (C-Ar), 96.7 (C−Ar), 82.1 (CH-Ar), 81.8 (CH-Ar), 80.4 (CH-Ar), 79.6 (CH-Ar), 62.1 (OCH_2CH_3), 61.7 (NCH_2CH_3), 52.1 (NCH_2CO), 30.99 ($CH(CH_3)_2$), 22.5 (CH-$(CH_3)_2$), 22.4 ($CH(CH_3)_2$), 17.9 (Ar-CH_3), 15.8 (NCH_2CH_3), 14.6 (OCH_2CH_3) ppm.

Hydrolysis Experiments. For hydrolysis studies, compounds **1a**, **1b**, and **4a** (1−2 mg/mL) were dissolved in MeOD-d_4/D_2O (5/95) solution, and the samples were analyzed by ^{1}H NMR spectroscopy. In order to force aquation of the complex, the chlorido ligands were abstracted by addition of 2 equiv of $AgNO_3$ in D_2O, and the solution was filtered to remove AgCl. In both cases, ^{1}H NMR spectra were recorded after 0.5, 24, 48, 72, and 120 h. To study a potential suppression of hydrolysis by the presence of chloride, we dissolved **1a** in 100 mM NaCl solution in D_2O (1−2 mg/mL), and a solution of **1a** in D_2O was placed in a capillary in the same NMR tube for reference.

pK_a Determination. pK_a values were determined by dissolving complexes **1a**, **1b**, and **4a** in MeOD-d_4/D_2O (5/95) solution. The pH values were measured directly in the NMR tubes with a pH meter Eco Scan pH6 equipped with a glass microcombination pH electrode (Orion 9826BN) and calibrated with standard buffer solutions of pH 4.00, 7.00, and 10.00. The pH titration was performed with NaOD (0.4−0.0004% in D_2O) and DNO_3 (0.4−0.0004% in D_2O). The pH values were plotted against the chemical shifts of the Ar_{cym}-H2/H6 protons of the arene ring in the ^{1}H NMR spectra, and the resulting curves were fitted using the Henderson−Hasselbalch equation with Microsoft Office Excel 2003, SP3 (Microsoft Corporation). The experimentally obtained pK_{a*} values were corrected with eq 1, in order to convert the pK_{a*} in D_2O to the corresponding pK_a values in aqueous solutions.[68]

$$pK_a = 0.929\, pK_{a*} + 0.42 \quad (1)$$

Reaction with Biomolecules Monitored by NMR Spectroscopy. 5′-GMP binding experiments were carried out by titrating solutions of the complexes **1a**, **1b**, and **4a** (1−2 mg/mL) in MeOD-d_4/D_2O (5/95) with a 5′-GMP solution (10 mg/mL D_2O) in 50 μL increments. The reaction was monitored by ^{1}H and $^{31}P\{^1H\}$ NMR spectroscopy until unreacted 5′-GMP was detected.

In order to investigate the reactivity of complexes with amino acids, a solution of **1a** (1 mg/mL) in MeOD-d_4/D_2O (5/95) was treated with equimolar amounts of Gly, Ala, Cys, Met, and His (pH of the solutions was in the range 5.5−7.1), and the ^{1}H NMR spectra were recorded after 5 min and 24 h.

Mass Spectrometry Studies on the Binding to Amino Acids and Proteins. Stock solutions of **1a**, **4a**, Gly, Cys, Met, His, ubiquitin (Ub), and cytochrome c (Cyt) (each 400 μM) were prepared in MeOH/H_2O = 10/90. Solutions of **1a** and **4a** were incubated with the selected amino acid at a 1:1 molar ratio for 1, 19, 24, and 48 h at 37 °C. In order to follow the competitive reaction of **1a** or **4a** with amino acids, reaction mixtures with compound:Gly:Met:His:Cys at a molar ratio of 1:1:1:1:1 were prepared and incubated for 19 h. For the protein binding studies, **1a** or **4a** and Ub or Cyt were mixed at 2:1 or 3:1 molar ratios, and aliquots were taken after 1, 19, and 48 h.

The samples were analyzed at concentrations ranging from 10−30 μM. Therefore, they were diluted with MeOH in case of the amino acid incubations and with MeOH/water/formic acid = 50/50/0.1 for the analysis of the protein samples.

ESI mass spectra were recorded on a Bruker esquire$_{3000}$ ion trap mass spectrometer by direct infusion with a flow rate of 4 μL/min. The experimental conditions were as follows: Capillary 4.5 kV, end plate offset 0.5 kV, skimmer 1 45.5 V, skimmer 2 6 V, cap exit offset 78.4 V, and dry temperature 200 °C. The spectra were recorded and processed using ESI Compass 1.3 and DataAnalysis 4.0 software (both Bruker, Bremen, Germany). Deconvolution was obtained by maximum entropy calculations with a mass step of m/z 0.1 and an instrument peak width of 1.

CDK2/Cyclin A Protein Kinase Inhibition Assay. The CDK2 peptide substrate, HHASPRK, and CDK2/Cyclin A protein complex were purchased from Enzo Life Sciences. Adenosine 5′-[γ-ferrocene] triphosphate (Fc-ATP) was synthesized according to the procedure published elsewhere.[69] Gold rod electrodes (99.99% purity) with surface area of 0.02 cm^2 were obtained from CH Instruments. All experiments were conducted in aqueous conditions using ultrapure water (18.2 MΩ cm) from a Millipore Milli-Q system.

Fabrication of Kinase Biosensor. The gold electrodes were cleaned by polishing with slurry of 1 μm Al_2O_3 until a mirror finish was obtained. After 5 min sonication in Milli-Q water, the gold electrodes were rinsed with water and ethanol. The electrodes were then cleaned electrochemically by cyclic voltammetry (CV) in 0.5 M H_2SO_4 in the range 0−1.2 V and then by cycling in the negative potential range from −0.6 to −2.3 V. Next, the gold electrodes were incubated with 2 mM lipoic acid NHS ester solution in ethanol for 3 days at 273 K. After extensive washing with freshly distilled ethanol, the gold electrodes were incubated with a 0.1 mM peptide solution in Milli-Q water for 18 h at 273 K. Consequently, the modified electrodes were rinsed with Milli-Q water and then incubated with 100 mM ethanolamine solution in absolute ethanol for 1 h. Finally, the electrodes were immersed in 10 mM dodecanethiol solution in ethanol for 20 min to block any unmodified gold surface.

Kinase-Catalyzed Phosphorylation Reaction. The peptide-modified gold electrodes were immersed in the kinase assay buffer based on 60 mM HEPES (pH 7.5), 3 mM $MnCl_2$, 3 mM $MgCl_2$, 0.5 μg/μL of PEG 20000, 3 μM sodium ortho-vanadate, 1 μg/mL CDK2/Cylin A protein kinase, and 200 μM Fc-ATP. The phosphorylation reaction was performed for 6 h at 37 °C in a heating block (VWR Scientific, USA). The modified gold

(68) Krezel, A.; Bal, W. *J. Inorg. Biochem.* **2004**, *98*, 161–166.

(69) Song, H.; Kerman, K.; Kraatz, H.-B. *Chem. Commun.* **2008**, 502–504.

electrodes were washed five times using the kinase assay buffer and 0.1 M phosphate buffer (pH 7.4) prior to the electrochemical measurement. For the inhibitor studies, the CDK2/Cyclin A protein and compounds **1a**, **1b**, or **4a** (1 mM, DMSO) were added to the kinase buffer, while maintaining the working concentration of the protein and inhibitor at 1 μg/mL and 20 μM, respectively. The DMSO concentration was maintained at a low level (< 2%). After 30 min, the kinase reaction was initiated by the addition of Fc-ATP and was followed by the procedure outlined above.

Electrochemical Experiments. All electrochemical experiments were carried out using a CH Instrument 660B system potentiostat (Austin, TX) at a 100 mV/s scan rate unless otherwise specified. The electrochemical measurements were performed in 0.1 M phosphate buffer (pH 7.4). Typical electrochemical experimental set up included a three-electrode system: a modified gold electrode as the working electrode, Ag/AgCl in 3 M KCl as the reference electrode, which was connected with the electrolyte via a salt bridge, and platinum wire as the counter electrode. For each electrode, CV was performed at a scan rate of 100 mV/s, and square-wave voltammetry (SWV) was recorded from 0.2 to 0.6 V, with an amplitude of 25 mV at 20 Hz frequency.

Cytotoxicity in Cancer Cell Lines. Cell Lines and Culture Conditions. CH1 cells (adenocarcinoma of the ovary) were a generous gift from Lloyd R. Kelland, CRC Centre for Cancer Therapeutics, Institute of Cancer Research, Sutton, U.K. SW480 (adenocarcinoma of the colon, human) and A549 (nonsmall cell lung cancer, human) cells were kindly provided by Brigitte Marian (Institute of Cancer Research, Department of Medicine I, Medical University of Vienna, Austria). All cell culture reagents were obtained from Sigma-Aldrich, Austria. Cells were grown in 75 cm^2 culture flasks (Iwaki) as adherent monolayer cultures in Eagle's minimal essential medium (MEM) supplemented with 10% heat-inactivated fetal calf serum, 1 mM sodium pyruvate, and 2 mM L-glutamine. Cultures were maintained at 37 °C in a humidified atmosphere containing 95% air and 5% CO_2.

MTT Assay Conditions. Cytotoxicity was determined by the colorimetric MTT (3-(4,5-dimethyl-2-thiazolyl)-2,5-diphenyl-2*H*-tetrazolium bromide, purchased from Fluka) microculture assay. For this purpose, cells were harvested from culture flasks by trypsinization and seeded in 100 μL aliquots MEM supplemented with 10% heat-inactivated fetal calf serum, 1 mM sodium pyruvate, 4 mM L-glutamine, and 1% nonessential amino acids (100 ×) into 96 well microculture plates (Iwaki). Cell densities of 1.5×10^3 cells/well (CH1), 2.5×10^3 cells/well (SW480), and 4×10^3 cells/well (A549) were chosen in order to ensure exponential growth of untreated controls throughout the experiment. Cells were allowed to settle and resume exponential growth for 24 h. The test compounds were dissolved in DMSO, serially diluted in the same medium such that the maximum DMSO content did not exceed 1%, and added in 100 μL aliquots to the microcultures (only the maximum concentration tested was added in 200 μL aliquots after removal of the medium). Cells were then exposed to the test compounds for 96 h. At the end of exposure, all media were replaced by 100 μL/well RPMI1640 culture medium (supplemented with 10% heat-inactivated fetal calf serum) plus 20 μL/well MTT solution in phosphate-buffered saline (5 mg/mL). After incubation for 4 h, the supernatants were removed, and the formazan crystals formed by viable cells were dissolved in 150 μL DMSO per well. Optical densities at 550 nm were measured with a microplate reader (Tecan Spectra Classic), using a reference wavelength of 690 nm to correct for unspecific absorption. The quantity of vital cells was expressed in terms of T/C values by comparison to untreated control microcultures, and 50% inhibitory concentrations (IC_{50}) were calculated from concentration effect curves by interpolation. Evaluation is based on means from three independent experiments, each comprising three replicates per concentration level.

Scheme 1. Synthetic Strategy to Ligands **a**, **b**, and **c**[60−62,71]

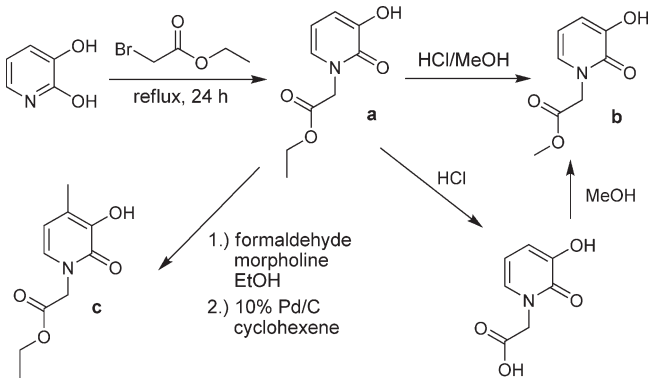

Results and Discussion

Synthesis and Characterization. Hydroxypyridones and their derivatives are a versatile class of ligands and behave as *O*,*O*-bidentates to form 5-membered chelate rings with metals. These 6-membered *N*-heterocycles are readily ionizable by deprotonation of the hydroxyl group, and thereby, the zwitterionic "aromatic" character of the molecule is introduced. They form stable metal complexes with a wide range of bi- or trivalent metals, including Al, Fe, Ga, V, Mo, Zn, etc.[70] In addition to those metals, complexes of 3-hydroxy-4-pyr(id)ones of Ru have been demonstrated to exhibit antitumor activity.[23−29] However, no data for 3-hydroxy-2-pyrones have been reported, a gap which we aim to fill with the present study by synthesizing a series of ruthenium(II)- and osmium(II)-arene complexes of alkoxycarbonylmethyl-3-hydroxy-2-pyridones.

The bidentate ligand 1-[(ethoxycarbonyl)methyl]-3-hydroxy-2(1*H*)-pyridone **a** (Scheme 1) was synthesized straightforwardly by *N*-alkylation of 2,3-dihydroxypyridine with ethyl bromoacetate, acting also as solvent in this reaction.[60] Recrystallization from ethanol (96%) gave rise to the pure compound (about 80% yield). In addition, the simple *N*-alkylation of 2,3-dihydroxypyridine with alkyl halides has been reported, but the synthetic procedures require harsh conditions and often result in poor yields.[60] The methyl ester **b** was obtained in excellent yield (99%) in a one-step procedure via acid-catalyzed transesterification of 1-[(ethoxycarbonyl)-methyl]-3-hydroxy-2-pyridone **a**.[61] Alternatively, **b** is also accessible in two steps, involving in the first step the hydrolysis of ethyl ester **a,** followed by esterification of the pyridone carboxylic acid.[71] In order to introduce regioselectively a methyl substituent at position 4 of the hydroxypyridone scaffold, the Mannich reaction was employed for mono aminomethylation and in a second step, the Mannich base was further transformed to the methyl-substituted *N*-[(ethoxycarbonyl)methyl]-3-hydroxy-4-methyl-2-(1*H*)-pyridone **c** under palladium-catalyzed transfer hydrogenolysis conditions.[62]

Ligands **a**, **b**, and **c** were converted in methanol into the corresponding complexes by activating the alkoxycarbonylmethyl-3-hydroxy-2-pyridones with sodium methoxide. The respective dimers $[(\eta^6\text{-}p\text{-cymene})MX(\mu\text{-}X)]_2$

(70) Thompson, K. H.; Barta, C. A.; Orvig, C. *Chem. Soc. Rev.* **2006**, *35*, 545–556.
(71) Rai, B. L.; Khodr, H.; Hider, R. C. *Tetrahedron* **1999**, *55*, 1129–1142.

Scheme 2. Synthesis of Complexes from Corresponding Ligands

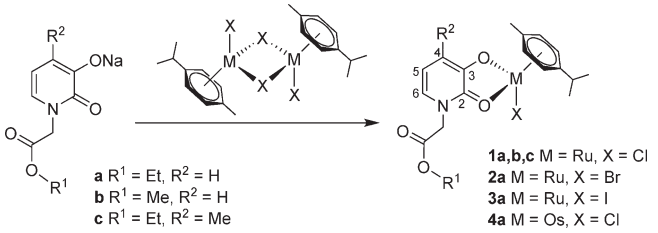

(X = Cl, Br, I; M = Ru, Os; cym = η^6-*p*-cymene) were added to this solution at RT to yield the products (57−93%) after recrystallization by slow diffusion of diethyl ether into a concentrated solution of dichloromethane (Scheme 2).

The ^{1}H NMR spectra of all complexes in $CDCl_3$ contain doublets assigned to each of the four cym ring protons with a coupling constant of about 6 Hz and two doublets for the cym isopropyl methyl groups due to slow epimerization of the chiral metal center and the presence of nonequivalent aromatic protons. However, in the ^{1}H NMR spectra of **1a** and **1b** in D_2O, conditions in which the complex will hydrolyze quickly to the aqua species (see below), only two doublets for the cym ring protons and a doublet for the two methyl groups of the cym isopropyl are observed.[22] Upon coordination of hydroxypyridone to the ruthenium center, H4, H5, and H6 protons give three sets of signals (two set of doublets in the case of **1c**). In the case of **1c**, the signal attributable to the H4 of hydroxypyridone is no longer present, instead a singlet at δ = 2.19 ppm appears, corresponding to the methyl substituent, accompanied by loss of coupling of H4 to H5 or H6.[62]

For all compounds, the methylene protons of the alkoxycarbonylmethyl-3-hydroxy-2-pyridones become diastereotopic upon complexation and show splitting of their resonances, if analyzed in noncoordinating solvents. The diastereotopic N−CH_2−CO protons adjacent to the pyridone ring give two doublets centered at δ = 5.1 and 4.2 ppm with a geminal coupling constant $^2J_{(H,H)}$ = 17 Hz as expected for an AB system. Similar observations were reported for complexes containing related hydroxypyridones.[46,61,72] If the ^{1}H NMR spectra are recorded in D_2O, the same protons give a singlet at δ = 4.8 ppm, which is comparable to the chemical shift in **a**, **b**, or **c** (δ = about 4.7 ppm).

Crystal structures of **1a** and **1b** were determined by X-ray diffraction analysis. The compounds exhibit pianostool configuration as usually observed for such metal−arene complexes.[13,25,29] The alkoxycarbonylmethyl-3-hydroxy-2-pyridones act as *O*,*O*-chelating bidentate ligands and form a five-membered chelate ring upon binding to the ruthenium(II) center (Figure 1, selected bond lengths and angles are given in Table 2). The ruthenium−centroid$_{arene}$ distances are 1.6397(7) and 1.6427(12) Å, and the Ru−Cl bond lengths are 2.4186(4) and 2.4166(7) Å in **1a** and **1b**, respectively. These parameters are very similar to those observed for a dinuclear RuCl(cym)(3-hydroxy-4-pyridone) complex.[26]

Stability in Aqueous Solution. The aquation of **1a**, **1b**, and **4a** was investigated by ^{1}H NMR spectroscopy in

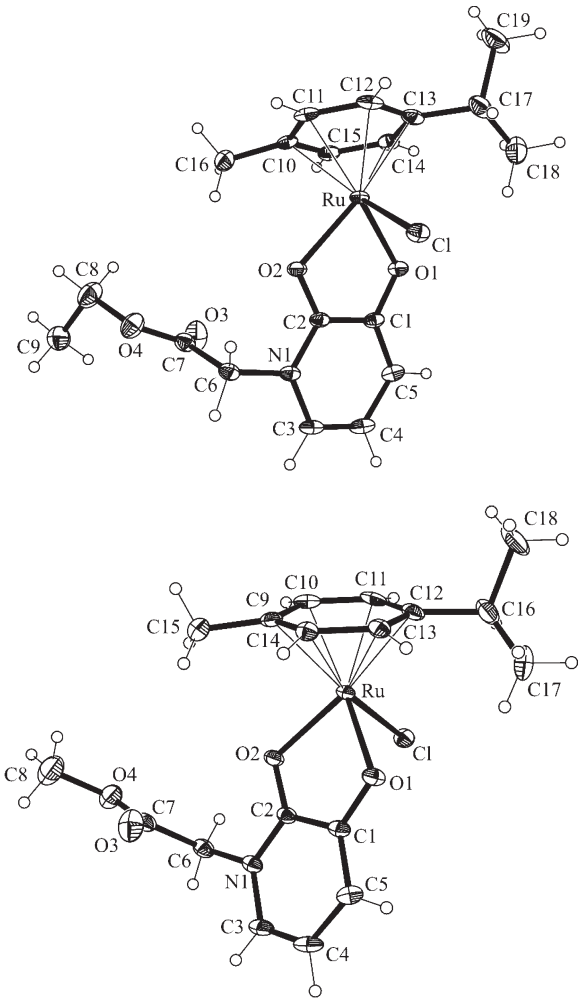

Figure 1. ORTEP plots of **1a** (top) and **1b** (bottom); thermal ellipsoids are drawn at 50% probability level.

D_2O/MeOD-d_4 (95/5) because of limited water solubility. Complexes **1a**, **1b**, and **4a** hydrolyze rapidly upon dissolution in water by exchange of the chlorido ligand with a neutral water molecule and exist predominantly as the charged monoaqua species of the general formula $[M(cym)(HP)(OH_2)]^+$ (see below). This result was confirmed by obtaining similar NMR spectra when hydrolysis was initiated by addition of equimolar amounts of $AgNO_3$. These data suggest immediate aquation after dissolution in aqueous environment. Furthermore, addition of 100 mM NaCl appears not to suppress hydrolysis as shown by ^{1}H NMR spectroscopy. Likewise, fast hydrolysis was also observed for M(arene) complexes containing anionic *O*,*O*-chelating ligands such as acac, maltolato, or other hydroxypyrones in comparison to relative high stability of *O*,*S*-, *O*,*N*-, and *N*,*N*-chelate complexes. This might be due to either the increased electron density at the metal center or possible interactions between hydrogen atoms of coordinated H_2O and the oxygen atoms of the *O*,*O*-chelating ligand, which in the case of acac was also proposed by DFT calculations.[4,24,73] When comparing the hydrolysis behavior of Ru and Os analogues, the Os compound **4a** is less water soluble and hydrolyzes

(72) Grote, Z.; Bonazzi, S.; Scopelliti, R.; Severin, K. *J. Am. Chem. Soc.* **2006**, *128*, 10382–10383.

(73) Melchart, M.; Habtemariam, A.; Parsons, S.; Sadler, P. J. *J. Inorg. Biochem.* **2007**, *101*, 1903–1912.

Table 2. Selected Bond Lengths (Å) and Bond Angles (deg) for **1a**, **1b**, and **5a**

	1a	1b	5a
Ru−(O═C)	2.0716(12)	2.0686(16)	2.0711(15)
Ru−(O−C)	2.1294(12)	2.1323(17)	2.0941(15)
Ru−Cl[a]	2.4186(4)	2.4166(7)	2.1227(17)
Ru(1)−centroid	1.6397(7)	1.6427(12)	1.6407(10)
O−Ru−O	78.75(5)	78.96(7)	79.82(6)
(C═O)−Ru−Cl[a]	85.51(4)	84.73(5)	82.03(6)
(C−O)−Ru−Cl[a]	84.51(3)	84.08(5)	82.60(6)

[a] In the case of **5a**, the values for the Ru−N bond length and the O−Ru−N angles are given.

significantly slower than the ruthenium analogue **1a** because of the higher lability of Ru than of Os complexes. The aqua species $[M(cym)(HP)(OH_2)]^+$ are stable for more than five days, and in contrast to analogous hydroxypyrone complexes,[22] no dimeric species of $[(cym)_2Ru_2(\mu-OH)_3]^+$ are formed.[23,74] The NMR data were essentially confirmed by electrospray ionization mass spectrometry (ESI-MS). Both **1a** and **4a** exhibit similar behavior in solution, with the chlorido ligand being released within an hour. This fact is supported by the presence of base peaks assignable to $[M(cym)(HP)]^+$ in the MS spectra at m/z 432.3 and 522.3 for **1a** and **4a**, respectively, and the peaks showing the characteristic isotope pattern for these metal compounds. Furthermore, transesterification to the methyl ester and hydrolysis of the ester moiety occurred for **1a** and **4a** in presence of methanol, however at low relative abundance (e.g., for **1a** at m/z 418.3 [10%] and 404.2 [5%]). These side products were observed at increased relative abundance during the protein binding experiments (see below) in the presence of formic acid (Figure S1 of the Supporting Information).

The pK_a values of **1a**, **1b**, and **4a** were determined by titrating the aqua species of the respective complexes with NaOD to afford the corresponding hydroxido complex and monitoring the deprotonation process by ^{1}H NMR spectroscopy (Table 3). The aqua species were generated by dissolving the complexes in D_2O containing 5% MeOD-d_4. The pK_a values were determined by plotting the chemical shifts of the proton signal of the arene ring Ar_{cym}-H2/H6 against the pH value (e.g., from 5.67 ppm at pH 2.78 to 5.29 at pH 10.03 for **1a**), and the inflection points of the sigmoid curves give the pK_{a*} values, which were corrected using eq 1 in order to consider the difference between D_2O and water and to yield the pK_a. The pK_a values determined for **1a**, **1b**, and **4a** are in a similar range as those of the structurally related hydroxypyr(id)ones.[22,25,29] As reported earlier, aqua ligands coordinated to osmium are significantly more acidic than at ruthenium centers.[22,75] Note that pK_a values strongly depend on the first coordination sphere and can easily be modified by replacing *O*,*O*-chelators by bidentate *N*,*N* ligands, which leads to a significant decrease in the pK_a values.[75,76]

Table 3. pK_a Values of **1a**, **1b**, and **4a** and Their in Vitro Anticancer Activity in Human Ovarian Cancer (CH1), Colon Cancer (SW480), and Nonsmall Cell Lung Cancer (A549) Cells (exposure time 96 h)[a]

		IC_{50} values/μM		
compound	pK_a	CH1	SW480	A549
1a	8.97	242 ± 29	> 320	> 320
1b	9.46	232 ± 7	> 320	> 320
4a	7.70	129 ± 7	> 320	> 320

[a] Values are means ± standard deviations obtained from at least three independent experiments.

Amino Acids as Binding Partners for Hydroxypyridone Complexes. Most metallodrugs are administered intravenously, and hence, they encounter a number of reactive biomolecules such as proteins in the bloodstream. Serum proteins can play a divergent role either in delivery of metal-based anticancer drugs to their cellular targets or in deactivating them even before reaching the target(s).[9,77] Therefore, the reaction of **1a** with the amino acids Gly, Ala, His, Met, and Cys was investigated to gain insight into the reactivity to biomolecules and potential metabolization. Histidine and methionine as well as cysteine have been chosen because they are known to undergo favorable binding interactions with ruthenium(II) anticancer complexes, whereas Gly and Ala served as nonselective references. For ^{1}H NMR studies, the amino acids were incubated with **1a** at equimolar ratios in D_2O/MeOH-d_4 (95/5), and the reaction was monitored for 24 h. It appears that the bidentate hydroxypyridone ligand was replaced by the respective amino acid within 24 h as signals assignable to the released hydroxypyridones appeared in the ^{1}H NMR spectra. Notably, Cys decomposes the complex within minutes, probably due to the strong *trans*-effect of the thiol functionality. A similar observation has been reported for related pyrone-derived complexes.[25] Similarly, the reaction of **1a** with 1 equiv of Met and His takes place immediately with quantitative release of the pyridone ligand within 24 h, possibly due to the ability of both amino acids to act as bidentate or tridentate chelating ligands (with the thioether of Met and *N*1 or *N*3 atoms of the imidazole moiety of His as third donors in addition to NH_2 and COOH). This hypothesis is supported by the mass spectrum of the reaction between **1a** and His in which the peak at m/z 346.1, which appeared after 48 h, was assigned to $[Ru(cym)(His - CO_2) - 2H]^+$ (1%). This indicates *N*,*N* chelation of His to the metal center. The reaction of Gly with **1a** was significantly slower than with all the other investigated amino acids. In the ^{1}H NMR spectra recorded after 24 h, there appeared two doublets at δ = 3.11 and 2.94 ppm with a geminal coupling constant of $^2J_{(H,H)}$ = 17 Hz. These signals were assigned to the Gly-CH_2 protons, which become diastereotopic upon coordination of Gly as an *N*,*O*-chelating ligand to the Ru(II)-arene center forming a five-membered ring. In analogy to related complexes,[24,25] no ruthenium dimer signals appeared within 24 h in the presence of amino acids (in ^{1}H NMR spectra signals at approximately 5.0 and 5.5 ppm would be indicative for this process).

In order to investigate the interaction of **1a** with amino acids (aa) by means of ESI-MS, **1a** was incubated with

(74) Berger, I.; Hanif, M.; Nazarov, A. A.; Hartinger, C. G.; John, R. O.; Kuznetsov, M. L.; Groessl, M.; Schmitt, F.; Zava, O.; Biba, F.; Arion, V. B.; Galanski, M.; Jakupec, M. A.; Juillerat-Jeanneret, L.; Dyson, P. J.; Keppler, B. K. *Chem.—Eur. J.* **2008**, *14*, 9046–9057.
(75) Peacock, A. F. A.; Habtemariam, A.; Fernandez, R.; Walland, V.; Fabbiani, F. P. A.; Parsons, S.; Aird, R. E.; Jodrell, D. I.; Sadler, P. J. *J. Am. Chem. Soc.* **2006**, *128*, 1739–1748.
(76) Fernandez, R.; Melchart, M.; Habtemariam, A.; Parsons, S.; Sadler, P. J. *Chem.—Eur. J.* **2004**, *10*, 5173–5179.
(77) Hartinger, C. G.; Keppler, B. K. *Electrophoresis* **2007**, *28*, 3436–3446.

one mol equiv of Gly, His, Met, or Cys at 37 °C in water/methanol (90/10). The samples were analyzed after 1, 24, and 48 h, and the trend to replace the pyridone ligand is already observable within1 h, however to different extents and with differing kinetics. After 48 h incubation of **1a** with Met or His, the major products were identified as $[Ru(cym)(aa) - H]^+$ as were for Cys and Gly but at lower relative abundance. To perform a competition experiment, we incubated **1a** with Gly, His, Cys, and Met at a molar ratio of 1:1:1:1:1 for 19 h, and the following trend for the formation of amino acid adducts was observed: Met ≥ His ≫ Cys > Gly (Table S1 and Figure S2 of the Supporting Information). The preference for Met and His might indicate enhanced stability of the formed adducts as compared to their Gly and Cys counterparts. The obvious feature of Cys, Met, and His as compared to Gly is the side chain with soft donors that can be directly involved in coordination to the metal center. Furthermore, when comparing Cys with His and Met, the side chains of the latter two aa are more flexible to act as *N*,*O*,*S* or *N*,*O*,*N* chelating ligands, whereas the Cys complex is more constrained. These observations are also supported by bis-aa adduct formation during the reaction of **1a** with Gly found at *m*/*z* 385.9 $[Ru(cym)(Gly)_2]^+$ and 367.9 $[Ru(cym)(Gly)_2-H_2O]^+$. In addition, the dinuclear species $[(cym)_2Ru_2(Gly) + H_2O]^+$was detected at *m*/*z* 654.9 (5%). However, species containing both Gly and the pyridone ligand were not observed. In analogy to the ^{1}H NMR experiments, Cys appears to degrade **1a**, which might be a reason for the low relative abundance of Cys adducts in the mass spectrum, and several peaks appeared in the range *m*/*z* 500−950, one of which was identified as dimeric $[(cym)_2Ru_2(Cys)_2 + H_2O]^+$ at *m*/*z* 731.8.

The reactivity of the osmium analogue **4a** toward amino acids is similar to that of **1a** as is the result of the competition experiment (Met≈His > Cys ≫ Gly). Again, the pyridone ligand is replaced in each case by the respective amino acid giving rise to $[Os(cym)(aa) - H]^+$ (aa = Met, His, Cys, Gly). Os has an even greater affinity for softer ligands compared to Ru, but ligand exchange rates are lower and replacement of the pyridone ligand is thus slower. Interesting features were observed in the mass spectrum of the reaction mixture containing His. In analogy to **1a**, a signal at *m*/*z* 480.3 $[Os^{II}(cym)(His) - H]^+$ was observed which was partly overlapping with a peak with the most abundant isotope at *m*/*z* 478.3. This signal might be related to $Os^{II/IV}$ oxidation (occurring probably during the ionization process in the ESI-MS source), which requires double deprotonation to balance the charge contributed by the metal center (Figure S3 of the Supporting Information). Furthermore, again a decarboxylated species was observed at *m*/*z* 434.4 $[Os^{IV}(cym)(His - CO_2) - 3H]^+$ (10%), and the peak at *m*/*z* 462.4 was assigned to $[Os^{II}(cym)(His - OH) - 2H]^+$ (10%). In the reaction with Gly, **4a** forms dinuclear species not observed for **1a** such as $[(cym)Os_2(\mu\text{-}OMe)_3]^+$ (*m*/*z* 743.4; 15%) and $[(cym)Os_2(\mu\text{-}OMe)_2(\mu-OH)]^+$ (*m*/*z* 729.3; 22%), probably because Gly is only a weak binding partner.

Reaction of 1a and 4a with Ubiquitin and Cytochrome c. In order to estimate the binding to proteins as potential targets in the bloodstream, we incubated **1a** and **4a** at molar ratios of 2:1 with ubiquitin (Ub) and 3:1 with cytochrome c (Cyt). The reaction mixtures were analyzed with an ESI-ion trap-MS, and the data was deconvoluted with the maximum entropy deconvolution algorithm. Ion traps deliver spectra of relatively low resolution; however, the identity of the formed species can be clearly identified in this case. Such ESI-MS experiments have been successfully employed for a diversity of biomolecule binding studies, in particular of metal complexes to DNA and proteins, including the characterization of the formed adducts and more sophisticated binding site characterization.[29,78−97]

1a reacts quickly with Ub, and already after 1 h, the peak at 8565 ± 2 Da assigned to unreacted ubiquitin has vanished, giving rise to a signal at 8802 ± 2 Da (100%), corresponding to the monoruthenated adduct $[Ub + Ru(cym)]^+$ and a bisadduct $[Ub + 2\ Ru(cym) - H]^+$ at 9035 ± 2 Da (8% after 48 h), again accompanied by loss of the pyridone ligand. Various other signals appeared at masses >9 kDa, stemming most probably from tertiary adducts formed with solvent molecules, which were gone after longer incubation, and as most intense signals remained after 19 and 48 h peaks at *m*/*z* 8802 ± 2 and *m*/*z* 9035 ± 2 Da assigned to $[Ub + Ru(cym)]^+$ (100%) and $[Ub + 2\ Ru(cym) - H]^+$ (7 and 8%), respectively.

4a reacts with ubiquitin in a similar manner as observed for **1a** but at a lower rate. Consequently, **4a** binds to ubiquitin to form [Ub + Os(cym)] adducts (Figure 2). After 19 h reaction time, the ubiquitin parent mass was

(78) Gibson, D.; Costello, C. E. *Eur. Mass Spectrom.* **1999**, *5*, 501–510.
(79) Peleg-Shulman, T.; Gibson, D. *J. Am. Chem. Soc.* **2001**, *123*, 3171–3172.
(80) Peleg-Shulman, T.; Najajreh, Y.; Gibson, D. *J. Inorg. Biochem.* **2002**, *91*, 306–311.
(81) Balter, L.; Gibson, D. *Rapid Commun. Mass Spectrom.* **2005**, *19*, 3666–3672.
(82) Wang, F.; Bella, J.; Parkinson, J. A.; Sadler, P. J. *J. Biol. Inorg. Chem.* **2005**, *10*, 147–155.
(83) Casini, A.; Gabbiani, C.; Mastrobuoni, G.; Pellicani, R. Z.; Intini, F. P.; Arnesano, F.; Natile, G.; Moneti, G.; Francese, S.; Messori, L. *Biochemistry* **2007**, *46*, 12220–12230.
(84) Hartinger, C. G.; Ang, W. H.; Casini, A.; Messori, L.; Keppler, B. K.; Dyson, P. J. *J. Anal. At. Spectrom.* **2007**, *22*, 960–967.
(85) Weidt, S. K.; Mackay, C. L.; Langridge-Smith, P. R. R.; Sadler, P. J. *Chem. Commun.* **2007**, 1719–1721.
(86) Hartinger, C. G.; Tsybin, Y. O.; Fuchser, J.; Dyson, P. J. *Inorg. Chem.* **2008**, *47*, 17–19.
(87) Egger, A. E.; Hartinger, C. G.; Ben Hamidane, H.; Tsybin, Y. O.; Keppler, B. K.; Dyson, P. J. *Inorg. Chem.* **2008**, *47*, 10626–10633.
(88) Hartinger, C. G.; Casini, A.; Duhot, C.; Tsybin, Y. O.; Messori, L.; Dyson, P. J. *J. Inorg. Biochem.* **2008**, *102*, 2136–2141.
(89) Casini, A.; Guerri, A.; Gabbiani, C.; Messori, L. *J. Inorg. Biochem.* **2008**, *102*, 995–1006.
(90) Gabbiani, C.; Casini, A.; Mastrobuoni, G.; Kirshenbaum, N.; Moshel, O.; Pieraccini, G.; Moneti, G.; Messori, L.; Gibson, D. *J. Biol. Inorg. Chem.* **2008**, *13*, 755–764.
(91) Renfrew, A. K.; Phillips, A. D.; Egger, A. E.; Hartinger, C. G.; Bosquain, S. S.; Nazarov, A. A.; Keppler, B. K.; Gonsalvi, L.; Peruzzini, M.; Dyson, P. J. *Organometallics* **2009**, *28*, 1165–1172.
(92) Casini, A.; Gabbiani, C.; Michelucci, E.; Pieraccini, G.; Moneti, G.; Dyson, P. J.; Messori, L. *J. Biol. Inorg. Chem.* **2009**, *14*, 761–770.
(93) Cubo, L.; Casini, A.; Gabbiani, C.; Mastrobuoni, G.; Messori, L.; Jimenez-Barbero, J.; Navarro-Ranninger, C.; Quiroga, A. G. *Chem.—Eur. J.* **2009**, *15*, 9139–9146.
(94) Groessl, M.; Terenghi, M.; Casini, A.; Elviri, L.; Lobinski, R.; Dyson, P. J. *J. Anal. At. Spectrom.* **2010**, *25*, 305–313.
(95) Mura, P.; Camalli, M.; Casini, A.; Gabbiani, C.; Messori, L. *J. Inorg. Biochem.* **2010**, *104*, 111–117.
(96) Groessl, M.; Tsybin, Y. O.; Hartinger, C. G.; Keppler, B. K.; Dyson, P. J. *J. Biol. Inorg. Chem.* **2010**, *15*, 677−688.
(97) Egger, A. E.; Hartinger, C. G.; Renfrew, A. K.; Dyson, P. J. *J. Biol. Inorg. Chem.* **2010**, *15*, 919−927.

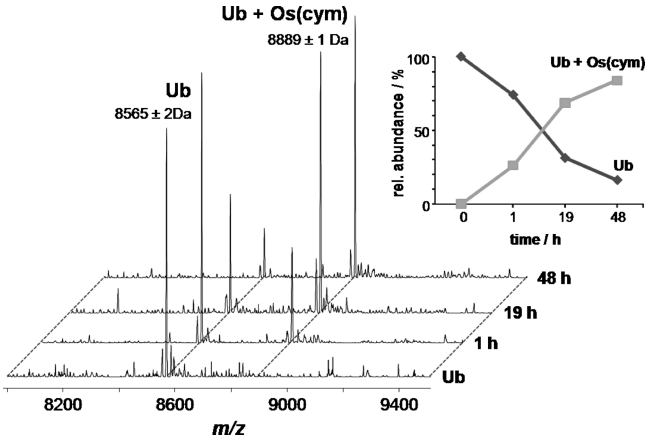

Figure 2. Time course for the reaction of **4a** with Ub. Inset shows the relative changes in the signal intensities for Ub and its Os(cym) adduct.

still present at 40% relative intensity, and in contrast to **1a**, no bisadduct was observable within this time period. Prolonging the reaction time to 48 h showed that the intensity of the unreacted protein decreased to 19% relative to the monoadduct. It appears as the reaction proceeds by forming only a limited number of adducts, whereas in the reaction of Ub with **1a** a multitude of species were detected. This might be related to the higher stability of the Os compound as compared to that of the Ru analogue.

In addition to the studies with Ub with potential His and Met binding sites, the reaction with cytochrome c (Cyt), a Cys containing heme protein, was monitored for both **1a** and **4a** by ESI-MS. Within 1 h incubation, no adducts were observed, but over the time course of the reaction, a series of different species was detected. After 19 h, a monoruthenated Cyt adduct was observed at 12597 ± 1 Da at similar relative intensity as unreacted Cyt (12363 ± 1 Da). Furthermore, a series of higher adducts were detected, including the bisadduct at 12831 ± 1 Da. As was the case for the reaction with ubiquitin, the pyridone ligand of **1a** is cleaved off during the reaction. The reaction of Cyt with **4a** revealed again higher stability of the Os compound. After 1 h incubation, the Cyt peak is the most abundant in the mass spectrum, with a monoadduct visible at 12686 ± 1 Da and possibly a series of aqua species, e.g., a signal at 12732 ± 1 Da was attributed to a trisaqua adduct. It seems as these species are mainly intermediates in the binding process and are converted into the trifunctionally bonded [Cyt + Os(cym)] as can be seen after an incubation time of 19 h, when the most intense signal corresponds already to the monometalated protein at 12686 ± 1 Da (100%) versus Cyt (50%), and no higher adducts were observed.

DNA as a Potential Target. Because DNA is thought to be one of the important targets for metal-based anticancer agents, the reactions of **1a**, **1b**, and **4a** with 5′-GMP were investigated by ^{1}H NMR spectroscopy in D_2O/MeOH (90/10), conditions under which immediately the aqua species are formed (see above). The reaction occurred in a quantitative manner within minutes, and the resulting adducts were stable in solution for more than

Scheme 3. Replacement of the Chlorido Ligand by 9-EtG; Counterion $CF_3SO_3^-$ Has Been Omitted for Clarity

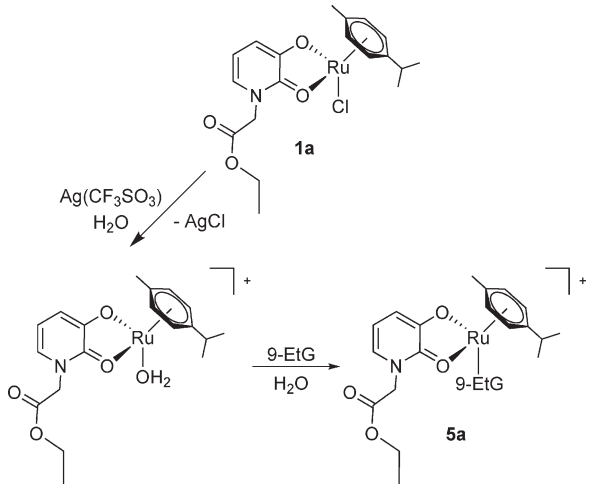

48 h. Upon addition of the metal complex, the H8 signal of 5′-GMP shifts from δ = 8.11 to 7.76 and 7.72 ppm due to the formation of isomers.[98] This change in chemical shift indicates binding to the *N*7 of the guanine moiety and implies that DNA may be a possible target for these Ru(II)−arene complexes as proposed for related organometallic ruthenium(II) compounds.[22]

In order to characterize the interaction of compound **1a** with guanine residues more in detail, **1a** was reacted with 9-ethyl guanine (9-EtG) to yield **5a**. The chlorido ligand of **1a** was abstracted by addition of $Ag(CF_3SO_3)$ (Scheme 3), AgCl was removed by filtration, and 9-ethylguanine was added to the filtrate and stirred for 24 h to afford **5a**. The molecular structure of **5a** was determined by X-ray diffraction analysis of a crystal grown from methanol/diethyl ether by the diffusion technique. This is the first example of a crystal structure of a Ru(arene)[hydroxypyr(id)one] complex bearing a 9-EtG moiety. As implied from the results of the NMR studies, the 9-ethylguanine is coordinated to ruthenium via its *N*7 atom (Figure 3). The Ru−$N7_{Gua}$ bond length in **5a** is 2.1227(17) Å and hence slightly shorter than that observed for a 9-EtG adduct of a Ph_2acac-Ru(cymene) complex [2.140(3) and 2.126(3) Å], whereas the Ru−O bond lengths are rather similar (for key bond lengths and angles see Table 2).[73]

Two molecules of **5a** are linked by hydrogen bonds between *N*3 and NH_2 of neighboring guanines to form a planar structure between the Ru centers, whereas in other cases a noncoplanar arrangement was observed.[99] In **5a**, both HP ligands point on different sides of the plane, whereas in a structure of a complex bearing Ph_2acac, both ligands are on the same side of the plane.[73] Furthermore, *N*1-H and NH_2 of 9-EtG are involved in hydrogen bonding to two oxygen atoms of the $CF_3SO_3^-$ counterion (Figure 3 and Figure S4 of the Supporting Information).

Evaluation of the in Vitro Anticancer Activity and CDK2 Inhibition. The antiproliferative activity of **1a**, **1b**, and **4a** was determined in human SW480 colon adenocarcinoma, CH1 ovarian cancer, and A549 nonsmall cell lung cancer cells by means of the MTT assay (Table 3); **1c**, **2a**, and **3a**

(98) Dorcier, A.; Hartinger, C. G.; Scopelliti, R.; Fish, R. H.; Keppler, B. K.; Dyson, P. J. *J. Inorg. Biochem.* **2008**, *102*, 1066–1076.

(99) Chen, H.; Parkinson, J. A.; Parsons, S.; Coxall, R. A.; Gould, R. O.; Sadler, P. J. *J. Am. Chem. Soc.* **2002**, *124*, 3064–3082.

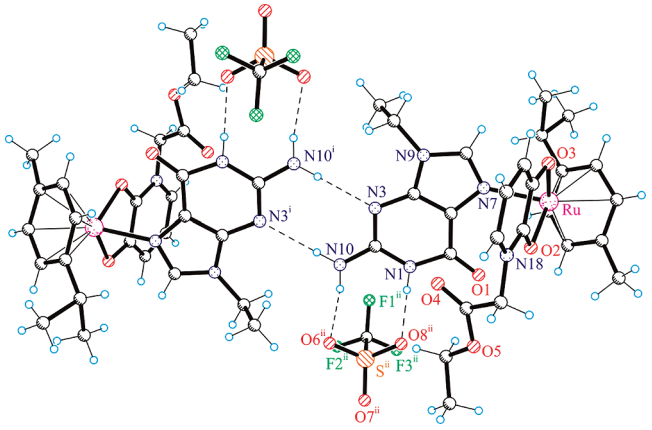

Figure 3. Part of the crystal structure of **5a** showing the coordinated 9-EtG pairing and short contacts to $CF_3SO_3^-$ counteranion via intermolecular hydrogen-bonding interactions N10−H···N3^i [N10···N3^i 3.032 Å, N10−H···N3^i 178.2°], N1−H···O8^{ii} [N1···O8^{ii} 2.909 Å, N1−H···O8^{ii} 177.2°], and N10−H···O6^{ii} [N10···O6^{ii} 3.006 Å, N10−H···O6^{ii} 169.1°]. Atoms marked with i and ii are at symmetry positions $-x, -y + 2, -z + 1$, and $-x + 1, -y + 1, -z + 1$.

were not sufficiently soluble in aqueous dilutions of DMSO stocks to a maximum DMSO content of 1% to be included in the biological assays. The ruthenium complexes **1a** and **1b** showed low anticancer activity in the most sensitive cell line with IC_{50} values of 242 and 232 μM, respectively, while that of the osmium complex **4a** is nearly 2 times lower (129 μM). This is one of the relatively few known examples that an osmium complex is more cytotoxic than its ruthenium analogue.

In an attempt to determine a possible CDK2/Cyclin A kinase inhibition of the Ru and Os complexes, a substrate peptide (HHASPRK) was immobilized onto an Au surface and Fc-ATP was employed as a cosubstrate in the kinase phosphorylation reaction assay.[69,100] Following the kinase-catalyzed phosphorylation reaction on the surface in the presence of the Fc-ATP bioconjugate, the electrochemical response was measured by cyclic voltammetry (CV) and square-wave voltammetry (SWV). The organometallic species do not exhibit redox activity in the region of interest, which makes the electrochemical peptide biosensor a valuable probe for inhibitor screening. The Ru and Os complexes inhibit the kinase activity at a concentration of 20 μM to a comparable extent as the known inhibitor R-roscovitine (Figures S6−S8 of the Supporting Information), which is currently undergoing clinical trials.[101] These data might indicate an interesting mode of action for this type of complexes, though the in vitro anticancer activity is only moderate. However, in vitro anticancer potency appears not to be a prerequisite in particular for ruthenium drug candidates, considering that NAMI-A failed the National Cancer Institute screening but entered clinical trials, and RAPTA compounds are excellent inhibitors of metastasis in vivo.[102−105] These facts support the requirement of improved biological tools with higher predictability in order to establish correlations between in vitro anticancer activity, target modulation, and efficacy in humans.

Conclusions

Organometallic compounds have emerged to an extensively studied class of anticancer chemotherapy drug candidates. Of particular interest are Ru(arene) and Os(arene) compounds, and on the basis of these scaffolds a series of compounds with a diversity of modes of action has been designed. Herein, we present Ru and Os complexes with hydroxypyridones, a compound family that can act as versatile ligands because of many options for derivatization, leading to compounds with particular chemical reactivity and biological properties. A series of Ru− and Os−(η^6-*p*-cymene) compounds was synthesized and characterized by standard methods. NMR studies revealed that the compounds hydrolyze quickly to the respective aqua species with pK_a values in the range 7.7−9.5 and the Os compound at the lower end of this scale. Those aqua species are stable for several days but react quickly, however to a different extent with the amino acids Met, Cys, His, Gly, and Ala, and form M(η^6-*p*-cymene)(amino acid) adducts upon loss of the hydroxypyridone ligand. The same types of adducts were observed in the reactions with ubiquitin and cytochrome c as determined by electrospray ionization mass spectrometry. In general, the Os complex **4a** appeared more stable than its Ru counterpart **1a**, indicated by a lower number of different adducts formed initially after incubation with the proteins. Longer reaction times lead in both cases to the formation of defined mono- or even bisadducts of the type [protein + M(η^6-*p*-cymene)]. In contrast to amino acids and proteins, 5′-GMP and 9-ethylguanine, employed as DNA models, did not induce cleavage of the metal−hydroxypyridone bond but coordinate monodentately via their *N*7 atoms to the metal center. In vitro anticancer activity assays in a series of human tumor cell lines revealed only low potency to inhibit the growth of tumor cells but potent CDK2/Cyclin A protein kinase inhibition by the Ru and Os complexes (similar to the drug candidate roscovitine). It appears as in this particular case (compare introduction) the reactivity of the compounds to biomolecules determines their in vitro anticancer activity, though a broader panel of complexes with different substitution pattern is required to draw definite conclusions.

Acknowledgment. We thank the Higher Education Commission of Pakistan, Austrian Exchange Service (ÖAD), Hochschuljubiläumsstiftung Vienna, Theodor-Körner-Fonds, FFG − Austrian Research Promotion Agency (811591), Austrian Council for Research and Technology Development (IS526001), COST D39 and CM0902, and Austrian Science Fund for financial support. We gratefully acknowledge Alexander Roller for collecting the X-ray diffraction data, Michaela Hejl for performing the in vitro anticancer assays, and Prof. Markus Galanski for recording the 2D NMR spectra.

Supporting Information Available: Amino acid and protein mass spectral data, molecular structure of **5a**, and CDK inhibition data as well as concentration−effect curves. This material is available free of charge via the Internet at http://pubs.acs.org.

(100) Kerman, K.; Song, H.; Duncan, J. S.; Litchfield, D. W.; Kraatz, H.-B. *Anal. Chem.* **2008**, *80*, 9395–9401.
(101) Krystof, V.; Uldrijan, S. *Curr. Drug Targets* **2010**, *11*, 291–302.
(102) Alessio, E.; Mestroni, G.; Bergamo, A.; Sava, G. *Curr. Top. Med. Chem.* **2004**, *4*, 1525–1535.
(103) Scolaro, C.; Bergamo, A.; Brescacin, L.; Delfino, R.; Cocchietto, M.; Laurenczy, G.; Geldbach, T. J.; Sava, G.; Dyson, P. J. *J. Med. Chem.* **2005**, *48*, 4161–4171.
(104) Bergamo, A.; Masi, A.; Dyson, P. J.; Sava, G. *Int. J. Oncol.* **2008**, *33*, 1281–1289.
(105) Chatterjee, S.; Kundu, S.; Bhattacharyya, A.; Hartinger, C. G.; Dyson, P. J. *J. Biol. Inorg. Chem.* **2008**, *13*, 1149–1155.

Is the Reactivity of M(II)–Arene Complexes of 3-Hydroxy-2(1*H*)-pyridones to Biomolecules the Anticancer Activity Determining Parameter?

Muhammad Hanif,[a] *Helena Henke,*[a,b] *Samuel M. Meier,*[a,b] *Sanela Martic,*[c] *Mahmoud Labib,*[c] *Wolfgang Kandioller,*[a] *Michael A. Jakupec,*[a,b] *Vladimir B. Arion,*[a,b] *Heinz-Bernhard Kraatz,*[c] *Bernhard K. Keppler,*[a,b] *Christian G. Hartinger*[a,b,]*

[a] University of Vienna, Institute of Inorganic Chemistry, Waehringer Str. 42, A-1090 Vienna, Austria.

[b] University of Vienna, Research Platform "Translational Cancer Therapy Research", Waehringer Str. 42, A-1090 Vienna, Austria.

[c] Department of Chemistry, The University of Western Ontario, London, Ontario, N6A 5B7, Canada.

Table of contents:

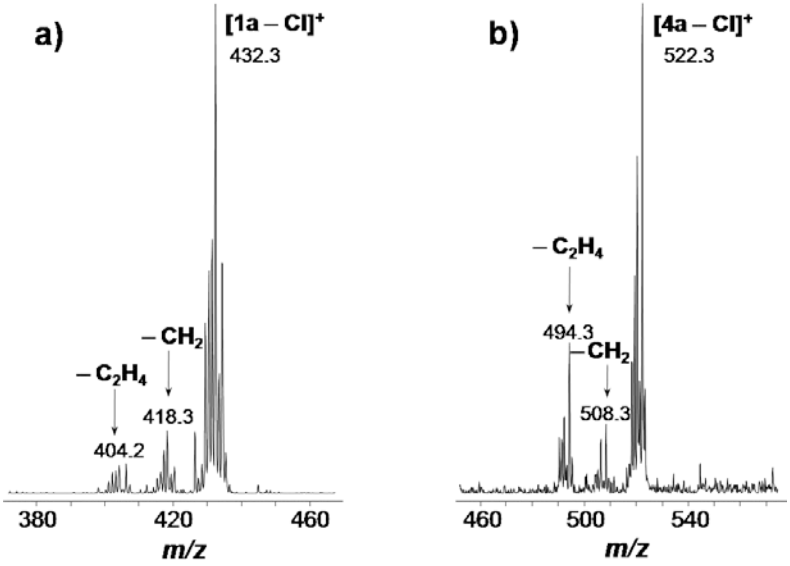

Figure S1. Electrospray ionization mass spectra for transesterification and hydrolysis of the ester moieties of (a) **1a** and (b) **4a** in presence of methanol and formic acid.

Table S1. In competitive experiments, **1a** and **4a** were incubated with Gly, His, Cys and Met at a molar ratio of 1 : 1 : 1 : 1 : 1 for 19 h and reaction mixtures were analyzed by ESI-MS (all *m/z* values contain standard deviations of ± 0.1).

Species	**Relative abundance (%)**		***m/z***	
	1a	**4a**	**1a**	**4a**
Met adduct	100	100	384.0	474.3
His adduct	66	96	390.0	480.3
Cys adduct	8	57	356.0	446.3
Gly adduct	1	0	310.0	400.2
1a	8	-	432.3	-
4a	-	0	-	522.3

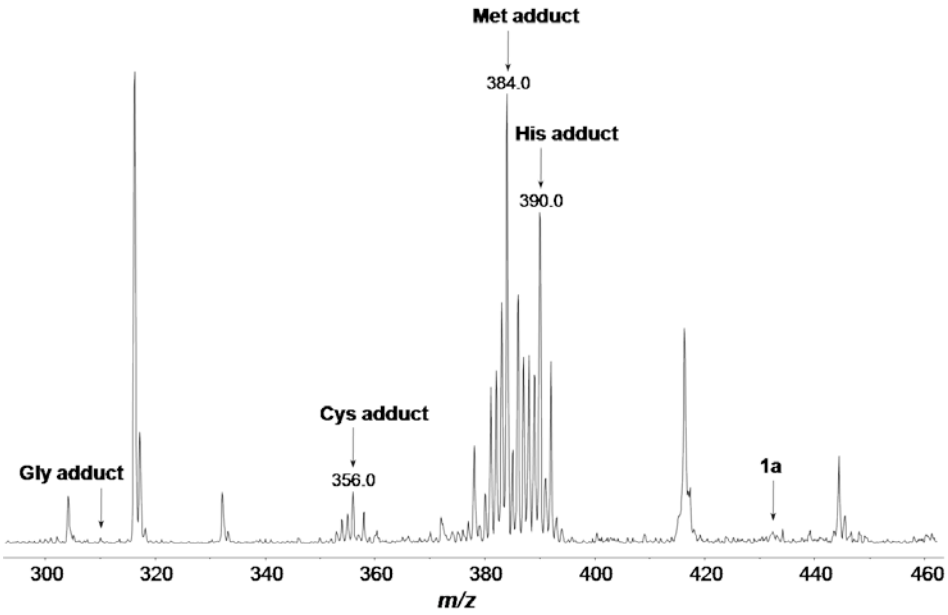

Figure S2. ESI mass spectrum for the competitive reaction of **1a** with Gly, His, Met and Cys.

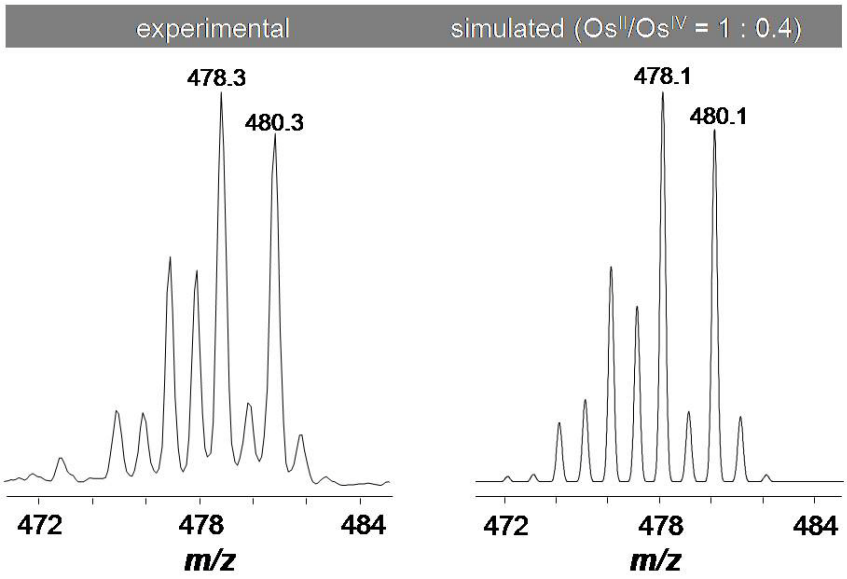

Figure S3. Redox processes observed in the mass spectrum of **4a**/His.

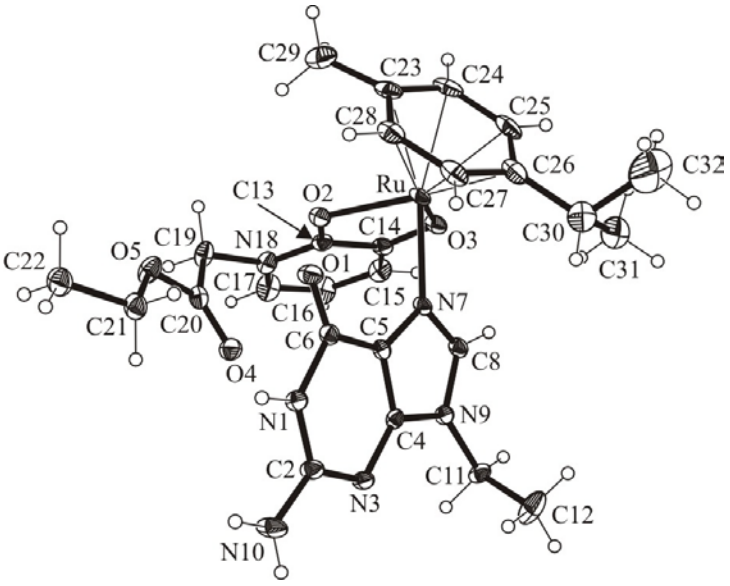

Figure S4. ORTEP plot of **5a** at 50% probability level.

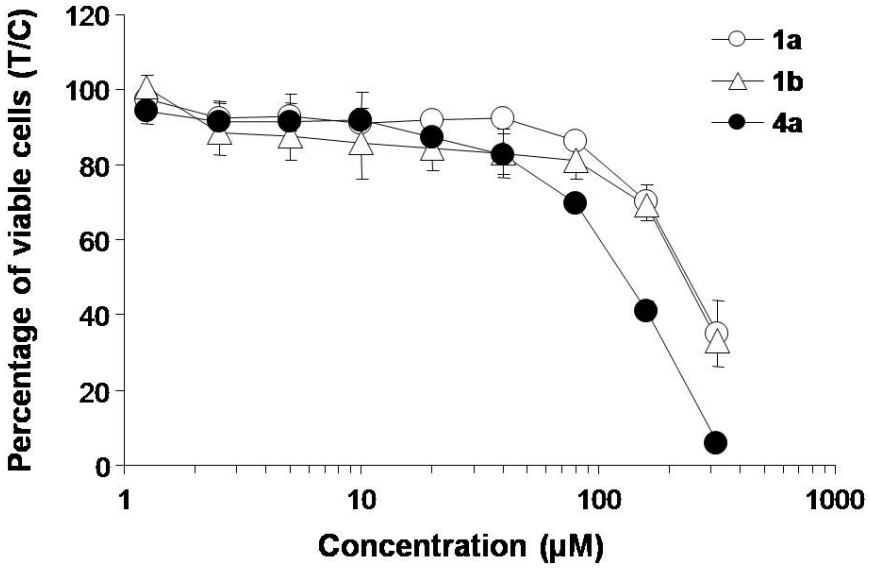

Figure S5. Concentration–effect curves of **1a**, **1b** and **4a** in CH1 ovarian cancer cells in the MTT assay (96 h exposure). Values are the means ± standard deviations from three independent experiments.

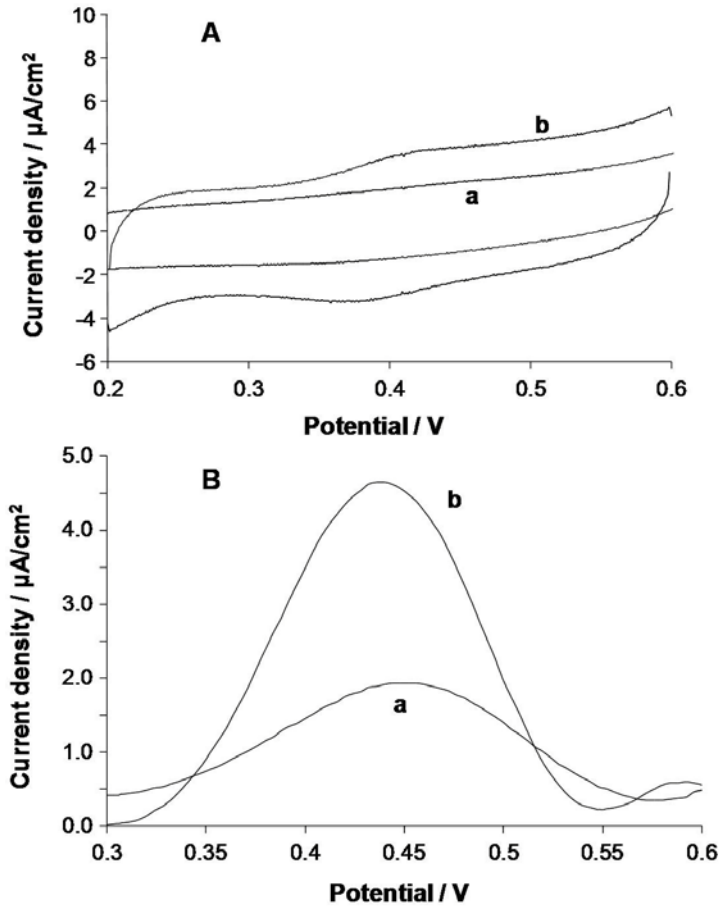

Figure S6. Cyclic voltammograms (A) and square-wave voltammograms (B) of 100 µM substrate peptide-modified Au surface electrodes for detection of CDK2/Cyclin A kinase (1 µg/ml) phosphorylation reactions. (a) in the presence of roscovitine (20 µM) and (b) in the absence of roscovitine. Measurements were taken in 0.1 M phosphate buffer solution (pH 7.4) versus Ag/AgCl as reference electrode and Pt wire as counter electrode at 100 mV/s.

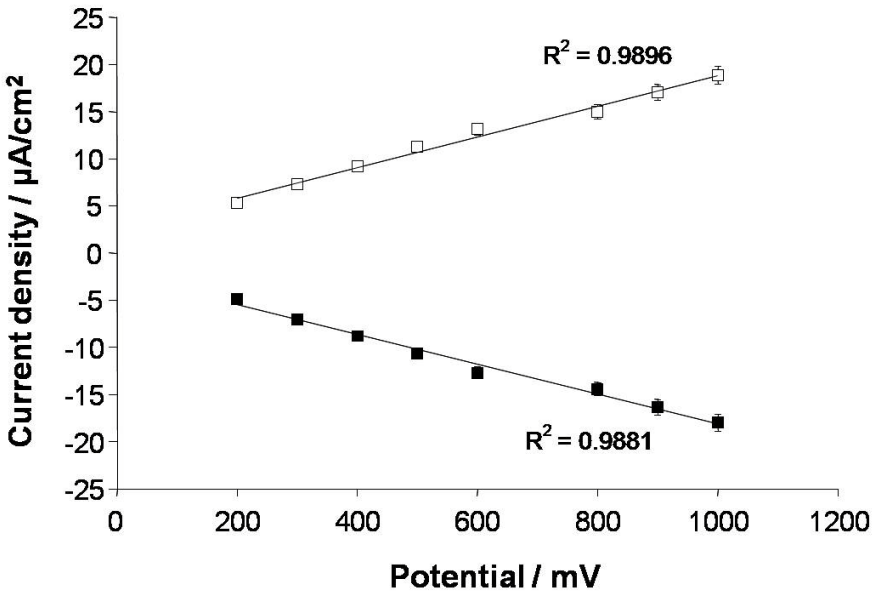

Figure S7. Plot of anodic and cathodic current density *vs.* scan rate in CDK2/Cyclin A kinase assay.

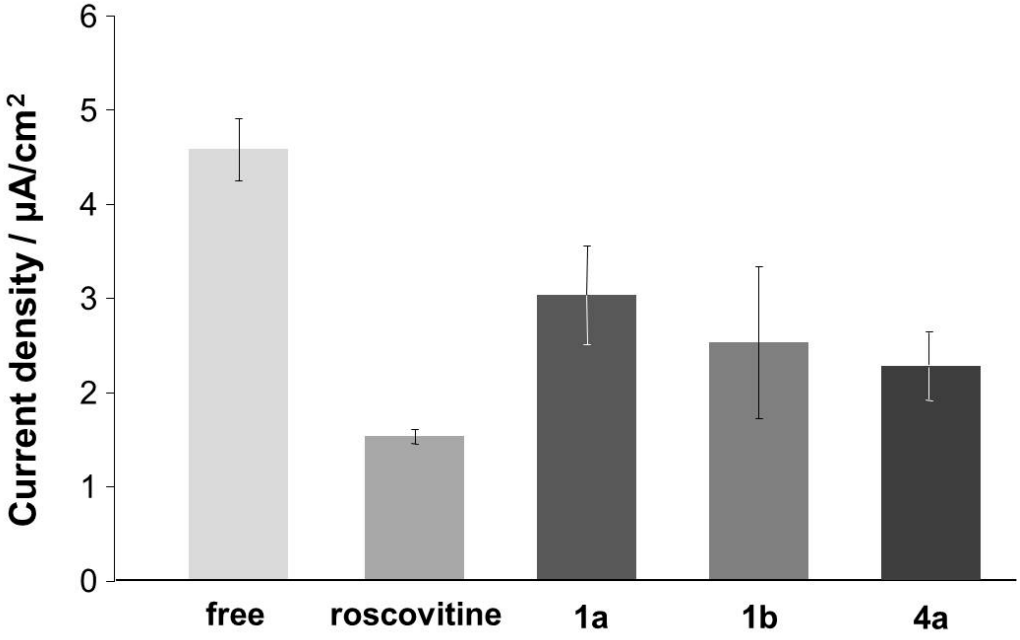

Figure S8. Plot for dependence of integrated current density in CDK2/Cyclin A kinase assays as a function of inhibitor type (inhibitor concentration = 20 µM in kinase buffer, 100 mV/s, 0.1 M phosphate buffer pH 7.4, triplicate measurements).

2.7 Tuning the Anticancer Activity of Ruthenium(II)–Arene Complexes of 3-Hydroxy-2-pyridone-Derived Ligands

Results and Discussion

As already discussed (see section 2.5), hydroxypyr(id)ones are are versatile molecules and a number of modifications or substitutions are possible on heterocyclic backbone of pyr(id)ones for fine-tuning the chemical and biological properties. Therefore, a series of alkoxycarbonylmethyl-3-hydroxy-2(1*H*)-pyridones and their mononuclear metal(II)–arene complexes was prepared (Fig. 17).

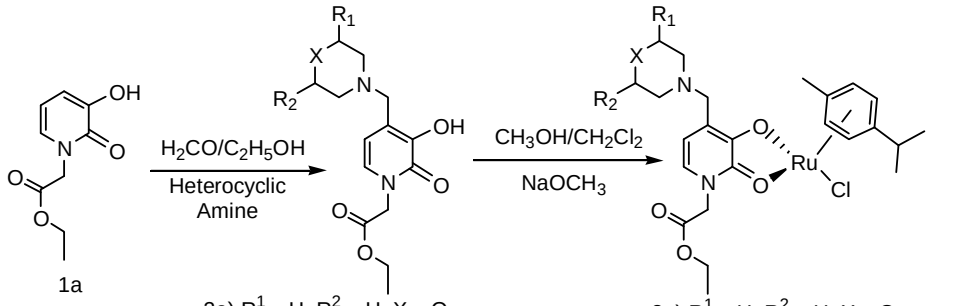

Figure 17. Synthetic strategy to 3-hydroxy-2-pyridone ligands and their Ru^{II}(arene) complexes.

The ligands (**2a-g)** were synthesized in high yields (76-91%) by Mannich reaction. The presence of an ortho directing group hydroxy group at position 3 of pyridone scaffold provides a strategy to introduce a substituent regioselectively at position 4. The Mannich reaction of *N*-[(ethoxycarbonyl)methyl]-3-hydroxy-2-(1*H*)-pyridone **1a** with formaldehyde and hetrocyclic secondary amines in ethanol/methanol resulted in 4-aminomethyl substituted products which were purified by recrystallization from ethanol (96%). The tertiary nitrogen of 4-aminomethyl substituted products is not a very good ligand for transition metals and it was thus expected to enhance the solubility of the resulting complexes without coordinating to the metal ion. All the

ligands were characterized by NMR spectroscopy, ESI-MS and elemental analysis. In the ^{1}H NMR spectra the H-4 signal disappeared and in the ^{13}C NMR spectra an additional quaternary carbon signal was observed for C-4 which further corroborates the substitution at position 4.

Subsequently, activation of **2a-g** with sodium methoxide and reaction with the [(η^6-cymene)$RuCl_2$] in methanol gave the Ru-arene complexes **3a-g** in reasonable yield 54-76% (Scheme 1).

All the complexes were characterized by 1D and 2D NMR spectroscopy, ESI-MS, elemental analysis, and the solid state structure of **3c** was determined by single crystal X-ray diffraction analysis. After complexation, the methylene protons of the alkoxycarbonylmethyl-3-hydroxy-2-pyridones become diastereotopic and show splitting of their resonances, if analyzed in non-coordinating solvents by ^{1}H NMR spectroscopy. The diastereotopic N–CH_2–CO protons adjacent to the pyridone ring give two doublets centered at δ = *ca.* 5.1 and *ca.* 4.2 ppm with a geminal coupling constant $^{2}J_{(H,H)}$ = 17 Hz. If the ^{1}H NMR spectra are recorded in D_2O, the same protons give a singlet at δ = 4.8 ppm which is comparable to the unbound ligands (δ = *ca.* 4.7 ppm). Similar observations were reported for complexes containing related hydroxypyridones.[123]

The molecular structure of **3c** was determined by X-ray diffraction analysis. The compound crystallizes in the triclinic *P*-1 space group and exhibits the typical piano-stool configuration as usually observed for such metal–arene complexes (Table 2).[19] The 3-hydroxy-2-pyridone acts as an *O,O*-chelating bidentate ligand and forms a five-membered chelate ring upon binding to the ruthenium(II) center (Figure 18). The ruthenium–centroid$_{arene}$ distance is 1.646 Å, and the Ru—Cl1, Ru—O1, and Ru—O2 bond lengths are 2.4287(6), 2.0834(15) and 2.1142(15) respectively. These parameters are very similar to those observed for RuCl(cym)(3-hydroxy-2-pyridone) complexes.[123]

---

[123] Hanif, Muhammad; Henke, Helena; Meier, Samuel M.; Martic, Sanela; Labib, Mahmoud; Kandioller, Wolfgang; Jakupec, Michael A.; Arion, Vladimir B.; Kraatz, Heinz-Bernhard; Keppler, Bernhard K.; Hartinger, Christian G.,Inorganic Chemistry 2010), 49(17), 7953-7963.

Table 2. Crystal data and details of data collection for **3c**.

Compound	**3c**
Chemical formula	$C_{25}H_{35}N_2O_4ClRu$
M (g mol^{-1})	564.07
Temperature (K)	100(2)
Crystal size (mm)	0.30 x 0.20 x 0.08
Crystal color, habit	red, block
Crystal system	triclinic
Space group	P-1
a (Å)	10.5181(4)
b (Å)	10.7150(4)
c (Å)	11.9231(5)
V (Å^3)	1212.84(8)
Z	2
D_c (g cm^{-3})	1.545
μ (cm^{-1})	7.91
F(000)	584
Θ range for data collection (°)	2.28 to 30.01
h range	-14/14
k range	-15/15
l range	-16/16
No. refls. used in refinement	7018
No. Parameters	299
R_{int}	0.0815
R_1 (obs.) [a)]	0.0369
wR_2 (all data) [b)]	0.0876
Flack parameter	0.01(5)
S [c)]	1.058

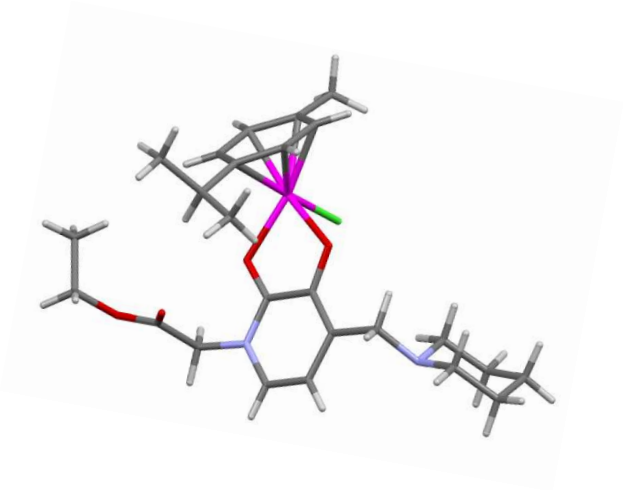

Figure 18. Molecular structure of **3c**.

Stability in aqueous solution

The aquation of **3a**, **3b** and **3c** was investigated by ^{1}H NMR spectroscopy in D_2O/MeOD-d_4 (95/5) and 0.02 M phosphate buffer (pH 7.4, 100 mM NaCl)/MeOD-d_4 (95/5), Methanol was used to increase the solubility. The complexes hydrolyze within minutes upon dissolution in water by exchange of the chlorido ligand with a water molecule and exist predominantly as cationic monoaqua species. The aqua species $[M(cym)(HP)(OH_2)]^+$ in case of **3a** and **3c** are stable for about 24 h, after which the dimeric species $[(cym)_2Ru_2(\mu\text{-}OH)_3]^+$ started to form, similarly to the analogous hydroxypyrone complexes.[124,125] The NMR data were confirmed by electrospray ionization mass spectrometry (ESI-MS). Complexes **3a** and **3b** exhibit similar behavior in solution with the chlorido ligand being released within half an hour and the resulting complexes $[M - Cl]^+$, where M = **3a** (*m/z* 531.2 ± 0.1, $m_{acc.}$ = *m/z* 531.1) or **3b** (*m/z* 547.10 ± 0.1, $m_{acc.}$ = *m/z* 547.1), remain the most intense signals for 24 h, the peaks showing the characteristic isotope pattern for the ruthenium

[124] A. F. A. Peacock, M. Melchart, R. J. Deeth, A. Habtemariam, S. Parsons and P. J. Sadler, *Chem. Eur. J.*, 2007, **13**, 2601-2613.

[125] W. Kandioller, C. G. Hartinger, A. A. Nazarov, J. Kasser, R. John, M. A. Jakupec, V. B. Arion, P. J. Dyson and B. K. Keppler, *J. Organomet. Chem.*, 2009, **694**, 922-929.

compounds. Both complexes slowly are converted into a methoxy-bridged dinuclear ruthenium(II) species, which is observable at *m/z* 565.0 ± 0.1 ($m_{acc.}$ = *m/z* 565.1) with relative abundances of 36 and 29% for **3a** and **3b**, respectively. Additionally, transesterification of the ethyl ester to the methyl derivative was observed as well as formation of the carboxylic acid. Interestingly, these reactions occur to a larger degree in **3b** where the signal corresponding to the methyl ester was found quite abundant (35%, *m/z* 533.1 ± 0.1, $m_{acc.}$ = *m/z* 533.1).

The pK_a values of **3a** and **3c** were determined by titration of the respective aqua complexes with NaOD to afford the corresponding hydroxido complex, and the deprotonation process was monitored by ^{1}H NMR spectroscopy. The aqua species were generated by dissolving the complexes in D_2O/MeOD-d_4 (95/5). The pK_a values were determined by plotting the chemical shifts of the proton signal of the arene ring Ar_{cym}-H2/H6 against the pD value and the inflection points of the sigmoid curves give the pK_{a*} values which were corrected using Eq. (1), in order to consider the difference between D_2O and water and to yield the pK_a. The pK_a values determined for **3a** and **3c** are 9.30 and 8.86, respectively and are in a similar range as those of structurally related hydroxypyr(id)ones.[123-125]

Biomolecules as Binding Partners

In order to evaluate their reactivity to and behavior in presence of potential biological binding partners, **3a** and **3b** were exposed to the amino acids (aa) His, Met and Cys and to the proteins Ub and Tf. His, Met and Cys have been chosen because they are known to coordinate preferably to soft metal centers often present in metal-based anticancer compounds. Ub serves as a model protein to characterize the adducts in proteinaceous environment by mass spectrometry at sufficient resolution and mass accuracy and Tf is used as an example of higher molecular weight (serum) proteins.

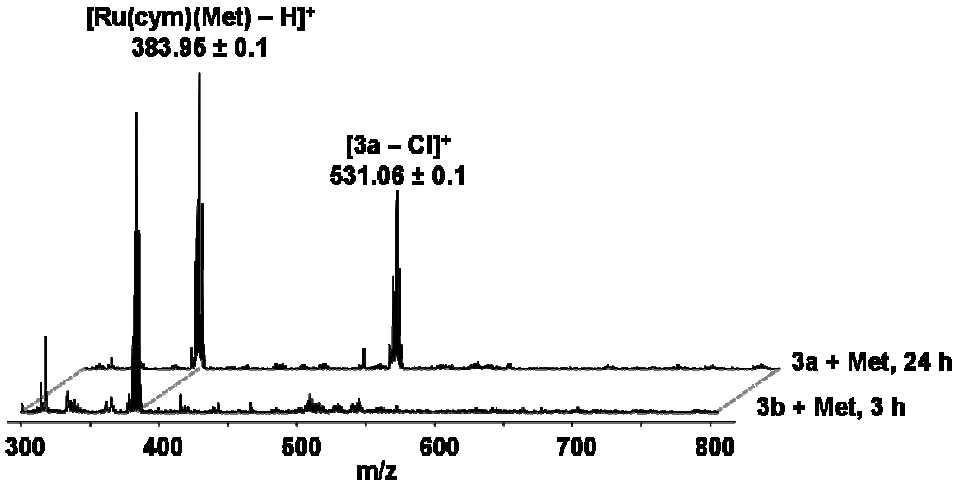

Figure 19. ESI-mass spectra of complexes **3a** and **3b** incubated with Met at a ratio of 1 : 1 for 3 and 24 h at 37 °C. In both cases, the adduct $[Ru(cym)(Met) - H]^+$ is selectively formed but at different rates.

The interaction of **3a** and **3b** with aa was investigated by incubating the complexes with one equivalent of His, Met, or Cys at 37 °C in water/methanol (90/10). The samples were analyzed after 0.5, 1, 3, 6 and 24 h. As already observed in previous studies,[123] Ru(II)-arene complexes containing hydroxypyridone ligands react very selectively with His or Met forming a complex-amino acid adduct of general formula $[Ru(cym)(aa) - H]^+$ accompanied by cleavage of the pyridone ligand, whereas Cys seems to decompose both complexes **3a** and **3b**, presumably due to the *trans* effect of the thiol group. In the case of the reaction between **3a** and His, the metal-amino acid-adduct $[Ru(cym)(His) - H]^+$ (*m/z* 390.0 ± 0.1) was already the most abundant ion in the spectrum after the first 3 h of incubation. In the course of the reaction, a methoxide species $[Ru_2(cym)_2(OMe)_3]^+$ (23% after 6 h, 0% after 24 h), formed presumably from an intermediate during the spraying process, was also completely converted into the His adduct. Complex **3a** reacted with Met to form selectively $[Ru(cym)(Met) - H]^+$ (*m/z* 384.0 ± 0.1) but at a considerably lower rate than **3b**. Replacing the morpholine-derivatized ligand by a thiomorpholine hydroxypyridone resulted in much faster kinetics when incubated with amino acid. Consequently, **3b** reacted quantitatively with both His and Met within 3 h forming the respective adduct and decomposed in the presence of Cys within the same time period (Fig. 19).

Reaction of 3a and 3b with Ubiquitin and apo-Transferrin

In order to estimate the binding to proteins as potential targets in the bloodstream, **3a** and **3b** were incubated at molar ratios of 2 : 1 with ubiquitin (Ub) and 4 : 1 with apo-transferrin (Tf). The reaction mixtures were analyzed by ESI-ion trap-MS, and the data was treated with the maximum entropy deconvolution algorithm. Ion traps deliver spectra of relatively low resolution; however, the identity of the formed species was unambiguous in this case.

Ru(II) complexes of unsubstituted hydroxypyridone were found to react quickly with Ub accompanied by ligand cleavage.[123] A similar observation was made for **3a** and **3b** which undergo the same process upon binding to the protein. The reaction of complex **3a** occurred quickly. After 3 h, the Ub peak at 8565 ± 5 Da had vanished, giving rise to a signal at 8803 ± 3 Da (100%), corresponding to the monoruthenated adduct $[Ub + Ru(cym)]^+$. The bis-adduct $[Ub + 2\ Ru(cym)]^+$ (8%) was also observable after 6 h though in low amounts. In contrast to the observations during the reactions with amino acids, complex **3b** reacted with Ub in a similar manner but at a lower rate (Fig. 20). Consequently, unreacted Ub was still found at 10% abundance after 3 h relative to the singly ruthenated adduct at 8803 ± 3 Da. Mono-adduct formation was completed after 6 h of incubation.

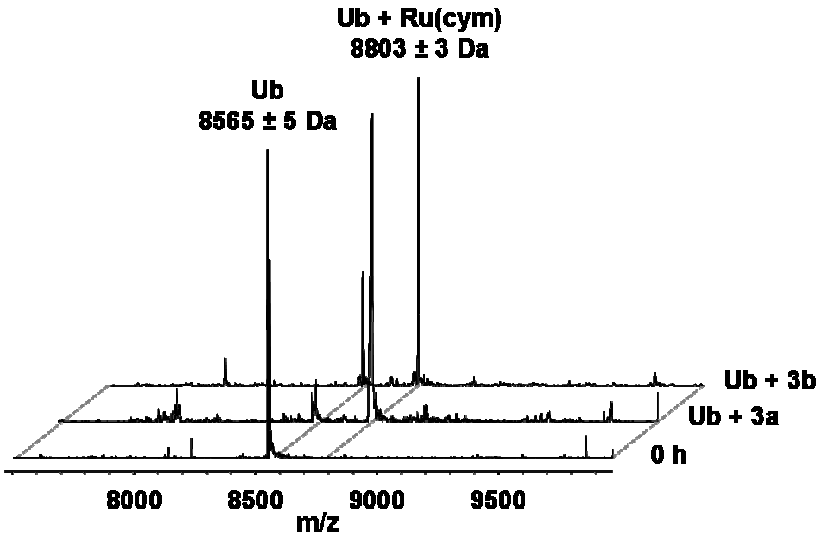

Figure 20. Deconvoluted ESI-mass spectra of Ub incubated with **3a** and **3b** at a ratio of 1 : 2 for 1 h at 37 °C. Protein adducts are formed via ligand loss and **3a** (16% unreacted Ub) exhibits faster kinetics compared to **3b** (36% unreacted Ub).

The reactivity of **3a** and **3b** towards apo-transferrin was investigated as a model for serum protein binding. Again, **3b** reacted at a considerable lower rate with apo-Tf than **3a** which can clearly be seen in the deconvoluted spectra recorded after 24 h of incubation despite the similar hydrolysis behavior (Fig. 21). With regard to the reactivity towards Ub where both complexes formed a mono-adduct quantitatively within 6 h hours, there is still unreacted Tf in considerable amounts present after 24 h of incubation. The excess of possible binding partners might thus have resulted in the non-selective formation of several multi-adducts. This in turn is an indication that **3a** and **3c** exhibit no selective affinity to bind into the binding pockets and that the complexes might prefer surface N- or S-donor containing amino acids.

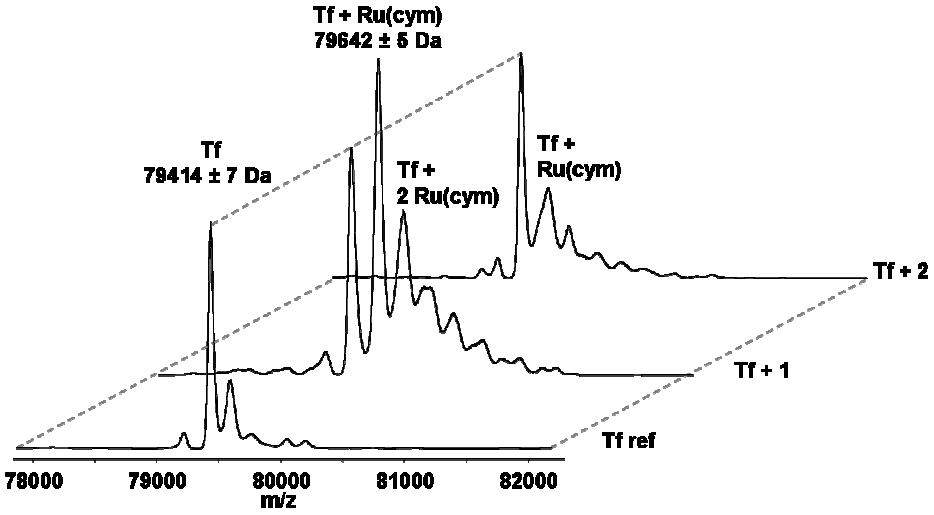

Figure 21. Deconvoluted ESI-MS spectra of Tf incubated with **3a** and **3b** at a molar ratio of 1 : 2 for 24 h at 37°C in 30mM bicarbonate buffer. Protein adducts are formed via ligand loss and **3a** exhibits faster kinetics compared to **3b**.

Reactivity with 5'-GMP

The reactions of **3a**, **3b** and **3c** with 5'-GMP were investigated by ^{1}H NMR spectroscopy in D_2O/MeOH (90/10), conditions under which immediately the aqua species are formed. The reaction occurred in a quantitative manner within minutes and the resulting adducts were stable in solution for more than 48 h. Upon addition

of the metal complex, the H8 signal of 5'-GMP shifts from δ = 8.11 to *ca*. 7.74 ppm. This change in chemical shift indicates binding to the *N*7 of the guanine moiety and implies that DNA may be a possible target for these Ru(II)–arene complexes.

Evaluation of the in vitro anticancer activity

The antiproliferative activity of **3a-3g** was determined in human SW480 colon adenocarcinoma, CH1 ovarian cancer and A549 non-small cell lung cancer cells by means of the MTT assay (Table 3). The ruthenium complexes **3b** and **3c** exhibit potent anticancer activity in all three tested cancer cell lines with IC_{50} values in the low micromolar range (e.g., in CH1 cell line IC_{50} values for **3b** and **3c** are 3.2 ± 0.3 and 3.4 ± 0.2 μM, respectively). Notably, despite minor structural differences between **3a** and **3b**, a remarkable difference in their tumor-inhibiting properties was observed, with **3b** being two orders of magnitude more cytotoxic than **3a.** The lower reactivity of **3b** towards Ub and Tfs as compared to **3a** gives a clue on its higher potency in *in vitro* anticancer tests.

Table 3. *In vitro* anticancer activity (mean IC_{50} values ± standard deviations) of **3a-3g** in human ovarian cancer (CH1), colon cancer (SW480) and non-small cell lung cancer (A549) cells (exposure time 96 h).

Compound	**IC_{50} values / µM**		
	CH1	SW480	A549
3a	229 ± 17	219 ± 7	487 ± 46
3b	3.2 ± 0.3	6.1 ± 0.3	6.2 ± 0.3
3c	3.4 ± 0.2	6.3 ± 0.1	6.0 ± 0.4
3d	28 ± 7	94 ± 16	364 ± 60
3e	56 ± 6	163 ± 16	> 640
3f	126 ± 45	279 ± 54	461 ± 24
3g	12 ± 1	68 ± 15	125 ± 34

Conclusions

Bioorganometallic chemistry is an emerging area of research and Ru(arene) complexes have been intensively investigated as anticancer chemotherapeutics. A series of 3-hydroxy-2-pyridones are prepared. The hydroxypyridones were then converted into [Ru(arene)(hydroxypyridone)Cl] complexes which were characterized chemically and biologically. The compounds hydrolyze quickly in aqueous solution to the respective aqua species as demonstrated by NMR studies. Those aqua species are stable for 48 h but react quickly, however to a different extent, with the amino acids Met, Cys, His and Gly and form M(η^6-*p*-cymene)(amino acid) adducts upon release of the hydroxypyridone ligand. The same behavior in adduct formation was ob-

served in reactions with ubiquitin and transferrin as determined by electrospray ionization mass spectrometry. *In vitro* anticancer activity assays in human tumor cell lines revealed promising anticancer activity with IC_{50} values in the low micromolar range. A remarkable difference in reactivity with biomolecules and anticancer activity was found between Ru(arene) complexes of morpholino and thiomorpholino derivatives, despite minor structural differences, the latter being two orders of magnitude more cytotoxic. The Ru(arene) complex with the thiomorpholino moiety reacts slowly with proteins such as Ub and Tf as determined by ESI-MS. Moreover, complexes react with DNA model 5'-GMP *via* their *N*7 atoms of guanine without cleavage of the metal–hydroxypyridone bond.

Experimental

Materials and methods

All reactions were carried out in dry solvents under an inert atmosphere. All chemicals were obtained from commercial suppliers and used as received and were of analytical grade. Methanol and CH_2Cl_2 were dried using standard procedures. $RuCl_3 \cdot xH_2O$ (40.4%) were purchased from Johnson Matthey, ubiquitin (bovine red blood cells) and human apo-transferrin from Sigma, α-terpinene from Acros, glycine and L-histidine from Merck, L-cysteine and 5'-GMP from Fluka, and L-methionine from Sigma-Aldrich. The solvents for ESI-MS studies were methanol (VWR Int., HiPerSolv CHROMANORM), formic acid (Fluka) and milliQ H_2O (18.2 MΩ, Synergy 185 UV Ultrapure, Millipore, France). The dimer bis[dichlorido(η^6-*p*-cymene)ruthenium(II)][126,127] and 1-[(ethoxycarbonyl)methyl]-3-hydroxy-2-(1*H*)-pyridinone[128] **1a** were synthesized using literature procedures.

^1H, $^{31}P\{^1H\}$ and $^{13}C\{^1H\}$ NMR spectra were recorded at 25 °C on a Bruker FT NMR spectrometer Avance III 500 MHz at 500.10 (^1H), 125.75 MHz ($^{13}C\{^1H\}$) and 202.44 MHz ($^{31}P\{^1H\}$). 2D NMR data were collected in a gradient-enhanced mode.

---

[126] M. A. Bennett, T. N. Huang, T. W. Matheson and A. K. Smith, *Inorg. Synth.*, 1982, **21**, 74-78.

[127] M. A. Bennett and A. K. Smith, *J. Chem. Soc., Dalton Trans.*, 1974, 233-241.

[128] M. Streater, P. D. Taylor, R. C. Hider and J. Porter, *J. Med. Chem.*, 1990, **33**, 1749-1755.

Melting points were measured on a Büchi B-540 apparatus and are uncorrected. Elemental analysis was done on a Perkin–Elmer 2400 CHN Elemental Analyzer by the Laboratory for Elemental Analysis, Faculty of Chemistry, University of Vienna. Electrospray ionization mass spectra were recorded on a Bruker esquire$_{3000}$ ion trap instrument.

X-ray diffraction measurements of **3c** were performed on a Bruker X8 APEXII CCD diffractometer at 100 K. The crystal was positioned at 35 mm from the detector and 1522 frames for 5 sec over 1° were measured. The data were processed using the SAINT software package.[129] Crystal data, data collection parameters, and structure refinement details are given in Table 2.

The structure was solved by direct methods and refined by full-matrix least-squares techniques. Non-hydrogen atoms were refined with anisotropic displacement parameters. H atoms were inserted at calculated positions and refined with a riding model. The following computer programs were used: structure solution, SHELXS-97; refinement, SHELXL-97;[130] molecular diagrams, ORTEP-3;[131] computer, Pentium IV; scattering factors.[132]

Synthesis

General procedure for ligands

Compounds **2a-g** were synthesized following a slightly modified literature procedure.[133] Aqueous formaldehyde (35%, 1.5 eq) and heterocyclic amine (1.2 eq) were stirred for 30 minutes with cooling (ice bath). The formed Mannich base was added dropwise to a suspension of 1-ethoxycarbonylmethyl-3-hydroxy-2(1*H*)-pyridinone **1a** (1 eq) in ethanol (96%). Stirring was continued at RT until a clear solution was

---

[129] M. R. Pressprich and J. Chambers, Bruker Analytical X-ray systems, Madison, 2004.

[130] G. M. Sheldrick, *Acta Crystallogr., Sect. A: Found. Crystallogr.*, 2008, **A64**, 112-122.

[131] L. J. Farrugia, *J. Appl. Crystallogr.*, 1997, **30**, 565.

[132] *International Tables for X-ray Crystallography*, Kluwer Academic Press, Dordrecht, The Netherlands, 1992.

[133] R. C. Fox and P. D. Taylor, *Synth. Commun.*, 1998, **28**, 1563-1574.

obtained after 8-24 h. The volume of the solvent was reduced to half of its original volume and kept at 4 °C overnight. The white precipitate formed was filtered and washed with cold ethanol (2×5 mL). Recrystallization from 96% ethanol gave the product as a white crystalline solid in high yield.

1-Ethoxycarbonylmethyl-3-hydroxy-4-morpholinomethyl-2(1*H*)-pyridone (2a)

2a was prepared by following the general procedure, using aqueous formaldehyde (35% in water, 0.980 g, 11.40 mmol), morpholine (0.800 g, 9.12 mmol) and 1-ethoxycarbonylmethyl-3-hydroxy-2(1*H*)-pyridinone **1a** (1.500 g, 7.6 mmol). Yield: 1.94 g (86%), m.p. 157–159 °C (decomp.), Elemental analysis found: C 56.37; H 6.89; N 9.18; calcd. for $C_{14}H_{20}N_2O_5$: C 56.75; H 6.80; N 9.45%. MS (ESI^+): *m/z*: 297.1 $[M + H]^+$; ^1H NMR (500.10 MHz, DMSO-d_6, 25 °C): δ = 7.12 (d, $^3J_{(H,H)}$ = 7 Hz, 1H, H6), 6.22 (d, $^3J_{(H,H)}$ = 7 Hz, 1H, H5), 4.71 (s, 2H, NCH_2CO), 4.14 (q, $^3J_{(H,H)}$ = 7 Hz, 2H, $CH_3C\underline{H}_2O$), 3.59 (t, $^3J_{(H,H)}$ = 4 Hz, 4H, H_{mor}), 3.38 (s, 2H, CH_2N), 3.35 (t, $^3J_{(H,H)}$ = 4 Hz, 4H, H_{mor}), 1.21 (t, $^3J_{(H,H)}$ =7 Hz, 3H, $C\underline{H}_3CH_2O$) ppm. $^{13}C\{^1H\}$ NMR (125.75 MHz, DMSO-d_6, 25 °C): δ = 168.5 ($\underline{C}OOEt$), 158.7 (C2), 144.6 (C3), 128.2 (C6), 125.5 (C4), 107.1 (C5), 66.7 (C_{mor}), 61.4 ($O\underline{C}H_2CH_3$), 55.8 (CH_2N), 53.7 (C_{mor}), 50.7 ($N\underline{C}H_2CO$), 14.5 ($OCH_2\underline{C}H_3$) ppm.

1-Ethoxycarbonylmethyl-3-hydroxy-4-thiomorpholinomethyl-2(1*H*)-pyridone (2b)

2b was prepared by following the general procedure, using aqueous formaldehyde (35% in water, 0.977 g, 11.40 mmol), thiomorpholine (0.941 g, 9.12 mmol) and 1-ethoxycarbonylmethyl-3-hydroxy-2(1*H*)-pyridinone **1a** (1.500 g, 7.60 mmol). Yield: 1.971 g (83%), m.p. 152–154 °C (decomp.), Elemental analysis, found: C 53.77; H 6.13; N 8.78; calcd. for $C_{14}H_{20}O_4N_2S$: C 53.83; H 6.45; N 8.97%. MS (ESI^+): *m/z*: 313.0 $[M + H]^+$; ^1H NMR (500.10 MHz, DMSO-d_6, 25 °C): δ = 7.12 (d, $^3J_{(H,H)}$ = 7 Hz, 1H, H6), 6.20 (d, $^3J_{(H,H)}$ = 7 Hz, 1H, H5), 4.70 (s, 2H, NCH_2CO), 4.14 (q, $^3J_{(H,H)}$ = 7 Hz, 2H, $CH_3C\underline{H}_2O$), 3.39 (s, 2H, CH_2N), 2.64 (m, 8H, $H_{thiomor}$), 1.21 (t, $^3J_{(H,H)}$ = 7 Hz, 3H, $C\underline{H}_3CH_2O$) ppm. $^{13}C\{^1H\}$ NMR (125.75 MHz, DMSO-d_6, 25 °C): δ =

168.4 (COOEt), 158.8 (C2), 144.4 (C3), 128.3 (C6), 125.6 (C4), 107.3 (C5), 65.8 ($C_{thiomor}$), 61.5 (OCH_2CH_3), 55.6 (CH_2N), 53.4 ($C_{thiomor}$), 50.6 (NCH_2CO), 14.5 (OCH_2CH_3) ppm.

1-Ethoxycarbonylmethyl-3-hydroxy-4-piperidinomethyl-2(1*H*)-pyridone (2c)

2c was prepared by following the general procedure, using aqueous formaldehyde (35% in water, 0.977 g, 11.40 mmol), piperidine (0.776 g, 9.12 mmol) and 1-ethoxycarbonylmethyl-3-hydroxy-2(1*H*)-pyridinone **1a** (1.500 g, 7.60 mmol). Yield: 1.767 g (79%), m.p. 132–133 °C (decomp.), Elemental analysis, found : C 61.20; H 7.44; N 9.36; calcd. for $C_{15}H_{22}O_4N_2$: C 61.21; H 7.53; N 9.52%. MS (ESI^+): *m/z*: 295.2 $[M + H]^+$; ^1H NMR (500.10 MHz, DMSO-d_6, 25 °C): δ = 7.07 (d, $^3J_{(H,H)}$ = 7 Hz, 1H, H6), 6.17 (d, $^3J_{(H,H)}$ = 7 Hz, 1H, H5), 4.71 (s, 2H, NCH_2CO), 4.14 (q, $^3J_{(H,H)}$ = 7 Hz, 2H, CH_3CH_2O), 3.37 (s, 2H, CH_2N), 2.37 (brs, 4H, H_{pip}), 1.50-1.53 (m, 4H, H_{pip}), 1.40-1.41 (m, 2H, H_{pip}), 1.21 (t, $^3J_{(H,H)}$ =7 Hz, 3H, CH_3CH_2O) ppm. $^{13}C\{^1H\}$ NMR (125.75 MHz, DMSO-d_6, 25 °C): δ = 168.6 (COOEt), 157.7 (C2), 144.8 (C3), 128.1 (C6), 125.9 (C4), 106.8 (C5), 61.4 (OCH_2CH_3), 56.7 (CH_2N), 54.4 (C_{pip}), 50.6 (NCH_2CO), 26.0 (C_{pip}), 24.2 (C_{pip}), 14.5 (OCH_2CH_3) ppm.

1-Ethoxycarbonylmethyl-3-hydroxy-4-(3-methylpiperidinomethyl-2(1*H*)-pyridinone (2d)

2d was prepared by following the general procedure, using aqueous formaldehyde (35% in water, 0.977 g, 11.40 mmol), 3-methylpiperidine (0.904 g, 9.12 mmol) and 1-ethoxycarbonylmethyl-3-hydroxy-2(1*H*)-pyridinone **1a** (1.500 g, 7.60 mmol). Yield: 1.855 g (78%), m.p. 119–121 °C (decomp.), Elemental analysis, found: C 61.86; H 7.69; N 8.83; calcd. for $C_{16}H_{24}O_4N_2 \cdot 0.1H_2O$: C 61.96; H 7.86; N 9.03%. MS (ESI^+): *m/z*: 309.1 $[M + H]^+$; ^1H NMR (500.10 MHz, DMSO-d_6, 25 °C): δ = 7.10 (d, $^3J_{(H,H)}$ = 7 Hz, 1H, H6), 6.16 (d, $^3J_{(H,H)}$ = 7 Hz, 1H, H5), 4.69 (s, 2H, NCH_2CO), 4.15 (q, $^3J_{(H,H)}$ = 7 Hz, 2H, CH_3CH_2O), 3.38 (s, 2H, CH_2N), 2.71-2.75 (m, 2H, H_{pip}), 1.90-1.94 (m, 2H, H_{pip}), 1.59-1.66 (m, 4H, H_{pip}), 1.45-1.50 (m, 1H, H_{pip}), 1.21 (t, $^3J_{(H,H)}$ = 7 Hz, 3H, CH_3CH_2O), 0.83 (d, $^3J_{(H,H)}$ = 6 Hz, 3H, CH_3)

ppm. $^{13}C\{^{1}H\}$ NMR (125.75 MHz, DMSO-d_6, 25 °C): δ = 168.8 (C<u>O</u>OEt), 157.7 (C2), 144.8 (C3), 128.2 (C6), 125.9 (C4), 106.8 (C5), 61.7 (C_{pip}), 61.4 (O<u>C</u>H_2CH_3), 56.5 (CH_2N), 53.9 (C_{pip}), 50.6 (N<u>C</u>H_2CO), 32.8 (C_{pip}), 31.2 (C_{pip}), 25.4 (C_{pip}), 19.9 (CH_3) 14.5 (OCH_2<u>C</u>H_3) ppm.

1-Ethoxycarbonylmethyl-3-hydroxy-4-(2,6-dimethylmorpholinomethyl-2(1*H*)-pyridinone (2e)

2e was prepared by following the general procedure, using aqueous formaldehyde (35% in water, 0.977 g, 11.40 mmol), 2,6-dimethylmorpholine (1.050 g, 9.12 mmol) and 1-ethoxycarbonylmethyl-3-hydroxy-2(1*H*)-pyridinone **1a** (1.500 g, 7.60 mmol). Yield: 1.873 g (76%), m.p. 158–159 °C (decomp.), Elemental analysis, found: C 59.38; H 7.44; N 8.60; calcd. for $C_{16}H_{24}O_5N_2$: C 59.24; H 7.7.46; N 8.64%. MS (ESI^+): *m/z*: 347.0 $[M + Na]^+$, 325.1 $[M + H]^+$; ^1H NMR (500.10 MHz, DMSO-d_6, 25 °C): δ = 7.11 (d, $^3J_{(H,H)}$ = 7 Hz, 1H, H6), 6.20 (d, $^3J_{(H,H)}$ = 7 Hz, 1H, H5), 4.70 (s, 2H, NCH_2CO), 4.15 (q, $^3J_{(H,H)}$ = 7 Hz, 2H, CH_3C<u>H</u>$_2O$), 3.55-3.59 (m, 2H, H_{mor}), 3.37 (s, 2H, CH_2N), 2.68 (d, $^3J_{(H,H)}$ = 10 Hz, 2H, H_{mor}), 1.70 (t, $^3J_{(H,H)}$ = 10 Hz, 2H, H_{mor}), 1.21 (t, $^3J_{(H,H)}$ = 7 Hz, 3H, C<u>H</u>$_3CH_2O$), 1.04 (d, $^3J_{(H,H)}$ = 6 Hz, 6H, CH_3) ppm. $^{13}C\{^{1}H\}$ NMR (125.75 MHz, DMSO-d_6, 25 °C): δ = 168.5 (C<u>O</u>OEt), 157.8 (C2), 144.6 (C3), 128.2 (C6), 125.4 (C4), 107.1 (C5), 71.5 (C_{mor}), 61.4 (O<u>C</u>H_2CH_3), 59.4 (CH_2N), 55.3 (C_{mor}), 50.7 (N<u>C</u>H_2CO), 19.4 (CH_3), 14.5 (OCH_2<u>C</u>H_3) ppm.

1-Ethoxycarbonylmethyl-3-hydroxy-4-(*N*-methylpiperazinomethyl-2(1*H*)-pyridinone (2f)

2f was prepared by following the general procedure, using aqueous formaldehyde (35% in water, 0.977 g, 11.40 mmol), 1-methylpiperazine (0.913 g, 9.12 mmol) and 1-ethoxycarbonylmethyl-3-hydroxy-2(1*H*)-pyridinone **1a** (1.500 g, 7.60 mmol). Yield: 2.138 g (91%), m.p. 150–152 °C (decomp.), Elemental analysis, found: C 58.11; H 7.44; N 13.57; calcd. for $C_{15}H_{23}O_4N_3$: C 58.24; H 7.49; N 13.58%. MS (ESI^+): *m/z*: 310.1 $[M + H]^+$; ^1H NMR (500.10 MHz, DMSO-d_6, 25 °C): δ = 7.11 (d, $^3J_{(H,H)}$ = 7 Hz, 1H, H6), 6.18 (d, $^3J_{(H,H)}$ = 7 Hz, 1H, H5), 4.71 (s, 2H, NCH_2CO), 4.15 (q, $^3J_{(H,H)}$ = 7 Hz, 2H, CH_3C<u>H</u>$_2O$), 3.39 (s, 2H, CH_2N), 2.37-2.41 (m, 8H, H_{pipz}), 2.17

(s, 3H, NCH_3), 1.21 (t, $^3J_{(H,H)}$ = 7 Hz, 3H, $C\underline{H}_3CH_2O$) ppm. $^{13}C\{^1H\}$ NMR (125.75 MHz, DMSO-d_6, 25 °C): δ = 168.5 ($\underline{C}OOEt$), 157.8 (C2), 144.6 (C3), 128.2 (C6), 125.7 (C4), 106.9 (C5), 61.4 ($O\underline{C}H_2CH_3$), 55.6 (CH_2N), 55.1 (C_{pipz}), 53.0 (C_{pipz}), 50.6 ($N\underline{C}H_2CO$), 46.1 (NCH_3), 14.5 ($OCH_2\underline{C}H_3$) ppm.

1-Ethoxycarbonylmethyl-3-hydroxy-4-(*N*-phenylpiperazinomethyl-2(1*H*)-pyridinone (2g)

2g was prepared by following the general procedure, using aqueous formaldehyde (35% in water, 0.977 g, 11.40 mmol), 1-phenylpiperazine (1.480 g, 9.12 mmol) and 1-ethoxycarbonylmethyl-3-hydroxy-2(1H)-pyridinone **1a** (1.500 g, 7.60 mmol). Yield: 2.512 g (89%), m.p. 161–162 °C (decomp.), Elemental analysis, found: C 64.53; H 6.86; N 11.39; calcd. for $C_{20}H_{25}O_4N_3$: C 64.67; H 6.78; N 11.31%. MS (ESI^+): *m/z*: 372.1 $[M + H]^+$; ^1H NMR (500.10 MHz, DMSO-d_6, 25 °C): δ = 7.20-7.23 (m, 2H, ph), 7.14 (d, $^3J_{(H,H)}$ = 7 Hz, 1H, H-6), 6.92-6.94 (m, 2H, ph), 6.76-6.79 (m, 1H, ph), 6.25 (d, $^3J_{(H,H)}$ = 7 Hz, 1H, H-5), 4.72 (s, 2H, NCH_2CO), 4.16 (q, $^3J_{(H,H)}$ = 7 Hz, 2H, $CH_3C\underline{H}_2O$), 3.46 (s, 2H, CH_2N), 3.15 (t, $^3J_{(H,H)}$ = 5 Hz, 4H, H_{pipz}), 2.56 (t, $^3J_{(H,H)}$ = 5 Hz, 4H, H_{pipz}),1.22 (t, $^3J_{(H,H)}$ =7 Hz, 3H, $C\underline{H}_3CH_2O$) ppm. $^{13}C\{^1H\}$ NMR (125.75 MHz, DMSO-d_6, 25 °C): δ = 168.5 ($\underline{C}OOEt$), 157.8 (C-2), 151.5 (C-ph), 144.6 (C-3), 129.4 (C-ph), 128.2 (C-6), 125.7 (C-4), 119.3 (C-ph), 115.9 (C-ph), 107.1 (C-5), 61.4 ($OO\underline{C}H_2CH_3$), 55.4 (CH_2N), 53.2 (C_{pipzn}), 50.7 ($N\underline{C}H_2CO$), 48.7 (C_{pipzn}), 14.5 ($OOCH_2\underline{C}H_3$) ppm.

General procedure for synthesis of complexs 3a-g:

A solution of **2a-g** (2.2 eq.) and NaOMe (3.5 eq.) in 20 ml MeOH was stirred for about 30 min. A solution of $[(\eta^6$-cymene)$RuCl(\mu$-$Cl)]_2$ (1.0 eq.) in 5 ml CH_2Cl_2 was added and the mixture was stirred for 2-3 h at RT. The solvent was removed under reduced pressure and the residue was redissolved in CH_2Cl_2, filtered to remove insoluble impurities and the filtrate was evaporated under vacuum. Recrystallization from CH_2Cl_2 and diethyl ether gave the pure product.

[Chlorido(η^6-*p*-cymene){*N*-[(ethoxycarbonyl)methyl]-3-oxo-κ*O*-(4-morpholinomethyl)-2-(1*H*)-pyridonato-κ*O*}ruthenium(II)] (3a)

The title compound was synthesized from *N*-[(ethoxycarbonyl)methyl]-3-hydroxy-(4-morpholinomethyl)-2-(1*H*)-pyridone (130 mg, 0.44 mmol), NaOMe (38 mg, 0.70 mmol) and [(η^6-*p*-cymene)RuCl(μ-Cl)]$_2$ (122 mg, 0.20 mmol) following the general procedure. Yield: 152 mg (67%), m.p. 214–216 °C (decomp.), Elemental analysis found C 51.16; H 5.85; N 4.75; calculated for $C_{24}H_{33}ClN_2O_5Ru$: C 50.92; H 5.88; N 4.95%; MS (ESI$^+$): *m/z* 531.2 [M – Cl]$^+$. ^{1}H NMR (500.10 MHz, $CDCl_3$, 25 °C): δ = 6.52 (brs, 1H, H6), 6.38 (d, $^3J_{(H,H)}$ = 7 Hz, 1H, H5), 5.52 (d, $^3J_{(H,H)}$ = 6 Hz; 1H, Ar-H), 5.49 (d, $^3J_{(H,H)}$ = 6 Hz, 1H, Ar-H), 5.24 (d, $^3J_{(H,H)}$ = 6 Hz, 1H, Ar-H), 5.23 (d, $^3J_{(H,H)}$ = 6 Hz, 1H, Ar-H), 5.10 (d, $^2J_{(H,H)}$ = 17 Hz, 1H, NCH_2CO), 4.27-4.30 (m, 2H, OCH_2CH_3), 4.22 (d, $^2J_{(H,H)}$ = 17 Hz, 1H, NCH_2CO), 3.75 (s, 2H, NCH_2), 3.67-3.73 (m, 4H, H_{mor}), 2.86-2.91 (m, 1H, C*H*$(CH_3)_2$), 2.53-2.60 (m, 4H, H_{mor}), 2.30 (s, 3H, Ar-CH_3), 1.33-1.36 (m, 9H, (C*H*$_3)_2$CH-Ar, OCH_2CH_3) ppm. ^{13}C{^{1}H} NMR (125.75 MHz, $CDCl_3$, 25 °C): δ = 167.0 (*C*OOEt), 166.4 (C3), 165.3 (C2), 120.3 (C4), 113.9 (C6), 105.7 (C5), 98.4 (C-Ar), 95.8 (C-Ar), 81.0 (C-Ar), 80.5 (C-Ar), 77.6 (C-Ar), 77.2 (C-Ar), 67.0 (C_{mor}), 66.8 (C_{mor}), 61.9 ($O\underline{C}H_2CH_3$), 55.2 (CH_2N), 53.6 (C_{mor}), 51.2 ($N\underline{C}H_2CO$), 31.1 ($\underline{C}H(CH_3)_2$), 22.5 ($CH(\underline{C}H_3)_2$), 22.3 ($CH(\underline{C}H_3)_2$), 18.5 (Ar-CH_3), 14.2 ($OCH_2\underline{C}H_3$) ppm.

[Chlorido(η^6-*p*-cymene){*N*-[(ethoxycarbonyl)methyl]-3-oxo-κ*O*-(4-thiomorpholinomethyl)-2-(1*H*)-pyridonato-κ*O*}ruthenium(II)] (3b)

The title compound was synthesized from *N*-[(ethoxycarbonyl)methyl]-3-hydroxy-(4-thiomorpholinomethyl)-2-(1*H*)-pyridone (137 mg, 0.44 mmol), NaOMe (38 mg, 0.70 mmol) and [(η^6-*p*-cymene)RuCl(μ-Cl)]$_2$ (122 mg, 0.20 mmol) following the general procedure. Yield: 135 mg (58%), m.p. >200 °C (decomp.), Elemental analysis found: C 49.35; H 5.62; N 4.65; calculated for $C_{24}H_{33}O_4N_2SClRu$: C 49.52; H 5.71; N 4.81%; MS (ESI$^+$): *m/z* 547.2 [M – Cl]$^+$. ^{1}H NMR (500.10 MHz, $CDCl_3$, 25 °C): δ = 6.51 (brs, 1H, H6), 6.39 (d, $^3J_{(H,H)}$ = 7 Hz, 1H, H5), 5.52 (d, $^3J_{(H,H)}$ = 6 Hz; 1H, Ar-H), 5.50 (d, $^3J_{(H,H)}$ = 6 Hz, 1H, Ar-H), 5.23 (d, $^3J_{(H,H)}$ = 6 Hz, 1H, Ar-H),

5.22 (d, $^{3}J_{(H,H)}$ = 6 Hz, 1H, Ar-H), 5.11 (d, $^{2}J_{(H,H)}$ = 17 Hz, 1H, NCH_2CO), 4.28-4.30 (m, 2H, OCH_2CH_3), 4.23 (d, $^{2}J_{(H,H)}$ = 17 Hz, 1H, NCH_2CO), 3.73 (s, 2H, NCH_2), 3.68-3.72 (m, 4H, H_{mor}), 2.87-2.91 (m, 1H, $CH(CH_3)_2$), 2.54-2.59 (m, 4H, H_{mor}), 2.31 (s, 3H, Ar-CH_3), 1.32-1.36 (m, 9H, $(CH_3)_2CH$-Ar, OCH_2CH_3) ppm. $^{13}C\{^{1}H\}$ NMR (125.75 MHz, $CDCl_3$, 25 °C): δ = 167.2 (*C*OOEt), 166.7 (C3), 165.4 (C2), 120.1 (C4), 113.8 (C6), 105.9 (C5), 98.6 (C-Ar), 95.5 (C-Ar), 81.1 (C-Ar), 80.6 (C-Ar), 77.8 (C-Ar), 77.1 (C-Ar), 67.3 (C_{mor}), 66.7 (C_{mor}), 61.9 ($O\underline{C}H_2CH_3$), 55.3 (CH_2N), 53.7 (C_{mor}), 51.3 ($N\underline{C}H_2CO$), 31.0 ($\underline{C}H(CH_3)_2$), 22.4 ($CH(\underline{C}H_3)_2$), 22.3 ($CH(\underline{C}H_3)_2$), 18.5 (Ar-CH_3), 14.2 ($OCH_2\underline{C}H_3$) ppm.

[Chlorido(η^6-*p*-cymene){*N*-[(ethoxycarbonyl)methyl]-3-oxo-κ*O*-(4-piperidinomethyl)-2-(1*H*)-pyridonato-κ*O*}ruthenium(II)] (3c)

The title compound was synthesized from *N*-[(ethoxycarbonyl)methyl]-3-hydroxy-(4-piperidinomethyl)-2-(1*H*)-pyridone (129 mg, 0.44 mmol), NaOMe (38 mg, 0.70 mmol) and [(η^6-*p*-cymene)RuCl(μ-Cl)]$_2$ (122 mg, 0.20 mmol) following the general procedure. Yield: 140 mg (62%), m.p. 215–217 °C (decomp.), Elemental analysis found: C 52.87; H 6.01; N 4.96; calculated for $C_{25}H_{35}O_4N_2ClRu$: C 53.23; H 6.25; N 4.97%; MS (ESI^+): *m/z* 565.1 $[M + H]^+$. ^{1}H NMR (500.10 MHz, $CDCl_3$, 25 °C): δ = 6.56 (brs, 1H, H6), 6.37 (d, $^{3}J_{(H,H)}$ = 7 Hz, 1H, H5), 5.52 (d, $^{3}J_{(H,H)}$ = 6 Hz; 1H, Ar-H), 5.50 (d, $^{3}J_{(H,H)}$ = 6 Hz, 1H, Ar-H), 5.24 (d, $^{3}J_{(H,H)}$ = 6 Hz, 2H, Ar-H), 5.07 (d, $^{2}J_{(H,H)}$ = 17 Hz, 1H, NCH_2CO), 4.28-4.30 (m, 2H, OCH_2CH_3), 4.25 (d, $^{2}J_{(H,H)}$ = 17 Hz, 1H, NCH_2CO), 3.82 (s, 2H, NCH_2), 3.67-3.69 (m, 2H, H_{pip}), 2.85-2.91 (m, 1H, $CH(CH_3)_2$), 2.57 (brs, 4H, H_{pip}), 2.30 (s, 3H, Ar-CH_3), 1.66 (brs, 4H, H_{pip}), 1.32-1.34 (m, 9H, $(CH_3)_2CH$-Ar, OCH_2CH_3) ppm. $^{13}C\{^{1}H\}$ NMR (125.75 MHz, $CDCl_3$, 25 °C): δ = 167.4 (*C*OOEt), 166.9 (C3), 162.3 (C2), 129.0 (C4), 126.3 (C6), 120.2 (C5), 98.4 (C-Ar), 95.7 (C-Ar), 80.9 (C-Ar), 80.5 (C-Ar), 77.6 (C-Ar), 77.2 (C-Ar), 61.9 ($O\underline{C}H_2CH_3$), 54.6 (CH_2N), 52.7 (C_{pip}), 51.3 ($N\underline{C}H_2CO$), 51.1 (C_{pip}), 31.1 ($\underline{C}H(CH_3)_2$), 26.0 (C_{pip}), 24.2 (C_{pip}), 22.4 ($CH(\underline{C}H_3)_2$), 22.3 ($CH(\underline{C}H_3)_2$), 18.5 (Ar-CH_3), 14.2 ($OCH_2\underline{C}H_3$) ppm.

[Chlorido(η^6-*p*-cymene){*N*-[(ethoxycarbonyl)methyl]-3-oxo-κ*O*-[4-(3-methylpiperidino)methyl]-2-(1*H*)-pyridonato-κ*O*}ruthenium(II)] (3d)

The title compound was synthesized from *N*-[(ethoxycarbonyl)methyl]-3-hydroxy-[4-(3-methylpiperidino)methyl]-2-(1*H*)-pyridone (136 mg, 0.44 mmol), NaOMe (38 mg, 0.70 mmol) and [(η^6-*p*-cymene)RuCl(μ-Cl)]$_2$ (122 mg, 0.20 mmol) following the general procedure. Yield: 141 mg (61%), m.p. 127–129 °C (decomp.), Elemental analysis found: C 53.79; H 6.17; N 4.90; calculated for $C_{26}H_{37}O_4N_2ClRu$: C 54.02; H 6.45; N 4.84%; MS (ESI$^+$): *m/z* 543.2 [M – Cl]$^+$. ^{1}H NMR (500.10 MHz, $CDCl_3$, 25 °C): δ = 6.45 (brs, 1H, H-6), 6.37 (d, $^3J_{(H,H)}$ = 6 Hz, 1H, H-5), 5.52 (d, $^3J_{(H,H)}$ = 6 Hz; 1H, Ar-H), 5.49 (d, $^3J_{(H,H)}$ = 6 Hz, 1H, Ar-H), 5.24 (d, $^3J_{(H,H)}$ = 6 Hz, 2H, Ar-H), 5.09 (d, $^2J_{(H,H)}$ = 17 Hz, 1H, NCH_2CO), 4.24-4.29 (m, 3H, OCH_2CH_3, NCH_2CO), 3.81 (s, 2H, NCH_2), 2.85-2.89 (m, 1H, C*H*$(CH_3)_2$), 2.82-2.83 (brs, 4H, H_{pip}), 2.29 (s, 3H, Ar-CH_3), 1.97-1.99 (m, 4H, H_{pip}), 1.61-1.69 (m, 1H, H_{pip}), 1.31-1.34 (m, 9H, (C*H*$_3)_2$CH-Ar, OCH_2CH_3), 0.86 (s, 3H, Pip-CH_3), ppm. ^{13}C{^{1}H} NMR (125.75 MHz, $CDCl_3$, 25 °C): δ = 168.0 (*C*OOEt), 166.7 (C3), 162.5 (C2), 128.4 (C4), 126.0 (C6), 119.2 (C5), 98.5 (C-Ar), 95.3 (C-Ar), 80.6 (C-Ar), 80.2 (C-Ar), 77.8 (C-Ar), 77.2 (C-Ar), 62.1 (C_{pip}), 61.5 ($O\underline{C}H_2CH_3$), 55.4 (CH_2N), 53.4 (C_{pip}), 51.5 ($N\underline{C}H_2CO$), 52.4 (C_{pip}), 31.2 ($\underline{C}H(CH_3)_2$), 26.3 (C_{pip}), 24.5 (C_{pip}), 22.4 ($CH(\underline{C}H_3)_2$), 22.3 ($CH(\underline{C}H_3)_2$), 18.5 (Ar-CH_3), 14.2 ($OCH_2\underline{C}H_3$) ppm.

[Chlorido(η^6-*p*-cymene){*N*-[(ethoxycarbonyl)methyl]-3-oxo-κ*O*-[4-(2,6-dimethylmorpholino)methyl]-2-(1*H*)-pyridonato-κ*O*}ruthenium(II)] (3e)

The title compound was synthesized from *N*-[(ethoxycarbonyl)methyl]-3-hydroxy-[4-(2,6-dimethylmorpholino)methyl]-2-(1*H*)-pyridone (143 mg, 0.44 mmol), NaOMe (38 mg, 0.70 mmol) and [(η^6-*p*-cymene)RuCl(μ-Cl)]$_2$ (122 mg, 0.20 mmol) following the general procedure. Yield: 128 mg (54%), m.p. 176–178 °C (decomp.), Elemental analysis found: C 52.27; H 6.05; N 4.71; calculated for $C_{26}H_{37}O_5N_2ClRu$: C 52.56; H 6.28; N 4.72%;: MS (ESI$^+$): *m/z* 559.2 [M – Cl]$^+$. ^{1}H NMR (500.10 MHz, $CDCl_3$, 25 °C): δ = 6.54 (brs, 1H, H6), 6.37 (d, $^3J_{(H,H)}$ = 7 Hz, 1H, H5), 5.51

(d, $^{3}J_{(H,H)}$ = 6 Hz; 1H, Ar-H), 5.49 (d, $^{3}J_{(H,H)}$ = 6 Hz, 1H, Ar-H), 5.25 (d, $^{3}J_{(H,H)}$ = 6 Hz, 1H, Ar-H), 5.23 (d, $^{3}J_{(H,H)}$ = 6 Hz, 1H, Ar-H), 5.09 (d, $^{2}J_{(H,H)}$ = 17 Hz, 1H, NCH_2CO), 4.26-4.29 (m, 2H, OCH_2CH_3), 4.23 (d, $^{2}J_{(H,H)}$ = 17 Hz, 1H, NCH_2CO), 3.73 (s, 2H, NCH_2), 3.63-3.69 (m, 4H, H_{mor}), 2.87-2.92 (m, 1H, $CH(CH_3)_2$), 2.54-2.58 (m, 2H, H_{mor}), 2.32 (s, 3H, Ar-CH_3), 1.34-1.37 (m, 9H, $(CH_3)_2CH$-Ar, OCH_2CH_3), 1.06 (d, $^{3}J_{(H,H)}$ = 6 Hz, 6H, CH_3) ppm. $^{13}C\{^{1}H\}$ NMR (125.75 MHz, $CDCl_3$, 25 °C): δ = 168.4 (*C*OOEt), 167.0 (C3), 165.4 (C2), 121.3 (C4), 114.2 (C6), 106.8 (C5), 98.6 (C-Ar), 95.4 (C-Ar), 81.3 (C-Ar), 80.6 (C-Ar), 77.8 (C-Ar), 77.1 (C-Ar), 69.2 (C_{mor}), 61.7 (OCH_2CH_3), 56.2 (CH_2N), 53.4 (C_{mor}), 51.3 (NCH_2CO), 31.2 ($CH(CH_3)_2$), 22.5 ($CH(CH_3)_2$), 22.3 ($CH(CH_3)_2$), 18.5 (Ar-CH_3), 14.2 (OCH_2CH_3) ppm.

[Chlorido(η^6-*p*-cymene){*N*-[(ethoxycarbonyl)methyl]-3-oxo-κ*O*-[4-(*N*-methylpiperazino)methyl]-2-(1*H*)-pyridonato-κ*O*}ruthenium(II)] (3f)

The title compound was synthesized from *N*-[(ethoxycarbonyl)methyl]-3-hydroxy-[4-(*N*-methylpiperazino)methyl]-2-(1*H*)-pyridone (136 mg, 0.44 mmol), NaOMe (38 mg, 0.70 mmol) and [(η^6-*p*-cymene)RuCl(μ-Cl)]$_2$ (122 mg, 0.20 mmol) following the general procedure. Yield: 134 mg (56%), m.p. 187–189 °C (decomp.), Elemental analysis found: C 50.69; H 5.92; N 7.23; calculated for $C_{25}H_{36}O_4N_3ClRu\cdot 0.25CH_2Cl_2$: C 50.52; H 6.13; N 7.00%; MS (ESI$^+$): *m/z* 544.2 [M – Cl]$^+$. ^{1}H NMR (500.10 MHz, $CDCl_3$, 25 °C): δ = 6.44 (d, $^{3}J_{(H,H)}$ = 7 Hz, 1H, H6), 6.37 (d, $^{3}J_{(H,H)}$ = 7 Hz, 1H, H5), 5.51 (d, $^{3}J_{(H,H)}$ = 6 Hz; 1H, Ar-H), 5.48 (d, $^{3}J_{(H,H)}$ = 6 Hz, 2H, Ar-H), 5.09 (d, $^{2}J_{(H,H)}$ = 17 Hz, 1H, NCH_2CO), 4.20-4.29 (m, 3H, OCH_2CH_3, NCH_2CO), 3.82 (s, 2H, NCH_2), 3.64-3.67 (m, 4H, H_{pipz}), 2.86-2.92 (m, 1H, $CH(CH_3)_2$), 2.46-2.54 (m, 4H, H_{pipz}), 2.33 (s, 3H, NCH_3), 2.29 (s, 3H, Ar-CH_3), 1.31-1.35 (m, 9H, $(CH_3)_2CH$-Ar, OCH_2CH_3) ppm. $^{13}C\{^{1}H\}$ NMR (125.75 MHz, $CDCl_3$, 25 °C): δ = 166.7 (*C*OOEt), 165.6 (C3), 164.8 (C2), 120.6 (C4), 114.4 (C6), 106.3 (C5), 98.5 (C-Ar), 95.6 (C-Ar), 81.2 (C-Ar), 80.7 (C-Ar), 77.4 (C-Ar), 77.1 (C-Ar), 61.9 (OCH_2CH_3), 55.8 (CH_2N), 55.2 (C_{pipz}), 53.7 (C_{pipz}), 51.3 (NCH_2CO), 47.1 (CH_3N), 31.0 ($CH(CH_3)_2$), 22.4 ($CH(CH_3)_2$), 22.3 ($CH(CH_3)_2$), 18.4 (Ar-CH_3), 14.2 (OCH_2CH_3) ppm.

[Chlorido(η^6-*p*-cymene){*N*-[(ethoxycarbonyl)methyl]-3-oxo-κ*O*-[4-(*N*-phenylpiperazino)methyl]-2-(1*H*)-pyridonato-κ*O*}ruthenium(II)] (3g)

The title compound was synthesized from *N*-[(ethoxycarbonyl)methyl]-3-hydroxy-[4-(*N*-phenylpiperazino)methyl]-2-(1*H*)-pyridone (163 mg, 0.44 mmol), NaOMe (38 mg, 0.70 mmol) and [(η^6-*p*-cymene)RuCl(μ-Cl)]$_2$ (122 mg, 0.20 mmol) following the general procedure. Yield: 195 mg (76%), m.p. 168–170 °C (decomp.), Elemental analysis found: C 55.86; H 5.76; N 6.60; calculated for $C_{30}H_{38}O_4N_3ClRu$: C 56.20; H 5.97; N 6.55%; MS (ESI$^+$): *m/z* 606.0 [M – Cl]$^+$. ^{1}H NMR (500.10 MHz, $CDCl_3$, 25 °C): δ = 7.25-7.29 (m, 2H, Ph), 6.93-6.95 (m, 2H, Ph), 6.84-6.87 (m, 1H, Ph), 6.51 (d, $^3J_{(H,H)}$ = 6 Hz, 1H, H6), 6.39 (d, $^3J_{(H,H)}$ = 7 Hz, 1H, H5), 5.52 (d, $^3J_{(H,H)}$ = 6 Hz; 1H, Ar-H), 5.50 (d, $^3J_{(H,H)}$ = 6 Hz, 1H, Ar-H), 5.25 (d, $^3J_{(H,H)}$ = 6 Hz, 2H, Ar-H), 5.11 (d, $^2J_{(H,H)}$ = 17 Hz, 1H, NC*H*$_2$CO), 4.27-4.30 (m, 2H, OC*H*$_2$CH$_3$), 4.22 (d, $^2J_{(H,H)}$ = 17 Hz, 1H, NC*H*$_2$CO), 3.84 (s, 2H, NCH$_2$), 3.21 (brs, 4H, H$_{pipz}$), 2.86-2.92 (m, 1H, C*H*(CH$_3$)$_2$), 2.70 (brs, 4H, H$_{pipz}$), 2.30 (s, 3H, Ar-CH$_3$), 1.33-1.36 (m, 9H, (C*H*$_3$)$_2$CH-Ar, OCH$_2$C*H*$_3$) ppm. ^{13}C{^{1}H} NMR (125.75 MHz, $CDCl_3$, 25 °C): δ = 167.1 (*C*OOEt), 165.2 (C3), 158.9 (C2), 151.4 (C-NPh), 129.1 (C4), 120.3 (C6), 119.5 (C-NPh), 116.0 (C5), 113.8 (C-NPh), 98.4 (C-Ar), 95.8 (C-Ar), 80.8 (C-Ar), 80.5 (C-Ar), 77.5 (C-Ar), 77.2 (C-Ar), 61.9 (O*C*H$_2$CH$_3$), 55.0 (C$_{pipz}$), 53.2(CH$_2$N), 51.2 (N*C*H$_2$CO), 49.1 (C$_{pipz}$), 31.1 (*C*H(CH$_3$)$_2$), 22.5 (CH(C̲H$_3$)$_2$), 22.4 (CH(C̲H$_3$)$_2$), 18.5 (Ar-CH$_3$), 14.2 (OCH$_2$*C*H$_3$) ppm.

Stability in aqueous solution

For hydrolysis studies, **3a**, **3b** and **3c** (1–2 mg/mL) were dissolved in D_2O/MeOD-d_4 (95/5) or 0.02 M phosphate buffer (pH 7.40, 100 mM NaCl)/MeOD-d_4 (95/5) and the samples were analyzed by ^{1}H NMR spectroscopy. The ^{1}H NMR spectra were recorded after 0.5, 24, 48, 72 and 120 h.

pK_a determination

pK_a values were determined by dissolving **3a** and **3c** in MeOD-d_4/D_2O (5/95) solution. The pH values were measured directly in the NMR tubes with an Eco Scan

pH6 pH meter equipped with a glass-micro combination pH electrode (Orion 9826BN) and calibrated with standard buffer solutions of pH 4.00, 7.00 and 10.00. The pH titration was performed with NaOD (0.4–0.0004% in D_2O) and DNO_3 (0.4–0.0004% in D_2O). The pH values were plotted against the chemical shifts of the Ar-$_{cym}$-H2/H6 protons of the arene ring in the ^{1}H NMR spectra and the resulting curves were fitted using the Henderson-Hasselbalch equation with Microsoft® Office Excel 2003, SP3 (Microsoft Corporation). The experimentally obtained pK_{a*} values were corrected with Eq. (1), in order to convert the pK_{a*} in D_2O to the corresponding pK_a values in aqueous solutions.[134]

$$pK_a = 0.929\ pK_{a*} + 0.42 \qquad (1)$$

Reaction with biomolecules monitored by NMR spectroscopy

5'-GMP binding experiments were carried out by titrating solutions of **3a**, **3b** and **3c** (1–2 mg/mL) in 0.02 M phosphate buffer (pH 7.4, 4 mM NaCl)/MeOD-d_4 (95/5) with a 5'-GMP solution (10 mg/mL D_2O) in 50 µL increments. The reaction was monitored by ^{1}H and ^{31}P{^{1}H} NMR spectroscopy until unreacted 5'-GMP was detected.

In order to investigate the reactivity of complexes with amino acids, solutions of **3a**, **3b** and **3c** (1 mg/mL) in 0.02 M phosphate buffer (pH 7.40, 100 mM NaCl)/MeOD-d_4 (95/5) were treated with equimolar amounts of Gly, Cys, Met and His and the ^{1}H NMR spectra were recorded after 5 min and 24 h.

Mass Spectrometry Studies on the Binding to Amino Acids and Proteins

Stock solutions of **3a**, **3b**, Cys, Met, His, ubiquitin (Ub) (each 400 µM) were prepared in MeOH/H_2O (90/10), and apo-transferrin (Tf) was dissolved in 50 mM ammonium bicarbonate buffer. Solutions of **3a** and **3b** were incubated with the amino acids at a 1 : 1 molar ratio at 37 °C and ESI-MS spectra were measured after 0.5, 1, 3, 6 and 24 h. For the protein binding studies, **3a** or **3b** and Ub or Tf were mixed at

[134] A. Krezel and W. Bal, *J. Inorg. Biochem.*, 2004, **98**, 161-166.

2 : 1 molar ratios, and aliquots were taken after 0.5, 1, 2, 3, 6 and/or 24 h. The samples were analyzed at concentrations ranging from 10-30 μM. Therefore, they were diluted with MeOH in case of the amino acids, with MeOH/water/formic acid (50/50/0.1) for the analysis of the Ub samples and with MeOH/water/formic acid (10/90/2) for the analysis of Tf samples. ESI-mass spectra were recorded on a Bruker esquire$_{3000}$ ion trap mass spectrometer by direct infusion with a flow rate of 4 μL/min. The experimental conditions were as follows: Capillary 4.5 kV, end plate offset 0.5 kV, skimmer 1 43.2 V, skimmer 2 6 V, octopole 2.62 V, cap exit offset 77.2 V, and dry temperature 200 °C. For Tf samples skimmer 1 was adjusted to 71.0 V, skimmer 2 to 20.0 V octopole to 2.78 V, capillary exit offset to 120.0 V and Trap Drive to 73.0 V. The spectra were recorded and processed using ESI Compass 1.3 and DataAnalysis 4.0 software (both Bruker, Bremen, Germany). Deconvolution was obtained by the maximum entropy deconvolution algorithm with a mass step of *m/z* 0.1 and an instrument peak width of 0.5-4.

Cytotoxicity in cancer cell lines

Cell lines and culture conditions. CH1 cells (adenocarcinoma of the ovary) were a generous gift from Lloyd R. Kelland, CRC Centre for Cancer Therapeutics, Institute of Cancer Research, Sutton, UK. SW480 (adenocarcinoma of the colon, human), and A549 (non-small cell lung cancer, human) cells were kindly provided by Brigitte Marian (Institute of Cancer Research, Department of Medicine I, Medical University of Vienna, Austria). All cell culture reagents were obtained from Sigma-Aldrich Austria. Cells were grown in 75 cm² culture flasks (Iwaki) as adherent monolayer cultures in Eagle's Minimal Essential Medium (MEM) supplemented with 10% heat-inactivated fetal calf serum, 1 mM sodium pyruvate and 2 mM L-glutamine. Cultures were maintained at 37 °C in a humidified atmosphere containing 95% air and 5% CO_2.

MTT assay conditions. Cytotoxicity was determined by the colorimetric MTT (3-(4,5-dimethyl-2-thiazolyl)-2,5-diphenyl-2*H*-tetrazolium bromide, purchased from Fluka) microculture assay. For this purpose, cells were harvested from culture flasks by trypsinization and seeded in 100 μL aliquots MEM supplemented with 10% heat-

inactivated fetal calf serum, 1 mM sodium pyruvate, 4 mM L-glutamine and 1% non-essential amino acids (100×) into 96-well microculture plates (Iwaki). Cell densities of 1.5×10^3 cells/well (CH1), 2.5×10^3 cells/well (SW480) and 4×10^3 cells/well (A549) were chosen in order to ensure exponential growth of untreated controls throughout the experiment. Cells were allowed to settle and resume exponential growth for 24 h. The test compounds were dissolved and serially diluted in the same medium and added in 100 µL aliquots to the microcultures (if necessary due to limited solubility, the maximum concentration tested was added in 200 µL aliquots after removal of the medium), and cells were exposed to the test compounds for 96 h. At the end of exposure, all media were replaced by 100 µL/well RPMI1640 culture medium (supplemented with 10% heat-inactivated fetal calf serum) plus 20 µL/well MTT solution in phosphate-buffered saline (5 mg/ml). After incubation for 4 h, the supernatants were removed, and the formazan crystals formed by viable cells were dissolved in 150 µL DMSO per well. Optical densities at 550 nm were measured with a microplate reader (Tecan Spectra Classic), using a reference wavelength of 690 nm to correct for unspecific absorption. The quantity of vital cells was expressed in terms of T/C values by comparison to untreated control microcultures, and 50% inhibitory concentrations (IC_{50}) were calculated from concentration-effect curves by interpolation. Evaluation is based on means from three independent experiments, each comprising three replicates per concentration level.

3. Conclusions and outlook

Bioorganometallic chemistry is a relatively new but a fervent area of research. It offers possibilities for the design and development of metal based drugs for specific therapeutic needs that are not readily accessible to organic compounds. In recent years, Ru(II)- and Os(II)-arene complexes have become the focus of interest and some examples appear to be promising anticancer drug candidates. The metal-arene motif is an excellent scaffold, with potential to fine-tune the anticancer activity and other drug-like properties such as stability and solubility. Moreover, conjugation of the metal-arene fragment to bioactive species (e.g.ethacrynic acid, tamoxifen, staurosporine or aspirin) or simple biomolecules (e.g.sugars or amino acids) can result in enhanced activity as well as specificity.

In this thesis, different strategies were employed, including coordination of biomolecules to the metal-arene unit, with the aim to improve pharmacological properties such as bioavailability, lipophilicity, solubility and anticancer activity. Cancer cells usually display enhanced glucose uptake under hypoxic conditions, due to overexpression of glycolytic enzymes and glucose transporters, as compared to healthy cells. Therefore, attaching a carbohydrate functionality to a metal-arene moiety appears a promising strategy to exploit biochemical and metabolic functions used for transport and accumulation of sugars in living organisms. This is discussed in the first part of this thesis which comprises the synthesis and biological evaluation of ruthenium(II)- and osmium(II)-arene compounds bearing sugar-derived bicyclophosphite ligands. The complexes were characterized with regard to their chemical stability in aqueous solution, reaction with proteins and the DNA models 5'-GMP and 9-ethylguanine. Different structural modifications such as change of arene, metal center and leaving group were made with regard to structure-activity relationships. [Ru(arene)(sugar-phosphite)Cl_2] complexes exhibit IC_{50} values from moderate to the low micromolar range and are prone to hydrolysis. They undergo aquation of the first halido ligand in aqueous solution, and additionally hydrolysis of a P–O

bond of the phosphite ligand, leading ultimately to the formation of dinuclear species.

The change of metal center from ruthenium to osmium has no significant impact on *in vitro* anticancer activity, despite a considerably lower rate of hydrolysis and lack of reactivity to 5'-GMP for a dichlorido-osmium analogue. In order to study the role of the leaving group, the dichlorido ligands were replaced with chelating biscarboxylates, *i.e.*, oxalate and malonate. This structural modification has a dramatic influence on the chemical and biological properties of the compounds. As expected, hydrolysis is markedly inhibited and *in vitro* anticancer activity is also considerably low in all tested cell lines. The reactivity of the organometallic species to the biological nucleophiles Met, Cys, Ub and 5'-GMP is also significantly reduced, and compared to the respective dichlorido complexes, essentially the same adducts are formed, but at a lowered rate.

Variation in the arene ligand of metal arene complexes has demonstrated strong influence on the antiproliferative activity. It appears that cytotoxicity is increased by increasing the lipophilicity of carbohydrate based complexes. The most lipophilic compound was the most active with IC_{50} values in the low micromolar range. The following order of cytotoxicity is observed with regard to variation of arene ligand with the same sugar moiety in the Ru(II) complexes: biphenyl > cymene > toluene > benzene. This trend is also observed when changing the carbohydrate-derived moiety. While keeping the same arene ligand, compound having the most lipophilic ligand was the most cytotoxic.

Overall, carbohydrate-based metal(arene) complexes have demonstrated promising anticancer activity in *in vitro* assays. However, in vivo experiments might give deeper insight on the potential of these compounds as chemotherapeutics, as the effect of increased glucose uptake due to enhanced glycolytic activity in cancer cells can only be exploited in living organisms.

The second part of this thesis deals with the synthesis and complexation of 3-hydroxy-2-pyridones to ruthenium(II)- and osmium(II)-arene moieties. Novel M^{II}(arene) half-sandwich complexes (M = Ru, Os) with 3-hydroxy-2-pyridone derived ligands were synthesized and characterized chemically and biologically. The

compounds undergo fast hydrolysis to the respective aqua species that are stable for several days but react quickly, however to a different extent, with the amino acids Met, Cys, His and Gly to form M(η^6-*p*-cymene)(amino acid) adducts upon cleavage of the hydroxypyridone ligand, as characterized by NMR spectroscopy and ESI mass spectrometry. A similar behavior was also observed during the reactions with the model proteins ubiquitin and cytochrome c to yield mainly [protein + M(η^6-*p*-cymene)] adducts (M = Ru, Os). Notably the ligand cleavage of the Os derivative was significantly slower than of its Ru analogue which could explain its higher activity in *in vitro* anticancer assays. Furthermore, reaction products with 5'-GMP were characterized, to proceed *via* coordination to the *N*7 of the guanine moiety, as demonstrated by ^{1}H NMR spectroscopy and X-ray diffraction analysis. In CDK2/Cyclin A protein kinase inhibition studies, the Ru complexes revealed potent activity, comparable to known inhibitors. Ru(arene) complexes of 3-hydroxy-2-pyridone substituted in a Mannich reaction with thiomorpholine and piperidine, have shown promising anticancer activity with IC_{50} values in the low micro molar range. However, a remarkable difference in cytotoxicity was found between Ru(arene) complexes of morpholine and thiomorpholine derivatives, the latter being two orders of magnitude more active, despite minor difference in their structures . It would be interesting to carry out further investigations on mode of action studies and certain enzyme inhibition assays for these two compounds to know more about difference in their mechanism of action.

In future, it would be interesting to evaluate the influence of further structural changes in the metal(II)-arene unit, particularly the conjugation of functional groups or bioactive segments to the arene ligand, modification of carbohydrate functionality, in particular by introducing a spacer between metal center and carbohydrate moiety, change in the nature of the donor system, and substitution at the pyridone backbone. Moreover, investigations on the mechanism of action at the molecular level would provide deeper insights and rationale for future drug design.

Curriculum Vitae

Mr. Muhammad Hanif
Institute of Inorganic Chemistry
University of Vienna, Wahringer Str. 42,
A-1090 Vienna, Austria
Home address: Forsthusgasse 2-8/2039
A-1200 Vienna, Austria
Telephone: +43-650-6677164
E-mail: Muhammad.hanif@univie.ac.at, mhanif171@yahoo.com

Education:

PhD (2007-to date), Bioinorganic Chemistry:
Supervisor: Prof. DDr. Bernhard K. Keppler;
Department of Inorganic Chemistry, Faculty of Chemistry, University of Vienna, Austria.

M.Phil (2006), Chemistry:
Thesis Supervisor**:** Prof. Dr. Saeed Ahmad
Department of Chemistry, University of Engineering and Technology Lahore, Pakistan.

M.Sc. (2002), Chemistry:
Government College of Science Lahore, University of the Punjab, Pakistan.

B.Sc. (1999), Major Chemistry, Zoology and Botany:
Government College of Sakargarh, University of the Punjab, Pakistan.

Publications:

1) Wolfgang Kandioller, Andrea Kurzwernhart, Muhammad Hanif, Samuel M. Meier, , Helena Henke, Bernhard K. Keppler, Christian G. Hartinger, **(Thio)Pyr(id)ones and metals: from natural products to metal-based drugs**, *Journal of Organometalic Chemistry (2010) in press.* (*Review Article)*

2) Muhammad Hanif, Samuel M. Meier, Wolfgang Kandioller, Michaela Hejl, Christian G. Hartinger, Alexey A. Nazarov, Vladimir B. Arion, Michael A. Jakupec, Paul J. Dyson, Bernhard K. Keppler, **From Kinetically Labile to Kinetically Inert Anticancer Ru(II)-Arene Complexes Bearing Carbohydrate-Derived Ligands**, *Journal of Inorganic Biochemistry (2010) in press.*

3) Muhammad Hanif, Patricia Schaaf, Wolfgang Kandioller, Michaela Hejl, Michael A. Jakupec, Vladimir B. Arion, Bernhard K. Keppler, Christian G. Hartinger; **Influence of the Arene Ligand and the Leaving Group on the Anticancer Activity of (Thio)maltol Ruthenium^{II}–Arene Complexes** *Australian Journal of Chemistry (2010) in press.*

4) Muhammad Hanif, Helena Henke, Samuel M. Meier, Sanela Martic, Mahmoud Labib, Wolfgang Kandioller, Michael A. Jakupec, Vladimir B. Arion, Heinz-Bernhard Kraatz, Bernhard K. Keppler, Christian G. Hartinger; **Is the Reactivity of M(II)–Arene Complexes of 3-Hydroxy-2(1H)-pyridones to Biomolecules the Anticancer Activity Determining Parameter?** *Inorganic Chemistry, 2010, 49 (17), 7953–7963.*

5) Muhammad Hanif, Alexey A. Nazarov, Christian G. Hartinger, Wolfgang Kandioller, Michael A. Jakupec, Vladimir B. Arion, Paul J. Dyson, Bernhard K. Keppler; **Osmium(II) versus Ruthenium(II)-Arene Carbohydrate-based Anticancer Compounds: Similarities and Differences**, *Dalton Transactions, 2010, 39, 7345–7352.*

6) Saeed Ahmad, Muhammad Hanif, Muhammad Monim-ul-Mehboob, Anvarhusein A. Isab, Sajjad Ahmad, **Silver(I) Complexation with Glutathione in the Presence of Tetramethylthiourea;** *Synthesis and Reactivity in Inorganic, Metal-Organic, and Nano-Metal Chemistry, 39 (2009) 45-49.*

7) Isabella Berger, Muhammad Hanif, Alexey A. Nazarov, Christian G. Hartinger, Roland O. John, Maxim L. Kuznetsov, Michael Groessl, Frederic Schmitt, Olivier Zava, Florian Biba, Vladimir B. Arion, Markus Galanski, Michael A. Jakupec, Lucienne Juillerat-Jeanneret, Paul J. Dyson, Bernhard K. Keppler, **In Vitro Anticancer Activity and Biologically- Relevant Metabolization of Organometallic Ruthenium Complexes with Carbohydrate based Ligands;** *Chemistry A European Journal, 14 (2008) 9046-9057***.**

8) Muhammad Hanif, Aisha Saddiqa, Shahida Hasnain, Saeed Ahmad, Ghulam Rabbani, Anvarhusein A. Isab, **Preparation, spectral characterization and antibacterial studies of silver (I) complexes of mercaptopyridine and thiomalate**; *Spectroscopy 22 (2008) 51–56.*

9) Muhammad Hanif, Saeed Ahmad, Muhammad Altaf, Helen Stoeckli-Evans, **Poly[bis(μ_2-cyanido)-κ^2C:N; κ^2N:C-(μ_2-N,N, N$^{/}$, N$^{/}$-tetramethylthiourea-κ^2S:S)disilver(I)];** *Acta Crystallogr., E63, m2594 (2007).*

10) Saeed Ahmad, Muhammad Monim-ul-Mehboob, Muhammad Hanif, Muhammad Altaf, Helen Stoeckli-Evans, **Bis(cyanido-κC)(ethane-1,2-diamine-k^{2}N,N$^{/}$)silver(II),** *Acta Crystallogr., E63, m2548 (2007).*

Abstracts Published:

1) Muhammad Hanif, Alexey A. Nazarov, Christian G. Hartinger, Isabella Berger, Michael A. Jakupec, Paul J. Dyson, Bernhard K. Keppler; **Influence of Arene Ligand, Metal Center and the Leaving Group on the in Vitro Anticancer Activity of Organometallic Compounds Linked with Carbohydrate Based Ligands**, *CHIMIA (2010), Vol. 64, Issue. No. 7/8, page 243***.**

2) Alexey A. Nazarov, Muhammad Hanif, Christian G. Hartinger, Bernhard K. Keppler, Paul J. Dyson; **Anticancer activity of Sugar-linked Ru(II) and Os(II) Complexes,** *Journal of Biological Inorganic Chemistry (2009), Vol. 14 (Suppl 1): page S90.*

3) Christian G. Hartinger, Alexey A. Nazarov, Isabella Berger, Muhammad Hanif, Maxim L. Kuznetsov, Michael Groessl, Frederic Schmitt, Olivier Zava, Michael A. Jakupec, Lucienne Juillerat-Jeanneret, Paul J. Dyson, Bernhard K. Keppler;

In Vitro Anticancer Activity and Biologically-Relevant Metabolization of Organometallic Ruthenium Complexes with Carbohydrate-based Ligands, *CHIMIA (2008), Vol. 62, Issue. No. 7/8, page 606.*

4) Saeed Ahmad, Muhammad Hanif, Muhammad Monim-ul-Mehboob, Anvarhusein A. Isab, **Silver(I) complexation with glutathione and tetramethylthiourea**, *Journal of Biological Inorganic Chemistry (2007), Vol. 12 (Suppl. 1), page S123.*

Contributions in Conferences/Symposiums/Workshops:

a) Oral Contributions:

1) Christian G. Hartinger, Wolfgang Kandioller, Muhammad Hanif, Andrea Kurzwernhart, Helena Henke, Robert Trondl, Caroline Bartel, Gerhard Mühlgassner, Michael A. Jakupec, M. G. Mendoza-Ferri, Alexey A. Nazarov, Bernhard K. Keppler; **Organometallic Pyrone and Pyridone Complexes as Anticancer Agents**, *5th International Symposium on Bioorganometallic Chemistry (ISBOMC10), July 5-9, 2010, Bochum, Germany.*

2) Muhammad Hanif, Christian G. Hartinger, Alexey A. Nazarov, Isabella Berger, Wolfgang Kandioller, Michael A. Jakupec, Paul J. Dyson, Bernhard K. Keppler; **Metal-Arene Complexes Linked with Carbohydrate Ligands: Cytotoxicity, Hydrolysis and Interaction with Biomolecules**, *6th Workshop on Inorganic Chemistry (6.WACÖ), March 29-30, 2010, Linz, Austria.*

3) Helena Henke, Muhammad Hanif, Christian G. Hartinger, Wolfgang Kandioller, Michael A. Jakupec, Vladimir B. Arion, Bernhard K. Keppler; **Synthesis and Cytotoxicity of Metal-Arene Complexes of 3-Hydroxy-2-pyridinone-Derived Ligands,** *6th Workshop on Inorganic Chemistry (6.WACÖ), March 29-30, 2010, Linz, Austria.*

4) Muhammad Hanif, Christian G. Hartinger, Alexey A. Nazarov, Isabella Berger, Michael A. Jakupec, Paul J. Dyson, Bernhard K. Keppler; **Controlling the Reactivity of Anticancer Active Organometallic Compounds**, *Bioinorganic*

Chemistry Gordon Research Conference (GRS), February 4-7, 2010, Ventura, California, USA. (Data Blitz)

5) Muhammad Hanif, Isabella Berger, Alexey A. Nazarov, Christian G. Hartinger, Michael A. Jakupec Bernhard K. Keppler, Paul J. Dyson; **In Vitro Anticancer Activity and Metabolization of Organometallic Ruthenium and Osmium Complexes with Carbohydrate-Based Ligands,** *10th International Symposium on Applied Bioinorganic Chemistry (ISABC 10), September 25 - 28, 2009, Debrecen, Hungary.*

6) Muhammad Hanif, Alexey A. Nazarov, Christian G. Hartinger, Michael A. Jakupec Bernhard K. Keppler, Paul J. Dyson; **Development of Anticancer Active RAPTA-C Analogues with Carbohydrate-Based Ligands,** *COST Action D39: Metallo-Drug Design and Action; 4th Annual Meeting and Workshop; September 24-25, 2009, Debrecen, Hungary.*

7) Alexey A. Nazarov, Muhammad Hanif, Christian G. Hartinger, Bernhard K. Keppler, Paul J. Dyson; **Anticancer activity of Sugar-linked Ru(II) and Os(II) Complexes,** *14th International Conference on Biological Inorganic Chemistry (ICBIC14), July 25-30, 2009, Nagoya, Japan.*

8) Muhammad Hanif, Isabella Berger, Alexey A. Nazarov, Christian G. Hartinger, Michael A. Jakupec Bernhard K. Keppler, Paul J. Dyson; **Anticancer Active RAPTA-C Analogues with Carbohydrate-Based Ligands: In Vitro Anticancer Activity and Metabolization,** *4th Asian Biological Inorganic Chemistry Conference (AsBIC IV), November 10-13, 2008, Jeju Island, South Korea.*

9) Saeed Ahmad, Muhammad Hanif, Muhammad Monim-ul-Mehboob, Anvarhusein A. Isab; **Silver(I) complexation with glutathione and tetramethylthiourea,** *13th International Conference on Biological Inorganic Chemistry (ICBIC13), July 15-20, 2007, Vienna, Austria.*

10) Muhammad Hanif, Saeed Ahmad, Muhammad Monim-ul-Mehboob, Anvarhusein A. Isab; **Synthesis and characterization of silver(I) complexes with 2-mercaptopyridine,** *1st International Chemistry Conference on Recent Challenges in Chemistry, November 1-3, 2006, Faisalabad, Pakistan.*

b) Poster Contributions:

1) Muhammad Hanif, Alexey A. Nazarov, Christian G. Hartinger, Isabella Berger, Michael A. Jakupec, Paul J. Dyson, Bernhard K. Keppler; **Influence of Arene Ligand, Metal Center and the Leaving Group on the in Vitro Anticancer Activity of Organometallic Compounds Linked with Carbohydrate Based Ligands**, *Swiss Chemical Society Meeting, Fall Meeting, September 16, 2010, Zürich, Switzerland.*

2) Alexey A. Nazarov, Muhammad Hanif, Lucienne Juillerat-Jeanneret, Christian G. Hartinger, Olivier Zava Michael A. Jakupec, Bernhard K. Keppler, Paul J. Dyson[a]; **Organometallic Ruthenium and Osmium Complexes with Carbohydrate-Based Ligands as Anticancer Agents**, *5th International Symposium on Bioorganometallic Chemistry (ISBOMC10), July 5-9, 2010, Bochum, Germany.*

3) Wolfgang Kandioller, Helena Henke, Muhammad Hanif, Patricia Schaaf, Caroline Bartel, Michael A. Jakupec, Alexey A. Nazarov, Christian G. Hartinger, Bernhard K. Keppler; **Pyrone vs. Pyridinone as Ligands for Ru-arene Anticancer Agents**; *10th European Biological Inorganic Chemistry Conference (EUROBIC10), June 22-26, 2009, Thessaloniki, Greece.*

4) Muhammad Hanif, Christian G. Hartinger, Alexey A. Nazarov, Isabella Berger, Michael A. Jakupec, Paul J. Dyson, Bernhard K. Keppler; **Controlling the Reactivity of Anticancer Active Organometallic Compounds,** *Bioinorganic Chemistry Gordon Research Conference (GRS), February 4-7, 2010, Ventura, California, USA.*

5) Alexey A. Nazarov, Muhammad Hanif, Christian G. Hartinger, Bernhard K. Keppler, Paul J. Dyson; **Anticancer activity of Sugar-linked Ru(II) and Os(II) Complexes,** *14th International Conference on Biological Inorganic Chemistry (ICBIC14), July 25-30, 2009, Nagoya, Japan.*

6) Alexey A. Nazarov, Muhammad Hanif, Julie Risse, Christian G. Hartinger, Bernhard K. Keppler, Paul J. Dyson; **Mono- and Polynuclear RAPTA-C Analogues with Carbohydrate-Based Ligand**; *6th European Workshop on Phosphorus Chemistry (EWPC-6), March 26-27, 2009, Florence, Italy.*

7) Christian G. Hartinger, Alexey A. Nazarov, Isabella Berger, Muhammad Hanif, Maxim L. Kuznetsov, Michael Groessl, Frederic Schmitt, Olivier Zava, Michael A. Jakupec, Lucienne Juillerat-Jeanneret, Paul J. Dyson, Bernhard K. Keppler; **In Vitro Anticancer Activity and Biologically-Relevant Metabolization of Organometallic Ruthenium Complexes with Carbohydrate-based Ligands**, *Swiss Chemical Society Fall Meeting, Zürich, Switzerland 2008.*

Work History:

1. 2007-2010 → research fellow, Department of Inorganic Chemistry, Faculty of Chemistry, University of Vienna, Austria

2. 2007 → junior scientist in Pakistan Atomic Energy Commission, declined.

3. 2005-2007 → chemistry teacher, Laurel Public High School Darogawala Lahore Pakistan.

4. 2003-2004 → chemist, Consolidated Chemical Lab (Pvt) Ltd. Kot Lakhpat Lahore Pakistan.

Research and Teaching Experience:

5. 2010 → Supervised one Master thesis, Department of Inorganic Chemistry, Faculty of Chemistry, University of Vienna, Austria.

6. 2009 → Supervised one Bachelor thesis, Department of Inorganic Chemistry, Faculty of Chemistry, University of Vienna, Austria.

7. 2007-2010 → Supervised undergraduate students in advanced inorganic synthetic lab courses on Biological Inorganic Chemistry and Coordination Chemistry, Department of Inorganic Chemistry, Faculty of Chemistry, University of Vienna, Austria.

8. 2007-2010 → PhD project, **"Ruthenium(II)- and Osmium(II)-Arene Anticancer Complexes: Synthesis, Cytotoxicity and Biologically Relevant Metabolization"** Department of Inorganic Chemistry, Faculty of Chemistry, University of Vienna, Austria.

9. 2005-2006 → M. Phil project, "**Synthesis, characterization and antimicrobial properties of silver (I) complexes of Thiones and Thiols"**

Fellowships/Awards/Grants:

- Fellowship for PhD studies in Austria by Higher Education Commission of Pakistan (2007-2010).
- Student Travel Award by Society of Biological Inorganic Chemistry to participate in 4th Asian Biological Inorganic Chemistry Conference, November 10-13, 2008, Jeju Island, South Korea.
- Travel Grant by Higher Education Commission of Pakistan to participate in 4th Asian Biological Inorganic Chemistry Conference, November 10-13, 2008, Jeju Island, South Korea.
- Travel Grant by Higher Education Commission of Pakistan to participate in Bioinorganic Chemistry Gordon Research Conference (GRS), February 4-7, 2010, Ventura, California, USA.
- Travel Award by University of Vienna Austria to participate in 10th International Symposium on Applied Bioinorganic Chemistry (ISABC 10), September 25 - 28, 2009, Debrecen, Hungary.